UNIVERSIDADE ESTADUAL DE CAMPINAS
Faculdade de Engenharia de Alimentos

KAMILA RAMPONI RODRIGUES DE GODOI FERNANDES

MATRIZES LIPÍDICAS À BASE DE ÁCIDO ESTEÁRICO: EFEITO DA INTERESTERIFICAÇÃO QUÍMICA, PROTOCOLOS DE CRISTALIZAÇÃO E POTENCIAL PARA OBTENÇÃO DE CARREADORES NANOESTRUTURADOS

STEARIC ACID-BASED LIPID SYSTEMS: EFFECTS OF CHEMICAL INTERESTERIFICATION, CRYSTALLIZATION PROTOCOLS AND POTENTIAL FOR OBTAINING NANOSTRUCTURED CARRIERS

Campinas
2023

KAMILA RAMPONI RODRIGUES DE GODOI FERNANDES

MATRIZES LIPÍDICAS À BASE DE ÁCIDO ESTEÁRICO: EFEITO DA INTERESTERIFICAÇÃO QUÍMICA, PROTOCOLOS DE CRISTALIZAÇÃO E POTENCIAL PARA OBTENÇÃO DE CARREADORES NANOESTRUTURADOS

STEARIC ACID-BASED LIPID SYSTEMS: EFFECTS OF CHEMICAL INTERESTERIFICATION, CRYSTALLIZATION PROTOCOLS AND POTENTIAL FOR OBTAINING NANOSTRUCTURED CARRIERS

Tese apresentada à Faculdade de Engenharia de Alimentos da Universidade Estadual de Campinas como parte dos requisitos exigidos para a obtenção do título de Doutora em Tecnologia de Alimentos.

Thesis presented to the Faculty of Food Engineering of the University of Campinas in partial fulfillment of the requirements for the degree of Doctor, in Food Technology.

Orientadora: Profª Drª Ana Paula Badan Ribeiro

ESTE EXEMPLAR CORRESPONDE À VERSÃO FINAL DA TESE DEFENDIDA PELA ALUNA KAMILA RAMPONI RODRIGUES DE GODOI FERNANDES E ORIENTADA PELA PROFª. DRª. ANA PAULA BADAN RIBEIRO.

Campinas
2023

Ficha catalográfica
Universidade Estadual de Campinas
Biblioteca da Faculdade de Engenharia de Alimentos
Claudia Aparecida Romano - CRB 8/5816

G547s

Godoi Fernandes, Kamila Ramponi Rodrigues, 1992-
Stearic acid-based lipid systems : effects of chemical interesterification, crystallization protocols and potential for obtaining nanostructured lipid carriers / Kamila Ramponi Rodrigues de Godoi Fernandes. – Campinas, SP : [s.n.], 2023.

Orientador: Ana Paula Badan Ribeiro.
Tese (doutorado) – Universidade Estadual de Campinas, Faculdade de Engenharia de Alimentos.

1. Interesterificação. 2. Ácido esteárico. 3. Carregadores lipídicos nanoestruturados. 4. Óleo de peixe. I. Ribeiro, Ana Paula Badan. II. Universidade Estadual de Campinas. Faculdade de Engenharia de Alimentos. III. Título.

Informações Complementares

Título em outro idioma: Matrizes lipídicas à base de ácido esteárico : efeito da interesterificação química, protocolos de cristalização e potencial para obtenção de carreadores lipídicos nanoestruturados.
Palavras-chave em inglês:
Interesterification
Stearic acid
Nanostructured lipidic carriers
Fish oil
Área de concentração: Tecnologia de Alimentos
Titulação: Doutora em Tecnologia de Alimentos
Banca examinadora:
Ana Paula Badan Ribeiro [Orientador]
Thaís Jordânia Silva
Valdecir Luccas
Mayara de Souza Queirós
Odalys García Cabrera
Data de defesa: 24-03-2023
Programa de Pós-Graduação: Tecnologia de Alimentos

Identificação e informações acadêmicas do(a) aluno(a)
- ORCID do autor: https://orcid.org/0000-0003-4115-0710
- Currículo Lattes do autor: http://lattes.cnpq.br/9644220881436403

BANCA EXAMINADORA

_____

Profª Drª Ana Paula Badan Ribeiro
Presidente

_____

Profª Drª Thaís Jordânia Silva
Membro Titular
Universidade Federal de São Carlos (UFSCAR)

_____

Prof. Dr. Valdecir Luccas
Membro Titular
Instituto de Tecnologia de Alimentos (ITAL)

_____

Drª Mayara de Souza Queirós
Membro Titular

_____

Drª Odalys García Cabrera
Membro Titular
Universidade Estadual de Campinas (UNICAMP)

A Ata de defesa com as respectivas assinaturas dos Membros Titulares encontra-se no SIGA/Sistema de Fluxo de Dissertações/Teses e na Secretaria do Programa de Pós-Graduação.

DEDICATÓRIA

À minha mãe Maristela e ao meu marido Fernando, dedico.

A mudança é o resultado final de toda a verdadeira aprendizagem (Leo Buscaglia)

AGRADECIMENTOS

Agradeço a Deus pela saúde e força para transpor os obstáculos e não me deixar desistir mesmo frente aos desafios durante todo o período de meu estudo.

À minha família, minha mãe Maristela, meu padrasto Ricardo e minhas avós, que sempre acreditaram no meu potencial e se alegraram com minhas vitórias.

Ao meu marido Fernando, pelo compartilhamento deste desafio dia-a-dia, por ser meu apoio e minha fonte de força em todos os momentos. Esta vitória também é sua!

Às velhas amigas, Letícia, Hellen, Renata, Ana Paula e Jussara, que mesmo distantes estiveram sempre presentes, sendo ombro amigo e apoio todo o tempo.

Às sempre melhores, Karina, Isadora e Letícia por compartilharem as agonias e dificuldades deste período desafiador sempre com muito bom humor e palavras de incentivo. Vencemos tudo isso, sempre juntas!

À todos os amigos que o Laboratório de Óleos e Gorduras me proporcionou, que foram essenciais no compartilhamento de conhecimento, discussões técnicas e boa companhia diária. Um agradecimento especial àqueles cujos laços fraternais se tornaram fortes e permaneceram, obrigada à Juila, Thaís, Kamila, Larissa, Renato, Gabriel e Valéria.

À minha parceira durante todo o doutorado, Mayanny, sou grata pelo compartilhamento de tanto conhecimento e por todo o carinho e paciência que tivemos uma com a outra por todo este período. Saiba que este trabalho é tão meu quanto seu.

À minha orientadora e amiga, Ana Paula, pela parceria e confiança de sempre. Obrigada pela paciência, ajuda e direcionamento durante todo o (longo) tempo de trabalho juntas.

Aos amigos da Cargill, Rodolfo, Tatiana e Flávio, pelo incentivo na reta final deste trabalho e pela amizade construída.

Aos membros da banca examinadora pela disponibilidade e considerações preciosas que certamente farão a diferença para a conclusão deste trabalho.

A todos que não foram citados, mas que participaram direta ou indiretamente deste período, agradeço de todo o meu coração.

O presente trabalho foi realizado com o apoio da Coordenação de Aperfeiçoamento de Pessoal de Nível Superior – Brasil (CAPES) – Código de financiamento 001 e do Conselho Nacional de Desenvolvimento Científico e Tecnológico (CNPq) que o fomentou através da bolsa de produtividade (Processo 303429/2018-6) concedida à orientadora Ana Paula Badan Ribeiro, e bolsa de doutorado à aluna Kamila Ramponi Rodrigues de Godoi Fernandes (Processo140789/2017-0). Agradecemos às agências de fomento pelo suporte financeiro que viabilizou a execução deste trabalho.

RESUMO

A interesterificação química é uma estratégia para fornecer propriedades físico-químicas e funcionais desejáveis para aplicação em alimentos além de favorecer a formação de cristais do tipo β' indefinidamente podendo proporcionar maior estabilidade em carreadores lipídicos nanoestruturados. Neste estudo, misturas lipídicas simples e quimicamente interesterificadas compostos por óleo de microalga totalmente hidrogenado (FHMO) e óleo de soja (SO) nas proporções (FHMO/SO): 90:10, 80:20, 70:30, 60:40 e 50:50 (p:p) foram avalidas quanto às características físico-químicas, e em função do comportamento de cristalização sob métodos rápidos e lentos. Este estudo inicial permitiu direcionar as melhores combinações de FHMO:SO para aplicação em carreadores lipídicos nanoestruturados (CLNs), que foram caracterizadas e, posteriormente, utilizados para encapsulação de óleo de peixe. Observou-se que o rearranjo dos triacilgliceróis (TAG) após a interesterificação levou a uma diminuição do TAG trissaturado e triinsaturado com um aumento concomitante dos TAGs monoinsaturados, impactando em redução nos parâmetros térmicos (teor de sólidos, ponto de fusão, tempo de indução e tamanho de cristais) e predominância dos cristais na forma β'. Os métodos de cristalização rápida e lenta indicaram que a baixa temperatura e o alto teor de tristearina podem atuar como uma semente de cristalização, acelerando o processo e tornando o sistema mais estável e denso, o que é mais acentuado para misturas simples quando comparados às misturas interesterificadas. A interesterificação, de fato, direcionou a cristalização à forma β' indefinidamente. Desta forma, seguiu-se com as proporções 90:10, 80: 20, 70:30 e 60:40 (FHMO:SO) de forma simples e interesterificada para aplicação em CLNs. Assim como na fração bulk, a maior proporção de FHMO influenciou diretamente nos parâmetros de cristalização dos CLNs, aumentando SFC, ponto de fusão e acelerando a cristalização, enquanto a reação de interesterificação influenciou na estabilidade do sistema com menor tamanho de gota e maior homogeneidade dos CNLs. As características físicas e a maior estabilidade ao longo do tempo indicaram que as proporções 70:30 e 60:40 (FHMO:SO) em frações simples ou interesterificadas têm potencial de uso como um sistema de entrega de compostos bioativos. Ao realizar a obtenção de NLCs com estas frações lipídicas já contendo óleo de peixe como composto encapsulado, observou-se que a combinação entre FHMO e SO como fase lipídica em NLCs foi adequada para o encapsulamento e que menores concentrações de FHMO e a reação de interesterificação impactam em menor resistência térmica e SFC a 25 °C, enquanto o tamanho da partícula, o PDI, o potencial zeta, a capacidade de encapsulação de óleo e índices de peróxido se mantiveram similares para todos os NLCs. Com o tempo, observou-se uma redução na estabilidade física e oxidativa de todas as partículas. Portanto, os carreadores lipídicos nanoestruturados de todas as composições aplicadas em NLCs no presente trabalho podem ser indicadas como um sistema adequado para proteger o óleo de peixe e proporcionar benefícios para aplicação em alimentos sem características de sabor e odor produzidos.

Palavras-chave: Interesterificação; Ácido Esteárico; Carreadores lipídicos nanoestruturados; Óleo de peixe.

ABSTRACT

Chemical interesterification is a strategy to provide desirable physical-chemical and functional properties for application in food. Aditionally, this reaction can favor the formation of β'-type crystals indefinitely, which can provide greater stability in nanostructured lipid carriers (NLC). In this study, simple and chemically interesterified lipid blends composed of fully hydrogenated microalgae oil (FHMO) and soybean oil (SO) in the proportions (FHMO/SO): 90:10, 80:20, 70:30, 60:40 and 50:50 (p:p) were evaluated according to physicochemical characteristics and crystallization behavior under fast and slow methods. This previous study of bulk phase allowed directing the best combinations of FHMO:SO for application in NLCs, which were characterized and subsequently used for encapsulation of fish oil. It was observed that the rearrangement of triacylglycerols (TAG) after interesterification led to a decrease in trisaturated and triunsaturated TAGs with a concomitant increase in monounsaturated TAGs, impacting a reduction in thermal parameters (SFC, melting point, induction time, crystal size) and predominance β' form crystals. The fast and slow crystallization methods indicated that low temperature and high tristearin content can act as a crystallization seed, accelerating the process and making the system more stable and dense, which is more pronounced for simple blends when compared to interesterified blends. Interesterification, in fact, direct the crystallization to the β' form indefinitely. In this way, the proportions 90:10, 80:20, 70:30 and 60:40 (FHMO:SO) were studied in a simple and interesterified blends for application in NLCs. As in the bulk fraction, the higher proportion of FHMO directly influenced the crystallization parameters of NLCs, increasing SFC, melting point and accelerating crystallization, while the interesterification reaction influenced the stability of the system with smaller droplet size and greater homogeneity of the NLCs. Physical characteristics and greater stability over time indicated that 70:30 and 60:40 (FHMO:SO) proportions in simple or interesterified fractions have potential for use as a delivery system for bioactive compounds. The NLCs obtained with these lipid fractions with fish oil as an encapsulated compound showed that the combination of FHMO and SO as a lipid phase in NLCs was adequate for encapsulation and lower concentrations of FHMO and interesterification reaction impact on lower thermal resistance and SFC at 25 °C, while particle size, PDI, zeta potential, oil encapsulation capacity and peroxide indices remained similar for all NLCs. Over time, a reduction in the physical and oxidative stability of all particles was observed. Therefore, the nanostructured lipid carriers of all composition applied in NLCs in the present work can be indicated as an adequate system to protect fish oil and provide benefits for application in foods without produced taste and odor characteristics.
Keywords: Interesterification, Stearic Acid, Nanostructured lipid carriers, Fish oil.

SUMÁRIO

1. **Introdução Geral** 15
2. **Objetivos** 18
   2.1. Objetivo geral 18
   2.2. Objetivos específicos 18
3. **Revisão bibliográfica** 19
   3.1. Lipídios 19
      3.1.1. Nanotecnologia aplicada à lipídios 20
      3.1.2. Tipos de nanopartículas lipídicas 22
   3.2. Obtenção de nanopartículas lipídicas por homogeneização a alta pressão (HAP) 24
   3.3. Propriedades gerais de NL 25
   3.4. Interesterificação lipídica 26
   3.5. Encapsulação de compostos bioativos 28
      3.5.1. Óleo de peixe 29
   3.6. Composição do CLN 30
      3.6.1. Bases lipídicas 30
      3.6.1.1. Óleo de soja 30
      3.6.1.2. Óleo de microalgas totalmente hidrogenado 31
      3.6.1.3. Emulsificante lecitina de soja 33
   3.7. Estado da arte 34

Referências 39

4. **Artigos** 46

   Artigo 1. EFFECT OF CHEMICAL INTERESTERIFICATION ON PHYSICO-CHEMICAL PROPERTIES OF SOYBEAN OIL AND FULLY HYDROGENATED MICROALGAE OIL BLENDS 46

   1. Introduction 48
   2. Material and methods 51
      2.1. Material 51
      2.2. Methods 51
      2.2.1. Preparation of simple blends 51
      2.2.2. Chemical interesterification 51
      2.2.3. Fatty acid composition 52
      2.2.4. Iodine value and saponification value 53

2.2.5. Triacylglycerol composition 53
2.2.6. Triacylglycerol regiospecific distribution 53
2.2.7. Thermal Behavior 54
2.2.8. Solid fat content (SFC) 54
2.2.9. Crystallization kinetics 54
2.2.10. Microstructure 56
2.2.11. Polymorphism 56
2.2.12. Statistical analysis 56
3. Results and discussion 56
3.1. Fatty acid composition 56
3.2. Triacylglycerol composition 59
3.3. Regioespecific distribution 64
3.4. Thermal behavior 65
3.5. Solid fat content (SFC) 71
3.6. Crystallization kinetics 78
3.7. Polymorphism 82
3.8. Microstructure 86
4. Conclusion 89
References 91
ARTIGO 2. EFFECT OF STATIC CRYSTALLIZATION PROTOCOL ON POLYMORPHISM AND MICROSTRUCTURE OF INTERESTERIFIED LIPID MATRICES RICH IN STEARIC ACID 100
1. Introduction 102
2. Material and methods 104
2.1. Material 104
2.2. Methods 104
2.2.1. Preparation of simple blends 104
2.2.1.1. Simple blend 104
2.2.1.2. Chemical interesterification 104
2.2.2. Lipid characterization 105
2.2.2.1. Fatty acid composition 105
2.2.2.2. Iodine value and saponification value 106
2.2.2.3. Triacylglycerol composition 106
2.2.2.4. Fatty acid regiospecific distribution 106
2.2.2.5. Microstructure 107
2.2.2.6. Polymorphism 107

2.2.3. Statistical analysis 107
3. Results and discussion 108
3.1. Fatty acid composition 108
3.2. Triacylglycerol composition 109
3.3. Regiospecific distribution 110
3.4 Polymorphism 112
3.5. Microstructure 120
4. Conclusion 132
References 137
ARTIGO 3. SIMPLE AND INTERESTERIFIED LIPID BLENDS FOR FORMULATING FOOD-GRADE NANOSTRUCTURED LIPID CARRIERS 144
1. Introduction 146
2. Material and methods 148
2.1. Material 148
2.2. Methods 149
2.2.1. Preparation of lipid blends 149
2.2.1.1. Preparation of simple blends 149
2.2.1.2. Preparation of chemically interesterified blends 149
2.2.2. Production of nanoparticles 150
2.2.3. Physical characteristics and stability of the nanoparticles 150
2.2.3.1. Melting behavior and recrystallization index 151
2.2.3.2. Solid fat content (SFC) 151
2.2.3.3. Polymorphism 151
2.2.3.4. Droplet size, size distribution, and polydispersity index 152
2.2.3.5. Zeta potential 152
2.2.3.6. Kinetic stability by Turbiscan measurements 153
2.2.4. Statistical analysis 154
3. Results and discussion 154
3.1. Physical characteristics of nanoparticles 154
3.1.1. Melting Behavior and Recrystallization index 154
3.1.2. Solid fat content (SFC) 159
3.1.3. Polymorphism 162
3.2. Stability of nanoparticles 165
3.2.1. Droplet size, size distribution, polydispersity index, and zeta potential 165
3.2.2. Physical stability by Turbiscan measurements 168

4. Conclusion 172
References 174
ARTIGO 4. INCORPORATION OF OMEGA-3 FATTY ACIDS IN NANOSTRUCTURED LIPID CARRIERS BASED ON SOYBEAN OIL AND FULLY HYDROGENATED MICROALGAE OIL: EFFECT OF SATURATED FATTY ACID CONTENT AND TRIACYLGLYCEROL COMPOSITION 184
1. Introduction 186
2. Material and methods 188
2.1. Material 188
2.2. Production of the lipid matrices 189
2.2.1. Simple blends 189
2.2.2. Chemically interesterified blends 189
2.3. Characterization of lipid matrices 190
2.3.1. Fatty acid composition 190
2.3.2. Triacylglycerol composition 190
2.3.3. Fatty acid regiospecific distribution 191
2.4. Production of the nanoparticles 191
2.4.1. Physical characteristics and stability of the nanoparticles 192
2.4.2. Physical characteristics of nanoparticles 192
2.4.2.1. Melting Behavior 192
2.4.2.2. Solid fat content (SFC) 192
2.5. Stability of nanoparticles 193
2.5.1. Droplet size, size distribution, and polydispersity index 193
2.5.2. Zeta potential 193
2.5.3. Kinetic stability by Turbiscan measurements 194
2.5.4. Peroxide value 195
2.5.5. Encapsulation efficiency (EE) 195
2.5.6. Statistical analysis 197
3. Results and Discussion 197
3.1. Characterization of the lipid phase 197
3.2. Physical characteristics of the nanoparticles 199
3.2.1. Melting Behavior 199
3.2.2. Solid fat content (SFC) 203
3.3. Characterization of the nanoparticles 206
3.3.1. Droplet size, size distribution, polydispersity index, and zeta potential 206

3.3.2. Physical stability by Turbiscan 212
3.3.3 Encapsulation efficiency (EE) 217
3.3.1. Oxidative state 220
4. Conclusion 222
5. **Discussão Geral** 234
6. **Conclusão geral** 244

1. Introdução Geral

Os óleos e gorduras são quimicamente reconhecidos como misturas multi-componentes de triacilgliceróis (TAGs), que são compostos por uma molécula de glicerol com ácidos graxos (AG) esterificados. Neste sentido, o tipo de AG presente no TAG pode definir as características micro e macroscópicas do material lipídico sendo que os óleos e gorduras em seu estado natural, inalterado, apresentam aplicação limitada. Assim, a técnica de interesterificação química surgiu como uma estratégia capaz de quebrar ligações ésteres entre o glicerol e os AG naturalmente presentes nas matérias-primas lipídicas, com posterior reorganização destes AG de forma aleatória, resultando em novos TAG e modificando as propriedades químicas, físicas e funcionais das gorduras.

Neste contexto, utilizando-se bases lipídicas em combinações inéditas e também avaliando-se a saudabilidade e custo dos blends, o presente estudo utilizou combinações de óleo de soja (SO), rico em ácidos graxos poli-insaturados e altamente disponível comercialmente, com óleo de microalgas totalmente hidrogenado (FHMO), considerada uma base inédita na combinação e rica em ácido esteárico, de efeito aterogênico neutro.

Estes materiais de partida foram, inicialmente, avaliados em diferentes proporções FHMO:SO (90:10, 80:20, 70:30, 60:40 e 50:50 m:m) em misturas simples e quimicamente interesterificadas com avaliações durante 60 dias em dois métodos de cristalização: cristalização rápida (5°C por 24 horas e manutenção a 25°C até os 60 dias de avaliação) e cristalização lenta (manutenção a 25°C durante todo o tempo de avaliação). Na sequência, selecionou-se as misturas com resultados mais promissores para aplicação em carreadores lipídicos nanoestruturados (NLC), considerando-se, também, o método de cristalização rápida como o mais indicado. Este direcionamento das bases ocorreu principalmente baseado na estabilidade do sistema lipídico ao longo do tempo, e ao aparecimento majoritário de cristais do tipo β', que possuem menor cristalinidade e, possivelmente, trariam maior estabilidade e capacidade de incorporação de compostos bioativos aos NLCs.

Assim, aplicou-se as misturas 90:10, 80:20, 70:30 e 60:40 (FHMO: SO m:m) de forma simples e quimicamente interesterificada como fase lipídica de NLCs compostos de água (88%), lecitina de soja enzimaticamente modificada

(2%) e lipídios (10%), obtidos por homogeneização a quente sob alta pressão. Esta aplicação visou apontar se havia diferença e qual poderia ser o benefício em utilizar maiores (ou menores) proporções de ácidos graxos saturados na fase lipídica dos NLCs, assim como discernir sobre o efeito da interesterificação química em escala nanométrica. Os NLCs produzidos foram acompanhados durante 60 dias, visualizando-se características mais promissoras nos NLCs produzidos com as frações 60:40 e 70:30 (FHMO:SO m:m).

Com isso, escolheu-se o óleo de peixe como composto bioativo para ser encapsulado, já que este óleo é rico em ácidos graxos essenciais - o teor de ácido docosaexaenoico (DHA) é de 70% - cujo consumo vem sendo apontado como decisivo para proteção à inúmeras doenças crônicas e degenerativas. Por suas características organolépticas indesejáveis, a nanoencapsulação é apontada como uma alternativa importante para viabilizar o aumento do consumo de óleo de peixe pela população. Portanto, verificou-se a capacidade de incorporação de óleo de peixe em NLCs produzidos a partir de frações lipídicas simples e interesterificadas de FHMO:SO (70:30 e 60:40 m:m) avaliando a estabilidade deste sistema durante 30 dias.

Neste sentido, conforme visualizado, o presente trabalho foi composto por etapas previamente definidas e interdependentes entre si, e divide-se da seguinte forma:

Capítulo 1. Este capítulo traz o primeiro artigo da tese e engloba os primeiros resultados sobre as frações lipídicas estudadas. Assim, as combinações de FHMO: SO (90:10, 80:20, 70:30, 80:20 e 90:10 m:m) foram obtidas de forma simples e quimicamente interesterificadas e avaliadas de acordo com a composição em ácidos graxos, composição em triacilgliceróis, distribuição regioespecífica de ácidos graxos, comportamento térmico, teor de sólidos, cinética de cristalização, polimorfismo e microestrutura.

Capítulo 2. Este capítulo apresenta o artigo com as avaliações das frações lipídicas obtidas nas mesmas proporções e condições de obtenção do Capítulo 1. Entretanto, nesta etapa os sistemas lipídicos simples e interesterificados foram cristalizados sob dois métodos: Método 1 (cristalização lenta – 25°C) e Método 2 (cristalização rápida – 24h a 5°C e depois, manutenção a 25°C). Para estas misturas, acompanhou-se as possíveis modificações e estabilidade

cristalina do sistema através de avaliações da microestrutura e do polimorfismo dos cristais durante 60 dias a 25°C.

Capítulo 3. Este capítulo inclui o artigo que inicia o estudo das nanoestruturas. Nesta etapa, as misturas mais promissoras para aplicação em NLCs são utilizadas como fração lipídica para tal. As misturas simples e quimicamente interesterificadas de FHMO: SO (m:m) nas proporções 90:10, 80:20, 70:30 e 60:40 foram aplicadas em NLCs. Estas estruturas foram avaliadas segundo o comportamento térmico, índice de recristalização, perfil de sólidos, polimorfismo, tamanho de partículas, índice de polidispersidade, potencial zeta e estabilidade da nanoemulsão por turbidimetria. As avaliações ocorreram ao longo de 60 dias a 25°C. Nesta etapa também foi realizada uma correlação direta com os capítulos anteriores ao identificar o quanto as características da fração lipídica (teor de saturados ou distribuição regioespecífica dos AGs nos TAGs) influenciam na estrutura final dos NLCs e na sua estabilidade do longo do tempo.

Capítulo 4. Último capítulo da tese, o artigo que esta contido nesta seção traz a finalização do estudo com a inclusão do composto bioativo, neste caso, o óleo de peixe, nos NLCs que foram previamente selecionados no Capítulo 3. Desta forma, os NLCs foram caracterizados quanto ao comportamento térmico, perfil de sólidos, tamanho de partícula, potencial zeta, índice de polidispersidade e estabilidade oxidativa por Turbiscan. Além destas, que já são capazes de avaliar o quanto a adição de óleo de peixe influencia nos parâmetros dos NLCs, também se avaliou a eficiência de encapsulação e a estabilidade oxidativa, já que o óleo de peixe poderia reduzir tal estabilidade ao agregar ácidos graxos poli-insaturados à nanoemulsão.

2. Objetivos

2.1. Objetivo geral

Avaliar o impacto do uso de bases lipídicas simples e interesterificadas na composição de carreadores lipídicos nanoestruturados para encapsulação de óleo de peixe.

2.2. Objetivos específicos

- Estudar as características físico-químicas e de cristalização de blends inéditos de óleo de microalgas totalmente hidrogenado e óleo de soja antes e após a reação de interesterificação;
- Avaliar o impacto da cristalização rápida (5°C/24h e, logo após, 25°C/24 horas) e lenta (25°C/24h) nos parâmetros dos blends FHMO:SO simples e interesterificados;
- Avaliar as características de cristalização, homogeneização e estabilidade de carreadores lipídicos nanoestruturados obtidos com frações lipídicas de FHMO:SO simples e interesterificadas;
- Inferir sobre a eficiência de encapsulação de óleo de peixe pelos carreadores lipídicos nanoestruturados contendo as frações lipídicas de FHMO:SO simples e interesterificadas;
- Inferir sobre o impacto do teor de ácidos graxos saturados (variação dos níveis de FHMO) e da modificação lipídica (interesterificação) nos parâmetros físico-químicos e de cristalização nos sistemas *bulk* e nos carreadores lipídicos nanoestruturados.

3. Revisão bibliográfica

3.1. Lipídios

Os lipídios correspondem a uma ampla variedade de compostos presentes ou originados por organismos vivos, incluindo ácidos graxos (AG) e seus derivados, esteroides, terpenos, carotenoides e ácidos biliares que possuem como característica comum a solubilidade em solventes orgânicos como dietil ésteres, hexano, benzeno, clorofórmio ou metanol, e insolubilidade em água (PÉREZ; LI; GUO, 2017).

É conhecido que os lipídios são nutrientes essenciais da dieta humana, apresentando papel vital mediante o fornecimento de AG essenciais e energia. Quimicamente, estes lipídios são reconhecidos como óleos e gorduras, tratando-se de misturas multi-componentes de triacilgliceróis (TAGs), que são ésteres de glicerol AG. Cada AG pode ocupar diferentes posições na molécula de glicerol (*sn-1*, *sn-2* ou *sn-3*), possibilitando uma grande diversidade de combinações. Com estas possibilidades, as propriedades físicas de óleos e gorduras também são diferenciadas: os óleos, geralmente compostos por majoritariamente de AG insaturados, encontram-se no estado líquido a temperatura ambiente; enquanto as gorduras, majoritariamente compostas por AG saturados, são sólidas a temperatura ambiente (CURI et al., 2002; O'BRIEN, 2004).

Os óleos e gorduras provêm consistência e características de fusão específicas aos produtos que os contêm. A presença de cadeias longas e saturadas aumenta o ponto de fusão dos TAGs, em razão de sua conformação linear, acarretando maior interação das moléculas e, consequentemente, permitindo melhor empacotamento das cadeias de AG. Além disso, podem atuar como meio de transferência de calor durante o processo de fritura e como carreadores de vitaminas lipossolúveis e aroma. Portanto, os lipídios afetam estrutura, estabilidade, sabor, aroma, qualidade de estocagem, características sensoriais e visuais dos alimentos. (O'BRIEN, 2004; O'KEEFE; SARNOSKI, 2017; SCRIMGEOUR, 2005).

Neste contexto, o comportamento e o controle da cristalização dos TAGs são essenciais. Durante a cristalização, a estrutura do cristal e da rede cristalina formada são determinados pelo tipo de nucleação (homogênea ou heterogênea),

taxa de resfriamento, agitação e composição da fase lipídica. A nucleação homogênea é pouco comum e ocorre sem influência de agente externo, já a heterogênea ocorre quando a nucleação é catalisada por elemento externo que atua como núcleo para a cristalização, facilitando-a. As taxas de resfriamento e agitação, influenciam no tamanho do cristal, já que um resfriamento rápido pode levar a formação de cristais menores. A composição da fase lipídica é diretamente relacionada à velocidade de cristalização, pois uma mistura heterogênea de TAGs promove cristalização de forma mais lenta do que em TAGs com comprimento de cadeia, níveis de saturação e posição dos AG semelhantes (PÉREZ; LI; GUO, 2017).

Portanto, diferentes padrões de cristalização resultam em formas cristalinas e empacotamentos moleculares distintos, o que caracteriza o polimorfismo do sistema. As principais formas polimórficas de cristais encontradas em óleos e gorduras são frequentemente denominadas de α, β’ e β, em ordem crescente de estabilidade, sendo a forma α menos estável e com menor ponto de fusão, a forma β’ de características intermediárias e a forma β é a mais estável e consequentemente, com maior temperatura de fusão (PÉREZ; LI; GUO, 2017; SATO; UENO, 2005).

Em adição às qualidades tecnológicas, do ponto de vista dietético e nutricional, os óleos e gorduras comestíveis são nutrientes essenciais da dieta humana, apresentando papel vital mediante o fornecimento de ácidos graxos essenciais e energia. Entretanto, diversos estudos têm relacionado o consumo de altas concentrações de gorduras saturadas e colesterol, com o aumento de colesterol total e da lipoproteína de baixa densidade (LDL) (SANTOS et al., 2013).

3.1.1. Nanotecnologia aplicada à lipídios

A nanotecnologia é definida como a compreensão e o controle da matéria em dimensões entre 1 e 100 nm, onde fenômenos únicos permitem novas aplicações. No campo da ciência e tecnologia de alimentos, o uso de nanotecnologia tem crescido de forma importante nos últimos anos em busca de

melhorias em produção, embalagem, shelf life e biodisponibilidade de nutrientes de forma geral (HULLA; SAHU; HAYES, 2015).

Neste contexto, o aumento na incidência de doenças relacionadas aos aspectos de alimentação como obesidade, doenças cardiovasculares, hipertensão e câncer tem levado a indústria de alimentos ao desenvolvimento contínuo de produtos com efeitos promotores da saúde, tendo os compostos funcionais como prioridade. Considera-se que, a médio e longo prazo, o enriquecimento de alimentos processados com componentes nutracêuticos, através do uso da nanotecnologia, consista em uma medida potencialmente efetiva para promoção da saúde de grandes populações (LIVNEY, 2015).

Neste sentido, os estudos de alimentos em nano-escala iniciaram-se focados no desenvolvimento de nanoemulsões, carreadores lipídicos nanoestruturados (CLN). emulsões tipo *pickering*. nanopartículas lipídicas sólidas (NLS) ou nanossuspensões constituídas de proteínas, polissacarídeos em combinações com componentes lipídicos ou minerais a fim de carrear compostos bioativos aumentando sua biodisponibilidade e seu consumo pela população (LIVNEY, 2015). Esta característica de tamanho, em combinação com a estrutura e a composição química de superfície, confere às nanopartículas características únicas de aplicação (LUYKX et al., 2008).

Na última década, as nanopartículas de natureza lipídica, ou nanopartículas lipídicas (NL) apresentaram-se como promissoras tecnologias de encapsulamento no campo de nanoestruturas. As vantagens englobam a possibilidade de produção com ingredientes naturais em escala industrial, grande diferenciação das propriedades físico-químicas das NL obtidas, além da capacidade de retenção de compostos de solubilidade bastante variável (YOON et al., 2013).

As NL são caracterizadas geralmente por dimensões entre 50 e 1000nm, mostrando-se fisiologicamente toleráveis, com estado físico sólido ou parcialmente sólido à temperatura ambiente ou corporal. Os componentes lipídicos podem compreender uma grande diversidade de moléculas, como triacilgliceróis, acilgliceróis parciais e lipídios minoritários (KAMBOJ et al., 2010).

Adicionalmente, mudanças nas propriedades físicas e funcionais dos lipídios permitem um vasto campo para o estudo de aplicação em NL, pois a cristalização de óleos e gorduras é relacionada à composição triacilglicerólica,

comportamento térmico e polimorfismo, que são características muito relevantes para incorporação de compostos bioativos e para formação das NL (YOON et al., 2013).

3.1.2. Tipos de nanopartículas lipídicas

As nanopartículas obtidas a partir de lipídios são atualmente divididas em duas categorias: nanopartículas lipídicas sólidas (NLS) e carreadores lipídicos nanoestruturados (CLN). A produção das NLS é baseada no conceito da substituição do centro aquoso de emulsões por lipídios sólidos. A primeira geração das NL foi produzida somente com matrizes lipídicas sólidas e emulsificantes e, em seguida, uma segunda geração, referente aos CLN. foi desenvolvida utilizando-se sistemas lipídicos sólidos, líquidos e emulsificantes (Figura 1) (BAGUL et al., 2018; BELOQUI et al., 2016; MÜLLER et al., 2016; POONIA et al., 2016; SOUTO et al., 2011).

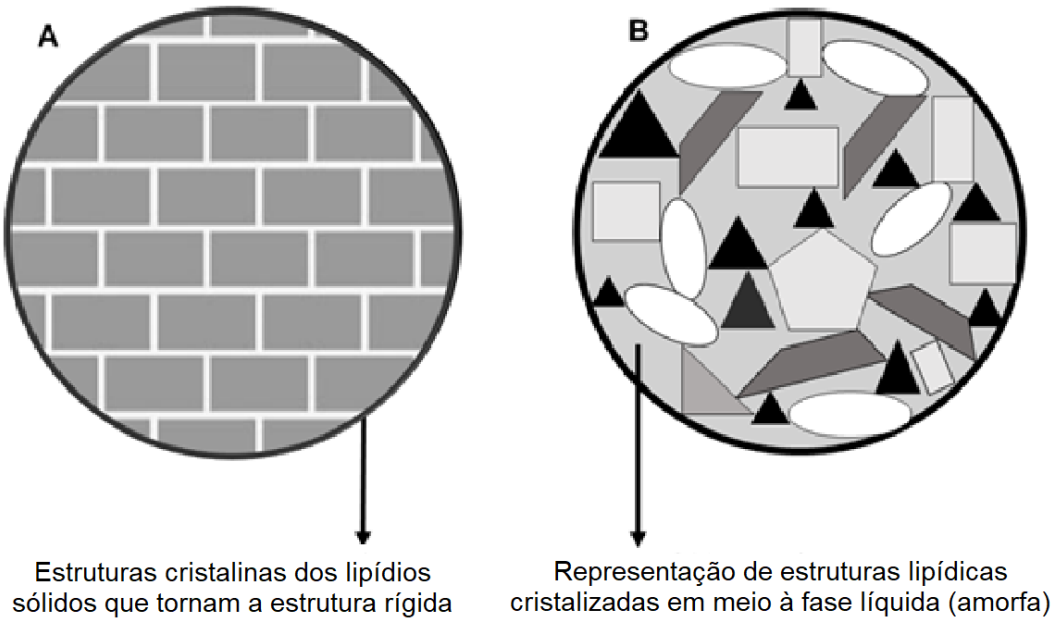

Figura 1. Representação esquemática de: A) Nanopartículas lipídicas sólidas (NLS); B) Carreadores lipídicos nanoestruturados (CLN).

As NLS e CLN são constituídas de fase lipídica, emulsificantes e água. As NLS são formadas por lipídios sólidos, ou seja, de alto ponto de fusão, enquanto os CLN possuem lipídios sólidos misturados com lipídios líquidos. Desta forma,

as NLS são geralmente compostas de 0,1% a 30% (m:m) de lipídios sólidos dispersos em meio aquoso estabilizados com emulsificantes na concentração de 0,5% a 5% (m:m) (ANTON et al., 2008; TAMJIDI et al., 2013).

Já os CLN, considerados a segunda geração de nanopartículas lipídicas, surgiram com o intuito de produzir uma matriz lipídica menos estruturada em relação à cristalinidade através do uso combinado de frações lipídicas sólidas e líquidas, capaz de obter melhor eficiência de encapsulação e evitar a liberação dos compostos incorporados durante a estocagem (KATOUZIAN et al., 2017; MÜLLER et al., 2016). As misturas utilizadas, no entanto, devem apresentar ponto de fusão superior à temperatura corporal, menor velocidade das transições polimórficas, bem como menor grau de cristalinidade, propriedades associadas à existência de domínios lipídicos líquidos no centro das partículas (MÜLLER et al., 2016; TAMJIDI et al., 2013). Com isso, para os CLN, o percentual de lipídios na formulação pode variar de 5 a 15% (m/m), com aproximadamente 95% (m:m) de fase aquosa, também estabilizados com emulsificantes nas proporções de 5 a 15% (BENOIT et al., 2016; PURI et al., 2009).

Do ponto de vista tecnológico, os CLNs podem aumentar a solubilidade dos compostos nutracêuticos tornando-os mais eficientes e reduzindo sua influência na aparência e características sensoriais dos produtos finais, como as bebidas, por exemplo.

Comparando-se as NLS e CLN em relação ao tamanho de partícula, os CLN são consideravelmente menores que as de NLS quando preparados com o mesmo procedimento, tipos e concentrações de emulsificantes e quantidade total de lipídios (FANG et al., 2008). Já em relação à estabilidade das partículas, estudos mostraram estabilidade física adequada por até 6 meses, mantendo-se o tamanho de partícula tanto para os NLS e quanto para os CLN (ELNAGGAR et al., 2011). Segundo Babazadeh et al. (2016), obtendo-se CLNs a partir de homogeneizador de alto cisalhamento e ultrassom para encapsulação de rutina, o tamanho de partícula se manteve estável ao longo do tempo (1, 15 e 45 dias) com 15nm para os CLNs sem composto bioativo e de 77 a 96 nm nos CLN com composto.

Com tais características, os CLN são capazes de aumentar a eficiência de encapsulação dos compostos bioativos, além de garantir a estabilidade química, biodisponibilidade e controle na liberação de compostos lipofílicos funcionais.

Portanto, os CLN são promissores como sistema de entrega em produtos alimentícios (MCCLEMENTS; JAFARI, 2018; TAMJIDI et al., 2013).

3.2. Obtenção de nanopartículas lipídicas por homogeneização a alta pressão (HAP)

Dentre os possíveis métodos utilizados para obtenção de NL, a homogeneização a alta pressão (HAP) consiste na técnica de maior potencial para preparação, uma vez que homogeneizadores de diferentes capacidades se encontram comercialmente disponíveis, sem dificuldades de transposição de escala e permite trabalhar em condições assépticas, o que caracteriza o método como altamente versátil e vantajoso (PARK et al., 2016). A técnica HAP é caracterizada pelo uso de pressão variável entre 100 e 2000 bar, em que forças de cisalhamento e cavitação rompem as partículas em escala nanométrica (MEHNERT e MÄDER, 2012). Para homogeneidade do sistema, toda a dispersão deve ser sujeita à mesma intensidade de energia, o que é possível com a HAP pela aplicação da mesma tensão de corte devido às dimensões reduzidas do orifício de saída do homogeneizador, geralmente inferior a 30µm (SOUTO et al., 2011).

O processo escolhido para o desenvolvimento deste trabalho, foi a técnica HAP a quente, que consiste no preparo de uma pré-emulsão com as matérias-primas lipídicas totalmente fundidas misturadas à água contendo emulsificante sob homogeneização de alta velocidade. Em seguida, esta pré-emulsão obtida é submetida à HAP, dando origem à nanoemulsão do tipo óleo/água (GUPTA et al., 2017; SOUTO et al., 2011). A etapa de homogeneização pode ser realizada em diferentes ciclos e diferentes pressões; em geral, de 2 a 5 ciclos, sob pressão de 500-1500 bar são suficientes (JAFARI et al., 2007). Estudo de Park et al. (2016) verificou que dois ou três ciclos de passagem pelo HAP é capaz de tornar mais homogêneo o tamanho das partículas e produzir CLN estáveis.

Considera-se que as características físico-químicas das NL obtidas por HAP sejam afetadas por um conjunto de parâmetros que incluem solubilidade do componente encapsulado, polimorfismo da matriz lipídica, natureza e concentração da fase lipídica e emulsificantes, temperatura de processo, força

de cisalhamento e número de ciclos de homogeneização efetuados (SOUTO et al.. 2011).

3.3. Propriedades gerais de NL

Após a obtenção, é de grande importância caracterizar as NL produzidas segundo suas propriedades físico-químicas, como o tamanho das partículas, ponto de fusão, potencial zeta, cristalinidade, polimorfismo e microestrutura (MCCLEMENTS, 2016).

O tamanho das nanopartículas é um dos fatores mais importantes, visto que pode influenciar suas propriedades físico-químicas e funcionais como propriedades ópticas, estabilidade, características de liberação e destino biológico (MCCLEMENTS; MCCLEMENTS, 2016).

Em relação ao ponto de fusão, considera-se que as dispersões coloidais podem apresentar ponto de fusão aproximadamente entre 5 a 20°C abaixo da temperatura do material lipídico em sua forma pura, assim como este parâmetro diminui com a diminuição do tamanho de partícula das nanoestruturas (KOVAČEVIĆ et al.. 2014).

O potencial zeta – PZ (potencial elétrico na superfície hidrodinâmica de corte em torno das partículas coloidais) é geralmente determinado como parâmetro característico para a carga de NL. A determinação do PZ tem sido principalmente empregada para informações sobre a estabilidade de formulações durante a estocagem ou instabilidade quando da interação com eletrólitos, permitindo importantes ajustes de formulação, determinação da estabilidade e das interações das NL com os diferentes compostos de inclusão, principalmente durante o período de estocagem (BUNJES e UNRUH, 2007).

O grau de cristalinidade e modificações polimórficas dos lipídios de composição dos CLN representam fatores fundamentais para o seu desenvolvimento, uma vez que estes parâmetros são fortemente correlacionados com a capacidade de incorporação de princípios ativos e taxas de liberação. Em geral, observa-se declínio na capacidade de manutenção dos ativos encapsulados conforme a sequência de transições polimórficas para as formas cristalinas de maior estabilidade (KATOUZIAN et al., 2017; MEHNERT; MÄDER, 2012; MÜLLER et al., 2016; TAMJIDI et al., 2013).

A morfologia das NL mostra-se bastante variável. Partículas esféricas oferecem maior potencial para liberação controlada e proteção de compostos bioativos, com vias de difusão mais longas e menor contato com meio aquoso. Além disso, requerem menor quantidade de emulsificante para sua estabilização devido à minimização da área superficial específica. Destaca-se que a ultraestrutura das NL deve ser considerada em estudos de obtenção devido às propriedades de incorporação e liberação de ativos (YOON et al., 2013).

Por fim, as propriedades de eficiência de encapsulação (EE) e capacidade de carga (CC) são definidas respectivamente, como: razão entre a fração do princípio encapsulado nas NL e o total do princípio incorporado à fase lipídica inicial (LIU e WU, 2010) e a razão do princípio ativo encapsulado em relação à fase lipídica inicial. O parâmetro pode ser determinado após quantificação da fração livre ou encapsulada do componente de interesse (NGUYEN et al., 2012), influenciando nas propriedades de liberação das NL (TAMJIDI et al., 2013), enquanto a CC mostra-se predominantemente influenciado pelo hábito polimórfico preferencial do sistema lipídico utilizado, pela solubilidade do composto encapsulado na matriz lipídica no estado líquido, e pela estrutura física da NL (NGUYEN et al., 2012). A manutenção destes parâmetros reside, principalmente, no desenvolvimento de estratégias para prevenção de modificações cristalinas durante a estocagem. Além do controle das transições entre as formas α, β' e β. Diversas sub-formas e suas interações com os diferentes emulsificantes devem ser consideradas no estudo de estabilidade das NL (MEHNERT e MADER, 2012; SOUTO et al., 2011).

3.4. Interesterificação lipídica

A interesterificação consiste na troca de posição dos ácidos graxos na molécula de glicerol formando novas estruturas triacilglicerólicas. Existem dois tipos de interesterificação: a química e a enzimática. No processo enzimático, biocatalisadores, tais como lipases microbianas, são utilizados para promover a migração acila seletiva nas moléculas glicerídicas. Na interesterificação química, que é utilizada neste trabalho, a reação é randômica e entropicamente dirigida até que o equilíbrio termodinâmico seja alcançado. O processo envolve a quebra simultânea de ligações ésteres existentes e formação de novas ligações nas

moléculas glicerídicas com o uso de catalisador, de forma aleatória. Esta modificação lipídica é capaz de alterar a composição química dos lipídios, resultando em mudanças nas propriedades físicas dos óleos e gorduras, como o comportamento térmico e de cristalização, ampliando o potencial de aplicação de matérias-primas ou misturas lipídicas (MARANGONI e ROSSEAU, 2002; O'BRIEN, 2009b; RIBEIRO et al., 2013).

A interesterificação química de misturas de *hardfats* com óleos líquidos representa a opção de maior versatilidade para produção de bases lipídicas com propriedades físico-químicas diferenciadas, face à diversidade de composição dos materiais de partida, resultando em matrizes lipídicas com desempenho compatível com aplicações em alimentos. Isso porque o polimorfo característico de uma gordura ou base oleosa dependente da distribuição dos AG nas moléculas de triacilglicerol, sendo o grau de randomização particularmente importante. Gorduras com baixa variabilidade de TAGs transformam-se rapidamente na forma estável β. Gorduras que consistem em distribuição randômica de TAGs podem apresentar a forma β' indefinidamente. Desta forma, o processo de interesterificação consiste em importante meio para estabilização da forma β'(RIBEIRO et al., 2009; 2010).

O primeiro estudo envolvendo o processo de interesterificação para aplicação em NL, datado de 2012, apontou as gorduras interesterificadas como diferenciadas quanto às propriedades de cristalização e polimorfismo preferencial devido à reorganização molecular e formação de classes e espécies triacilglicerólicas específicas com boa aplicabilidade (HOLSER, 2012).

De forma bastante recente, Reis et al. (2020) estudaram o comportamento do óleo de buriti enzimaticamente interesterificado em NLCs e observaram que a reação reduziu o teor de triacilgliceróis trissaturados e afetou as propriedades físico-químicas das partículas resultando em menor tamanho de partícula, alta estabilidade e alta capacidade antioxidante com potencial para aplicações nutricionais e biológicas.

SILVA et al. (2022), ao produzir CLNs a partir de fases lipídicas interesterificadas e apenas misturadas compostas de óleo de soja como lipídio líquido e óleos totalmente hidrogenados de palma, soja, microalgas e crambe como lipídios sólidos, observaram que as nanoestruturas foram influenciadas pela interesterificação química e pela composição do lipídio sólido utilizado,

principalmente em relação ao tamanho da cadeia de ácidos graxos. A interesterificação resultou em menores tamanhos de partícula e reduziu a temperatura de fusão, indicando cristalinidade diminuída e uma estrutura menos organizada favorecendo os cristais na forma β', o que é uma característica positiva para a incorporação de compostos bioativos.

Assim, os sistemas desenvolvidos no presente estudo são considerados bastante atuais e inovadores, principalmente no que diz respeito à composição dos NLCs, e apresentam bom potencial para aplicações alimentícias. Com isso, reforçamos que o emprego de frações lipídicas modificadas por interesterificação química em NL é uma abordagem promissora.

3.5. Encapsulação de compostos bioativos

Naturalmente, os fitoquímicos naturais podem estar presentes em inúmeros alimentos, contudo, seu consumo e absorção podem ser prejudicados por diversos fatores. Como alternativa, estes fitoquímicos podem ser isolados de sua origem natural e convertidos em ingredientes funcionais para incorporação em alimentos, suplementos ou produtos farmacêuticos, que tem sido objeto de pesquisas na atualidade para promoção de saúde e bem-estar (MCCLEMENTS, 2020).

Tal incorporação pode melhorar significativamente os aspectos sensoriais e nutricionais, além de aumentar a vida útil de alimentos e bebidas. Entretanto, o enriquecimento é considerado um desafio, visto que muitos compostos bioativos se associam firmemente à matriz alimentar ou são altamente lipofílicos, resultando em baixa absorção e biodisponibilidade limitada, além de serem quimicamente instáveis (DAN, 2016; WEISS et al., 2008).

Estudos dos últimos 10 anos apontam que os sistemas de encapsulação são capazes de superar problemas associados à absorção intestinal lenta e reduzida e à instabilidade termodinâmica. Comparando-se as nanoemulsões em NLS e CLN (MEHNERT e MADER, 2012) estas podem variar, principalmente, em função da estabilidade oxidativa (TIKEKAR e NITIN, 2011) e liberação controlada dos compostos (MEHNERT e MADER, 2012).

3.5.1. Óleo de peixe

O óleo de peixe é reconhecido pelos níveis elevados de ácidos graxos poliinsaturados de cadeia longa, incluindo ácido eicosapentaenóico (EPA; 20: 5n-3), ácido docosahexaenóico (DHA; 22: 6n-3) e ácido alfa-linolênico ou ALA (18:3n-3), considerados os principais representantes da família do ômega-3 de origem marinha e essenciais aos mamíferos (FARD et al., 2019).

O teor dos ácidos graxos poli-insaturados presentes no óleo de peixe é variável. A significância destes teores reside em sua importância biológica, visto que a presença e o consequente consumo de EPA e DHA está associada a diversos efeitos metabólicos e fisiológicos, como a redução do risco de doenças cardiovasculares através da diminuição dos níveis séricos de triglicérides, LDL colesterol e colesterol total, controle da pressão sanguínea, contribuição para o sistema de coagulação e prevenção de câncer e doenças degenerativas (KRIS-ETHERTON; GRIEGER; ETHERTON, 2009). Na fase gestacional, a ingestão adequada especialmente de DHA, é imprescindível devido à transferência deste ácido graxo da mãe para o feto e atuação direta no desenvolvimento do cérebro e retina. Além do mais, o DHA tem demonstrado evitar casos de prematuridade ao atuar como um anti-inflamatório e como fator protetivo para o sistema imune e cognitivo (SWANSON; BLOCK; MOUSA, 2012).

Devido aos citados efeitos benéficos, diversas agências e organizações de saúde ao redor do mundo tem recomendado o consumo adequado de ácidos graxos ômega 3, principalmente EPA e DHA. Segundo a Organização das Nações Unidas (ONU), este consumo deve alcançar 250 mg/dia de EPA e DHA para homens e mulheres adultas, enquanto a American Heart Association (AHA) recomenda cerca de 1g/dia de EPA e DHA para pacientes com doença coronariana e 2 a 4g/dia para pacientes que requerem redução dos níveis séricos de triglicérides (KRIS-ETHERTON; GRIEGER; ETHERTON, 2009). Com isso, nota-se que, apesar dos benefícios comprovados, ainda há dualidade em relação à recomendação destes ácidos graxos para o efeito funcional. No Brasil, a ANVISA possui recomendação diária de ingestão de ômega-3 apenas para suplementos alimentares indicando que quantidades abaixo de 100mg/porção não exercem os efeitos desejados (BRASIL, 2014).

O consumo de peixes no Brasil e no mundo, apesar de ter apresentado aumento nos últimos anos, é considerado insuficiente para assegurar a funcionalidade biológica associada aos ácidos graxos poli-insaturados ômega 3 (INSTITUTO BRASILEIRO DE GEOGRAFIA E ESTATISTICA, 2019). Em contrapartida, a incorporação de dosagens maiores que 100mg/porção apresenta limitações tecnológicas e sensoriais levando à baixa aceitação dos produtos. É importante destacar que, além do odor e sabor peculiares e desagradáveis, os ácidos graxos poli-insaturados presentes no óleo de peixe são altamente instáveis e sensíveis à oxidação lipídica sob condições normais. Além disso, a oxidação destes ácidos graxos está associada à liberação de moléculas voláteis que prejudicam o aroma e sabor do óleo, assim como produzem componentes tóxicos à saúde humana, como os radicais livres (GHORBANZADE et al., 2017; KHOSHNOUDI-NIA; FORGHANI; JAFARI, 2020).

Neste sentido, a encapsulação do óleo de peixe vem sendo apontada já há alguns anos como uma alternativa em potencial para fornecer ao consumidor alimentos estáveis, funcionais, seguros e com características sensoriais agradáveis (DRUSCH et al., 2006; KHOSHNOUDI-NIA; FORGHANI; JAFARI, 2022).

3.6. Composição do CLN

3.6.1. Bases lipídicas

3.6.1.1. Óleo de soja

A soja (*Glycina máxima)* é a principal oleaginosa produzida no mundo devido às suas características agronômicas e sua aplicabilidade, visto que é uma leguminosa com altas concentrações de proteína, obtendo-se o óleo como importante co-produto (FAGERIA et al., 2010).

O óleo de soja é caracterizado por altas concentrações de ácidos graxos insaturados (80-90%) como o ácido linoleico (aproximadamente 55%) que pertence à classe de ácidos graxos ômega 6 e, em menor quantidade, pelo ácido linolênico (aproximadamente 7%), que pertence à categoria ômega 3. Comparando-se com outros óleos ricos nestes mesmos ácidos graxos como algodão, milho e girassol, a soja mostra-se como uma importante alternativa de obtenção de óleo rico em ácidos graxos essenciais com diversas vantagens

competitivas no aspecto econômico. O óleo de soja possui custo mais baixo do que óleos de girassol, cártamo e milho com elevada disponibilidade mundial, ampla faixa de temperatura com característica líquida, além de características nutricionais desejáveis ao consumo (ASBRIDGE, 2015; HAMMOND et al., 2005).

O uso de óleo de soja é indicado para produção de *shortenings* e produtos de base lipídica que requeiram a forma polimórfica preferencial β – cristais quebradiços usados em massa folhada, por exemplo - e possui características interessantes para desenvolvimento de formulações lipídicas com redução de ácidos graxos saturados (DEMODARAN et al., 2010).

3.6.1.2. Óleo de microalgas totalmente hidrogenado

As algas microscópicas ou microalgas e os seus extratos são utilizados desde o início do século XX. Com isso, no decorrer dos anos, a indústria buscou avançar na tecnologia de obtenção e extração de diversos componentes das microalgas a fim de comercializar e ampliar suas aplicações, incluindo alimentos, suplementos, alimentos para animais e aquicultura, bem como cosméticos e biocombustíveis (KURATKO AND SALEM, 2013). As microalgas são as fontes primárias de vida marinha, fornecendo inclusive os ácidos graxos essenciais bioacumulados nos peixes. No entanto, semelhante ao óleo de peixe, os ácidos graxos ômega-3 do óleo de microalgas são altamente instáveis à oxidação quando são expostos ao oxigênio, calor, luz e certas substâncias, como os íons metálicos (O'BRIEN, 2009a).

O rendimento de óleo extraído de microalgas pode variar de acordo com a espécie, visto que estes organismos são capazes de alterar seu metabolismo conforme mudanças na composição química do meio de cultura, podendo conter entre 15-75 % de lipídios a partir de seu peso seco, dependendo da forma de cultivo (COHEN et al., 1995). A extração do óleo de microalgas pode ser realizada por processos como prensagem mecânica, extração por solventes, fluídos supercríticos ou centrifugação. Logo após a extração, o óleo deve ser processado rapidamente, visto que sua composição favorece reações oxidativas e carreia um odor característico, portanto, o óleo deve ser refinado, branqueado e desodorizado (O'BRIEN, 2009a).

Ao final, a composição em ácidos graxos dos óleos extraídos de microalgas pode variar de espécie para espécie e é dependente do método de extração, porém, há uma faixa padrão para os ácidos graxos presentes, sendo constituídos majoritariamente de ácidos graxos insaturados como o palmitoleico, oleico, linoleico e linolênico, seguido pelos ácidos graxos saturados palmítico, esteárico e mirístico, em pequenas quantidades (13,6-58,9%), com média de 25%; dentre os monoinsaturados, a variação pode ser de 2,1 – 46,1% com média de 25%, distribuído principalmente em ácido palmitoleico (cerca de 0,5 – 44,8%) e ácido oleico (0,1% a 35,5%); dentre os ácidos graxos poli-insaturados, o ácido linolênico pode estar presente em teores entre 0,1 – 24,3% sendo que os ácidos linoleico e linolênico são predominantes em quase todas as espécies de microalgas (BASOVA, 2005; O'BRIEN, 2009a).

No estudo de Nascimento et al. (2013) avaliou-se a composição em ácidos graxos de óleos advindos de diversos tipos de microalgas. Dentre eles, o óleo de *Botrycoccus braunii*. apresentou cerca de 77% de ácido oleico, ácido margárico (2,65%), palmítico (7,17%) e ainda proporções de ácidos linoleico (5,16%) e linolênico (5,34%). Estas proporções, no entanto, não foram as mesmas observadas por outros autores, pois pode haver uma diversidade de linhagens e condições de cultivo das microalgas, o que torna sua identificação específica ainda mais dificultada.

Dentre as modificações possíveis em óleos comestíveis como o óleo de microalgas, a hidrogenação é realizada com o intuito de modificar a composição, estrutura e consistência de um óleo. Seu resultado é a redução do grau de insaturação do óleo e aumento de seu ponto de fusão, associado ao aumento da estabilidade oxidativa e funcionalidade das frações semi-sólidas produzidas (RIBEIRO et al., 2007).

A hidrogenação parcial modifica a plasticidade da base lipídica e gera ácidos graxos *trans*. Trata-se de uma reação exotérmica, irreversível, que envolve três fases distintas: sólida (fase com catalisador), líquida (fase oleosa) e gasosa (ação do hidrogênio). A reação ocorre dentro dos sítios ativos do catalisador, normalmente o níquel, onde o hidrogênio gasoso entra em contato com as duplas ligações dos ácidos graxos insaturados presentes no óleo ou gordura dando origem a reações de saturação ou isomerização. As duplas ligações podem ser reposicionadas (isomerização de posição) ou modificadas

da configuração *cis* para uma forma termodinamicamente mais estável pelo mecanismo de *trans*-isomerização (GHOTRA et al., 2002). Já a hidrogenação total, realizada para obtenção dos *hardfats*, elimina todas as duplas ligações de ácidos graxos insaturados, permitindo o uso destes materiais como aditivos de cristalização em óleos vegetais capazes de alterar o hábito polimórfico e o comportamento de cristalização da matriz lipídica (OLIVEIRA et al.. 2015).

A hidrogenação total do óleo de microalgas, devido a sua composição supracitada, possibilita a obtenção de uma versão totalmente hidrogenada com composição em ácidos graxos majoritária de ácido esteárico (C18:0 – 90,88%) seguido por ácido palmítico (C16:0 – 6,22%), apontado como um método de obtenção de baixo custo e alta eficiência para produção de fontes lipídicas ricas em ácido esteárico, visto que triestearina (grau técnico), por exemplo, possui cerca de 65% de ácido esteárico e alto custo, com possibilidade de presença de ácido elaídico (C18:1 *trans*) (OLIVEIRA et al., 2011; RIBEIRO et al., 2013a).

Em particular, teor expressivo de ácido esteárico no *hardfat* mostra-se favorável ao uso destes componentes em NL devido ao efeito aterogênico neutro associado a este ácido graxo, que não apresenta efeito adverso sobre o risco de doenças cardiovasculares (VALENZUELA et al. 2011).

3.6.1.3. Emulsificante lecitina de soja

A lecitina de soja pode ser definida como um subproduto do processamento do óleo, caracterizado por uma mistura complexa de fosfolipídios e triacilgliceróis. A lecitina obtida a partir da soja corresponde à maior parte da lecitina comercial. O teor e a distribuição dos fosfolipídios garantem a propriedade emulsificante da lecitina sendo que, para soja, a composição majoritária é de fosfatidilcolina (PC) (13% - 18%), seguida por fosfatidiletanolamina (PE) (10% -15%), fosfatidilinositol (PI) (10% -15%) e ácido fosfatídico (PA) (5% -12) (CHIPLUNKAR e PRATAP, 2017).

A lecitina de soja é amplamente utilizada nas indústrias alimentícia e farmacêutica como agente anti-salpicante em margarinas, anti-espumante em lubrificantes e em diversos produtos como emulsificante (CHIPLUNKAR e PRATAP, 2017).

A lecitina de soja modificada enzimaticamente, proposta para o desenvolvimento deste trabalho, é requerida devido ao aumento na capacidade emulsificante em emulsões do tipo óleo em água através da hidrólise parcial das ligações ésteres pelo uso da enzima fosfolipase, que remove os grupos acila da posição sn-2 dos fosfolipídios aumentando a razão de lisofosfolipídios/fosfolipídios (WENDEL AND STAFF, 1995).

3.7. Estado da arte

O uso de NLS e CLN para carreamento de compostos funcionais ou bioativos revela-se como um dos mais importantes assuntos para a tecnologia de alimentos, visando a entrega, liberação controlada e proteção destes componentes durante o processamento industrial. Devido às dimensões nanométricas estes sistemas podem aumentar a solubilidade e biodisponibilidade dos compostos de inclusão, além de prevenir reações químicas indesejáveis e controlar a liberação, especialmente daqueles componentes caracterizados por baixa solubilidade em matrizes aquosas. Adicionalmente, a influência das interações físico-químicas entre materiais em nanoescala pode superar alguns problemas típicos que caracterizam o uso de sistemas em macro e microescala para entrega de compostos bioativos, tais como a compatibilidade com a matriz alimentar, efeitos de agregação e separação de fases; e a perda de atividade funcional, em função da exposição à luz e ao oxigênio (DAN, 2016). Os principais compostos funcionais lipofílicos referem-se aos carotenoides, antioxidantes lipossolúveis (tocoferóis e polifenóis), vitaminas lipossolúveis e fitoesteróis (Tamjidi et al., 2013; Livney, 2015). Desta forma, a utilização de nanoestruturas mostra-se uma alternativa promissora e diferenciada para o carreamento e proteção destes compostos em sistemas alimentícios (MOZAFARI. et al., 2006; WEISS et al., 2006). Para atingir características desejáveis, inúmeras composições têm sido estudadas quanto às propriedades de proteção e liberação de compostos bioativos.

Na busca por materiais inéditos para constituição de NLS, Shtay et al. (2018) utilizaram 5% (m:m) manteiga de cacau como fase lipídica, misturas de 1,5% de emulsificantes (lactato estoroil-2 de sódio, monoglicerídeos e triacilgliceróis) e a HAP como técnica de preparo a 1000bar. Ao longo de 3 meses

de armazenamento, as NLS mostraram-se pequenas (cerca de 112,7nm) e estáveis.

Witayaudom e Klinkesorn (2017), além de avaliarem uma matriz inédita na obtenção de CLNs, o óleo do caroço do fruto rambutan (*Nephelium lappaceum L*.), também verificaram o efeito de diferentes concentrações de Tween 80 como emulsificante e a temperatura de cristalização (5 e 25°C) na estabilidade dos CNLs. Como resultado, verificaram que um aumento na concentração do emulsificante levou à diminuição do potencial zeta e do tamanho de partícula, porém sem efeito no índice de polidispersidade, enquanto a temperatura de solidificação afetou a microestrutura, o comportamento de fusão e a estabilidade dos CLNs, sendo que a condição de cristalização inicial a 5°C resultou em CLNs mais estáveis e monodispersos.

Matérias-primas de origem animal também vem sendo testadas nos últimos anos. Queirós et al. (2020) obtiveram nanoemulsões de gordura do leite produzidas por HAP a quente e estabilizada por proteínas de soro de leite isoladas (pH 4,0 ou 7,0) ou caseinato de sódio (NaCas pH 7,0) avaliados por 60 dias de armazenamento a 25° C. Nestas condições, os autores observaram que partículas menores e distribuição mais homogênea foram obtidas com uso de caseinato de sódio e pH 7,0, resultando em um sistema emulsionado estável ao longo de todo o tempo de avaliação. O sistema foi considerado adequado para entrega de compostos bioativos e melhoria das propriedades sensoriais de alimentos gordurosos.

Além de novos materiais de obtenção, diversos compostos bioativos, cuja incorporação ou biodisponibilidade é limitada, vem sendo estudados para serem encapsulados em nanoestruturas lipídicas. A luteína, composto bioativo de baixa solubilidade muito usado para aplicação dérmica, dificilmente consegue ser incorporado em produtos para este fim. Desta forma, buscou-se encapsular a luteína em CLN (9% de lipídios sólidos e líquidos misturados: tripalmitato de glicerila, cetil palmitato, cera de carnaúba, triacilglicerol caprílico) ou NLS (frações sólidas dos lipídios citados) produzidas por HAP a quente, apresentaram tamanho médio das partículas de 150 a 350nm, potencial zeta de 40 a 63mV, com boa estabilidade em um mês de armazenamento. Os CLN apresentaram capacidade de proteção superior às NLS, pois impediram a

degradação da luteína quando exposta a radiação UV além de aumentar em 19% a absorção dérmica.

O α-tocoferol é um composto lipossolúvel com funções antioxidantes que faz parte do grupo de moléculas denominadas coletivamente de vitamina E. Por causa de sua afinidade por lipídios, o alfa-tocoferol está presente no tecido adiposo, nas lipoproteínas circulantes e nas membranas celulares, protegendo os ácidos graxos poli-insaturados da peroxidação lipídica sendo essencial, principalmente, nas primeiras fases da vida (DA MATA et al., 2020). Contudo, este composto é altamente sensível à presença de oxigênio, pH e temperatura, sofrendo degradação durante o processamento e armazenamento de alimentos, bem como pelo transporte através do sistema digestivo (LIANG et al., 2010). Visando a proteção de α-tocoferol, Pinto, Barros e Fonseca (2018) obtiveram CLNs a partir de óleos vegetais diversos, obtendo-se estabilidade física considerada adequada com o uso de óleo de girassol, amêndoa doce, oliva e coco. Tal estabilidade foi avaliada segundo o tamanho de partícula (de 240–315 nm) e o potencial zeta (variando entre -45,6 a -55,1 mV). Adicionalmente, os pesquisadores conseguiram, através da nano encapsulação, manter 79,4% do composto bioativo aprisionado, com liberação efetuada de forma controlada.

Os polifenóis, de maneira geral, são muito conhecidos pelos seus benefícios na prevenção de diversas doenças, sendo utilizados como alimento ou nas indústrias cosmética e farmacêutica. Contudo, várias condições ambientais como a luz, temperatura e oxigênio, podem afetar a estabilidade físico-química dos polifenóis, comprometendo sua bioatividade. Para superar estas limitações, a nanoencpsulação tem sido vista como uma alternativa importante (PIMENTEL-MORAL et al., 2018).

Estudando-se a incorporação de epigalocatequina-galato (EGCG) em nanopartículas, Park et al. (2016) obtiveram CLN a partir de homogeneização a alta pressão a quente (aproximadamente 700bar, 3 ciclos) utilizando-se alginato e quitosana (0,01% de cada). Como resultados, observaram que houve alta eficiência de encapsulação e preservação da atividade antioxidante do composto, com tamanhos de partícula próximo a 200nm, potencial zeta próximo a 30mV sendo que a incorporação do composto contribuiu para o aumento destes parâmetros.

Matos-Jr et al. (2017) estudaram NL constituídas de óleo de palma totalmente hidrogenado e óleo de palmiste interesterificados e lecitina de soja como emulsificante para incorporação de ácido ascórbico. As partículas foram obtidas de 5 maneiras distintas: 1) Emulsão com proporção de material ativo: veículo de 1: 7 a uma velocidade de homogeneização de 5000 rpm; 2) Emulsão com a proporção de 1:10 e a velocidade de homogeneização de 5000 rpm; 3) emulsão com proporção de 1: 7 a uma velocidade de homogeneização de 10.000 rpm; 4) Emulsão com proporção de 1:10 com velocidade de 10.000 rpm; 5) Dispersão com a proporção de 1:10. Desta forma. os pesquisadores observaram que as metodologias de obtenção 1 a 4 não apresentaram diferenças significativas para as análises de eficiência de encapsulação, tamanho de partícula e atividade de água enquanto a dispersão apresentou resultado inferior para eficiência de encapsulação e atividade de água com maior tamanho de partícula, o que indica que a dispersão foi mais eficaz em manter a estabilidade do ácido ascórbico.

A curcumina é outro composto bastante visado para nanoencapsulação. Para tanto, Ma et al. (2017) avaliaram o efeito de diferentes tipos de óleo (triacilgliceróis de cadeia média, óleo de canola e óleo de linhaça), diferentes tratamentos (aquecimento, ultrassom e micro-ondas), emulsificantes tween-80, lecitina, isolado proteico do soro de leite e acácia. Com isso, a curcumina apresentou maior solubilidade em triacilgliceróis de cadeia média e, enquanto o tamanho de partícula foi correlacionado com a concentração da fase oleosa, aumentando conforme a concentração também aumentava. O tipo de óleo e concentração não foram significativos para o potencial zeta, mas favoreceram o aumento do tamanho de partícula ao longo do tempo e aumento da decomposição da curcumina. Os CLNs contendo triacilgliceróis de cadeia média foram mais estáveis em função do tempo.

Visando-se o uso de compostos hipocolesterolêmicos, o estudo de Soleimanian et al. (2018) objetivou a encapsulação de β sitosterol em CLNs formuladas por cera de própolis pura ou misturas de cera com gliceril-beenato (10% m:m) em diversas proporções, contendo lecitina e tween-80 (6% m:m) como emulsificantes e obtidos por homogeneização a alto cisalhamento (1400rpm por 10 minutos) seguida por ultrassom (8 minutos). Estas condições resultaram em tamanho de partícula de 80 a 150nm, sendo que, quanto maior o

teor de cera, maior o tamanho de partícula. O uso de β sitosterol, no entanto, apresentou efeito contrário. O CLN, segundo análise de microscopia eletrônica de transmissão, apresentou superfície esférica e lisa.

Outro trabalho objetivando o desenvolvimento de CLNs com fitoesteróis foi realizado por Santos et al. (2019) utilizando-se óleo de girassol rico em oleico, óleo de canola e crambe totalmente hidrogenados. Os pesquisadores observaram que o tamanho de partícula variou de 148,23 a 342,10 nm e potencial zeta −22,27 e −29,70 mV com características adequadas para uso em diversos produtos alimentícios como pastas, margarinas e bebidas.

Os ácidos graxos poli-insaturados, alguns considerados essenciais ao consumo humano, podem melhorar o valor nutricional de alimentos fortificados, mas são extremamente propensos à oxidação. Desta forma, estudos tem avaliado a nanoencapsulação de ômega 3 ou óleos fonte destes ácidos graxos, como foi feito por Azizi et al. (2018) com CLN constituída por proteína de soro de leite (WPI) como emulsificante em misturas de ácidos láurico, palmítico e esteárico, e água. Os resultados indicaram que, principalmente o ácido láurico influenciou a estabilidade física das partículas diminuindo seu tamanho e o número de poros da superfície e sendo mais eficaz na proteção do composto contra a oxidação do que os ácidos palmítico e esteárico.

Por outro lado, estudos realizaram a obtenção de CLN contendo ômega 3 como constituinte, à exemplo de Lacatusu et al,z (2013), que utilizaram óleo de peixe enriquecido com ácidos graxos ω-3 para obter nanocarreadores lipídicos estáveis para encapsulação de luteína. O tamanho de partícula dos CLNs contendo luteína ficou abaixo de 200 nm com alta eficiência de aprisionamento (88,5%) enquanto o perfil de liberação *in vitro* mostrou que foi possível garantir uma liberação controlada de luteína.

Como observado, a nanoencapsulação tem se destacado como alternativa principal para garantir proteção e ação de compostos bioativos. Assim, inúmeros materiais lipídicos sólidos e líquidos estão sendo estudados para compor CLN ou SLN buscando-se alcançar efetividade e estabilidade adequados para tais fins.

Referências

ANTON, N.; BENOIT, J.P., SAULNIER, P. **Design and production of nanoparticles formulated from nano-emulsion templates—A review**. Journal Control. Release.128:185–199, 2008.

ASBRIDGE, D. D. Soybeans vs.Other vegetable oils as a source of edible oil products. In: ERICKSON, D. R. (Ed.). . **Pratical Handbook and soybean processing and utilization**. Illinois: AOCS Press, 2015. p. 1–9.

AZIZI, M. et al. Improvement of physicochemical properties of encapsulated echium oil using nanostructured lipid carriers. **Food Chemistry**, v. 246, n. September 2017, p. 448–456, 2018.

BABAZADEH, A.; GHANBARZADEH, B.; HAMISHEHKAR, H. Novel nanostructured lipid carriers as a promising food grade delivery system for rutin. **Journal of Functional Foods**, v. 26, p. 167–175, 2016.

BASOVA, M. M. Fatty acid composition of lipids in microalgae. **International Journal on Algae**, v. 7, n. 1, p. 33–57, 2005.

BELOQUI, A. et al. Nanostructured lipid carriers : Promising drug delivery systems for future clinics. **Nanomedicine: Nanotechnology, Biology, and Medicine**, v. 12, n. 1, p. 143–161, 2016.

BRASIL. Informe Técnico n. 63, de 3 de outubro de 2014. **ANVISA – Agência Nacional de Vigilância Sanitária**, 2014.

BUNJES, H.; UNRUH, T. Characterization of lipid nanoparticles by differential scanning calorimetry, X-ray and neutron scattering. **Advanced Drug Delivery Reviews**, v. 59, n. 6, p. 379–402, 2007.

CHIPLUNKAR, P. P.; PRATAP, A. P. Ultrasound Assisted Synthesis of Hydroxylated Soybean Lecithin from Crude Soybean Lecithin as an Emulsifier. **Journal of Oleo Science**. v. 1108, n. 10, p. 1101–1108, 2017.

COHEN, Z.; NORMAN, H. A.; HEIMER, Y. M. Microalgae as a source of omega3 fatty acids. **World Review of Nutrition and Dietetics**, v. 77, p. 1–31, 1995.

CURI, R. et al. **Entendendo a gordura: os ácidos graxos**. 1ª ed. Editora Manole, 2002.

DA MATA, A. M. B. et al. Dietary Lipid Intake Influences the Alpha-tocopherol Levels in Human Milk. **Journal of pediatric gastroenterology and nutrition**,

v. 70, n. 6, p. 858–863, 2020.

DAN, N. Compound release from nanostructured lipid carriers (NLCs). **Journal of Food Engineering**, v. 171, p. 37–43, 2016.

DEMODARAN, S.; PARKIN, K. L.; FENNEMA, O. L. **Química de Alimentos de Fennema**. Forth edit ed. Porto Alegre: Editora Artmed, 2010.

DRUSCH, S. et al. Physicochemical characterization and oxidative stability of fish oil encapsulated in an amorphous matrix containing trehalose. **Food Research International**, v. 39, n. 7, p. 807–815, 2006.

ELNAGGAR, Y. S. R.; EL-MASSIK, M. A.; ABDALLAH, O. Y. Fabrication, appraisal, and transdermal permeation of sildenafil citrate-loaded nanostructured lipid carriers versus solid lipid nanoparticles. **International journal of nanomedicine**, v. 6, p. 3195–3205, 2011.

FAGERIA, N. K.; BALIGAR, V. C.; JONES, C. A. Growth and Mineral Nutrition of Field Crops. In: Third Edit ed. Boca Raton: CRC Press, p. 551, 2010.

FANG, J. Y. et al. Lipid nanoparticles as vehicles for topical psoralen delivery: Solid lipid nanoparticles (SLN) versus nanostructured lipid carriers (NLC). **European Journal of Pharmaceutics and Biopharmaceutics**, v. 70, n. 2, p. 633–640, 2008.

FARD, S. G. et al. How does high DHA fish oil affect health? A systematic review of evidence. **Critical Reviews in Food Science and Nutrition**, v. 59, n. 11, p. 1684–1727, 2019.

GHORBANZADE, T. et al. Nano-encapsulation of fish oil in nano-liposomes and its application in fortification of yogurt. **Food Chemistry**, v. 216, p. 146–152, 2017.

GHOTRA, B. S.; DYAL, S. D.; NARINE, S. S. Lipid shortenings: A review. **Food Research International**, v. 35, n. 10, p. 1015–1048, 2002.

GUPTA, S. et al. Systematic Approach for the Formulation and Optimization of Solid Lipid Nanoparticles of Efavirenz by High Pressure Homogenization Using Design of Experiments for Brain Targeting and Enhanced Bioavailability. v. 2017, 2017.

HAMMOND, E. G. et al. Soybean Oil. **Bailey's Industrial Oil and Fat Products**, n. 1, p. 577–653, 2005.

HOLSER, R. Encapsulation of polyunsaturated fatty acid esters with solid lipid particles. **Lipid Insights**, v. 5, p. 1–5, 2012.

HULLA, J. E.; SAHU, S. C.; HAYES, A. W. Nanotechnology: History and future. **Human and Experimental Toxicology**, v. 34, n. 12, p. 1318–1321, 2015.

INSTITUTO BRASILEIRO DE GEOGRAFIA E ESTATISTICA, I. **Pesquisa de Orçamentos Familiares 2017 - 2018 - Primeiros Resultados**. 2019.

JAFARI, S. M.; HE, Y.; BHANDARI, B. Effectiveness of encapsulating biopolymers to produce sub-micron emulsions by high energy emulsification techniques. **Food Research International**, v. 40, n. 7, p. 862–873, 2007.

KAMBOJ, S.; BALA, S.; NAIR, A. B. Solid Lipid Nanoparticles An Effective Lipid Based Technology For Poorly Water Soluble Drugs, **International Journal Of Pharmaceutical Sciences Review And Research**, 5 (2). 78-90, 2010.

KATOUZIAN, I. et al. Formulation and application of a new generation of lipid nano-carriers for the food bioactive ingredients. **Trends in Food Science and Technology**, v. 68, p. 14–25, 2017.

KHOSHNOUDI-NIA, S.; FORGHANI, Z.; JAFARI, S. M. A systematic review and meta-analysis of fish oil encapsulation within different micro/nanocarriers. **Critical Reviews in Food Science and Nutrition**, v. 62, n. 8, p. 2061 - 2082, 2022.

KOVAČEVIĆ, A. B. et al. Solid lipid nanoparticles (SLN) stabilized with polyhydroxy surfactants: Preparation, characterization and physical stability investigation. **Colloids and Surfaces A: Physicochemical and Engineering Aspects**, v. 444, p. 15–25, 2014.

KRIS-ETHERTON, P. M.; GRIEGER, J. A.; ETHERTON, T. D. Dietary reference intakes for DHA and EPA. **Prostaglandins Leukotrienes and Essential Fatty Acids**, v. 81, n. 2–3, p. 99–104, 2009.

KURATKO, C. N.; SALEM, N. Docosahexaenoic acid from algal oil. **European Journal of Lipid Science and Technology**, v. 115, n. 9, p. 965–976, 2013.

LACATUSU, I. et al. Lipid nanoparticles based on omega-3 fatty acids as effective carriers for lutein delivery. Preparation and in vitro characterization studies. **Journal of Functional Foods**, v. 5, n. 3, p. 1260–1269, 2013.

LIANG, L. et al. In vitro release of α-tocopherol from emulsion-loaded β-lactoglobulin gels. **International Dairy Journal**, v. 20, n. 3, p. 176–181, 2010.

LIU, C. H.; WU, C. T. Optimization of nanostructured lipid carriers for lutein delivery. **Colloids and Surfaces A: Physicochemical and Engineering Aspects**, v. 353, n. 2–3, p. 149–156, 2010.

LIVNEY, Y. D. Nanostructured delivery systems in food: Latest developments and potential future directions. **Current Opinion in Food Science**, v. 3, p. 125–135, 2015.

LUYKX, D. M. et al. A review of analytical methods for the identification and characterization of nano delivery systems in food. **J Agric Food Chem**, v. 56, n. 18, p. 8231–8247, 2008.

MA, P. et al. Preparation of curcumin-loaded emulsion using high pressure homogenization : Impact of oil phase and concentration on physicochemical stability. **LWT - Food Science and Technology**, v. 84, p. 34–46, 2017.

MATOS-JR, F. E. et al. Effect of feed preparation on the properties and stability of ascorbic acid microparticles produced by spray chilling. **LWT - Food Science and Technology**, v. 75, p. 251–260, 2017.

MARANGONI, A. G.; ROSSEAU, D. The effects of interesterification on the physical properties of fats. In: MARANGONI, A. G.; NARINE, S. S. **Physical Properties of Lipids**. New York: Marcell Dekker Inc., 2002.

MCCLEMENTS, D. J. Advances in nanoparticle and microparticle delivery systems for increasing the dispersibility, stability, and bioactivity of phytochemicals. **Biotechnology Advances**, v. 38, n. August 2018, p. 107287, 2020.

MCCLEMENTS, D. J.; JAFARI, S. M. Chapter 1 - General Aspects of Nanoemulsions and Their Formulation. In: JAFARI, S. M.; MCCLEMENTS, D. J. **Nanoemulsions**. Academic Press, p. 3–20, 2018.

MCCLEMENTS, D. J. Standardization of Nanoparticle Characterization : Methods for Testing Properties , Stability , and Functionality of Edible Nanoparticles. **Crit Rev Food Sci Nutr**. v. 8398, p. 1334 - 1362, 2016.

MEHNERT, W.; MÄDER, K. Solid lipid nanoparticles: Production, characterization and applications. **Advanced Drug Delivery Reviews**, v. 64, n. SUPPL., p. 83–101, 2012.

MÜLLER, R. H. et al. Nanostructured Lipid Carriers (NLC): The Second Generation of Solid Lipid Nanoparticles. In: DRAGICEVIC, N.; MAIBACH, H. I. **Percutaneous Penetration Enhancers Chemical Methods in Penetration Enhancement: Nanocarriers**. Berlin, Heidelberg: Springer Berlin Heidelberg, p. 161–185, 2016.

NASCIMENTO, I. A. et al. Screening Microalgae Strains for Biodiesel

Production: Lipid Productivity and Estimation of Fuel Quality Based on Fatty Acids Profiles as Selective Criteria. **Bioenergy Research**, v. 6, n. 1, p. 1–13, 2013.

NGUYEN, H. M. et al. Enhanced payload and photo-protection for pesticides using nanostructured lipid carriers with corn oil as liquid lipid. **Journal of Microencapsulation**, v. 29, n. 6, p. 596–604, 2012.

O'BRIEN, R. D. Interesterification. In: **Fats and Oils: Formulating and Processing for Applications**. CRC Press,. p. 122–132. 2009a

O'BRIEN, R. D. Chapter 1 - Raw Materials. In: **Fats and Oils: Formulating and Processing for Applications**. Third Edit ed. Boca Raton: CRC Press,. p. 1–66. 2009b

O'KEEFE, S. F.; SARNOSKI, P. J. Nomenclature and Classification of Lipids. In: AKOH, C. C. **Food Lipids: Chemistry, Nutrition, and Biotechnology**. Fourth Edi ed. Boca Raton. p. 1029. 2017.

OLIVEIRA, G. M. et al. Effect of the addition of hardfats on technological properties of palm oil : solid fat content , consistency and crystallization kinetic. **International Congress on Engineering and Food.**, 2011.

OLIVEIRA, G. M. et al. Hard fats as additives in palm oil and its relationships to crystallization process and polymorphism. **LWT - Food Science and Technology**, v. 63, n. 2, p. 1163–1170, 2015.

PARK, S. J. et al. Fabrication and optimization of EGCG-loaded nanoparticles by high pressure homogenization. **Journal of Applied Polymer**. v. 43269, p. 1–7, 2016.

PÉREZ, B.; LI, J.; GUO, Z. Chemistry and properties of lipids and phospholipids. In: AKOH, C. C. **Food Lipids: Chemistry, Nutrition, and Biotechnology**. Fouth Edit ed. Boca Raton: CRC Press, p. 1029. 2017.

PIMENTEL-MORAL, S. et al. Lipid nanocarriers for the loading of polyphenols – A comprehensive review. **Advances in Colloid and Interface Science**, v. 260, p. 85–94, 2018.

PINTO, F.; DE BARROS, D. P. C.; FONSECA, L. P. Design of multifunctional nanostructured lipid carriers enriched with α-tocopherol using vegetable oils. **Industrial Crops and Products**, 2018.

POONIA, N. et al. Nanostructured lipid carriers : versatile oral delivery vehicle. v. 2, 2016.

PURI, A. et al. Lipid-Based Nanoparticles as Pharmaceutical Drug Carriers : From Concepts to Clinic. v. 26, n. 6, p. 523–580, 2009.

QUEIRÓS, M. S. et al. Milk fat nanoemulsions stabilized by dairy proteins. **Journal of Food Science and Technology**, v. 57, n. 9, p. 3295–3304, 2020.

REIS, L. V. C. et al. Evaluation of nanostructured lipid carriers produced with interesterified buriti oil. **Food Technology and Biotechnology**, v. 58, n. 3, p. 284–294, 2020.

RIBEIRO, A. P. B. et al. Interesterificação química: Alternativa para obtenção de gorduras zero trans. **Quimica Nova**, v. 30, n. 5, p. 1295–1300, 2007.

RIBEIRO, A. P. B. et al. Instrumental Methods for the Evaluation of Interesterified Fats. **Food Analytical Methods**, v. 2, n. 4, p. 281–302, 2009.

RIBEIRO, A. P. B. et al. Hardfats as crystallization modifiers of cocoa butter. **European Journal of Lipid Science and Technology**, v. 115, p. 1462–1473, 2013a.

SANTOS, R. et al. I Diretriz sobre o consumo de Gorduras e Saúde Cardiovascular. **Arquivo Brasileiro de Cardiologia**, v. 100, p. 1–40, 2013.

SANTOS, V. S. et al. Nanostructured lipid carriers loaded with free phytosterols for food applications. **Food Chemistry**, v. 298, n. May, p. 125053, 2019.

SATO, K.; UENO, S. Polymorphism in fats and oils. **Bailey's Industrial Oil and Fat Products**, v. 1, p. 77–120, 2005.

SCRIMGEOUR, C. Chemistry of Fatty Acids. **Bailey's Industrial Oil and Fat Products**, p. 1–43, 2005.

SHTAY, R.; PING, C.; SCHWARZ, K. Development and characterization of solid lipid nanoparticles (SLNs) made of cocoa butter : A factorial design study. **Journal of Food Engineering**, v. 231, p. 30–41, 2018.

SILVA, M. G. et al. Developed and characterization of nanostructured lipid carriers containing food-grade interesterified lipid phase for food application. **Food Research International**, v. 155, n. October 2021, p. 111119, 2022.

SOLEIMANIAN, Y. et al. Propolis wax nanostructured lipid carrier for delivery of β sitosterol: Effect of formulation variables on physicochemical properties. **Food Chemistry**, v. 260, n. March, p. 97–105, 2018.

SOUTO, E. et al. Nanopartículas de lipídios sólidos: métodos clássicos de produção laboratorial. **Quimica Nova**, v. 34, n. 8, p. 1323–1327, 2011.

SWANSON, D.; BLOCK, R.; MOUSA, S. A. Omega-3 Fatty Acids EPA and

DHA: Health Benefits Throughout Life. **Advances in Nutrition**, v. 3, n. 1, p. 1–7, 2012.

TAMJIDI, F. et al. Nanostructured lipid carriers (NLC): A potential delivery system for bioactive food molecules. **Innovative Food Science and Emerging Technologies**, v. 19, p. 29–43, 2013.

TIKEKAR, R. V; NITIN, N. Effect of physical state (solid vs. liquid) of lipid core on the rate of transport of oxygen and free radicals in solid lipid nanoparticles and emulsion. **Soft Matter**, v. 7, n. 18, p. 8149–8157, 2011.

VALENZUELA, A.; DELPLANQUE, B.; TAVELLA, M. Stearic acid: a possible substitute for *trans* fatty acids from industrial origin. **Grasas y Aceites**, v. 62, n. 2, p. 131–138, 2011.

WEISS, J. et al. Solid lipid nanoparticles as delivery systems for bioactive food components. **Food Biophysics**, v. 3, n. 2, p. 146–154, 2008.

WENDEL, A.; STAFF, U. Lecithin. In: **Kirk-Othmer Encyclopedia of Chemical Technology**. p. 1–19. 1995.

WITAYAUDOM, P.; KLINKESORN, U. Effect of surfactant concentration and solidification temperature on the characteristics and stability of nanostructured lipid carrier (NLC) prepared from rambutan (Nephelium lappaceum L.) kernel fat. **Journal of Colloid and Interface Science**, v. 505, p. 1082–1092, 2017.

YOON, G.; PARK, J. W.; YOON, I.-S. Solid lipid nanoparticles (SLNs) and nanostructured lipid carriers (NLCs): recent advances in drug delivery. **Journal of Pharmaceutical Investigation**, v. 43, n. 5, p. 353–362, 2013.

4. Artigos

Artigo 1. EFFECT OF CHEMICAL INTERESTERIFICATION ON PHYSICO-CHEMICAL PROPERTIES OF SOYBEAN OIL AND FULLY HYDROGENATED MICROALGAE OIL BLENDS

Kamila Ramponi Rodrigues de Godoi Fernandes[1], Mayanny Gomes da Silva[1], Lisandro Pavie Cardoso[2], Ana Paula Badan Ribeiro[1]

[1]Department of Engineering and Food Technology, School of Food Engineering, University of Campinas, Brazil

[2]Department of Applied Physics, Institute of Physics, University of Campinas, Brazil

Corresponding author: kamila.ramponi@hotmail.com

(Manuscrito submetido ao Periódico *Food Research International*)

Abstract: The chemical interesterification is a strategy to provide desirable physical, chemical, and functional properties to lipid materials without causing the formation of *trans* isomers. In this study, simple and structured lipid blends obtained by chemical interesterification, composed of fully hydrogenated microalgae oil (FHMO) and soybean oil (SO) in the ratios (FHMO/SO): 90:10, 80:20, 70:30, 60:40, and 50:50 (w:w) were evaluated for fatty acid (FA) composition, triacylglycerol composition (TAG), regiospecific distribution, thermal behavior, solid fat content (SFC), crystallization kinetics, polymorphism, and microstructure. The rearrangement of TAG after the interesterification led to a decrease in trissaturated and tri-unsaturated TAG and an increase in monounsaturated TAG, with changes in the physicochemical characteristics when compared to simple lipid blends. The reduction in SFC profile for all temperatures studied, reduction of maximum SFC at 25 °C, and increase in crystallization induction time was also observed. In general, a wide melting range and lower melting point was observed in the thermal behavior after interesterification, affecting the crystal morphology for all blends. A reduction of crystal size was observed, with a predominant morphology of spherulites before the randomization, and disk- and needle-shaped crystals after randomization, due to the predominance of polymorphic β' form crystals. The small crystal size and the β' form can enhance the applications of the interesterified blends in specialty fats for confectionery, margarine, and bakery products.

Keywords: Lipid crystallization, randomization, solid fat content, differential scanning calorimetry, microstructure, polymorphism.

1. Introduction

The majority of natural fats and oils present limited application due to their particular fatty acid and triacylglycerol compositions. The chemical composition of fat partly defines its physical and functional properties and depends on the fatty acid structure and its distribution on the glycerol backbone (Marangoni & Rosseau, 2002).

The use of trans fatty acids has stood out as a current subject concerning industrial fats and health. However, the high consumption of trans fatty acids increases the risk of all-case mortality by 34% and coronary heart disease by 28%, and for every 1% increase in daily energy obtained from trans fats, the mortality raises by 12% (Bösch et al., 2021). Thus, the elimination of trans fatty acids has been one of the priority targets in the World Health Organization (WHO) 13th General Programme of Work, which guides the five-year work of WHO in 2019–2023 monitoring all countries in this goal. In this sense, countries should adapt their legislation for eliminating and reducing the trans fatty acids, with a limitation of 2 g of industrially-produced trans-fatty acids per 100 g of total fat, or should ban on the production or use of partially hydrogenated fat as an ingredient in all foods until 2023 (World Health Organization, 2020).

Although saturated fatty acids can be used to replace the technical characteristics of the trans fatty acids in foods, the high consumption of saturated fatty acids can cause cardiometabolic risk and weight gain. According to European Food Safety Authority (EFSA), the intake of these fatty acids should be below 10% of total energy, with the replacement of the energy contained in this fat for monounsaturated and polyunsaturated fats. However, this replacement can impact the consistency and flavor of food products (Bösch et al., 2021; Brouwer, 2020).

Thus, many techniques have been used to modulate these fatty acids distribution, modifying the final macroscopic lipid characteristics, mainly to replace the trans and saturated fatty acids in food products. The interesterification is a strategy that allows obtaining new and desirable physical, chemical, and functional properties of fats and oils, once it can break ester bonds between glycerol and fatty acids naturally present in the raw materials and redistribute them on the glycerol molecules, forming new bonds on the glyceride molecules,

that is, new triacylglycerols. This event can affect the polymorphism, solid fat content, and fat microstructure of the lipid system producing semi-solid lipid systems free of *trans* isomers (Ribeiro et al., 2017; Ribeiro et al., 2009; Rosseau & Marangoni, 2002).

The interesterification process can be done enzymatically or chemically. The enzymatic interesterification is catalyzed by highly selective regio-specific lipases for a particular type of fatty acid on the glycerol molecule. All the event is carried out under mild reaction conditions, with the lower formation of side reactions, lower waste generation, and ease recovery when compared to chemical interesterification; however, it is a more expensive and time-consuming process (Sivakanthan & Madhujith, 2020). In turn, the chemical interesterification leads to a random distribution of fatty acids on the glycerol molecules until reaching a thermodynamic equilibrium, using a chemical catalyst and high temperature (approximately 100 °C) (Ribeiro et al., 2007).

The selection of lipid raw material to obtain new interesterified systems is very important. In general, the lipid raw materials are mixed to form blends aimed to increase the technological applications of the natural forms. Several studies have shown lipid combinations using highly unsaturated liquid vegetable oil and highly saturated materials, such as fully hydrogenated oils or vegetable oil with a high concentration of saturated fats, to widen their commercial value.

Rashid et al. (2016a) compared both chemical and enzymatic interesterified blends of palm oil and palm kernel oil (25:75 w:w) and found that the chemical interesterification led to significant changes in the TAG composition, reducing the eutectic interaction and improving the use of blends in foods applications. Similarly Rashid, et al. (2016b) studied the chemical interesterification of blends of palm stearin and rice bran oil in the mass ratio of 100:0, 70:30, 50:50, 30:70, and 0:100 (w:w) and obtained suitable fats for application in margarine. Ribeiro et al. (2017) studied the enzymatic and chemical interesterification of high oleic sunflower oil (HOSO) and fully hydrogenated soybean oil (FHSO) in a weight ratio of 50:50 (w/w). Zhang et al. (2019) used various combinations between palm oil and beef tallow, soybean oil, palm stearin, palm olein, palm mid fraction, and palm kernel oil and obtained potential fats for several applications in food specialty fats. Berčíková et al. (2020) obtained chemically interesterified structured blends based on not cholesterol-raising fatty acids (stearic, behenic,

arachidic, and oleic acids) and high oleic sunflower oil and fully hydrogenated erucic rapeseed oil with physical properties similar to industrial shortenings.

In addition, Oliveira et al. (2017) studied chemical interesterified blends of palm stearin and patawa oil at different ratios (30:70, 40:60, 50:50, and 60:40) and reported that the blend 50:50 can be used in fatty products due to appropriate melting point and SFC, similar to that of soft table margarine, with plastic and spreadable consistency at refrigeration temperature.

Therefore, interesterification has proven to be an effective process to improve the use of several lipid raw materials. Soybean is a conventional and important raw material, and the principal oilseed produced in the world due to agronomic characteristics and applicability, resulting in low-cost and highly available oil (Asbridge, 2015; Fageria et al., 2010; Hammond et al., 2005). Soybean oil (SO) has desirable nutritional characteristics due to its high unsaturated fatty acids content (approximately 55% of linoleic acid and 7% of linolenic acid) and is indicated to shortening production and lipid products that require β form habit (Asbridge, 2015; Demodaran et al., 2010; Fageria et al., 2010; Hammond et al., 2005).

Novel oil sources have been studied worldwide. Microalgae oils can have a variable fatty acid composition according to the algae species, with an emphasis on palmitoleic, oleic, linoleic, and linolenic fatty acids (Basova, 2005; O'Brien, 2009). In turn, fully hydrogenated microalgae oil (FHMO) consists of a totally hydrogenated matrix containing approximately 90% (w:w) of stearic acid, which is positive from a nutritional point of view, once this fatty acid does not cause adverse effects on the risk of cardiovascular diseases (Crupkin & Zambelli, 2008; Ribeiro et al., 2017). Thus, considering the health benefits of FHMO, the homogeneity of the triacylglycerols, and its strategic production potential, it was selected as a solid lipid phase to study the behavior of this hardfat when subjected to chemical interesterification, an unprecedented approach in the literature. It is worth mentioning that although previous studies have investigated the enzymatic interesterification of microalgae oil (Bogevik et al. 2018; Wang et al. 2015), none of them addressed different species and fatty acid composition of the microalgae, which justifies the novelty of the present study.

Therefore, this study developed lipid blends from simple and interesterified blends of FHMO and SO at different ratios, aiming to obtain fat products with

better physical and chemical properties and desirable functionality to be applied in the food, cosmetic, and pharmaceutical industries.

2. Material and methods

2.1. Material

Refined soybean oil (SO) was purchased in the local market; fully hydrogenated microalgae oil (FHMO) was donated by SGS Agriculture and Industry Ltd. (Ponta Grossa, PR, Brazil) from AlgaWiseTM Ultra Omega-9 Algae Oil (TerraVia Holdings, San Francisco, CA, USA); sodium methoxide anhydrous powder, 99% purity, was supplied by Sigma Aldrich. The simple and chemical interesterified fats were produced from SO and FHMO blends at different ratios (FHMO/SO).

2.2. Methods

2.2.1. Preparation of simple blends

The FHMO and SO were heated until total melting and mixed under magnetic stirring at a weight ratio (FHMO: SO; w:w) of 90:10, 80:20, 70:30, 60:40, and 50:50. The blends were maintained under agitation for 3 minutes at 70°C to destroy the crystalline memory.

2.2.2. Chemical interesterification

The reactions were performed according to the FHMO and SO ratios described in Section 2.2.1. For the chemical interesterification, on a laboratory scale, each blend was heated until 100 °C under magnetic stirring (500rpm) for 20 minutes under vacuum to remove moisture. Then, each blend was interesterified using 1.54% of sodium methoxide, according to the quantity of free fatty acids and peroxide value of SO and FHMO, as described by Desmet Ballestra (Figure 1), and the optimization was performed as described by Grimaldi et al. (2005). Sodium methoxide was added and the blends were dried at 100 °C, under magnetic stirring (500rpm) for 20 minutes under vacuum. Then, citric acid solution (5g/100mL) was added to stop the reaction. The interesterified samples were washed with distilled water (80°C). For drying, the blends were heated until

100 °C under magnetic stirring for 20min under vacuum. After the reaction, FFA and partial acylglycerols (diacylglycerols and monoacylglycerols) were removed as described by Rousseau & Marangoni (1998) with modifications. The interesterified blends were melted and mixed with an equal volume of 96% ethanol at 40–50 °C in a separation funnel. The ethanol phase was extracted, and the procedure was repeated three times. The samples were stored in glass vials at 25°C until the moment of analysis.

Figure 1. Schematic form to calculate the total quantity of sodium methoxide used in the chemical interesterification reaction.

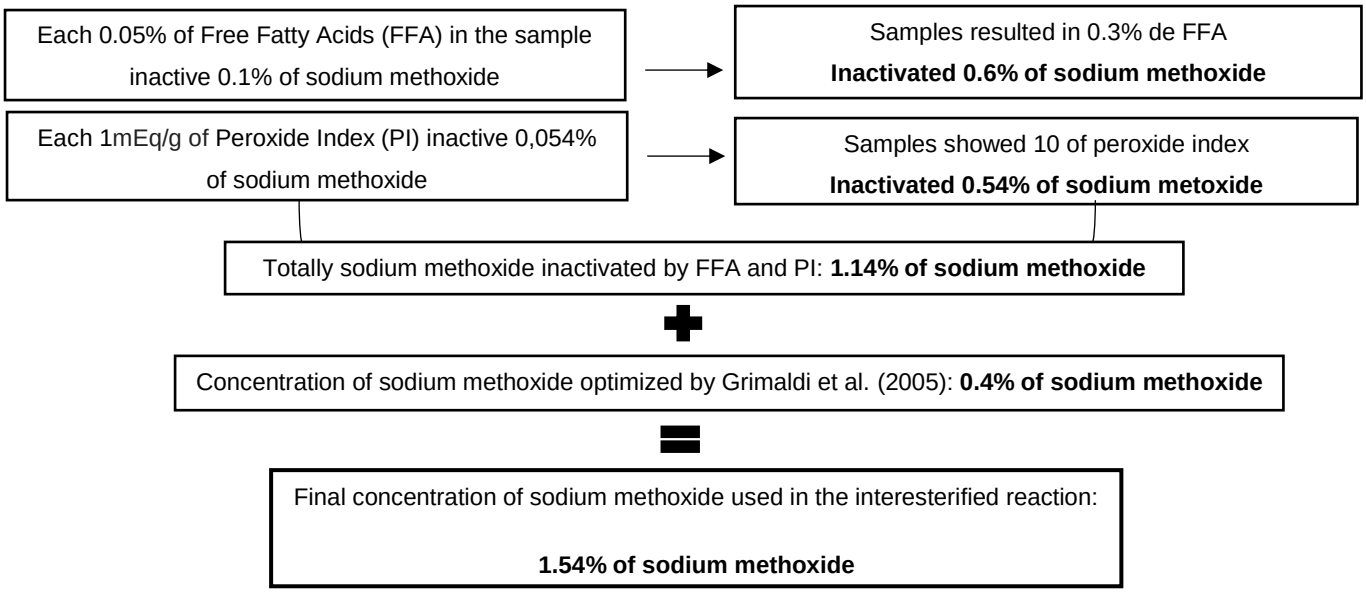

2.2.3. Fatty acid composition

The fatty acid composition was determined using a gas chromatograph (CGC) Agilent Series 6850 (Santa Clara, California, USA) with an FID detector, after esterification according to Hartman & Lago (1973). The methyl esters were separated according to AOCS Cf 1-96 (AOCS, 2009) using a capillary column Agilent-DB-23 (50% cyanopropyl – methylpolysiloxane), length 60 m, internal diameter 0.25 mm, and film thickness 0.25 μm; The operation conditions were: flow rate of 1.0 ml/min; linear velocity of 24 cm/s; injector temperature of 250 °C; detector temperature of 280 °C/min; oven temperature of 110 °C for 5 min, 110 -

215 °C at 5 °C/min, 215 °C for 34 min; helium as a carrier gas; injected volume of 1.0 µL/min and split ratio of 1:50. Individual fatty acid methyl esters were identified by comparison of retention times to commercial standards and quantified based on relative peak areas. The fatty acid composition of the blends was calculated according to the respective mass fractions in the blends.

2.2.4. Iodine value and saponification value

The iodine and saponification values were determined according to AOCS Cd 1c-85 and Cd 31-94 (AOCS, 2009), respectively.

2.2.5. Triacylglycerol composition

Triacylglycerol (TAG) composition was determined using a gas chromatograph CGC Agilent 6850 Series GC System (Santa Clara, California, USA). A capillary column Agilent - DB-17 HT (50% phenyl- 50% methylpolysiloxane) 15 m in length, 0.25 mm internal diameter, and 0.15 µm of film thickness was used. The operation conditions were: injector temperature 360 °C; detector temperature of 375 °C/min; oven temperature from 250°C to 350 °C at 5 °C/min, 350 °C for 20 min; helium as a carrier gas; injected volume of 1.0 µL/min and split ratio of 1:100. TAG were identified by comparison of retention times and the quantification was based on relative peak areas (Antoniosi Filho et al., 1995). The TAG composition of the blends was determined according to the composition of SO and FHMO and the respective mass fractions in the blends regarding the trissaturated (S_3), dissaturated (S_2U), monossaturated (SU_2) triunsaturated (U_3) triacylglycerols.

2.2.6. Triacylglycerol regiospecific distribution

Proton-decoupled 13C NMR (Nuclear Magnetic Resonance) was used to analyze the positional distribution of different fatty acids (saturated/unsaturated) on the TAG backbone. Lipid samples were dissolved in deuterated chloroform in NMR tubes, and NMR spectra were recorded on a Bruker Advance DPX spectrometer operating at 300 MHz. The determination of 13C was performed at

a frequency of 75.8 MHz, with a 5 mm multinuclear probe operating at 30°C (Vlahov, 1998).

2.2.7. Thermal Behavior

The thermal analysis was performed in a differential scanning calorimeter (DSC) TA Q2000 coupled to an RCS90 Refrigerated Cooling System (TA Instruments, Waters LLC, New Castle) according to the AOCS method Cj 1-94, with adaptations (AOCS, 2009) using Universal V4.7A for data processing (TA Instruments, Waters LLC, New Castle). The analysis conditions were: sample weight: 10 mg; crystallization curves: 10 min (80°C); 80°C to -40°C (10°C/min); melting curves: 30 min at -40°C; and -40°C to 80°C (5°C/min). The results were evaluated for the following parameters: initial crystallization and melting temperatures (T_i), peak crystallization and melting temperatures (T_p), and crystallization and melting enthalpies (ΔH) (Campos, 2005).

2.2.8. Solid fat content (SFC)

The SFC as a function of temperature was determined by a low-resolution NMR spectrometer (Bruker pc 120 Minispec). The samples were melted and maintained at 0 °C for 1 hour, and the analyses were carried out according to the AOCS Cd 16b-93 (AOCS, 2009) direct method, with sequential measurements at controlled temperatures of 10, 15, 20, 25, 30, 35, 40, 45, 50, 55, 60, and 65 °C using high precision dry baths (TCON 2000, 0-70 °C). The melting point was calculated for the temperature corresponding to 4% solids content obtained from the SFC curves given by NMR (Ribeiro et al. 2009). The analyses were performed in triplicate.

2.2.9. Crystallization kinetics

The samples were placed in a liquid state in a dry bath system (Peltier Tcon 2000, Duratech, USA) at 70°C for 1 h. The solid fat content (SFC) was determined at 25°C (± 0.5°C) at 60-second intervals, in triplicate, using a low-

resolution nuclear magnetic resonance (NMR) spectrometer Bruker pc120 Minispec, with temperature control using a thermostatic bath (+/- 0.5°C) (Wassell & Young, 2007).

The crystallization kinetics was determined by the original Avrami equation (Equation 1), which is the most used model to describe the isothermal phase transformation kinetics, and used for the crystallization study at 25 °C (Marangoni, 1998; Wright et al., 2000). This model characterizes the induction period (ƮSFC) corresponding to the onset of crystal formation and the maximum solid content (SFC_{max}). Induction time is graphically attained and corresponds to the time needed for a stable nucleus of critical size to be formed in a liquid phase (Marangoni, 1998)

$$\frac{SFC(t)}{SFC_{máx}} = 1 - e^{-kt^n} \qquad \text{Equation 1}$$

where SFC(t) corresponds to the solid fat content (%) as a function of time, 1 is the solid fat content limit when time tends to infinite, k is the Avrami constant (min^n), which takes into account both crystal nucleation and growth rate, and *n* is the Avrami exponent, which indicates crystal growth mechanism according to Table 1 (Wright et al., 2000). The equation was linearized and applied to the results during the first 20 minutes of crystallization to determine the k and n values.

Table 1. Avrami Exponent (*n*) for different crystal growth and crystal nucleation.

Crystal growth	Crystal nucleation	Avrami exponent (*n*)	Description of crystal growth and nucleation
3	1	3 + 1 = 4	Spherulite growth with sporadic nucleation
3	0	3 + 0 = 3	Spherulite growth with instantaneous nucleation
2	1	2 + 1 = 3	Disk growth with sporadic nucleation
2	0	2 + 0 = 2	Disk growth with instantaneous nucleation
1	1	1 + 1 = 2	Needle growth with sporadic nucleation
1	0	1 + 0 = 1	Needle growth with instantaneous nucleation

2.2.10. Microstructure

The samples were evaluated by polarized light microscopy (PLM). For that, a drop of the melted sample was placed on a glass slide at 80 °C with the aid of a capillary tube, covered with a coverslip, and stored in an incubation chamber at 25 °C for 24 hours until stabilization. The images were taken from three different visual fields, at a magnification of 40 X, and a single representative image was selected to represent the systems (Campos, 2005). The software Image Pro Plus (version 7.0, Media Cybernetics) was used to take the images.

2.2.11. Polymorphism

The polymorphic habit of the samples was determined by X-ray diffraction according to the AOCS Cj 2-95 method (AOCS, 2009). The determinations were made in a Philips diffractometer (PW 1710) using Bragg-Brentano geometry (θ:2θ) with Cu-Kα radiation (λ = 1.54056Å, 40 KV, and 30 mA). The measurements were obtained with steps of 0.02 ° in 2θ and an acquisition time of 2 seconds, with scans from 2 to 40° (scale 2θ). The identification of the crystalline forms was carried out on the characteristic short spacing of the crystals (Chopin-Doroteo et al., 2011; Dassanayake et al., 2011; Yap et al., 1989).

2.2.12. Statistical analysis

The results were subjected to analysis of variance (ANOVA) using the software STATISTICA Version 8 (StatSoft Inc., Tulsa, OK). Tukey tests were applied for comparisons of means, at a 5% significance level ($p<0.05$).

3. Results and discussion

3.1. Fatty acid composition

As expected, SO used in this study showed fatty acid composition consistent with the results in the literature (O'Brien. 2009a). In turn, due to its

original composition rich in oleic acid, FHMO resulted in fully hydrogenated oil with high stearic acid content (92.85%). As reported by Ribeiro et al. (2017) and Ribeiro et al. (2009b), fully hydrogenated soybean oil is the most similar in terms of stearic acid contents due to its original composition rich in oleic, linoleic, and linolenic acids. However, the maximum stearic acid content in this raw material was 86%, about 5% lower than FHMO.

It is worth noting that, despite being a homogeneous matrix in fatty acids and triacylglycerols, and predominantly saturated fatty acids, stearic acid (C18:0) has a neutral atherogenic effect, i.e., it cannot increase the levels of high-density lipoproteins, also called LDL cholesterol (Mensink, 2005). Although this effect has been observed in several studies, the mechanism is not well elucidated.

When consumed, fatty acids are emulsified in the duodenum by bile acids, leading to the formation of micelles. These micelles, formed by esters of cholesterol, triacylglycerols, and phospholipids, are then digested by lipases. Concerning the long-chain fatty acids, after absorption, they are esterified back to triacylglycerols by acyltransferases and released into the lymphatic circulation as chylomicrons (Curi et al., 2002). For stearic acid, this event can occur differently, once according to Sampath & Ntambi (2005), stearic acid may have lower absorption efficiency in the intestine due to the higher chain length. Conversion of stearate from stearic acid to oleate can also occur via the enzyme stearoyl-CoA desaturase. It is known that oleate is the preferred substrate for the synthesis of triglycerides and other complex lipids, and is therefore utilized by the body and does not directly impact the increase of cholesterol levels. Furthermore, the animal organism is able to perform the transformation to oleic acid by introducing a double bond between carbon atoms 9 and 10 catalyzed by the enzyme Δ-9 desaturase (Curi et al., 2002). Although not completely elucidated, these are some factors of the neutral atherogenic effect of stearic acid.

As can be seen in Table 2, high levels of saturated fatty acids were observed in the blends due to the addition of FHMO, with a reduction of 33.42% in the blend with the highest content of FHMO, 90:10, when compared to the blend with the lowest content of FHMO, 50:50. Although these values are considered high, the FA are mostly represented by stearic acid, with levels of 83.71 and 48.18% in the blends 90:10 and 50:50, respectively. Therefore, even

with high saturated fatty acids levels, there is still a greater healthiness associated with the blends.

Table 2. Fatty acid composition (%) of raw materials (SO and FHMO) and the respective mixtures.

Fatty acids (%)	FHMO	SO	90:10 (w:w)	80:20 (w:w)	70:30 (w:w)	60:40 (w:w)	50:50 (w:w)
C 12:0 – Lauric acid	0.15±0.02	0.02±0.01	0.14±0.01	0.13±0.01	0.11±0.01	0.10±0.01	0.09±0.01
C14:0 – Mirístic acid	0.47±0.01	0.10±0.02	0.43±0.00	0.39±0.00	0.35±0.00	0.32±0.01	0.28±0.01
C16:0- Palmític acid	5.52±0.01	11.10±0.24	6.06±0.03	6.62±0.05	7.18±0.07	7.74±0.10	8.29±0.12
C18:0 – Stearic acid	92.85±0.10	3.74±0.35	83.71±0.08	74.83±0.04	65.94±0.04	57.06±0.07	48.18±0.12
C18:1 – Oleic acid	-	24.53±2.28	2.60±0.32	5.03±0.54	7.47±0.76	9.90±0.97	12.34±1.19
C18:2 – Linoleic acid	0.12±0.01	52.70±2.15	5.37±0.21	10.62±0.43	15.87±0.64	21.12±0.86	26.37±1.07
C18:3 – Linolenic acid	-	6.39±0.50	0.63±0.05	1.28±0.10	1.91±0.15	2.56±0.20	3.19±0.26
C20:0 – Araquidic acid	0.95±0.01	0.48±0.10	0.90±0.01	0.86±0.02	0.81±0.03	0.76±0.04	0.72±0.05
C22:0 – Behenic acid	-	0.51±0.03	0.10±0.02	0.15±0.02	0.19±0.02	0.24±0.02	0.28±0.02
∑ **Saturated**	99.94±0.10	16.14±0.76	91.36±0.12	83.01±0.14	74.65±0.16	66.30±0.18	57.94±0.02
∑ **Monounsaturated**	-	24.77±2.31	2.63±0.01	5.10±0.02	7.56±0.04	10.03±0.05	12.49±0.07
∑ **Polyunsaturated**	0.12±0.1	59.09±2.62	6.01±0.04	11.90±0.08	17.78±0.11	23.67±0.15	29.57±0.18
S. I.	190±5.44	193±42.66	-	-	-	-	-
I.I. (I_2/100g)	129±2.64	0.33± 0.07	-	-	-	-	-

FHMO: Fully hydrogenated microalgae oil; SO: soybean oil; S.I: Saponification Index; I.I.: Iodine Index.

From a technological point of view, the addition of fully hydrogenated oils containing mostly long-chain saturated fatty acids, such as C18, is necessary for lipid bases that require higher melting point, thermal and mechanical strength, in addition to being used as crystallization inducers or as hard stock fats. The range of blends can provide these characteristics in different ways, once the different SO and FHMO contents provide distinct profiles for lipid blends. Regarding the saturated fatty acid content, the blend 90:10 showed specificity for saturated and unsaturated fatty acid levels, which were 91.36% saturated acids, reducing to 83.01, 74.65, 66.30, and 57.94% in the blends 80:20, 70:30, 60:40, and 50:50, respectively. The saturated and unsaturated fatty acid contents of the raw materials also affected the iodine value (I.V.) and the saponification value (S.V.),

which was considered adequate due to the predominantly unsaturated characteristic of SO and fully saturated characteristic of FHMO.

3.2. Triacylglycerol composition

The triacylglycerol (TAG) composition has a direct correlation with the physical properties of fats. When the system is subjected to chemical interesterification, complete randomization of fatty acids occurs according to the laws of probability (Rosseau & Marangoni, 2002). Thus, the chemical interesterification reactions can modulate such composition, changing several properties in the simple matrices.

For all blends, before and after randomization, there was a predominance of triestearin (SSS) due to the significant stearic acid content of FHMO, observed in the fatty acid composition, and higher TAG S3, S2U, and U3 contents in the simple blends when compared to those obtained by randomization, with the formation of new TAG S2U, as shown in Figure 2.

Figure 2. Triacylglycerol classes (TAG) (%) of FHMO: SO in simple or interesterified blends. Simple (S) and Interesterified (I) blends of fully hydrogenated microalgae oil (FHMO) and soybean oil (SO) in the respective proportions (w:w): 90:10, 80:20, 70:30, 60:40 e 50:50.

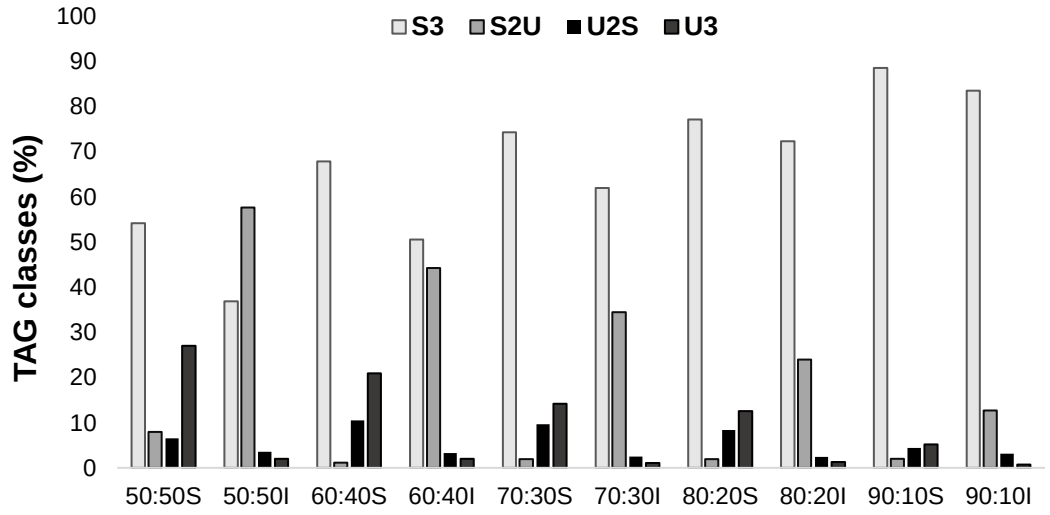

Triacylglycerols: S_3 (trisaturated), S_2U (disaturated–monounsaturated), SU_2 (monosaturated-diunsaturated) and U_3 (triunsaturated). Mean between sample injection triplicates.

A similar result was found by Ribeiro et al. (2017); Ribeiro, et al. (2009), and Ribeiro et al. (2018), who also reported a significant increase in S2U content and reduction of S3 and U3 in various matrices, with a slight increase in U2S. These modifications modulate the physical and thermal properties of lipid bases since there was a reduction of up to 40 °C in the melting point of blends, increasing their applicability, especially at room temperature (Rosseau & Marangoni, 2002).

Regarding TAGs, a predominance of S3 was observed for the simple blends with a majority composition of SSS (tristearin) and PSS (palmitic/stearic/stearic acid), with the other TAGs also present in SO. This pattern was modified after the interesterification, with the formation of new TAGs, differently from those observed in the raw materials, still with a predominance of SSS. In general, when comparing the simple fraction to its interesterified counterpart, there was an increase in PSS and SOO contents, with maintenance or decrease in SSS after the reaction, except for the blend 90:10, with higher amounts of FHMO and, consequently, stearic acid and SSS. A reduction in SSS contents and an increase in more unsaturated TAGs were observed with the addition of SO to FHMO.

Table 3 shows the contribution of each TAG in the blends made from simple and interesterified blends. The simple blend 90:10 presented 73.57% SSS and 11.35% PSS before interesterification, which changed to 63.45% SSS, 16.46% PSS, and 8.17% SSO after interesterification. The simple blend 80:20 showed 60.58% SSS and 13.36% PSS, while the interesterified fraction was composed of 54.85% SSS, 15.02% SSO, and 13.98% PSS. The simple blend 70:30 showed 63.51% SSS and 8.44% PSS, and the interesterified fraction was characterized by 44.66% SSS, 21.98% SSO, and 12.96% PSS. The simple blend 60:40 had 55.96% SSS and 8.61% PSS, while the interesterified fraction resulted in 33.80% SSS, 23.52% SSO, and 12.96% PSS. Finally, the simple blend 50:50 showed 48.41% SSS, 10.30% OLL, and 7.68% PSS, and the corresponding interesterified fraction showed a predominance of SSO, SSS, and SSL, with percentages of 23.58, 23.08, and 12.07%, respectively. Thus, the results for the individual TAGs confirm the findings of triacylglycerol classes, once the addition of SO led to higher TAG U3 concentrations with an emphasis on the predominance of OLL in the blend 50:50, with a reduction of S3, represented by SSS. In turn, despite the high SSS levels after interesterification reaction due to

the high stearic acid content in FHMO, the process led to an increase in SSO for all blends, confirming the increase in S2U.

These characteristics generate extreme melting points (very high or very low), which directly impacts their use at the temperatures of industrial interest, which are 5 °C for refrigerated products or 25 °C for products that require stability at room temperature. However, an increase in S2U broadens the possibilities of use by providing fats with greater plasticity. Plastic fats are used in the food industry for various applications due to their appropriate physical properties such as wider melting range, slower melting, higher total melting at body temperature, adequate solid fat content to ensure firmness to chilled products, and stability at room temperature, which also impacts the crystalline structure and polymorphic form, ensuring softness, texture, pleasant mouthfeel, and satisfactory air incorporation to numerous products (Lee et al., 2008; Pacheco et al., 2013).

Table 3. Triacylglycerols composition (%) of raw materials (SO and FHMO) and the respective mixtures.

TAG	NC	FHMO	SO	90:10S	90:10I	80:20S	80:20I	70:30S	70:30I	60:40S	60:40I	50:50S	50:50I
PPP	48	0.69±0.12	-	0.55±0.10	0.94±0.15	0.20±0.10	1.06±0.17	0,28±0,24	1.01±0.19	0.66±0.24	0.75±0.21	0.68±0.14	0.65±0.12
POP		-	1,07±0.34	-	-	0.22±0.10	-	1.08±1.08	-	1.12±0.07	-	0.28±0.12	-
PLP	50	-	2,11±0.34	-	-	0.88±0.22	-	0.42±0.17	-	-	-	7.68±1.40	-
PPS		3.79±0.39	-	3.01±0.30	2.62±0.19	2.94±0.22	2.36±0.03	2.07±1.27	2.19±0.12	2.56±0.42	2.45±0.19	1.41±0.16	2.46±0.41
POO		-	5,71±0.90	2.42±0.93	-	2.75±0.18	-	1.42±1.34	-	2.97±0.25	-	4.32±0.46	-
PPO		-	-	-	0.17±0.02	-	0.49±0.16	-	0.70±0.23	-	0.81±0.14	-	1.29±0.32
PLO	52	-	10,62±1.22	-	-	4.09±1.82	-	3.40±1.30±	-	3.16±1.49	-	5.89±0.06	-
PLL		-	12,57±0.70	0.34±0.30	-	-	-	3.59±1.25	-	4.35±1.39	-	0.62±0.25	-
PLnL		-	2,09±0.45	-	-	-	-	1.24±1.25	-	-	-	-	-
PSS		15.45±0.43	-	11.35±1.37	16.46±0.51	13.36±1.15	13.98±1.14	8.44±1.28	12.96±1.47	8.61±1.18	13.48±0.01	1.88±0.58	10.59±1.91
PSO			-	-	1.66±0.14	-	4.47±0.47	-	6.66±1.22	-	6.83±0.07	-	9.25±0.39
OOO		-	8,75±1.04	-	-	3.43±1.08	-	3.06±1.27	-	4.8±1.04	-	6.45±2.11	-
OLO		-	14,20±0.90	-	-	4.36±1.35	-	3.90±1.28	-	2.77±2.17	-	8.07±0.08	-
OLL		-	19,05±1.22	-	-	2.42±1.33	-	3.09±1.43	-	4.87±3.76	-	10.30±1.15	-
LLL		-	18,48±1.07	-	-	2.34±0.47	-	2.84±1.51	-	6.01±4.24	-	6.16±0.66	-
LLnL		-	5,35±0.99	-	-	1.55±0.58	-	1.26±1.23	-	-	-	-	-
PSL		-	0.91±0.14	-	-	-	0.62±0.26	-	1.02±0.04	-	1.69±0.32	-	3.16±1.37
SSO	54	-	-	-	8.17±0.87	-	15.02±0.03	-	21.98±1.36	-	23.52±0.84	-	23.58±3.51
SSL		-	-	-	1.6±0.14	-	2.55±0.07	-	4.10±0.70	-	8.5±1.66	-	12.07±2.25
SSLn		-	-	-	-	-	0.84±0.01	-	1.49±0.06	-	2.82±0.15	-	4.66±2.71
SLLn		-	-	-	0.62±0.18	-	0.62±0.36	-	1.49±0.06	-	1.11±0.10	-	-
SLL		-	-	-	2.08±0.34	-	1.83±0.21	-	1.80±0.19	-	2.20±1.60	-	2.21±1.78
SLLn		-	-	-	-	-	-	-	-	-	-	-	1.36±0.76
SLnLn		-	-	-	0.42±0.15	-	-	-	0.51±0.06	-	-	-	-
LLL		-	-	-	0.51±0.16	-	0.59±0.58	-	0.37±0.22	-	0.90±0.44	-	0.90±0.39

LLLn		-	-	-	0.24±0.16	-	0.29±0.23	-	0.35±0.02	-	0.65±0.24	-	0.69±0.22
LLnLn		-	-	-	-	-	0.15±0.06	-	0.19±0.04	2.46±2.54	0.42±0.08	-	0.50±0.09
SSS		78.38±0.45	-	73.57±2.75	63.45±0.96	60.58±4.87	54.85±0.59	63.51±1.18	44.66±0.17	55.96±7.30	33.80±0.41	48.41±2.75	23.08±3.86
SSA	56	1.68±0.24	-	-	0.16±0.09	0.94±0.51	-	0.40±0.05	-		-	-	0.56±0.26
ΣS_3		98.32±0.24	-	88.48±0.87	83.47±1.28	77.08±0.66	72.26±1.54	74.30±2.14	61.93±1.57	67.81±7.36	50.77±0.37	54.18±2.17	36.85±6.11
ΣS_2U		1.68±0.24	3.19±0.60	1.99±0.67	12.67±1.13	1.90±0.11	23.98±0.28	1.89±0.66	34.47±2.10	1.12±0.46	45.66±2.06	7.97±1.44	57.59±7,08
ΣSU_2		-	30.99±0.93	4.39±1.21	3.12±0.64	8.40±0.05	2.45±0.57	9.66±1.13	2.49±0.25	10.48±3.58	2.09±1.71	6.52±0.31	3.55±1.05
ΣU_3		-	65.82±0.70	5.18±0.27	0.75±0.21	12.56±0.83	1.32±0.68	14.15±0.86	1.11±0.28	20.89±4.68	2.51±	27.01±3.88	2.01±0.22

Simple (S) and Interesterified (I) blends of fully hydrogenated microalgae oil (FHMO) and soybean oil (SO) in the respective proportions (w:w): 90:10, 80:20, 70:30, 60:40 e 50:50; Triacylglycerols (TAG); Number of carbons (NC); Trisaturated (S3), Disaturated-monounsaturated (S2U); monosaturated-diunsaturated (SU2), triunsaturated (U3). Mean between sample injection triplicates.

3.3. Regioespecific distribution

The analysis of TAG regiospecificity allows the identification of fatty acids distribution in the glycerol molecule before and after randomization. This technique has been widely used for vegetable oils and fats to evaluate the rearrangement of fatty acids after the interesterification, which is performed randomly by the chemical process (Guedes et al., 2014; Ifeduba et al., 2016; Speranza et al., 2015).

Figures 3 and 4 show the unsaturated and saturated fatty acids levels esterified at the different sites of the glycerol molecule (sn-1,3 and sn-2). In a characteristic configuration of natural vegetable oils and fats, lipid raw materials have the saturated fatty acids esterified mostly in the sn 1,3 position, while the unsaturated fatty acids are preferentially located in the sn-2 position (Silva et al., 2009).

Figure 3. Distribution of the fatty acids (%) at the sn-1,3 position on the TAG of fully hydrogenated microalgae oil (FHMO) and soybean oil (SO) in simple (S) and interesterified mixtures (I) in concentrations of 90:10, 80:20, 70:30, 60:40 and 50:50 (FHMO:SO) (w:w).

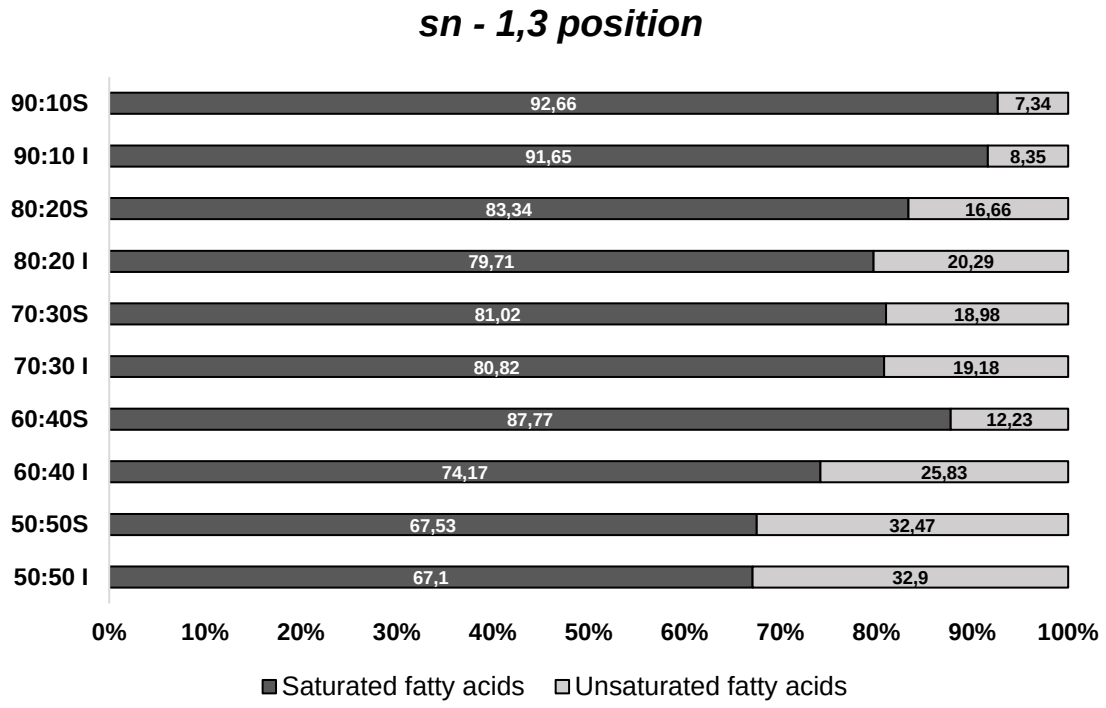

Figure 4. Distribution of the fatty acids (%) at the sn-2 position on the TAG of fully hydrogenated microalgae oil (FHMO) and soybean oil (SO) in simple (S) and interesterified mixtures (I) in concentrations of 90:10, 80:20, 70:30, 60:40 and 50:50 (FHMO/SO) (w:w).

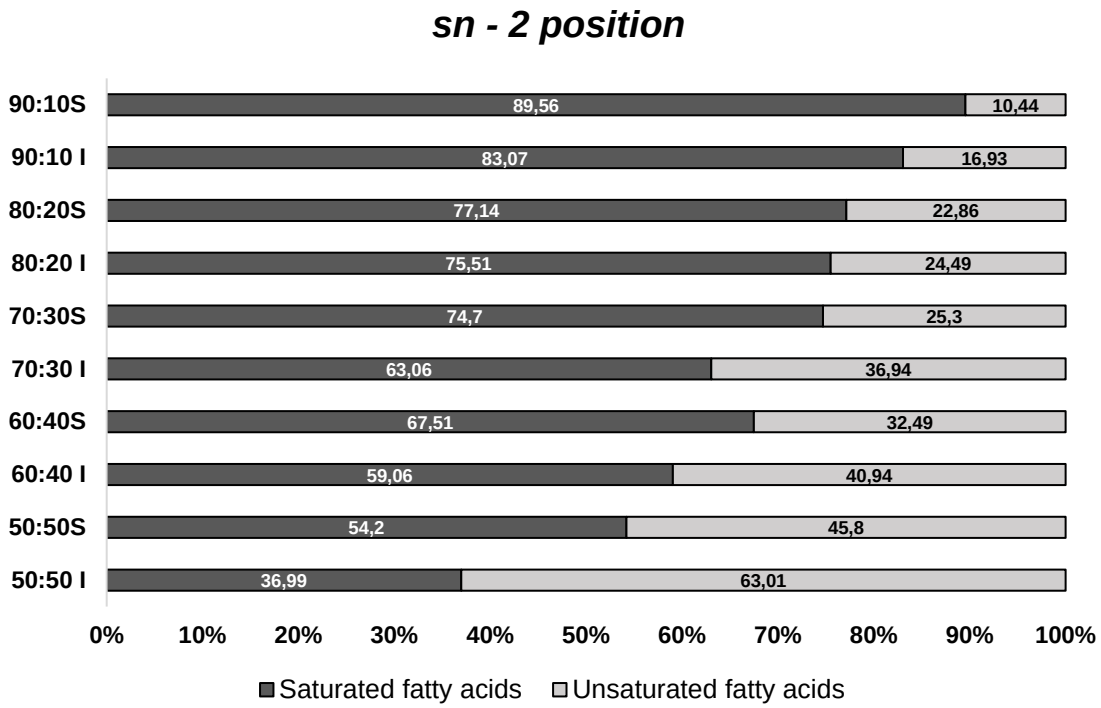

3.4. Thermal behavior

The chemical interesterification also modulates the thermal behavior due to the randomization of the triacylglycerol composition of the lipid matrices (Ribeiro et al., 2009; Rosseau & Marangoni, 2002). In the first studies on the chemical interesterification of blends of fully hydrogenated soybean oil and different liquid oils, although new curves referring to the formation of new TAGs were observed, the randomization did not change the shape of the crystallization curve, only reducing the enthalpy of the existing peaks, indicating that less energy is required to crystallize or melt the whole randomized system, due to less variation and distribution of polymorphic forms (Zeitoun et al., 1993).

The thermograms of the crystallization and melting behavior of the blends were analyzed before and after interesterification (Figure 5). Before randomization, the blends showed two crystallization peaks only at the ratios 90:10 and 80:20, possibly related to TAG S3 and U3, majority constituents of FHMO and SO, respectively, as well as the difficulty of interaction between these

components in the system. After the addition of SO, a simple exothermic peak was observed, possibly due to greater interaction or co-crystallization by the similarity of the chains in the raw materials, which are mostly composed of 18 carbons, with β-polymorphism. Also, the proportions closer to the mass balance of SO and FHMO led to an increase in compatibility due to the reduction of TAG S3 and U3.

Figure 5. Thermal behavior of crystallization and melting of simple (S) or interesterified (I) mixtures in the respective proportions: (FHMO/SO w:w): 90:10, 80:20, 70:30, 60:40 e 50:50.

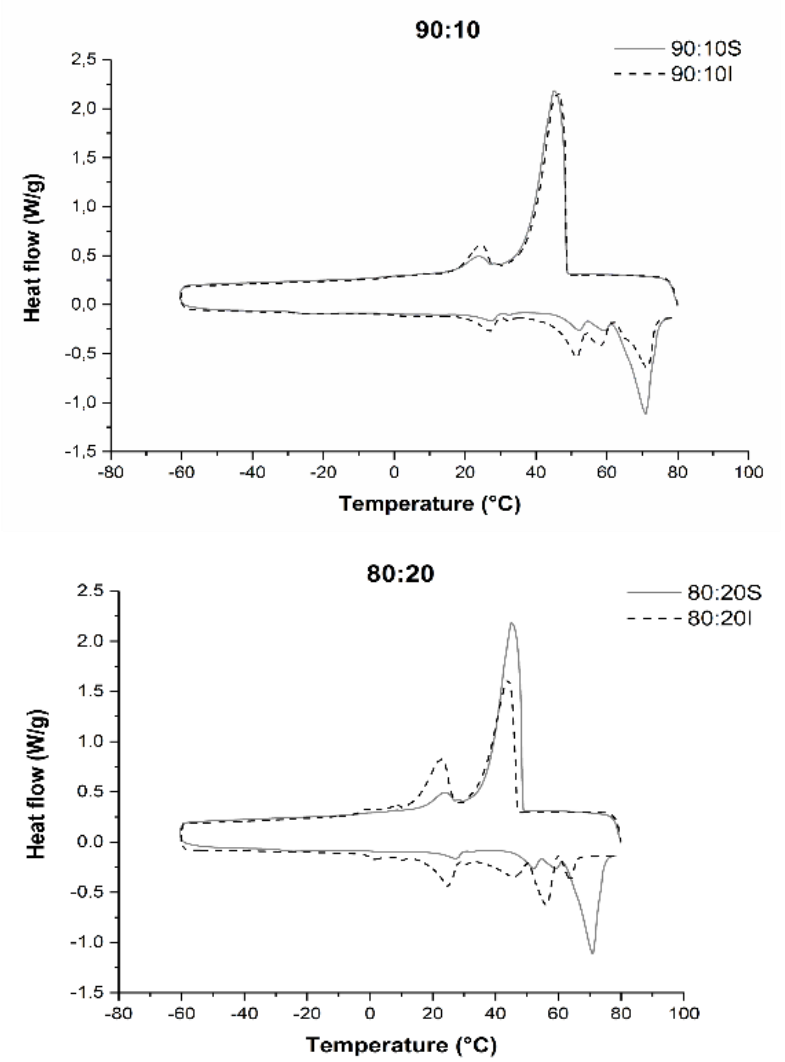

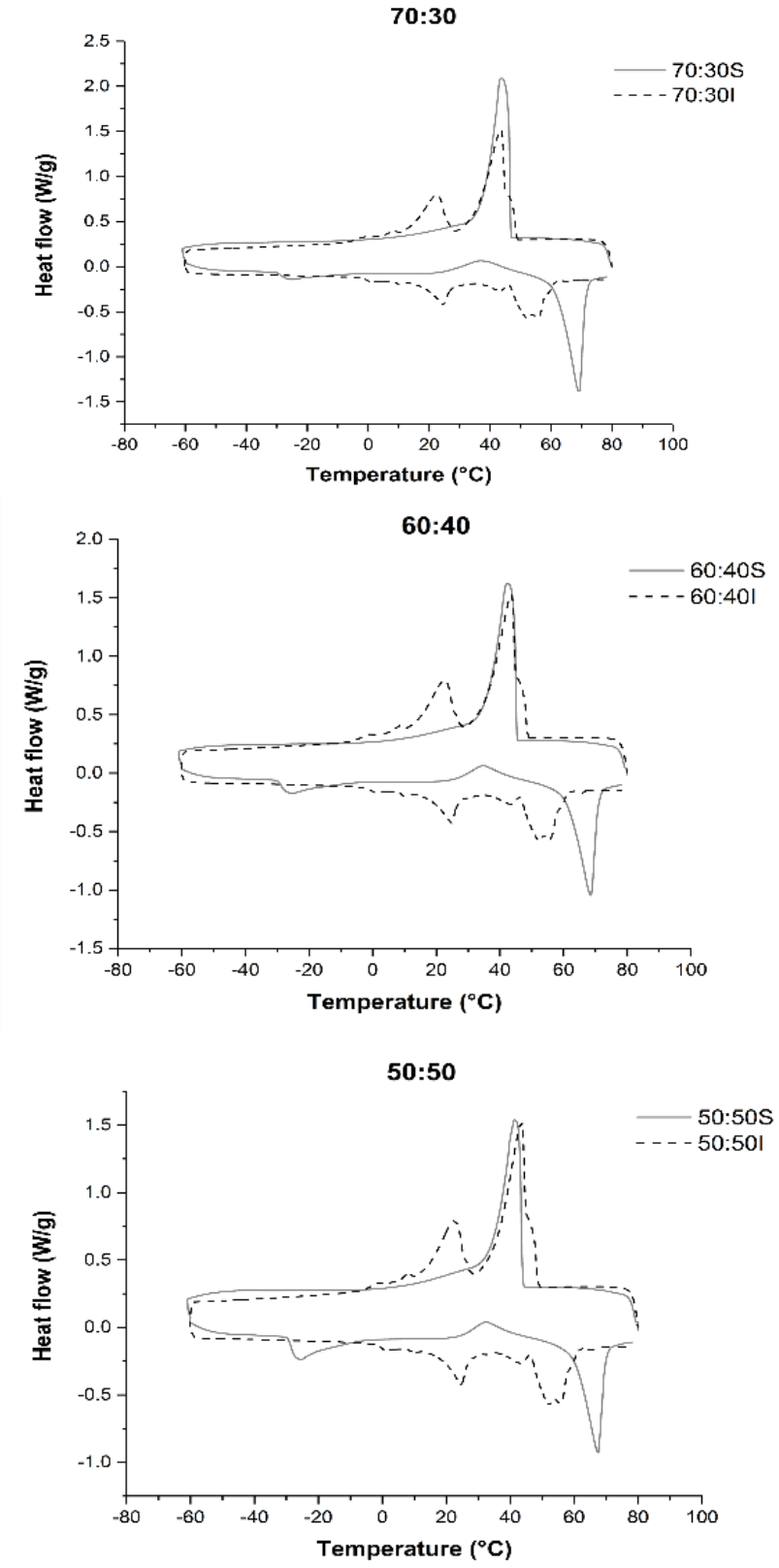

SO: Soybean oil; FHMO: Fully hydrogenated microalgae oil.

After randomization, all blends showed two exothermic peaks with a reduction in ΔH values for the first peak, indicating a lower contribution of more saturated TAGs in the interesterified blends, which was evidenced by the decrease in S_3 TAGs. In the second peak, there was an increase in ΔH values due to the intense formation of S_2U TAGs. Similarly, Ribeiro et al (2018) also reported a change in the crystallization profiles before and after the chemical interesterification. Two peaks appeared in the simple blend of high oleic sunflower oil and fully hydrogenated crambe oil, with a lower intensity, and after interesterification the second peak indicating increased in S_2U concentrations. Furthermore, there was a reduction in the intensity of the peaks after interesterification, probably due to a mixed crystallization from instantaneous and sporadic nuclei, which can be confirmed by the analyses of crystallization isotherm and microstructure (Ribeiro, et al., 2009b). Similar findings were also reported by Berčíková et al. (2020); Ribeiro et al. (2017); Ribeiro et al. (2009); Ribeiro et al. (2017), and Ribeiro et al. (2018), who found an intense formation of S_2U and decrease of S_3 after interesterification of blends of liquid oils and fully hydrogenated oils from various sources, resulting in two exothermic peaks referring to S_3 and SU_2 TAG fractions, respectively.

The analysis of the thermal parameters of the blends (Tables 3 and 4) indicated that the FHMO concentration in the simple blends was proportional to the initial crystallization temperature ranging from 49.02 °C (90:10) to 44.43 °C (50:50); and melting temperature, ranging from 54.09 °C (90:10) to -30.36 °C (50:50). When comparing the simple and interesterified blends in the same ratio, there was a slight reduction in all Tic with the FHMO reduction, with values of 0.35, 1.51, 2.65, 3.5, and 5.78 °C for the ratios 90:10, 80:20; 70:30; 60:40; and 50:50, respectively, with an intense reduction in Tif (~26.0°C) for all ratios. These results are due to the effect of randomization, which led to a decrease in S_3 and U_3 and an increase in S_2U for all ratios.

Table 3. Thermal behavior of crystallization of simple (S) or interesterified (I) blends in the respective proportions: (FHMO:SO w:w): 90:10, 80:20, 70:30, 60:40 e 50:50.

CRYSTALLIZATION						
Raw materials						
	T_i (°C)	**T_{p1}(°C)**	**∆H1 (J/g)**	**T_{p2} (°C)**	**∆H2 (J/g)**	**T_F(°C)**
FHMO	50.82±0.16	46.57±0.35	116.73±1.75			16.62±0.29
SO	-10.98±1.21	-20.57±0.36	12.13±1.70			-55.55±0.91
Blends						
	T_i (°C)	**T_{p1}(°C)**	**∆H1 (J/g)**	**T_{p2} (°C)**	**∆H2 (J/g)**	**T_F(°C)**
90:10S	49.02±0.08a	44.60±0.63b	104.73±1.49a			12.46±4.17 ab
90:10I	49.36±0.14a	46.63±0.69a	86.47±0.93b	24.63±0.36a	14.12±0.61c	3.57±1.06d
80:20S	47.98±0.08b	43.96±0.55bc	96.14±3.15ab			13.99±4.17ª
80:20I	46.47±0.53cd	43.95±0.41bc	63.73±0.07c	22.29±0.76b	24.06±2.60b	-6.76±1.39e
70:30S	46.98±0.08c	46.96±0.55bc	87.12±3.27b			11.98±2.37abc
70:30I	44.33±0.21e	42.51±0.81cd	45.29±0.48d	21.48±0.50bc	34.79±0.66a	-8.14±1.28e
60:40S	45.75±0.08d	42.28±0.36cd	71.49±9.42c			5.97±2.42cd
60:40I	42.25±0.14f	39.88±0.09e	33.14±0.23e	20.28±0.18c	39.38±0.68a	-10.51±1.92e
50:50S	44.43±0.35e	41.47±1.20d	64.17±1.55c			6.68±1.35bcd
50:50I	38.65±0.64g	36.63±0.76f	19.80±1.14f	18.17±0.82d	36.74±3.87a	-8.47±1.60e

SO: Soybean oil; FHMO: Fully hydrogenated microalgae oil. The letters in columns indicates the statistical differences by the Tukey test (P<0,05); Same letters did not show statistical differences between them.

Table 4. Thermal behavior of melting of simple (S) or interesterified (I) mixtures in the respective proportions: (FHMO/SO w:w): 90:10, 80:20, 70:30, 60:40 e 50:50.

	MELTING							
	Raw materials							
	T_i (°C)	**T_{p1}(°C)**	**∆H1 (J/g)**	**T_{p2} (°C)**	**∆H2 (J/g)**	**T_{p3} (°C)**	**∆H3 (J/g)**	**T_F(°C)**
FHMO	49.83±0.40	52.12±5.69	55.50±1.62	64.26±0.03	64.27±6.74	70.38±0.02	20.42±0.91	71.73±3.74
SO	-37.88±1.72	-25.07±2.42	48.79±3.70	-	-	-	-	48.79±3.70
	Blends							
	T_i (°C)	**T_{p1}(°C)**	**∆H1 (J/g)**	**T_{p2} (°C)**	**∆H2 (J/g)**	**T_{p3} (°C)**	**∆H3 (J/g)**	**T_F(°C)**
90:10S	54.09±0.57a	70.74±0.31a	125.43±1.40a	-	-	-	-	76.53±1.23a
90:10I	28.04±0.28b	33.05±0.05c	37.52±0.85e	42.21±0.16de	59.06±3.84a	65.25±0.14a	2.39±0.45a	64.15±0.65c
80:20S	56.79±0.61a	62.90±0.09b	107.50±0.70ab	-	-	-	-	75.19±0.87ab
80:20I	-2.74±0.43c	25.43±0.62c	66.80±12.93c	56.56±0.37b	36.78±7.02cd	63.73±0.07b	11.51±13.94[a]	66.83±0.78c
70:30S	54.51±2.68a	66.95±0.09ab	92.21±3.49b	-	-	-	-	73.64±0.09ab
70:30I	-4.64±0.51cd	24.01±0.11c	70.45±8.42c	55.24±0.17bc	40.94±0.72c	-	-	59.96±0.45d
60:40S	-27.14±5.71e	-22.20±5.52d	12.20±7.79e	68.67±0.11a	74.65±8.04[a]	-	-	75.70±1.63ab
60:40I	-3.92±0.37cd	23.13±0.01c	38.56±0.31d	53.41±0.04cd	37.72±0.26cd	-	-	57.31±0.37e
50:50S	-30.36±0.37e	-25.45±0.02d	23.18±3.55de	66.11±2.85a	60.04±3.81b	-	-	75.22±0.24ab
50:50I	-9.92±2.95d	20.36±0.33c	39.43±8.47d	49.77±0.49e	25.49±2.07d	-	-	54.23±0.43f

The letters in columns indicates the statistical differences by the Tukey test (P<0,05); Same letters did not show statistical differences between them.

Ribeiro et al. (2009) also reported lower S_3 and higher S_2U levels after randomization and increased crystallization speed as a function of the addition of fully hydrogenated soybean oil (FHSO). Berčíková et al. (2020) reported a similar behavior in fully hydrogenated oil matrices with high contents of long-chain fatty acids with neutral atherogenic effect (stearic, arachidic, and behenic acid), which

were selected as sources for the blends made with high oleic sunflower oil and fully hydrogenated erucic canola oil in different proportions subjected to modification by chemical interesterification. The authors reported a decrease in Tic with increasing saturated fatty acid contents in the blends, changes in the crystallization properties after chemical interesterification, and a decrease in high melting point TAG S3.

The results of the thermal parameters showed a shift and change in enthalpy (ΔH) of the exothermic peaks (crystallization). The increase in FHMO promoted uniformity of the crystallization curve, with an increase in ΔH, showing greater participation of more unsaturated TAGs in the interesterified systems. Concerning the endothermic peaks (melting) of FHMO:SO (w:w) at the ratios 70:30, 60:40, and 50:50 after randomization, new peaks were formed for the blends 90:10 and 80:20, indicating greater regularity in the triacylglycerol distribution, especially in the systems with lower FHMO concentrations. Berčíková et al. (2020) also reported the disappearance of the endothermic peaks of highly saturated TAGs, with the formation of new, broader, and less defined peaks after chemical interesterification.

The results of this study are very similar to the studies of those authors, confirming the effect of the continuous lipid phase and the modification of thermal parameters caused by the balanced fatty acids distribution after interesterification. This characteristic facilitates the use of lipid blends in various products, reducing the incompatibility between the raw materials and broadening their applicability once it prevents phase separation at specific temperatures.

3.5. Solid fat content (SFC)

Studies have shown changes in the SFC after chemical interesterification, favoring more linear profiles, according to the great variability of the triacylglycerol species formed (Gunstone et al., 2007; Martini et al., 2005; Rosseau & Marangoni, 2002). In addition, the SFC results can guide the application of the fat obtained, ensuring spreadability characteristics and minimizing waxiness during consumption (O'Brien, 2004).

As expected, the SFC profiles of the blends of the present study (Figure 6) were proportional to the amount of FHMO, due to the content of saturated fatty

acids in the hardfat composition, mainly stearic acid (C18:0 - 93% w:w), which has a high melting point. A similar result was reported by Berčíková et al. (2020), who evaluated the effect of different saturated fatty acids on interesterified matrices with up to 20% variation in SFC at 40 °C, and observed a gradual and constant melting. In addition, Guedes et al. (2014) found that the SFC of the blends was dependent on the addition of fully hydrogenated crambe oil to soybean oil, for all temperatures studied.

Figure 6. Solid fat content (SFC) profile for the simple (S) and interesterified (I) mixtures in the respective proportions (FHMO/SO w:w): 90:10, 80:20, 70:30, 60:40, 50:50.

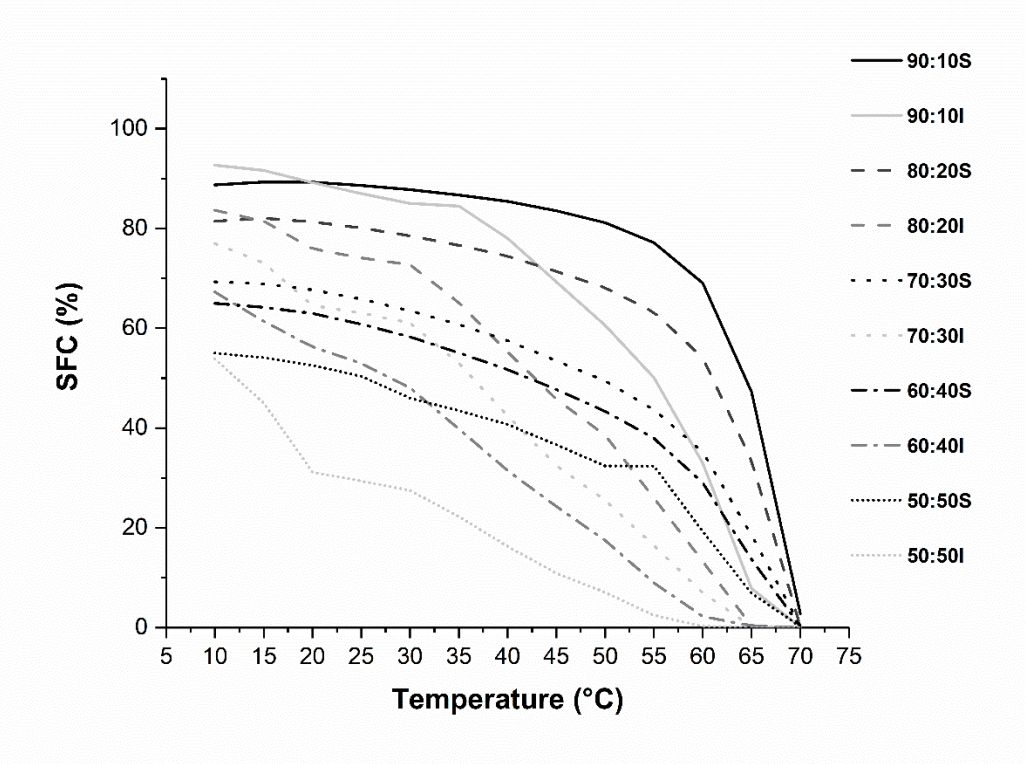

FHMO: Fully hydrogenated microalgae oil; SO: Soybean oil.

A slight differentiation in the solid fat profiles was observed as a function of randomization. With less pronounced curves, the interesterified blends showed an almost linear decrease in SFC from 35 °C until the complete melting of the blends (65 to 70 °C). For all ratios, the simple blends showed higher SFC values when compared to the interesterified fats.

The differentiation between blends after randomization is mainly due to the TAG reorganization since the increase in SFC is closely related to higher S_3 TAGs concentrations in the simple blends, while the SFC reduction is due to the presence of S_2U TAGs formed after randomization. The present results

corroborate the findings of Berčíková et al. (2020), Ribeiro et al. (2017); Rashid, et al. (2016), and Ribeiro et al. (2017, 2018), who studied combinations of diverse liquid and solid lipid matrices and reported lower SFC levels after interesterification, due to the reduction in S_3 and simultaneous increase in S_2U. This differentiation ensures greater fat plasticity, leading to the slope of the curve for the fats subjected to chemical interesterification (Guedes et al., 2014; O'Brien, 2004).

In palm stearin-rich systems, which contain stearic acid as the major fatty acid, as well as FHMO, there was an increase in SFC as a function of the stearin content due to high melting point TAGs. However, blends made with palm stearin and cottonseed oil provided better melting properties and spreadability at application temperature, and randomization provided lower SFC and fats more suitable for use in products such as margarine and chocolates, which require good spreadability and melting at body temperature (Rashid, Safuan, et al., 2016). Similarly, the present study showed high SFC contents (above 32%) for the simple blends for all application temperatures (25°C and 35°C), while only the interesterified blend 50:50 showed adequate spreadability, with SFC of 22% at 35 °C.

Furthermore, as observed in the thermal behavior, the TAG modification reduced the Tif by approximately 20 °C for all ratios studied, providing a fast-complete melting of the interesterified blends, as shown by the SFC curve. The representative melting point (MP) of the blend consists of the temperature corresponding to 4% of solids (Karabulut et al., 2004; Kok et al., 1999; Ribeiro, Basso, Grimaldi, Gioielli, & Gonçalves, 2009).

Thus, the blends of this study showed a reduction in MP as a function of the FHMO contents and TAG reorganization since the blends showed a 5 °C reduction in MP after randomization except for the blend 90:10 (Table 5) when compared to their simple counterparts. A similar result was reported by Ribeiro et al. (2017), who observed that the fat obtained by chemical interesterification exhibited a lower melting temperature than the non-interesterified blends.

Table 5. Melting point of simple (S) and interesterified (I) mixtures in the respective proportions (FHMO:SO w:w): 90:10, 80:20, 70:30, 60:40, 50:50.

Melting point (°C)									
90:10S	**90:10I**	**80:20S**	**80:20I**	**70:30S**	**70:30I**	**60:40S**	**60:40I**	**50:50S**	**50:50I**
70a	70a	70a	65b	70a	65b	70a	65b	70a	65b

The letters in columns indicates the statistical differences by the Tukey test (P<0,05); Same letters did not show statistical differences between them. FHMO: Fully hydrogenated microalgae oil; SO: Soybean oil.

The differences before and after randomization are probably due to the TAG composition of the blends. Although they still contained high stearic acid levels, randomization increased S_2U TAGs, with greater variability of fatty acids esterified to glycerol, with a reduction mainly in the U_3 TAG levels.

According to Bot & Flöter (2013) and O'Brien (2004), S_2U TAGs, which were the majority after randomization, present a melting range of 27 to 42 °C covering body temperature and providing greater plasticity and technological functionality to the products. The author divided TAG into regions according to the physical state of TAG, consisting of refrigeration (-10 to 5 °C), room (10 and 30 °C), body (30 to 45 °C), and higher temperatures (above 50 °C). Due to their composition in unsaturated fatty acids, U3 TAGs are classified as liquids at the refrigeration temperature since they have a low melting point; SU2 TAGs are in liquid the second region since they are liquid from 10 °C up to room temperature (~25 °C), S_2U TAGs are classified in the third region since they melt near body temperature, while S_3 TAGs are considered high melting point TAGs, with melting temperatures above 50 °C.

However, it is known that lipid raw materials of vegetable, animal, or microbial origin are not composed of pure TAGs. They consist of a blend of TAGs with the most diverse liquid characteristics, which when in combination generate melting ranges that can define the technological applicability of the fat. The simple blend 90:10 presented higher S_3 contents (88.4%), with similar distribution for the other triacylglycerol classes (1.99, 4.38, and 5.18% for S_2U, SU_2, and U_3, respectively), which directly impacted the higher initial melting temperature (54.09 °C) and crystallization temperature (49.02 °C). Consequently, a higher enthalpy was associated with these thermal processes, and the final melting

temperature determined by DSC was very similar to that observed in the 4% solids profile, with values of 76.53 and 70 °C, respectively.

Similar results were observed for the other simple blends. The decrease in FHMO reduced the S_3 contents, which were 77.07, 74.29, 67.81, and 54.17% in the blends 80:20, 70:30, 60:40, and 50:50, respectively, with a proportional increase mainly in SU_2 and SU_3 contents. Therefore, the initial crystallization and melting temperatures decreased as a function of the S_3 content in the simple blends, as well as the enthalpy and final melting temperature, which varied from 76.53 °C (maximum value in the blend 90:10) to 75.22 °C (minimum value in the blend 50:50), with the same melting temperature according to the SFC profile.

However, after randomization, these parameters changed along with the distribution of the triacylglycerol classes. The interesterified blends showed lower S_3 contents with an expressive increase in S_2U, which may broaden their application, due to the greater contribution of S_2U TAGs in the thermal parameters, which increases the fat plasticity. These blends presented S_3 and S_2U contents of 83.47 and 12.67%, 72.25 and 23.97%, 61.93 and 34.47%, 50.52 and 44.20%, and 36.85 and 57.58%, for the blends 90:10, 80:20, 70:30, 60:40, and 50:50 respectively. Thus, there was an inversion of majority TAGs as a function of the addition of SO in the blends, which directly impacted the thermal parameters, with a reduction of the initial crystallization temperature from 49.36 to 38.65 °C for the formulations with higher FHMO and SO contents, respectively. In addition, a reduction of the initial melting temperature from 28.04 to -9.92 °C was observed, which shows the strong influence of the TAG composition on the thermal behavior of fats. A reduction in the final melting temperature was also observed when compared to the simple blends, which can be directly correlated to the results of the solids profile, reducing from 66.15 to 54.23 °C for the blends with higher FHMO and SO contents, respectively.

The TAG composition can also guide the technological application of these blends as a function of the SFC and thermal behavior. SFC below 25 °C characterize the hardness of the fat, while SFC values between 25 and 30 °C indicate the resistance of the fat to heating/melting. The onset of melting occurs from 27 to 33 °C followed by the release of flavor and freshness of the product in the mouth. The presence of a solid fat fraction at temperatures above 35 °C can

lead to an unpleasant waxy aftertaste (Bot & Flöter, 2013; Michael Eskin & List, 2017).

In this context, the characteristics of blends with different FHMO:SO ratios allow using all simple blends in bouillon cubes, soups, granules, and matrices for micro and nanoparticles, which require strength and physical stability at room temperature (25° C) with SFC higher than 10%, fast crystallization, and melting point higher than body temperature (above 35 °C) with possible targeting to the most stable β-polymorph, once these applications do not require aeration, creaminess, and plasticity. Regarding the interesterified blends, the blend 50:50 exhibited higher plasticity and possibility of applications. The other blends can be used as coating materials in lipid nanoparticles, providing stability and good incorporation once the interesterification reaction can guide the crystals to the β' polymorph indefinitely.

The SFC also allows assessing the compatibility between the raw materials used in the simple blends and their profile after interesterification by identifying possible interactions through the iso-solids diagram or compatibility diagram (Figure 7).

Figure 7. Isosolid diagrams of FHMO:SO in simple (A) and interesterified (B) blends.

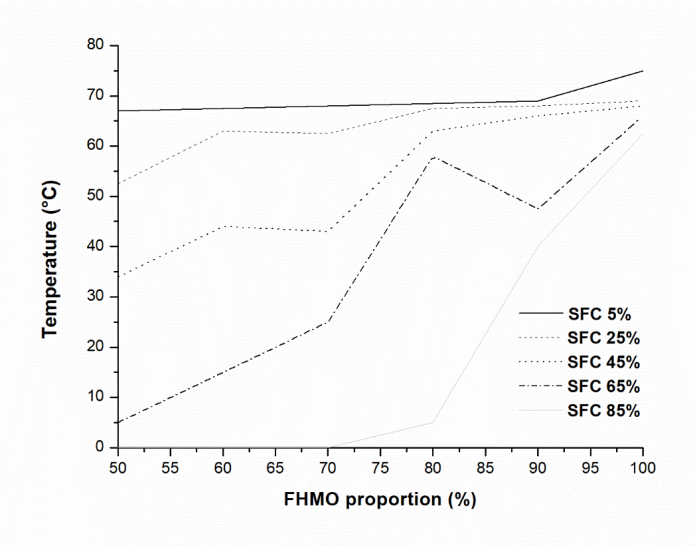

A

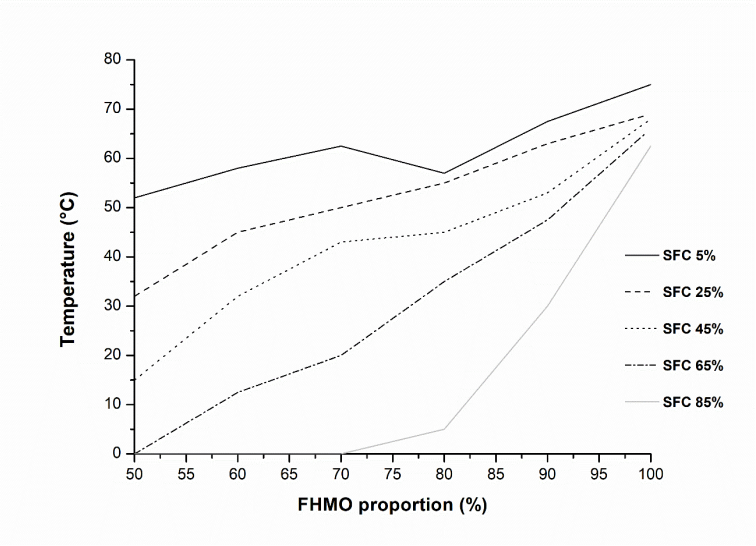

B

This diagram allows the identification of the mode of interaction between the raw materials in the blend, which can generate continuous, eutectic, or monothetic solid solution systems. A eutectic effect was observed for the simple blends containing 70% and 90% of FHMO, with depressions in the curves for the various solid contents. This result is due to the interaction between oil and hard fat, with a large amplitude of melting points due to the majority TAGs of each raw material, with a predominance of S3 and U3 in FHMO and SO, respectively (D'Agostini, 2014). This effect indicates an incompatibility between the raw materials and is considered undesirable once it can lead to early softening of the blends, which is usually reduced or eliminated after interesterification.

In the interesterified blends, the depression in the solids curve was observed only for the blend with 80% FHMO and 5% SFC, which can be classified as a eutectic point at these ratios. This result is due to the variation of the blend components including molecular volume, polymorphic form, and less variation in melting point. It was not a standard behavior along the SFC curves, thus there was more compatibility between OS and FHMO after the interesterification due to the increase and predominance of S2U TAGs with an intermediate melting point, characterizing monothetic systems.

3.6. Crystallization kinetics

As observed in the thermal behavior, the modification of the TAG distribution by the chemical interesterification changes the energy requirements for melting or crystallization of the system, modulating the growth rate and the size of the crystals formed (Foubert et al., 2006). In this study, Avrami's model was used to describe the kinetics of crystallization by nucleation and crystal growth under isothermal conditions, providing information about the nature of the crystallization process. In this model, the constant k is the crystallization rate constant, and the Avrami exponent (n), also called the crystallization index, indicates the crystal growth mechanism, which can occur by instantaneous nucleation (nuclei appearing altogether at the beginning of the process) or sporadic nucleation (number of nuclei increasing linearly with time) in the form of needles, disks, or spherulites (Wright et al., 2000).

As can be seen in the graphical representation of the crystallization isotherms at 25 °C (Figure 8), the simple blends stabilized faster than the interesterified blends. In addition, before the reaction, the curves had hyperbola characteristics becoming sigmoidal due to the lower crystallization rate after interesterification. This modification was also reported by Ribeiro et al. (2009).

Figure 8. Crystallization kinetics for the simple (S) and interesterified (I) mixtures in the respective proportions (FHMO/SO w:w): 90:10, 80:20, 70:30, 60:40, 50:50.

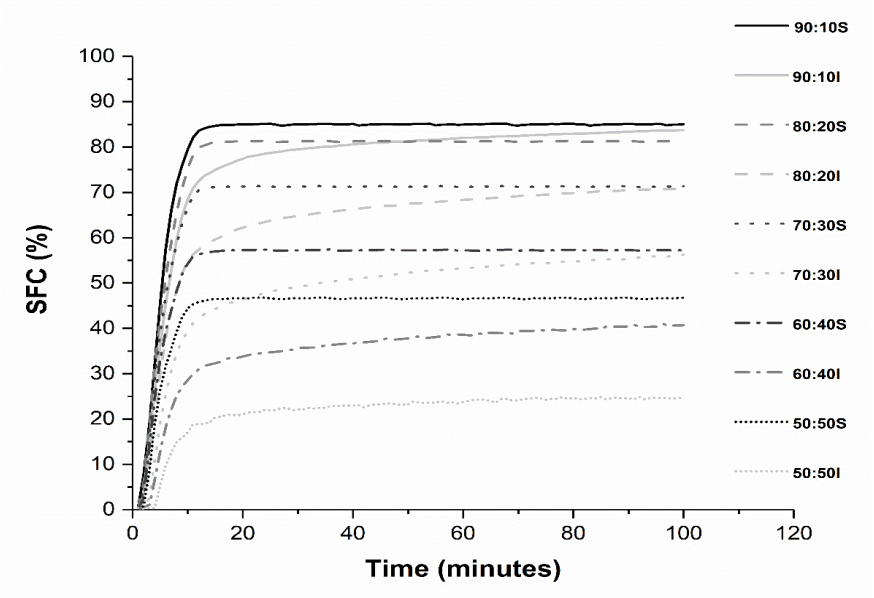

. FHMO: Fully hydrogenated microalgae oil; SO: Soybean oil.

The results of Avrami and isothermal curve parameters are presented in Table 6. As expected, the addition of SO to FHMO led to a reduction in the maximum solid content (SFCmax) and the interesterified blends had lower SFCmax when compared to the simple blends. Therefore, fatty acid randomization decreased the SFCmax for all concentrations studied due to the decrease in S3 TAGs and simultaneous increase in S2U TAG, ranging from 2.08 to 21.88% for the blends 90:10 and 50:50, respectively, before and after the reaction. Regarding the crystallization induction time (ƮSFC), the simple blends showed similar induction times (2 minutes), while the interesterified blends showed longer time, as a function of SO concentration (from 2 to 4.25 minutes). This is an important parameter for defining the applicability of the lipid bases since the formation of the triacylglycerol species S2U and SU2 contributes to higher ƮSFC values, which is associated with greater polymorphic homogeneity at 25 °C, due to the longer time for TAG organization in the crystal network, allowing better organization (Rosseau & Marangoni, 2002).

Reductions in SFCmax and ƮSFC in interesterified fats were observed by Ribeiro, et al. (2009), and Ribeiro et al. (2009) for fully hydrogenated canola oil and cottonseed oil blends, and fully hydrogenated soybean oil and soybean oil blends, respectively, which was also related to the lower TAG S_3 percentages and simultaneous increase in S_2U and SU_2 contents after interesterification.

Regarding Avrami's parameters, the k values showed a lower crystallization rate in the interesterified blends when compared to the respective simple blends, which agrees with the results of SFCmax and ƮSFC. However, the k values of the blends made with different FHMO and SO ratios varied from 0.03 for the simple blends at 90:10, 80:20, 70:30, and 60:40 to 0.01 for the respective interesterified blends, while the blend 50:50 presented a variation from 0.02 to 0.06 in the simple blend and interesterified blend, respectively. Similar changes were observed by Zhu et al. (2018), who attributed the results to the high TAG S_3 contents in the simple blends, mainly triestearin (SSS), which can act as a crystallization inducer due to its high melting point. In contrast, a reduction of the k-value was observed with a reduction of approximately 13% of SSS after interesterification (Meng et al., 2011).

Table 6. Crystallization kinetics parameters for the simple (S) and interesterified (I) mixtures in the respective proportions (FHMO/SO w:w): 90:10, 80:20, 70:30, 60:40, 50:50.

Sample	$\tau_{SFC\ (min)}$	SFC $_{máx\ (\%)}$	Half-time	K $_{(min^{-n})}$	*n*	R^2	ΔSFC
90:10S	2±0.00b	85.13±2.38a	4.86±0.00a	0.03±0.00a	2.03±0.00	0.99±0.00	2.08
90:10I	2±0.00b	83.69±0.08ac	5.82±0.04a	0.01±0.00a	1.41±0.00a	0.98±0.01	
80:20S	2±0.00b	81.36±4.16bc	4.99±0.92a	0.03±0.02a	1.92±0.00a	0.99±0.03	10.44
80:20I	2.3±0.58b	70.92±6.32bc	6.14±0.81a	0.01±0.04a	1.00±0.04a	0.95±0.02	
70:30S	2±0.00b	71.37±6.01c	4.86±0.12a	0.03±0.02a	1.95±0.00a	0.99±0.00	15.13
70:30I	3.3±1.00ab	56.24±0.78d	7.87±0.38a	0.01±0.00a	1.00±0.00a	0.93±0.00	
60:40S	2±0.00ab	57.43±0.31d	4.72±0.24a	0.03±0.01a	2.00±0.00a	0.99±0.00	16.32
60:40I	3.3±1.15a	41.11±10.62d	4.72±2.28a	0.01±0.04a	1.00±0.00a	0.95±0.02	
50:50S	2.66±0.58ab	46.77±0.22d	4.90±0.00a	0.02±0.00a	2.15±0.00a	0.99±0.01	21.88
50:50I	4.25±0.01ab	24.84±0.05e	8.01±0.00a	0.06±0.00a	1.12±0.00a	0.94±0.01	

FHMO: Fully hydrogenated microalgae oil; SO: Soybean oil; τ_{SFC}: Induction period, SFCmáx: maximum solid fat content, k: Avrami constant, n: Avrami exponent (n) and R^2: respective coefficients of determination. The letters in columns indicates the statistical differences by the Tukey test (P<0,05); Same letters did not show statistical differences between them.

In general, n value, which indicates the type of nucleation and crystal morphology, is an integer value. However, fractional numbers may indicate crystal formation with similar morphology and different or simultaneous types of nucleation (sporadic and instantaneous). In this study, fractional numbers were observed in the vast majority of the blends, with differentiation between the fractions before and after randomization with values of n = 1 or n= 2, respectively. This result indicates that nucleation was preferentially instantaneous in the single blends, with the formation of needle-shaped crystals, i.e., the crystalline nuclei appear all at once at the onset of crystallization. In turn, nucleation after randomization may change or not, with the formation of needle- or disk-shaped

crystals, and instantaneous or sporadic nucleation in all the interesterified blends (Marangoni & Campos, 2005; Martini et al., 2005). Therefore, the TAG modifications by chemical interesterification may not affect the crystal morphology and nucleation mechanism in the blends, only leading to a change in crystallization dynamics, making it sporadic, which is consistent with the results of longer induction time for crystal formation after the reaction.

The random fatty acids distribution in glycerol molecules shows less thermodynamically favorable crystal growth, requiring more energy than simple blends, affecting the crystallization rate properties, rather than the crystal morphology or type of nucleation (Ribeiro et al., 2009).

In addition to these parameters, the crystallization half-time was evaluated, which corresponds to the time required to crystallize 50% of the total lipid system. This time was always shorter for the simple blends when compared to the corresponding interesterified fractions, which was expected due to the higher crystallization rate and shorter induction time of the blends before randomization. Zhu et al. (2018) correlated the crystallization half-time and polymorphic transition, an important parameter of fat applicability in foods. The authors reported that the polymorphic transition rate was inversely proportional to the half-life, i.e., the faster the crystallization, the slower the polymorphic transition, which may drive the application of the matrices produced.

Considering the fatty acid composition of the raw materials and the high tristearin content of FHMO, there was a correlation with the study of Ribeiro et al.(2009), who used SO associated with fully hydrogenated soybean oil (FHSO) in simple and chemically interesterified blends. As observed in the present study, soybean oil had high unsaturated fatty acids levels, mainly polyunsaturated FA, represented by linoleic, oleic, and linolenic acids, respectively. Therefore, the total hydrogenation of this lipid matrix led to an increase in fully saturated 18-carbon fatty acid, stearic acid, by 87%. Similarly, Ribeiro et al. (2009) reported a reduction of SFC max and an increase in crystallization induction time after interesterification of blends made with higher SO contents (SO: FHSO 90:10 to 50:50; w:w). This result was also associated with decreased S3 contents, increased S2U, and a simultaneous increase in SU2. The changes in the triacylglycerol profile were different from that observed for the association of SO and FHMO in the present study. Due to the higher stearic acid and triesterarin

levels, there was no increase in SU2 contents, with an increase in S2U, despite the important change observed in the crystallization parameters after interesterification.

Herrera et al. (1999) also associated the slower crystallization with the formation of acylglycerols (mono- and diacylglycerols) after the interesterification reaction. This event was not observed in the present study, once a washing step with heated ethanol was performed after the interesterification reaction, as described by Narine e Marangoni (1999), aimed at removing possible remaining acylglycerols from the interesterification, through polarity and affinity with the ethanol fraction.

Regarding the Avrami parameters, Ribeiro et al., 2009b observed a reduction in the crystallization rate after the chemical interesterification and a predominance of disk- or needle-shaped crystals with sporadic or instantaneous nucleation due to the value of n=2. However, a change in crystal structure and nucleation was observed in the blends, with the predominance of SO and n=3, which indicates the formation of spherulitic crystals, similar to the present study, considering that the maximum SO ratio used in this study was 50%.

3.7. Polymorphism

In general, the more heterogeneous the triacylglycerol structure, the lower tendency to form β-polymorphs (Oh et al., 2005). Therefore, it was expected that the simple blends and those with higher proportions of FHMO would stabilize in the polymorphic β-form, due to the high stearic acid content and, consequently, higher tristearin content in the blends.

Concerning the raw materials alone, the polymorphic α habit was observed in the FHMO, with an intense peak of 4.12 Å, characteristic of fully hydrogenated oils at the onset of crystallization (Ribeiro et al., 2017). This polymorphic form is the most unstable form, usually detected early in the crystallization process, which can transform into the more stable β' and β forms over time, once the polymorphic transformation always occurs monotropically towards the most stable form (Sato & Ueno, 2005). Soybean oil was not evaluated for the polymorphic form because there was no crystalline phase at the temperature of

analysis. However, it is known that SO is characterized by the β polymorph, which is considered the most stable form (Demodaran et al., 2010; O'Brien, 2009).

Regarding the simple blends, there was a predominance of polymorphic β form, followed by β' form after the interesterification, except for the blend 80:20I, which showed polymorphic β and β' simultaneously, less sharp peaks, and a larger liquid region, indicating lower crystallinity of the blends at the temperature of analysis. These results are consistent with the SFC results, once the interesterified blends showed lower SFC, which is the amount of crystallized fat when compared to the simple blends at 25 °C. Lower crystallinity was also observed for the FHMO:SO blends with increasing the SO contents for both the simple and interesterified blends, with less sharp peaks, and a more pronounced appearance of the liquid region.

As reported by Rosseau & Marangoni (2002), the results of the present study proved that the chemical interesterification of the blends can be an important tool to stabilize the polymorphic β′ form, while the formation of TAGs with a wide variety of fatty acids leads to a less ordered packing and less dense crystalline structures. Therefore, the interesterified blends showed β' form (peaks mostly at 4.2 and 3.8Å), while the simple blends showed polymorphic β form (peak at 4.55Å), as presented in Figure 9.

The SSS type TAGs, which was present in expressive amounts in the blends, mainly in the simple blends, have a high melting point (60-73 °C) while the new TAGs (SU2 and S2U) formed after the interesterification have an average melting point between 27 °C and 42 °C, which may cause modifications in the crystal morphology of fats and changes in the types and content of polymorphs. Thus, simple blends are more likely to present β-type crystals, while interesterified blends are more likely to present β' crystals (Rosseau & Marangoni, 2002; Zhu et al., 2019).

Similar findings were reported by Ribeiro et al. (2017), Narine and Humphrey (2004), Rashid et al., 2016; Ribeiro, et al. (2009a), and Zhu et al. (2019), who observed peaks of strong intensity before randomization, characterizing the β-form with concomitant presence of the β′ polymorph, at low intensity, while two peaks of variable intensity were observed after the reaction, corresponding only to the β' polymorph. According to some authors, this behavior is due to crystal formation favored by the triacylglycerol composition (Metin &

Hartel, 2005). The authors also related the dominance of the polymorphic β-form in the simple blends to the fully hydrogenated oil content, as stated by Marangoni & Rosseau (2002).

Knowledge about the crystal structure of lipid bases is important in formulating fats for application in various products since each crystalline form presents distinct properties related to plasticity, texture, solubility, and aeration (O'Brien, 2004). Fats that have crystals in the β′ form are softer and ensure good aeration properties, while those characterized by the β form have low aeration capacity and can cause a sandy perception in products (Takeuchi et al., 2002). Therefore, interesterified blends with a predominance of the polymorphic β′ habit have greater applicability, especially in fatty products such as margarines, confectionery, and bakery products (Oh et al., 2005).

Figure 9. Micrographs obtained at 20x and ray-x diffraction for the simple (S) and interesterified (I) mixtures and the respective diffractograms indicates for all proportions (FHMO/SO w:w): 90:10, 80:20, 70:30, 60:40, 50:50.

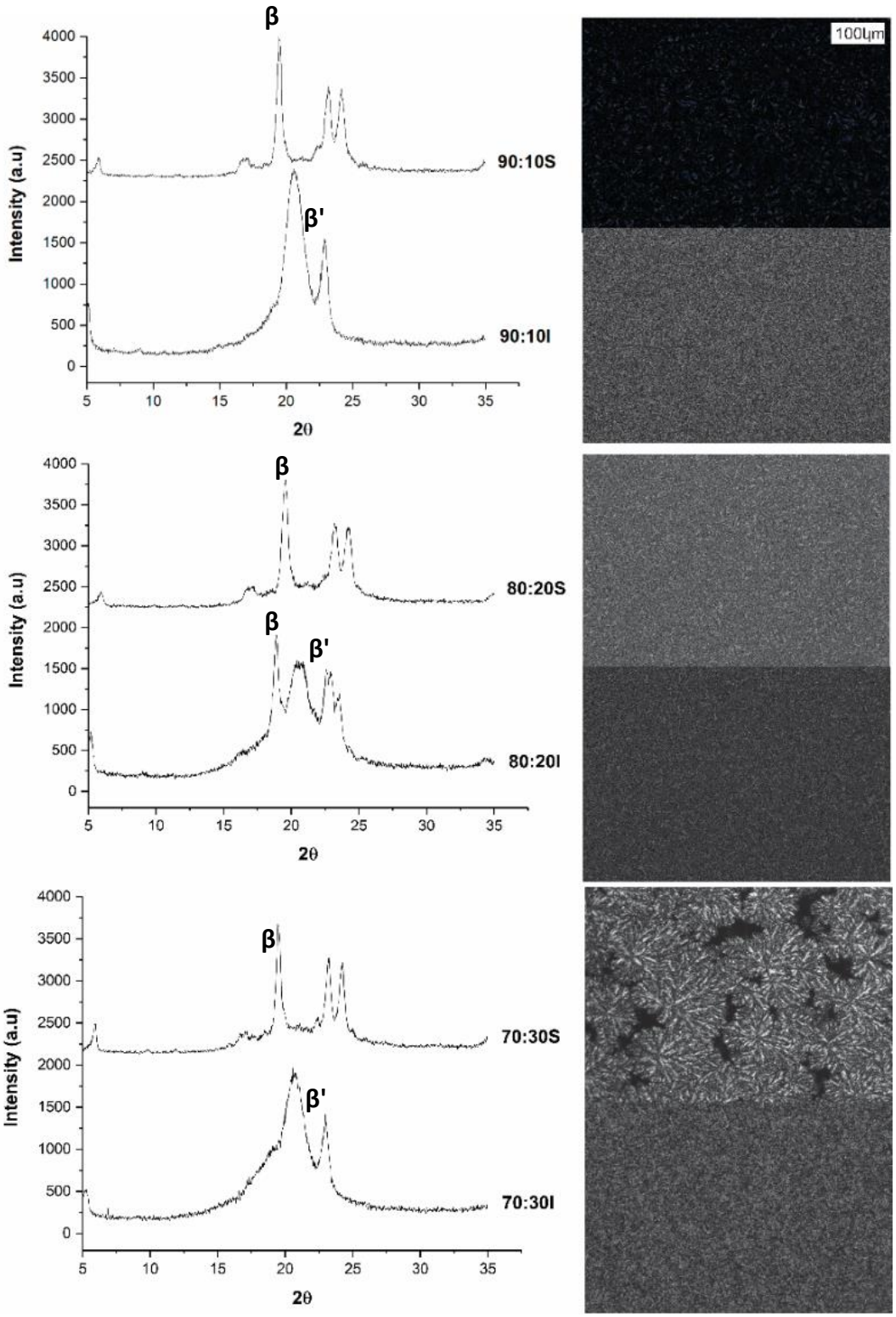

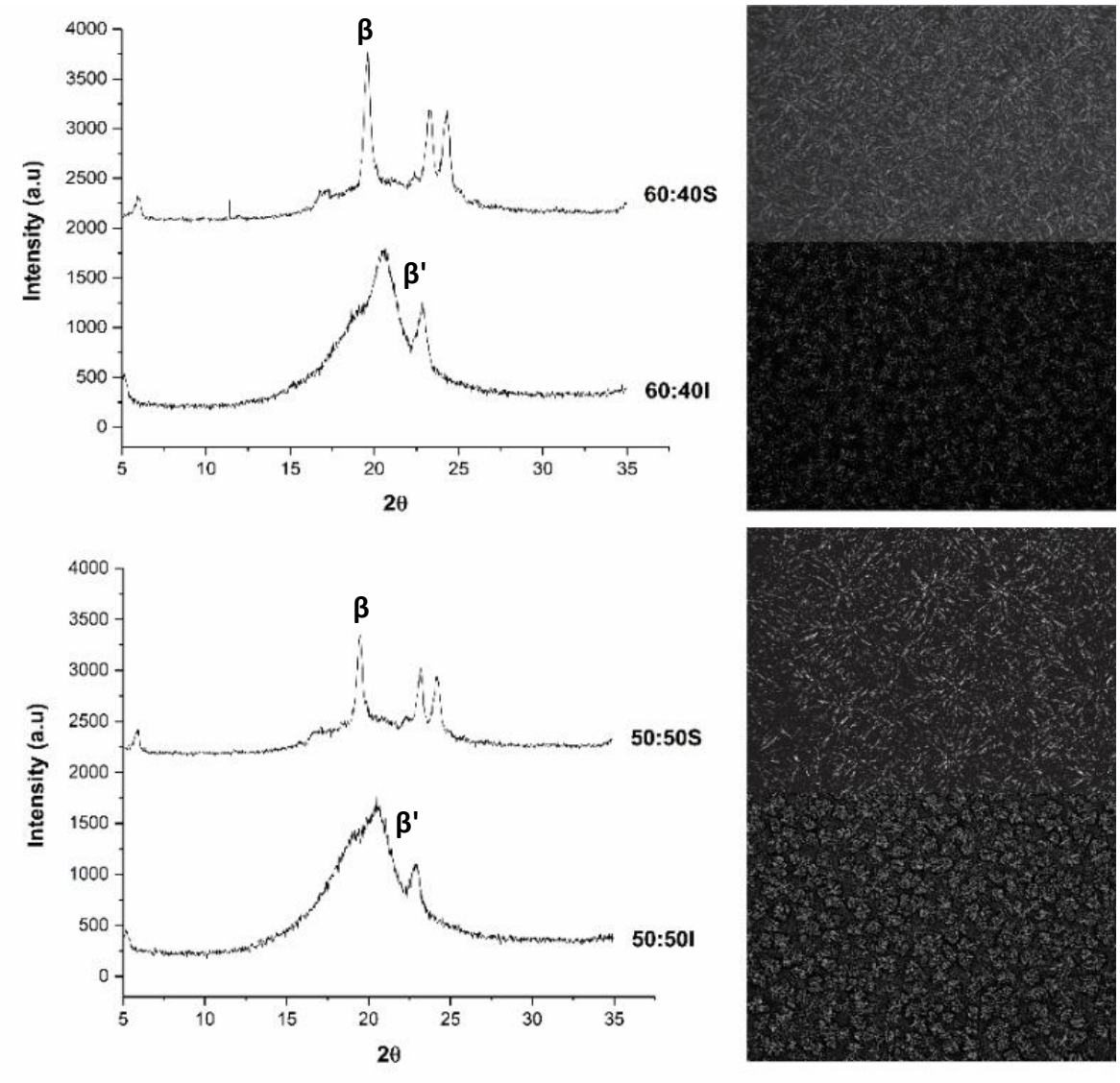

FHMO: Fully hydrogenated microalgae oil; SO: Soybean oil.

3.8. Microstructure

As also observed for the polymorphism, the different molecular packing affects the morphological characteristics and the density of the crystal network, which in turn defines the fat behavior regarding the attributes texture, appearance, and functionality (Rousseau et al., 1998). The lipid composition, as well as the crystallization conditions and the SFC, directly affect the different polymorphic

and morphological forms of crystals, which can be detected by polarized light microscopy analysis (Kamarulzamana, et al., 2016).

Previous studies have reported that interesterification promotes visible changes in crystal morphology mainly concerning the crystal size, with the presence of smaller crystals after the reaction (Rosseau & Marangoni, 2002)

As can be seen in Table 7 and Figure 9, the non-randomized blends showed larger disk-shaped crystals, with a maximum diameter of 32.66±4.61 μm for the blend 90:10S, and mean diameter ranging from 18.91±1.19 (90:10S) to 13.66±0.79 μm (50:50I), as observed in the microstructure and confirmed by the Avrami parameters. After randomization, smaller needle- or disk-shaped crystals were observed (mean diameter 16.55±0.94 to 12.55±0.49 μm), as shown by Avrami's exponent. Despite the smaller crystal size, there was an increase in the crystallized area in the interesterified blends, except for 90:10S, which was similar to its single fraction. However, the fractal dimension of the blends was regular, with no great changes before and after randomization.

Table 7. Parameters of crystalline networks formed before (S) or after randomization (I) in the mixtures in the respective proportions (FHMO/SO w:w): 90:10, 80:20, 70:30, 60:40, 50:50.

Samples	Maximum diameter (μm)	Mean diameter (μm)	Crystalized area (%)	Clusters	Singles
90:10S	32.66±3.41a	18.91±1.19bc	43.24±3.14a	707±77.94cde	735.66±81.56de
90:10I	24.43±1.91a	14.89±0.68c	41.00±9.03a	1066±92.97a	1366.33±320.74abc
80:20S	21.15±0.26a	13.47±0.15c	31.35±3.36ab	889.33±5.13abcd	1702.5±113.24ab
80:20I	22.38±4.26a	13.96±2.22c	37.12±13.13a	1018.33±70.59ab	1660.66±61.93ab
70:30S	28.50±0.63a	17.49±0.25a	29.07±1.31ab	540.33±30.66e	727±59.25de
70:30I	26.88±1.85a	16.55±0.94abc	43.36±1.18a	754±198.93bcde	995.33±233.79cde
60:40S	26.15±6.32a	15.94±3.46ab	27.01±13.72b	671.66±142.97de	765.66±157.48cde
60:40I	20.09±0.84a	12.55±0.49c	30.63±5.45ab	1066.66±76.29a	1887±285.81a
50:50S	24.03±0.79a	14.67±0.33c	19.40±3.89b	684±69.72cde	558.66±147.12e
50:50I	21.38±1.23a	13.66±0.79c	27.92±4.04ab	955.66±41.05abc	1214.66±368.69abcd

FHMO: Fully hydrogenated microalgae oil; SO: Soybean oil.

These results are interesting from an application point of view, once crystals smaller than 30 μm do not cause a sandiness sensation when consumed in lipid-based products (Herrera and Falabella, et al., 1999). Therefore, the interesterification process was effective in reducing the crystal size for all the blends studied, possibly providing physical stability and expanding the possibilities of application of the lipid base. This finding corroborates the polymorph results since the interesterification process modified the crystal habit of the fats, with a significant predominance of the β′ polymorph after the reaction, characterized by smaller crystals and plasticity desirable in products such as margarines and fats for bakery and confectionery products. On the other hand, polymorph β tends to produce large granular crystals, resulting in products with low aeration potential, which may impair the macroscopic properties of some foods. The simple blends of this study presented mostly polymorphic β form due to the higher melting point, attributed to TAG S_3 and less variability of fatty acids present in glycerol, which dominate the crystal morphology and high crystal dimensions, as observed in the microstructure analysis (Shi et al., 2005).

In addition to the maximum and mean crystal diameters of the blends, the crystal area, and the crystal distribution was also different before and after randomization. Thus, the interesterified blends, which had a smaller crystal diameter, also had a greater crystal area, except for the blend 90:10, which had a larger crystal diameter, and similar crystallized area before and after the reaction. Regarding the other blends, there was an increase in the crystallized area from 31.35 to 37.32% when comparing the simple blend 80:20 with its interesterified counterpart; 29.07 to 47.36% for the blend 70:30; 27.01 to 30.63% for the blend 60:40, and 19.40 to 27.92% for the blend 50:50, thus a decrease in the crystallized area was observed for all blends studied, as well as the crystal diameters, which may have affected the crystal distribution. Besides the formation of smaller crystals, a higher crystal formation may have occurred in the interesterified blends, which led to an increase in crystallized area, and consequently a higher tendency to agglomeration and an increase in the number of single crystals.

Crystal agglomeration can be defined as the intergrowth of crystal aggregates formed by particle collisions and the binding/attraction energy between them. Thus, the size distribution, as well as the number of crystals, can

directly affect the aggregation rate or breakup of agglomerates, although the dynamics of formation and maintenance of crystal agglomerates are not yet fully elucidated. It is known that the smaller the crystal size, the larger the contact surface for interaction with other crystals; and the larger the number of crystals in the medium, the greater the probability of collisions and consequently cluster formation (Brunsteiner et al., 2005). Thus, due to the increase in the absolute number of crystals with simultaneous reduction of the crystal diameter in the interesterified blends, the greater formation of agglomerates can be confirmed through the evaluation of the crystallized area and cluster formation, which was higher for these blends when compared to the interesterified blends. These results may be due to changes in the triacylglycerol composition, which leads to a modification of the bonding forces between the elements in a cluster (intra-particle) and between clusters (inter-particle) giving rise to the formation of different structures (Shi et al., 2005).

Similar microstructure results were observed by Ribeiro et al. (2009a), who reported that the crystal morphology was modified after randomization from a large spherulite in the simple blends to a small disk-shaped crystal, with a granular structure. In turn, Ahmadi et al. (2008), Rashid et al. (2016), and Ribeiro et al. (2018) found that besides changing the polymorphism of the blends, the chemical interesterification modified the large disk-shaped crystals, associated with the β polymorphism, to needle-shaped crystals, which are associated with the polymorphic β' form. The authors also related these transformations to the triestearin contents before and after the reaction, since a significant TAG S_3 reduction was observed after interesterification.

Therefore, as discussed in the polymorphism analysis, interesterification led to the formation of smaller crystals, characteristic of the β' polymorphic form, which tends to form aerated products, with increased applicability.

4. Conclusion

The chemical interesterification process of lipidic raw materials combined in a novel way (different proportions of soybean oil and fully hydrogenated microalgae oil) allowed the comparison of systems before and after the reaction. When comparing the simple blends with their interesterified fractions, the latter

presented distinct characteristics such as lower melting point, higher linearity of the solids profile, higher compatibility between the raw materials, as well a reduction in maximum solids content at isothermal equilibrium, longer crystallization induction time due to differentiation of thermal behavior and, consequently, morphological and polymorphic modification, guiding stabilization towards the higher amount of crystals, lower crystal diameter, and formation of β' configuration.

These results are mainly due to the rearrangement of fatty acids in the glycerol molecule by the interesterification reaction, with a reduction of TAG S_3 and simultaneous increase of S_2U. The final characteristics of the structured fats enabled greater applicability in lipid-based products requiring aeration such as margarine and bakery and confectionery products.

In addition, blends made with FHMO contents starting at 60% resulted in blends with high SFC contents and slower melting, which are ideal characteristics for application in products requiring greater thermal stability such as bouillon cubes, soups, and granules, as well as lipid micro- and nanoparticles.

CRediT authorship contribution statement

Kamila Ramponi Rodrigues de Godoi Fernandes: Conceptualization, Methodology, Investigation, Formal analysis, Writing – original draft. Mayanny Gomes da Silva: Methodology, Formal analysis, Review. Lisandro Pavie Cardoso: Supervision, Resources. Ana Paula Badan Ribeiro: Conceptualization, Writing – review & editing, Supervision, Funding acquisition, Resources, Project administration.

Declaration of Competing Interest

The authors declare that they have no known competing financial interests or personal relationships that could have appeared to influence the work reported in this paper.

Acknowledgments

Ana Paula Badan Ribeiro thank CNPq (303429/2018-6) for productivity grant and São Paulo Research Foundation-FAPESP (16/11261-8). Kamila Ramponi Rodrigues de Godoi Fernandes thank CNPq (140789/2017-0) for PhD

scholarship grant. Lisandro Pavie Cardoso thank CNPq (302626/2016-6 and 307896/2019-6) for productivity grant. This study was financed in part by the “Coordenação de Aperfeiçoamento de Pessoal de Nível Superior - Brazil (CAPES)”–Finance Code 001.

References

Ahmadi, L., Wright, A. J., & Marangoni, A. G. (2008). *Chemical and enzymatic interesterification of tristearin / triolein-rich blends : Microstructure and polymorphism*. 1025–1034. https://doi.org/10.1002/ejlt.200800059

Antoniosi Filho, N. R. A., Mendes, O. L., & Lanças, F. M. (1995). Computer prediction of triacylglycerol composition of vegetable oils by HRGC. *Chromatographia*, *40*(9–10), 557–562. https://doi.org/10.1007/BF02290268

AOCS. (2009). *Official methods and recommended practices of the American Oil Chemists’ Society* (6th Edition). https://doi.org/http://dx.doi.org/10.1002/0471740039.vec0152

Asbridge, D. D. (2015). Soybeans vs.Other vegetable oils as a source of edible oil products. In D. R. Erickson (Ed.), *Pratical Handbook and soybean processing and utilization* (pp. 1–9). AOCS Press.

Ballestra, D. (2012). *Produce trans-free fats - Interchem® Technology*. https://www.desmetballestra.com/oils-fats/fat-modification/interesterification/chemical-interesterification

Basova, M. M. (2005). Fatty acid composition of lipids in microalgae. *International Journal on Algae*, *7*(1), 33–57. https://doi.org/10.1615/InterJAlgae.v7.i1.30

Berčíková, M., Šimková, A., Hudecová, K., Kyselka, J., Filip, V., & Hrádková, I. (2020). Physical Properties of Structured Fats and Fat Blends Based on the Long Chain Fatty Acids. *Food Biophysics*, *15*(1), 143–152. https://doi.org/10.1007/s11483-019-09609-8

Bogevik, A. S., Nygren, H., Balle, T., Haugsgjerd, B. O., & Kousoulaki, K. (2018). Enzymatic Interesterification of Heterotrophic Microalgal Oil with Rapeseed Oil to Decrease the Levels of Tripalmitin. *European Journal of Lipid Science and Technology*, *120*(7), 1–10. https://doi.org/10.1002/ejlt.201800063

Bösch, S., Westerman, L., Renshaw, N., & Pravst, I. (2021). Trans Fat Free by 2023—A Building Block of the COVID-19 Response. *Frontiers in Nutrition*, *8*(March), 1–7. https://doi.org/10.3389/fnut.2021.645750

Bot, A., & Flöter, E. (2013). Application in Fat-Continuous Emulsions (Spreads). *Edible Oil Processing (2nd Edition)*, 223–249. https://app.knovel.com/hotlink/khtml/id:kt011ARUX6/edible-oil-processing/application-in-fat-continuous

Brouwer, I. A. (2020). The public health rationale for reducing saturated fat intakes: Is a maximum of 10% energy intake a good recommendation? *Nutrition Bulletin*, *45*(3), 271–280. https://doi.org/10.1111/nbu.12449

Brunsteiner, M., Jones, A. G., Pratola, F., Price, S. L., & Simons, S. J. R. (2005). Toward a Molecular Understanding of Crystal Agglomeration. *Crystal Growth & Design*, *5*(1), 3–16. https://doi.org/10.1021/cg049837m

Campos, R. (2005). Fat Crystal Networks. In *Fat Crystal Networks* (pp. 267–349). Marcell Dekker Inc.

Chopin-Doroteo, M., Morales-Rueda, J. A., Dibildox-Alvarado, E., Charó-Alonso, M. A., de la Peña-Gil, A., & Toro-Vazquez, J. F. (2011). The Effect of Shearing in the Thermo-mechanical Properties of Candelilla Wax and Candelilla Wax-Tripalmitin Organogels. *Food Biophysics*, *6*(3), 359–376. https://doi.org/10.1007/s11483-011-9212-5

Crupkin, M., & Zambelli, A. (2008). Detrimental impact of trans fats on human health: Stearic acid-rich fats as possible substitutes. *Comprehensive Reviews in Food Science and Food Safety*, *7*(3), 271–279. https://doi.org/10.1111/j.1541-4337.2008.00045.x

Curi, R., Procópio, J., Myasaka, C. K., & Pompéia, C. (2002). *Entendendo a gordura: os ácidos graxos* (1ª). Editora Manole.

D'Agostini, D. (2014). Obtenção de lipídios estruturados por interesterificação de triacilgliceróis de cadeia média e longa. Universidade de São Paulo.

Dassanayake, L. S. K., Kodali, D. R., & Ueno, S. (2011). Formation of oleogels based on edible lipid materials. *Current Opinion in Colloid and Interface Science*, *16*(5), 432–439. https://doi.org/10.1016/j.cocis.2011.05.005

Demodaran, S., Parkin, K. L., & Fennema, O. L. (2010). *Química de Alimentos de Fennema* (Forth edit). Editora Artmed.

Fageria, N. K., Baligar, V. C., & Jones, C. A. (2010). *Growth and Mineral*

Nutrition of Field Crops (Third Edit, p. 551). CRC Press.

Foubert, I., Dewettinck, K., Janssen, G., & Vanrolleghem, P. A. (2006). Modelling two-step isothermal fat crystallization. *Journal of Food Engineering*, *75*(4), 551–559. https://doi.org/10.1016/j.jfoodeng.2005.04.038

Grimaldi, R., Gonçalves, L. A. G., & Ando, M. Y. (2005). Otimização da reação de interesterificaç ão química do óleo de palma. *Quimica Nova*, *28*(4), 633–636. https://doi.org/10.1590/s0100-40422005000400015

Guedes, A. M. M., Ming, C. C., Ribeiro, A. P. B., Silva, R. C., Gioielli, L. A., & Gonçalves, L. A. G. (2014). Physicochemical Properties of Interesterified Blends of Fully Hydrogenated Crambe abyssinica Oil and Soybean Oil. *Journal of American Oil Chemistry Society*, *91*(1), 111–123.

Gunstone, F. D., Harwood, J. L., & Dijkstra, A. T. (2007). The Lipid Handbook. In *The lipid handbook* (3ª Edição, pp. 37–141). CRC Press.

Hammond, E. G., Johnson, L. a, Su, C., Wang, T., & White, P. J. (2005). Soybean Oil. *Bailey's Industrial Oil and Fat Products*, *1*, 577–653. https://doi.org/10.1002/047167849X.bio041

Hartman, L., & Lago, R. C. A. (1973). Rapid preparation of fatty acid methyl esters from lipids. *Lab. Pract.*, *22*(January), 475-476,494.

Herrera, M. L., De León Gatti, M., & Hartel, R. W. (1999). A kinetic analysis of crystallization of a milk fat model system. *Food Research International*, *32*(4), 289–298. https://doi.org/10.1016/S0963-9969(99)00083-6

Herrera, M. L., Falabella, C., Melgarejo, M., & Añón, M. C. (1999). Isothermal crystallization of hydrogenated sunflower oil: II. Growth and solid fat content. *JAOCS, Journal of the American Oil Chemists' Society*, *76*(1), 1–6. https://doi.org/10.1007/s11746-999-0039-x

Hrádková, I. (2017). Effects of chemical interesterification on the triacylglycerols, solid fat contents and crystallization kinetics of palm oil-based fats. *Proceedings of the 20th USENIX Security Symposium*, *2*(1), 369–376. https://doi.org/10.1016/j.foodres.2018.05.01

Ifeduba, E. A., Martini, S., & Akoh, C. C. (2016). Enzymatic Interesterification of High Oleic Sunflower Oil and Tripalmitin or Tristearin. *JAOCS, Journal of the American Oil Chemists' Society*, *93*(1), 61–67. https://doi.org/10.1007/s11746-015-2756-7

Karabulut, I., Turan, S., & Ergin, G. (2004). Effects of chemical interesterification on solid fat content and slip melting point of fat/oil blends. *European Food Research and Technology*, *218*(3), 224–229. https://doi.org/10.1007/s00217-003-0847-4

Kok, L. L., Fehr, W. R., Hammond, E. G., & White, P. J. (1999). Trans-free margarine from highly saturated soybean oil. *JAOCS, Journal of the American Oil Chemists' Society*, *76*(10), 1175–1181. https://doi.org/10.1007/s11746-999-0092-5

Lee, J. H. ., Akoh, C. C. ., Himmelsbach, D. S. ., & Lee, K. (2008). Preparation of Interesterified Plastic Fats from Fats and Oils Free of Trans Fatty Acid. *Journal of Agricultural and Food Chemistry*, *56*, 4039–4046.

Marangoni, A. G. (1998). On the use and misuse of the avrami equation in characterization of the kinetics of fat crystallization. *Journal of the American Oil Chemists' Society*, *75*(10), 1465–1467. https://doi.org/10.1007/s11746-998-0203-8

Marangoni, A. G., & Campos, R. (2005). Fat Crystal Networks. In *Methodology* (Issue August). https://doi.org/10.1002/047167849X.bio008

Marangoni, A. G., & Rosseau, D. (2002). The effects of interesterification on the physical properties of fats. In A. G. Marangoni & S. S. Narine (Eds.), *Physical Properties of Lipids*. Marcell Dekker Inc.

Martini, S., Herrera, M. L., & Marangoni, A. (2005). New technologies to determine solid fat content on-line. *JAOCS, Journal of the American Oil Chemists' Society*, *82*(5), 313–317. https://doi.org/10.1007/s11746-005-1072-7

Meng, Z., Liu, Y. F., Jin, Q. Z., Huang, J. H., Song, Z. H., Wang, F. Y., & Wang, X. G. (2011). Comparative analysis of lipid composition and thermal, polymorphic, and crystallization behaviors of granular crystals formed in beef tallow and palm oil. *Journal of Agricultural and Food Chemistry*, *59*(4), 1432–1441. https://doi.org/10.1021/jf103875f

Mensink, R. P. (2005). Effects of stearic acid on plasma lipid and lipoproteins in humans. In *Lipids* (Vol. 40, Issue 12, pp. 1201–1205). https://doi.org/10.1007/s11745-005-1486-x

Metin, S., & Hartel, R. W. (2005). Fats and Oils. *Bailey's Industrial Oil and Fat Products*, 45–76.

Michael Eskin, N. A., & List, G. R. (2017). Food applications of lipids. *Food Lipids: Chemistry, Nutrition, and Biotechnology, Fourth Edition*, 421–451. https://doi.org/10.1201/9781315151854

Narine, S. S., & Humphrey, K. L. (2004). A comparison of lipid shortening functionality as a function of molecular ensemble and shear: Microstructure, polymorphism, solid fat content and texture. *Food Research International*, *37*(1), 28–38. https://doi.org/10.1016/j.foodres.2003.09.013

Narine, Suresh S., & Marangoni, A. G. (1999). Microscopic and rheological studies of fat crystal networks. *Journal of Crystal Growth*, *198–199*(pt 2), 1315–1319. https://doi.org/10.1016/S0022-0248(98)01016-1

O'Brien, R.D. (2009). Chapter 1 - Raw Materials. In *Fats and Oils: Formulating and Processing for Applications* (Third Edit, pp. 1–66). CRC Press.

O'Brien, Richard D. (2004). Fats and oils: formulating and processing for applications. In *New York*.

Oh, J. H., McCurdy, A. R., Clark, S., & Swanson, B. G. (2005). Stabilizing polymorphic transitions of tristearin using diacylglycerols and sucrose polyesters. *JAOCS, Journal of the American Oil Chemists' Society*, *82*(1), 13–19. https://doi.org/10.1007/s11746-005-1036-y

Oliveira, P. D., Rodrigues, A. M. C., Bezerra, C. V., & Silva, L. H. M. (2017). Chemical interesterification of blends with palm stearin and patawa oil. *Food Chemistry*, *215*, 369–376. https://doi.org/10.1016/j.foodchem.2016.07.165

Pacheco, C., Palla, C., Crapiste, G. H. ., & Carrín, M. E. (2013). Optimization of Reaction Conditions in the Enzymatic Interesterification of Soybean Oil and Fully Hydrogenated Soybean Oil to Produce Plastic Fats. *Journal of American Oil Chemistry Society*, *90*, 391–400. https://doi.org/10.1007/s11746-012-2182-z

Rashid, N. A., Kamarulzamana, N. A., & Omarb, Z. (2016). Effect of chemical and enzymatic interesterification on the physicochemical properties of palm oil and. Palm kernel oil blends. *Jurnal Teknologi*, *2*, 19–25. www.jurnalteknologi.utm.my

Rashid, N. A., Safuan, T. S. S. T., Kelana, A. T., Zuher, M. A., & Omar, Z. (2016). Effects of chemical interesterification on the physicochemical properties of palm stearin and rice bran oil blends. *Jurnal Teknologi*, *5*, 21–

27.

Ribeiro, A. P. B., Basso, R. C., Grimaldi, R., Gioielli, L. A., dos Santos, A. O., Cardoso, L. P., & Guaraldo Gonçalves, L. A. (2009a). Influence of chemical interesterification on thermal behavior, microstructure, polymorphism and crystallization properties of canola oil and fully hydrogenated cottonseed oil blends. *Food Research International*, *42*(8), 1153–1162. https://doi.org/10.1016/j.foodres.2009.05.016

Ribeiro, A. P. B., Basso, R. C., Grimaldi, R., Gioielli, L. A., & Gonçalves, L. A. G. (2009). Instrumental Methods for the Evaluation of Interesterified Fats. *Food Analytical Methods*, *2*(4), 281–302.

Ribeiro, A. P. B., Grimaldi, R., Gioielli, L. A., Dos Santos, A. O., Cardoso, L. P., & Gonçalves, L. A. G. (2009b). Thermal behavior, microstructure, polymorphism, and crystallization properties of zero trans fats from soybean oil and fully hydrogenated soybean oil. *Food Biophysics*, *4*(2), 106–118. https://doi.org/10.1007/s11483-009-9106-y

Ribeiro, A. P. B., Grimaldi, R., Gioielli, L. A., Dos Santos, A. O., Cardoso, L. P., & Gonçalves, L. A. G. (2009c). Thermal behavior, microstructure, polymorphism, and crystallization properties of zero trans fats from soybean oil and fully hydrogenated soybean oil. *Food Biophysics*, *4*(2), 106–118. https://doi.org/10.1007/s11483-009-9106-y

Ribeiro, A. P. B., Leite, J. M., De Moura, N., Grimaldi, R., & Gonçalves, L. A. G. (2007). Interesterificação química: Alternativa para obtenção de gorduras zero trans. *Quimica Nova*, *30*(5), 1295–1300. https://doi.org/10.1590/S0100-40422007000500043

Ribeiro, A. P. B., Masuchi, M. H., Grimaldi, R., & Gonçalves, L. A. G. (2009). Interesterificação química de óleo de soja e óleo de soja totalmente hidrogenado: influência do tempo de reação. *Química Nova*, *32*(4), 939–945. https://doi.org/10.1590/s0100-40422009000400021

Ribeiro, M. D. M. M., Ming, C. C., Lopes, T. I. B., Grimaldi, R., Marsaioli, A. J., & Gonçalves, L. A. G. (2017). Synthesis of structured lipids containing behenic acid from fully hydrogenated Crambe abyssinica oil by enzymatic interesterification. *Journal of Food Science and Technology*, *54*(5), 1146–1157. https://doi.org/10.1007/s13197-017-2540-9

Ribeiro, M. D. M. M., Ming, C. C., Lopes, T. I. B., Grimaldi, R., Marsaioli, A. J., &

Gonçalves, L. A. G. (2018). Enzymatic synthesis of structured lipids from liquid and fully hydrogenated high oleic sunflower oil. *International Journal of Food Properties*, *21*(1), 702–716. https://doi.org/10.1080/10942912.2018.1454943

Ribeiro, M. D. M., Ming, C. C., Silvestre, I. M., Grimaldi, R., & Ap. G. Gonçalves, L. (2017). Comparison between enzymatic and chemical interesterification of high oleic sunflower oil and fully hydrogenated soybean oil. *European Journal of Lipid Science and Technology*, *119*(2), 1–9. https://doi.org/10.1002/ejlt.201500473

Rosseau, D., & Marangoni, A. G. (2002). Chemical Interesterification of Food Lipids: Theory and Practice. In C. C. Akoh & D. B. Min (Eds.), *Food Lipids : Chemistry, Nutrition, and Biotechnology* (Second Edi, p. 1014). Marcel Dekker, Inc.

Rousseau, D., & Marangoni, A. G. (1998). The effects of interesterification on physical and sensory attributes of butterfat and butterfat-canola oil spreads. *Food Research International*, *31*(5), 381–388. https://doi.org/10.1016/S0963-9969(98)00100-8

Rousseau, D., Marangoni, A. G., & Jeffrey, K. R. (1998). The influence of chemical interesterification on the physicochemical properties of complex fat systems. 2. morphology and polymorphism. *JAOCS, Journal of the American Oil Chemists' Society*, *75*(12), 1833–1839. https://doi.org/10.1007/s11746-998-0339-6

Sampath, H., & Ntambi, J. M. (2005). The fate and intermediary metabolism of stearic acid. *Lipids*, *40*(12), 1187–1191. https://doi.org/10.1007/s11745-005-1484-z

Sato, K., & Ueno, S. (2005). Polymorphism in fats and oils. *Bailey's Industrial Oil and Fat Products*, *1*, 77–120. http://onlinelibrary.wiley.com/doi/10.1002/047167849X.bio020/full

Shi, Y., Liang, B., & Hartel, R. W. (2005). Crystal morphology, microstructure, and textural properties of model lipid systems. *JAOCS, Journal of the American Oil Chemists' Society*, *82*(6), 399–408. https://doi.org/10.1007/s11746-005-1084-3

Sivakanthan, S., & Madhujith, T. (2020). Current trends in applications of enzymatic interesterification of fats and oils: A review. *Lwt*, *132*(July),

109880. https://doi.org/10.1016/j.lwt.2020.109880

Speranza, P., Macedo, G., & Ribeiro, A. P. B. (2015). Lipase catalyzed interesterification of Amazonian patauá oil and palm stearin for preparation of specific-structured oils. *Journal of Food Science and Technology*, *52*, 8268–8275.

Takeuchi, M., Ueno, S., & Sato, K. (2002). Crystallization kinetics of polymorphic forms of a molecular compound constructed by SOS (1,3-distearoyl-2-oleoyl-sn-glycerol) and SSO (1,2-distearoyl-3-oleoyl-rac-glycerol). *Food Research International*, *35*(10), 919–926. https://doi.org/10.1016/S0963-9969(02)00154-0

Wang, J., Wang, X. D., Zhao, X. Y., Liu, X., Dong, T., & Wu, F. A. (2015). From microalgae oil to produce novel structured triacylglycerols enriched with unsaturated fatty acids. *Bioresource Technology*, *184*, 405–414. https://doi.org/10.1016/j.biortech.2014.09.133

Wassell, P., & Young, N. W. G. (2007). Food applications of trans fatty acid substitutes. *International Journal Of Food Science And Technology*, *42*(5), 503–517. https://doi.org/10.1111/j.1365-2621.2007.01571.x

World Health Organization. (2020). *Countdown To 2023: WHO report on global trans-fat elimination 2020.* (Vol. 5, Issue May).

Wright, A. J., Narine, S. S., & Marangoni, A. G. (2000). Comparison of experimental techniques used in lipid crystallization studies. *Journal of the American Oil Chemists' Society*, *77*(12), 1239–1242.

Yap, P., Man, J. De, & Man, L. De. (1989). Polymorphism of palm oil and palm oil products. *Journal of the American Oil Chemist's Society*, *66*(5), 693–697. https://doi.org/10.1007/BF02669954

Zeitoun, M. A. M., Neff, W. E., List, G. R., & Mounts, T. L. (1993). Physical properties of interesterified fat blends. *Journal of the American Oil Chemists' Society*, *70*(5), 467–471. https://doi.org/10.1007/BF02542577

Zhang, Z., Lee, W. J., Zhou, H., & Wang, Y. (2019). Effects of chemical interesterification on the triacylglycerols, solid fat contents and crystallization kinetics of palm oil-based fats. *Food and Function*, *10*(11), 7553–7564. https://doi.org/10.1039/c9fo01648a

Zhu, T., Weng, H. tian, Zhang, X., Wu, H., & Li, B. (2018). Mechanistic insight into the relationship between triacylglycerol and crystallization of lipase-

catalyzed interesterified blend of palm stearin and vegetable oil. *Food Chemistry*, *260*(March), 306–316. https://doi.org/10.1016/j.foodchem.2018.03.147

Zhu, Tingwei, Zhang, X., Wu, H., & Li, B. (2019). Comparative study on crystallization behaviors of physical blend- and interesterified blend-based special fats. *Journal of Food Engineering*, *241*(May 2018), 33–40. https://doi.org/10.1016/j.jfoodeng.2018.08.005

ARTIGO 2. EFFECT OF STATIC CRYSTALLIZATION PROTOCOL ON POLYMORPHISM AND MICROSTRUCTURE OF INTERESTERIFIED LIPID MATRICES RICH IN STEARIC ACID

Kamila Ramponi Rodrigues de Godoi Fernandes[1], Mayanny Gomes da Silva[1], Lisandro Pavie Cardoso[2], Ana Paula Badan Ribeiro[1]

[1]Department of Engineering and Food Technology, School of Food Engineering, University of Campinas, Brazil

[2]Department of Applied Physics, Institute of Physics, University of Campinas, Brazil

Corresponding author: kamila.ramponi@hotmail.com

(Manuscrito submetido ao Periódico Food Research International)

Abstract: This study evaluated simple and chemical interesterified blends of soybean oil (SO) and fully hydrogenated microalgae oil (FHMO) in different proportions (FHMO: SO w:w): 90:10, 80:20, 70:30, 60:40, and 50:50, subjected to two crystallization methods, as follows: Method 1 (slow crystallization): samples were completely melted and maintained at 25°C for 60 days; Method 2 (quick crystallization): samples were completely melted and maintained at 5°C for 24 hours, with subsequent storage at 25°C for 60 days. The FHMO was composed of 92.85% of saturated fatty acids, mainly stearic acid, and consequently with a high level of trisaturated triacylglycerols in simple and interesterified blends, represented by tristearin. The interesterification process reduced trisaturated fatty acids and increased monosaturated triacylglycerols fatty acids levels, leading to important changes in the physical and microstructural behavior. Concerning the crystallization method 1, the interesterified blends showed β' polymorphic form, while the simple blends showed the β form probably due to the high saturated and homogenous triacylglycerols (StStSt and PStSt) levels. These characteristics remained until 30 days of storage at 25°C, with the formation of the β' form in the simple blend 50:50. This result is due to the late crystallization of unsaturated triacylglycerols present in SO, which corroborated with the microstructure modifications for the same time and conditions. Smaller crystals and larger crystallized area were observed over time, which was directly proportional to the FHMO content. In turn, the crystallization method 2 presented similar behaviors, with β form in the simple blends and β' form the interesterified blends until 7 days of storage. After this period, the interesterified blends 70:30, 60:40, and 50:50 showed β polymorphic form, and the coexistence of β' e β polymorphic form after 15 days. This result is possibly due to the late crystallization of unsaturated triacylglycerols of SO. In the microstructure analysis, the quick crystallization method resulted in larger crystallized area and lower crystal size when compared to the slow method, once the low temperature allowed the formation of a large number of crystals in a shorter time. A decrease in mean and maximum diameter of crystals was also observed as a function of time. The low temperature and high tristearin content can act as a seed of crystallization, accelerating the process and making the system more stable and denser, which is more pronounced for simple blends when compared to

interesterified blends. The smaller crystals and the presence of β' crystals can improve the application of interesterified blends.
Keywords: Soybean oil, Fully hydrogenated microalgae oil, Lipid crystallization, Interesterification, Slow crystallization, Quick crystallization.

1. Introduction

The interesterification process allows to obtain new lipid matrices troughs the reorganization of fatty acids position in the triacylglycerol backbone become these matrices highly applicable in foods. Triacylglycerols composed of saturated fatty acids have high melting points and are generally solid at room temperature, whereas triacylglycerols consisting of unsaturated fatty acids are usually liquid at room temperature. The chemical interesterification allows producing a blend of fats and oils, with a rearrangement of the fatty acids in the glycerol molecules, creating new triacylglycerol species with desirable physical, chemical, and functional properties (O'Brien, 2009).

The lipid composition and the crystallization conditions influence the crystalline habit, leading to the formation of different polymorphs and morphological forms (Rousseau et al., 1998). It is known that the crystallization process is divided into two phases: nucleation and crystal growth. Nucleation involves the formation of aggregates of molecules that exceed a critical size and are, therefore, stable. Once a crystalline nucleus has formed, it begins to grow by incorporating other triacylglycerol molecules (Ribeiro, et al., 2009; Rogers et al., 2008). The properties of crystals, such as size, morphology, and polymorphic form, influence the fat structure, which, in turn, affects the behavior of the fat in terms of texture, appearance, and functionality.

In addition, the storage time of lipid matrices can define the physical stability. Multicomponent materials, such as fats and oils, tend to exhibit a mixture of crystal types, affecting significantly the polymorphic transitions. The transformation rate is dependent on the homogeneity degree of triacylglycerols. Fats with low variability of triacylglycerols rapidly transform into the stable form β, while fats with a random distribution of triacylglycerols can present the β' form indefinitely in a long period of storage. Generally, triacylglycerols first crystallize

in polymorphic forms α and β', although the β form is the most stable (Sato & Ueno, 2005).

The type of crystal formed according to the crystallization method can guide the application of fats in foods. The β' crystals are small and present suitable morphology for the plasticity characteristics, which are desirable in products such as margarine, shortenings, and fat for bakery and pastry. In turn, the β polymorphic form tends to produce wide granular crystals, generating sandy products with low potential for aeration, which may compromise the macroscopic properties of some kinds of food (Sato & Ueno, 2005). Thus, considering the application requirements, the chemical interesterification of fats may be an effective process to stabilize the crystal fats in the β′ polymorphic form by promoting the randomization of fatty acids in triacylglycerols, resulting in more disordered packing of terminal methyl groups, which is associated to the formation of crystal lattices of lower density (Ribeiro et al., 2009).

In this context, soybean oil (SO) is a good choice for use in interesterification, once it is a low-cost and highly available oil, besides having desirable nutritional characteristics due to their fatty acid composition rich in linoleic acid (55%) and linolenic acid (7%) (Asbridge, 2015; Demodaran et al., 2010; Fageria et al., 2010; Hammond et al., 2005). Thus, from a health perspective, lipid matrices with high content of stearic acid may be a good alternative to obtain interesterified fats, once stearic acid does not cause adverse effects on the risk of cardiovascular disease when compared to the other saturated fatty acids. Although the mechanism is not well elucidated, it can be related to the large carbon chain length (18C) that cause less absorption in the gut or the transformation of stearate to oleate, which is the preferred substrate for the synthesis of triacylglycerols (Mensink, 2005; Sampath & Ntambi, 2005).

The fully hydrogenated microalgae oil (FHMO) is a novel and unexplored raw material, composed of approximately 92% of stearic acid and consequent high homogeneity in triacylglycerols composition, represented mainly by tristearin, a pure triacylglycerol. The present study used different proportions of SO and FHMO to produce simple and chemical interesterified blends. As previously mentioned, the chemical interesterification reaction is capable to reorder the fatty acids in the glycerol molecule resulting in heterogeneous triacylglycerols and, possibly, more unstable crystals, β'. The aim of this study

was investigate the effect of the interesterification process in two static crystallization methods (quick or slow crystallization) during 60 days of storage time using lipid matrices rich in stearic acid.

2. Material and methods

2.1. Material

Refined soybean oil (SO) was purchased in local market; fully hydrogenated microalgae oil (FHMO) was obtained and provided by SGS Agriculture and Industry Ltd. (Ponta Grossa, PR, Brazil) from AlgaWiseTM Ultra Omega-9 Algae Oil (TerraVia Holdings, San Francisco, CA, USA); sodium methoxide anhydrous powder, 99% purity, was supplied by Sigma Aldrich. The simple and chemical interesterified fats were obtained from SO and FHMO blends at the different ratios (FHMO/SO).

2.2. Methods

2.2.1. Preparation of simple blends

2.2.1.1. Simple blend

The FHMO and SO were heated until total melting and mixed under magnetic stirring at a weight ratio (FHMO: SO) of 90:10, 80:20, 70:30, 60:40, and 50:50 w:w. The blends were maintained under agitation for 3 minutes to destroy the crystalline memory.

2.2.1.2. Chemical interesterification

The reactions were performed according to the FHMO and SO ratios described in Section 2.2.1. For the chemical interesterification, on a laboratory scale, each blend was heated until 100°C under magnetic stirring (500rpm) for 20 minutes under vacuum to remove moisture. Then, each blend was interesterified using 1.54% of sodium methoxide, according to the quantity of free

fatty acids and peroxide value of SO and FHMO, as described by Desmet Ballestra, and the optimization was performed as described by Grimaldi et al. (2005). Sodium methoxide was added to the dried blends at 100°C, under magnetic stirring (500rpm) for 20 minutes under vacuum. Then, citric acid solution (5g/100mL) was added to stop the reaction. The interesterified samples were washed with distilled water (80°C). For drying, the blends were heated until 100°C under magnetic stirring for 20min under vacuum. After the reaction, free fatty acids and partial acylglycerols (diacylglycerols and monoacylglycerols) were removed as described by Rousseau & Marangoni (1998) with modifications. The interesterified blends were melted and mixed with an equal volume of 96% ethanol at 40–50 °C in a separatory funnel. The ethanol phase was then extracted, and the procedure was repeated three times. The samples were stored in glass vials according to the temperatures studied (25 or 5°C) for the static crystallization.

2.2.2. Lipid characterization

2.2.2.1. Fatty acid composition

The fatty acid composition was determined using a gas chromatograph CGC Agilent Series 6850 (Santa Clara, California, USA) with an FID detector, after esterification according to Hartman & Lago (1973). The methyl esters were separated according to AOCS Cf 1-96 (AOCS, 2009) using a capillary column Agilent-DB-23 (50% cyanopropyl – methylpolysiloxane), length 60 m, internal diameter 0.25 mm, and film thickness 0.25 µm; The operation conditions were: flow rate of 1.0 ml/min; linear velocity of 24 cm/s; injector temperature of 250 °C; detector temperature of 280 °C/min; oven temperature of 110 °C for 5 min, 110 - 215 °C at 5 °C/min, 215 °C for 34 min; helium as a carrier gas; injected volume of 1.0 µL/min and split ratio of 1:50. Individual fatty acid methyl esters were identified by comparison of retention times to commercial standards, and quantified based on relative peak areas. The fatty acid composition of the blends was calculated according to the respective mass fractions in the blends.

2.2.2.2. Iodine value and saponification value

The iodine and saponification values were determined according to AOCS Cd 1c-85 and Cd 31-94 (AOCS, 2009), respectively.

2.2.2.3. Triacylglycerol composition

The triacylglycerol (TAG) composition was determined using a gas chromatograph CGC Agilent 6850 Series GC System (Santa Clara, California, USA). A capillary column Agilent - DB-17 HT (50% phenyl- 50% methylpolysiloxane) 15 m in length, 0.25 mm internal diameter, and 0.15 μm of film thickness was used. The operation conditions were: injector temperature 360 °C; detector temperature of 375 °C/min; oven temperature from 250°C to 350 °C at 5 °C/min, 350 °C for 20 min; helium as a carrier gas; injected volume of 1.0 μL/min and split ratio of 1:100. TAG were identified by comparison of retention times and the quantification was based on relative peak areas (Antoniosi Filho et al., 1995) The TAG composition of the blends was determined according to the composition of SO and FHMO and the respective mass fractions in the blends regarding the trissaturated (S_3), dissaturated (S_2U), monossaturated (SU_2) triunsaturated (U_3) TAG.

2.2.2.4. Fatty acid regiospecific distribution

Proton-decoupled 13C NMR (Nuclear Magnetic Resonance) was used to analyze the positional distribution of different fatty acids (saturated/unsaturated) on the TAG backbone. Lipid samples were dissolved in deuterated chloroform in NMR tubes, and NMR spectra were recorded on a Bruker Advance DPX spectrometer operating at 300 MHz. The determination of 13C was performed at a frequency of 75.8 MHz, with a 5 mm multinuclear probe operating at 30°C (Vlahov, 1998).

2.2.2.5. Microstructure

The samples were evaluated by polarized light microscopy (PLM). For that, a drop of the melted sample was placed on a glass slide at 80 °C with the aid of a capillary tube, covered with a coverslip, and stored in an incubation chamber according to two crystallization methods, as follows: method 1) static crystallization and storage at 25°C with determinations on day 1, 7, 15, 30, and 60 of storage; method 2) static crystallization at 5°C for 24 hours and storage at 25°C with determinations on day 1, 7, 15, 30, and 60 of storage. The images were taken from three different visual fields, at a magnification of 40 X, and a single representative image was selected to represent the systems (Campos, 2005). The software Image Pro Plus (version 7.0, Media Cybernetics) was used to take the images

2.2.2.6. Polymorphism

The polymorphic habit of the samples was determined by X-ray diffraction according to the AOCS Cj 2-95 method (AOCS, 2009). The determinations were made in a Philips diffractometer (PW 1710) using Bragg-Brentano geometry (θ:2θ) with Cu-Kα radiation (λ = 1.54056Å, 40 KV, and 30 mA). The measurements were obtained with steps of 0.02 ° in 2θ and acquisition time of 2 seconds, with scans from 2 to 40° (scale 2θ). The identification of the crystalline forms was carried out from the characteristic short spacing of the crystals (Chopin-Doroteo et al., 2011; Dassanayake et al., 2011; Yap et al., 1989). The determinations were performed for two crystallization methods, as follows: method 1) static crystallization and storage at 25°C with determinations on day 1, 7, 15, 30, and 60 of storage; method 2) static crystallization at 5°C for 24 hours and storage at 25°C with determinations on day 1, 7, 15, 30, and 60 of storage.

2.2.3. Statistical analysis

The results were subjected to analysis of variance (ANOVA) using the software STATISTICA Version 8 (StatSoft Inc., Tulsa, OK). Tukey tests were

applied for statistical comparisons of means, at a 5% significance level ($p<0.05$).

3. Results and discussion

3.1. Fatty acid composition

As expected, the SO showed fatty acid composition consistent with literature results, containing mostly linoleic, oleic, palmitic, and linolenic acids with 52.70, 24.53, 11.10, and 6.39%, respectively (O'Brien. 2009). In turn, FHMO resulted in fully hydrogenated oil with high stearic acid content (92.85%), due to its original composition rich in oleic acid, followed by palmitic acid (5.52%). The iodine value (I.V) and saponification value (S.V) of the raw materials were also considered adequate according to fatty acid composition, with IV values of 193 and 0.33 for SO and FHMO, respectively, inversely proportional to the degree of unsaturation, since it measures the amount of iodine absorbed per 100g of sample. The SV was 190 and 193 for the SO and FHMO, respectively. For the blends, there was an increase in the amount of saturated fatty acids as a function of the addition of FHMO (Figure 1), and the results are presented in the Table in Appendix 1.

Figure 1. Fatty acid composition of the blends composed by FHMO: SO (w:w) in the proportions: 90:10, 80:20, 70:30, 60:40 e 50:50.

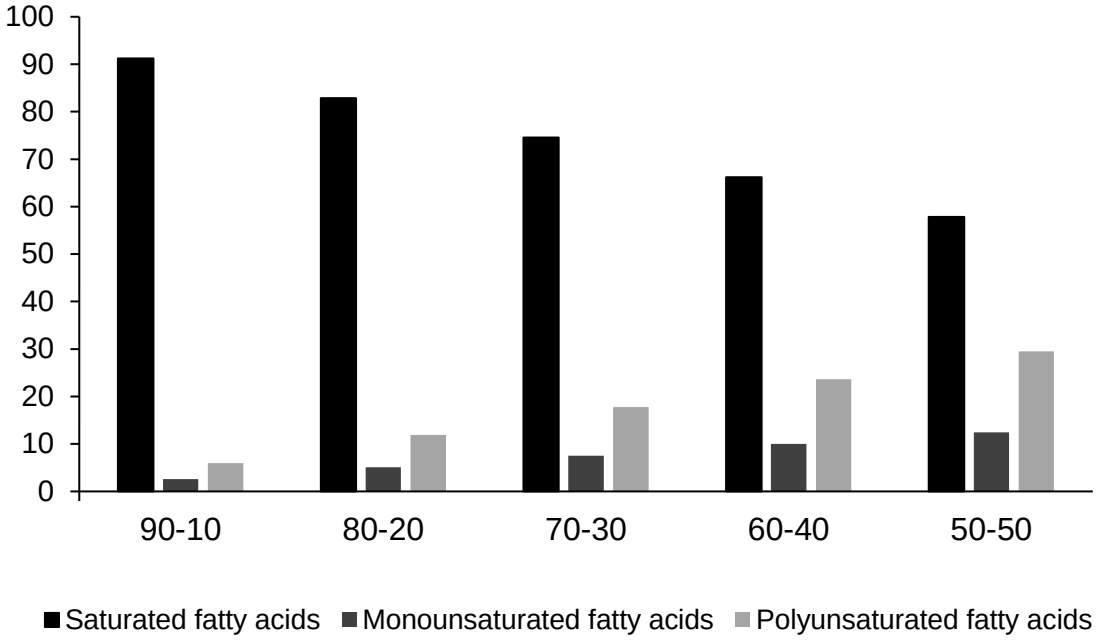

FHMO: Fully hydrogenated microalgae oil; SO: Soybean oil.

3.2. Triacylglycerol composition

The triacylglycerol profile is the main parameter to be evaluated in interesterified matrices for technological applications, which has a direct correlation with the physical properties of fats (Rosseau & Marangoni, 2002). In this context, the chemical interesterification reaction can alter several physical and crystallization properties of the original matrices by modulating their composition.

A modification in the triacylglycerol composition was observed for the blends of this study (Table 1) with decreased contents of trisaturated (S_3), monosaturated (U_2S), and triunsaturated (U_3) triacylglycerols (TAG), and a concomitant increase in disaturated triacylglycerols (S_2U) forall proportions of the interesterified blends when compared to the simple blends, with a predominance of triestearin (StStSt) before and after the reaction, due to the expressive stearic acid content of FHMO. Such composition also favored the presence of stearic acid in the triacylglycerols formed.

Table 1. Triacylglycerol classes (TAG) (%) of FHMO: SO in simple (S) or interesterified blends (I).

Blends	S_3	S_2U	SU_2	U_3
90:10S	88.47±0.86%	1.99±0.67%	4.38±01.20%	5.18±0.27%
90:10I	83.47±1.28%	12.67±1.13%	3.12±0.64%	0.75±0.21%
80:20S	77.07±0.66%	1.90±0.10%	8.39±0.25%	12.55±0.83%
80:20I	72.25±1.54%	23.97±0.28%	2.44±0.05%	1.32±0.67%
70:30S	74.29±2.14%	1.89±0.66%	9.65±1.12%	14.15±0.85%
70:30I	61.93±1.56%	34.47±2.09%	2.49±0.25%	1.10±0.27%
60:40S	67.81±7.35%	1.11±0.46%	10.48±3.58%	20.88±3.58%
60:40I	50.52±0.39%	44.20±2.09%	3.30±1.71%	1.96±1.71%
50:50S	54.17±2.16%	7.97±1.44%	6.51±0.30%	27.00±3.88%
50:50I	36.85±6.11%	57.58±7.07%	3.54±1.04%	2.01±0.22%

Triacylglycerols: S_3 (trisaturated), S_2U (disaturated–monounsaturated), SU_2 (monosaturated-diunsaturated) and U_3 (triunsaturated). Mean between sample injection triplicates.

The reduction in TAG S_3 and U_3 contents after interesterification was more intense in the blends containing higher SO contents, as well as an increase in S_2U. Similar results were reported by Ribeiro et al. (2017), Ribeiro, et al. (2009), and Ribeiro et al. (2018), who evaluated different matrices and also found a significant increase in S_2U content and reduction of S_3 and U_3, with a slight increase in SU_2. These modifications can modulate the physical and thermal properties of lipid bases (Rosseau & Marangoni, 2002).

The main TAGs identified in the blends were StStSt and PStSt/StPSt, corresponding to 73.57 and 11.35%, respectively, in the simple blend 90:10, with a reduction to 23.08% and 10.59%, respectively, after randomization. The modulation of the TAG profile led to a concomitant increase in SSO, SSL, and SSLn TAGs due to the greater contribution of SO. The results of triacylglycerol composition can be found in Appendix 2 as supplementary material.

3.3. Regiospecific distribution

TAG regiospecificity analysis shows the distribution of fatty acids in the glycerol molecule before and after randomization (Guedes et al., 2014; Ifeduba et al., 2016; Speranza et al., 2015). Table 2 shows the unsaturated and saturated

fatty acids contents esterified at the different sites of the glycerol molecule (sn-1,3 and sn-2).

Table 2. Distribution of the fatty acids (%) at the sn-1,3 and sn-2 position on the TAG of fully hydrogenated microalgae oil (FHMO) and soybean oil (SO) in simple (S) and interesterified blends (I) in concentrations of 90:10, 80:20, 70:30, 60:40 and 50:50 (FHMO/SO) (w:w).

Blends	sn-1,3		sn-2	
	Saturated	**Unsaturated**	**Saturated**	**Unsaturated**
90:10S	92,66 ± 0,83	7,34 ± 0,07	89,56 ± 0,65	10,44 ± 0,03
90:10I	91,65 ± 0,89	8,34 ± 0,02	83,07 ± 0,77	16,93 ± 0,31
80:20S	83,34 ± 0,98	16,65 ± 0,55	77,14 ± 0,41	22,86 ± 0,09
80:20I	79,71 ± 0,88	20,29 ± 0,28	75,51 ± 0,67	24,49 ± 0,65
70:30S	81,02 ± 0,72	18,98 ± 0,36	74,70 ± 0,77	25,30 ± 0,43
70:30I	80,82 ± 0,99	19,18 ± 0,34	63,06 ± 0,53	36,94 ± 0,11
60:40S	74,17 ± 0,65	25,83 ± 0,11	67,51 ± 0,44	32,49 ± 0,38
60:40I	87,77 ± 0,74	12,22 ± 0,22	59,06 ± 0,91	40,94 ± 0,33
50:50S	67,53 ± 078	32,47 ± 0,56	54,20 ± 0,51	45,80 ± 0,40
50:50I	67,00 ± 0,45	33,00 ± 0,18	36,99 ± 0,24	63,01 ± 0,55

FHMO: Fully hydrogenated microalgae oil; SO: Soybean oil.

Although it consists of a combination of a vegetable raw material, represented by SO, and a raw material of microbial origin, the FHMO, the regiospecificity analysis showed a typical behavior of natural vegetable oils. The saturated fatty acids were mostly esterified at the sn 1,3 position, while the unsaturated acids were located at the sn-2 position of the glycerol molecules (Silva et al., 2009). The analysis of the fatty acid composition showed that the saturated fractions possibly refer to stearic acid (C18:0), present in about 92% of FHMO, while the unsaturated fractions refer mainly to linoleic acid (C18:2) and oleic acid (C18:1), present in significant amounts in SO (52.7% and 24.53%, respectively).

The chemical interesterification of the blends led to a decrease in the amount of saturated fatty acids in all positions for the formulations with FHMO in a majority manner: 90:10 (S: 92.66%; I: 91.65%), 80:20 (S: 83.34%; I: 79.71%) and 70:30 (S: 81.02%; I: 80.82%), while the blend 60:40 (FHMO:SO) (w:w) showed a 12% increase in the sn 1-3 position, with no change for the equal ratios

(50:50). In response, the same concentrations showed increased unsaturated fatty acid contents at all binding sites of the glycerol molecules.

However, similar results were observed for esterification at the sn-2 position for all blends studied, with decreased amounts of saturated and increased unsaturated fatty acids, with fatty acid migration proportional to the SO concentration.

3.4 Polymorphism

In addition to the randomization by the interesterification reaction, the crystallization conditions and other factors such as stabilization time and temperature can influence the final polymorphic form of the lipid systems, as well as the transition between the different forms, called monotropic transition, referring to the transformation of less stable forms (α or β') into more stable forms (β). In a diffractogram, the β' form is characterized by spacings of 3.8 and 4.2Å, while the β form is characterized by a spacing of 4.6Å. Fats with low TAG variability quickly stabilize in the β form, while fats with random TAG distribution, such as interesterified fats, can exhibit the β' form indefinitely (Sato & Ueno, 2005). However, the different polymorphic forms can coexist at certain temperatures once fats are complex mixtures of TAGs (Chong et al., 2007).

In general, the more heterogeneous the TAG structure, the less tendency to form β-polymorphs (Oh et al., 2005). Therefore, the polymorphic form of the simple and interesterified blends was studied under different crystallization conditions: slow crystallization, at 25°C (crystallization method 1) and quick crystallization, at 5 °C (crystallization method 2) for 24 hours, with subsequent storage at room temperature (25 °C) for up to 60 days (Figures 2 to 5 and Tables 3 and 4;).

Figure 2. XRD patterns at 25 °C in different storage times for Crystallization Method 1 (24h/25°C) of the simple blends (S).

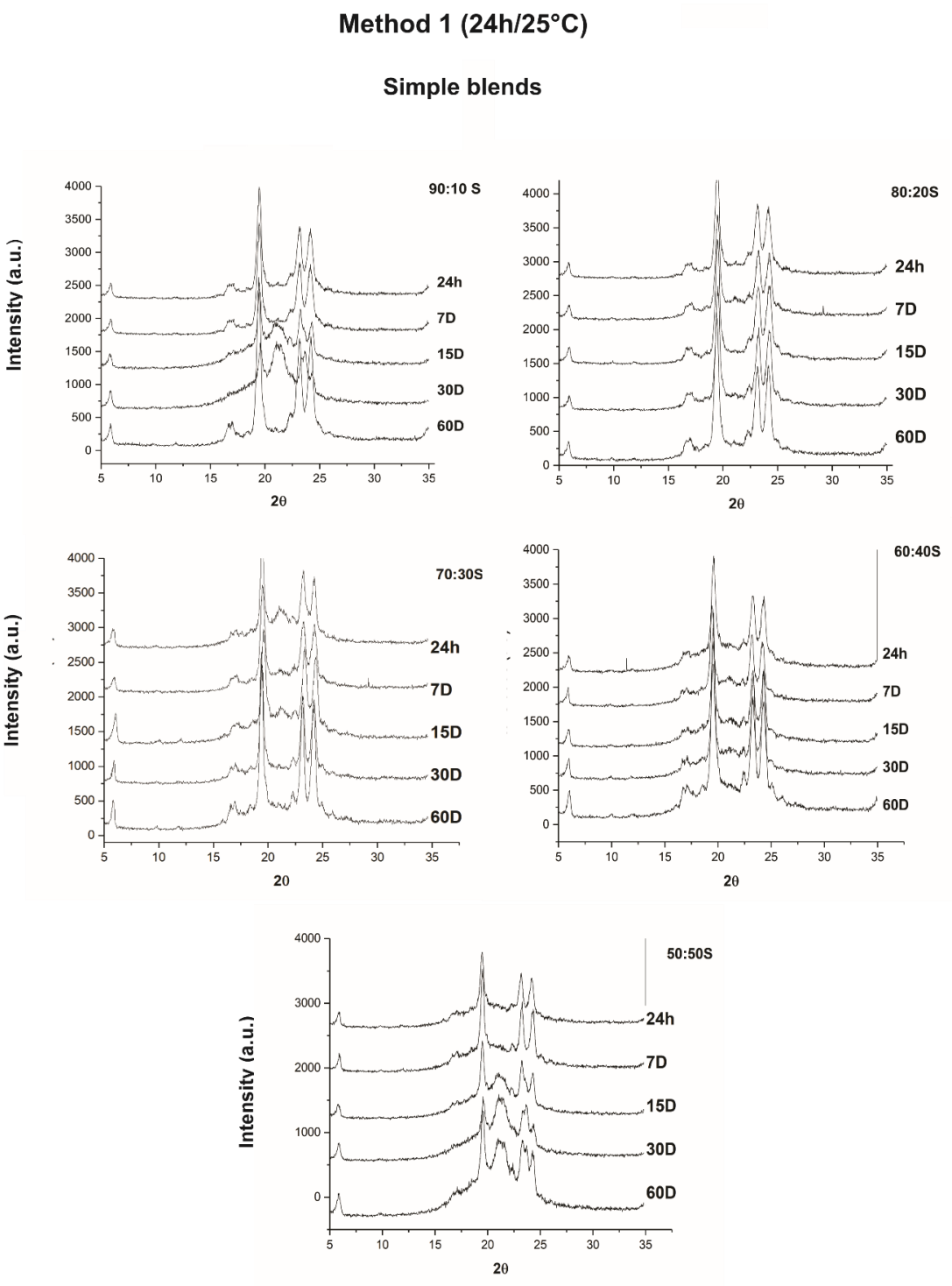

SO: soybean oil; FHMO: fully hydrogenated microalgae oil.

Figure 3. XRD patterns at 25 °C in different storage times for Crystallization Method 1 (25°C over time) of the interesterified blends (I).

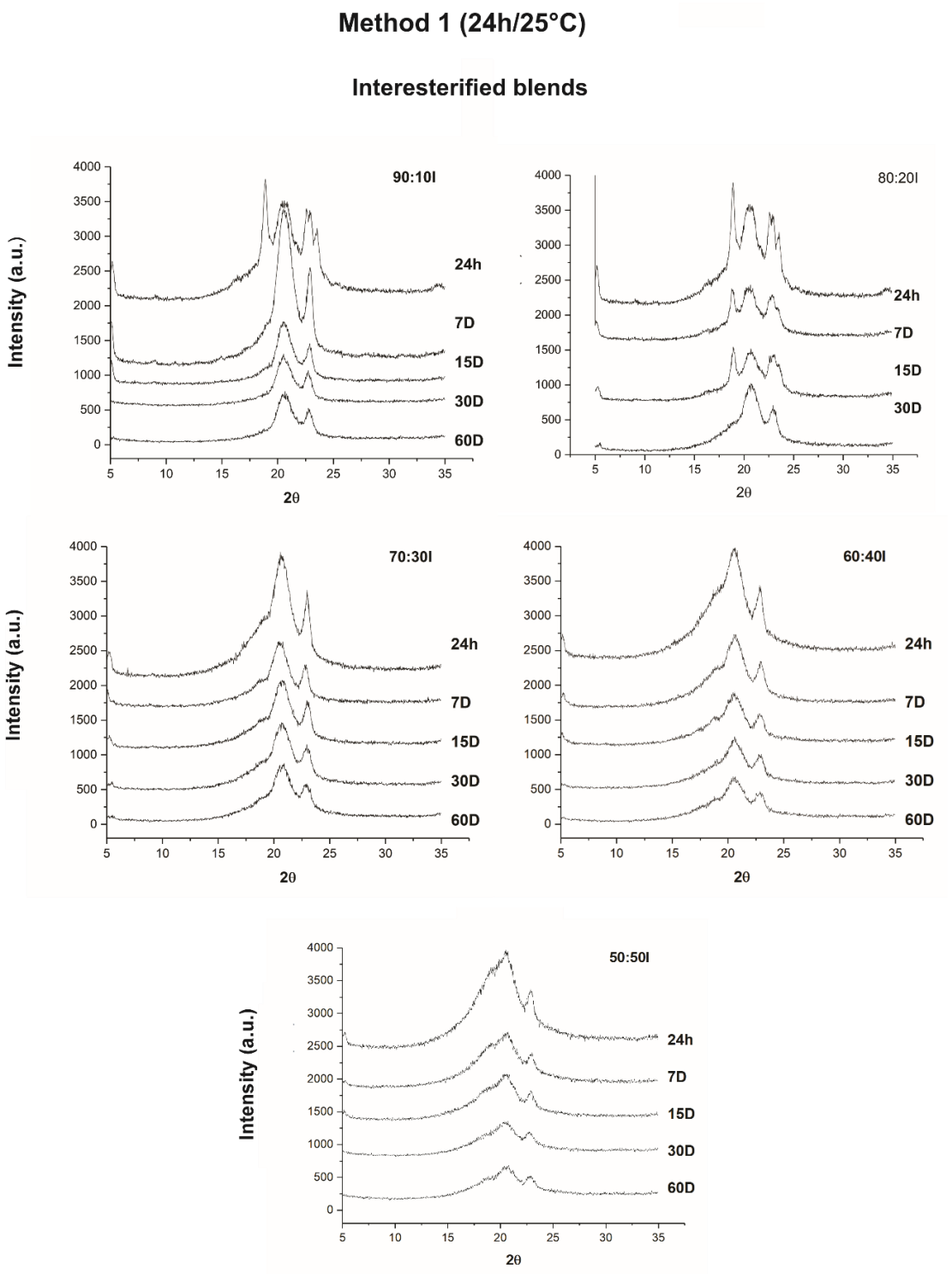

SO: soybean oil; FHMO: fully hydrogenated microalgae oil.

Figure 4. XRD patterns at 25 °C in different storage times for Crystallization Method 2 (24h/5°C and 24h/25°C) of the simple blends (S).

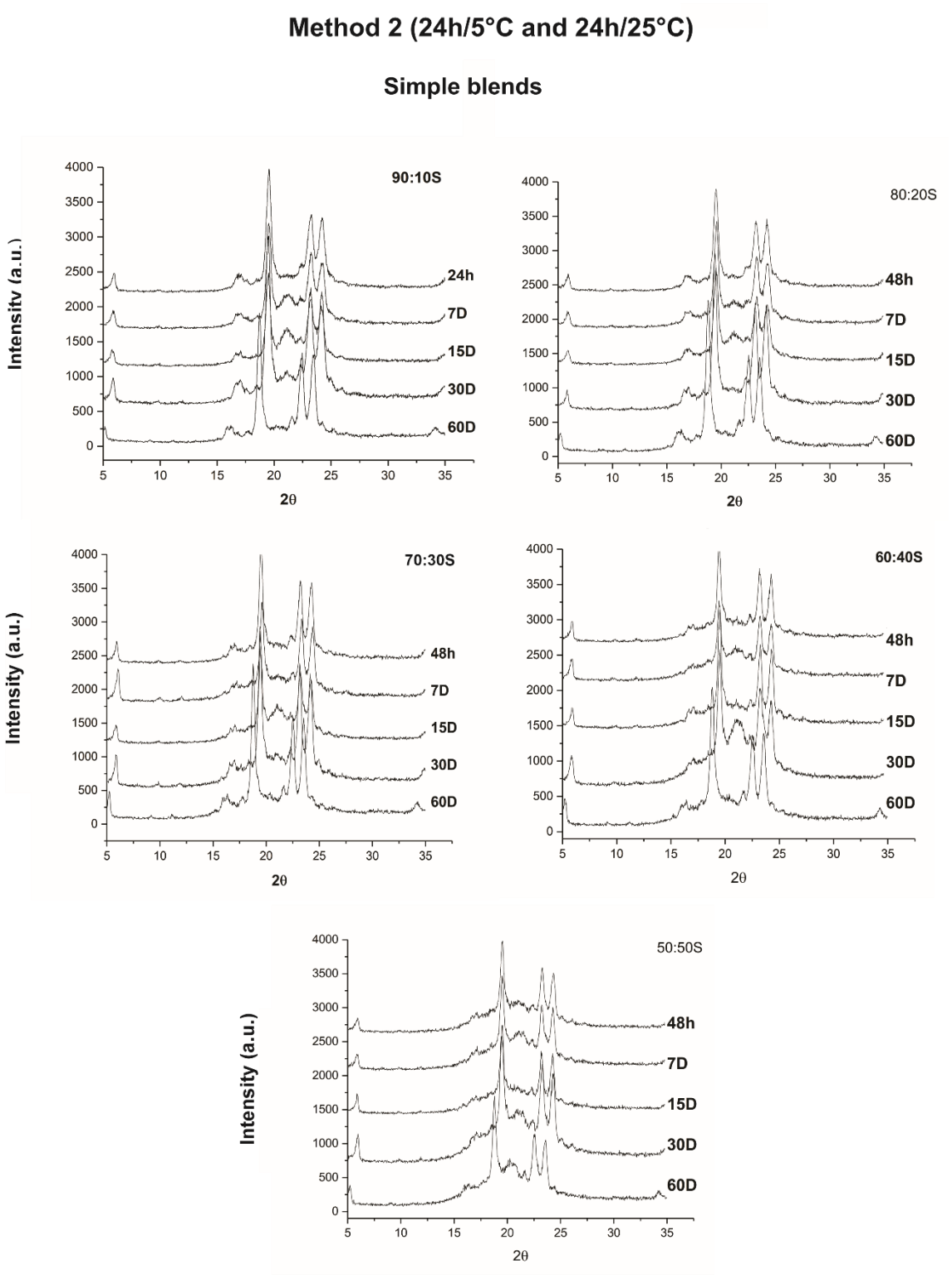

Figure 5. XRD patterns at 25 °C in different storage times for Crystallization Method 2 (24h/5°C and 24h/25°C) of the interesterified blends (I).

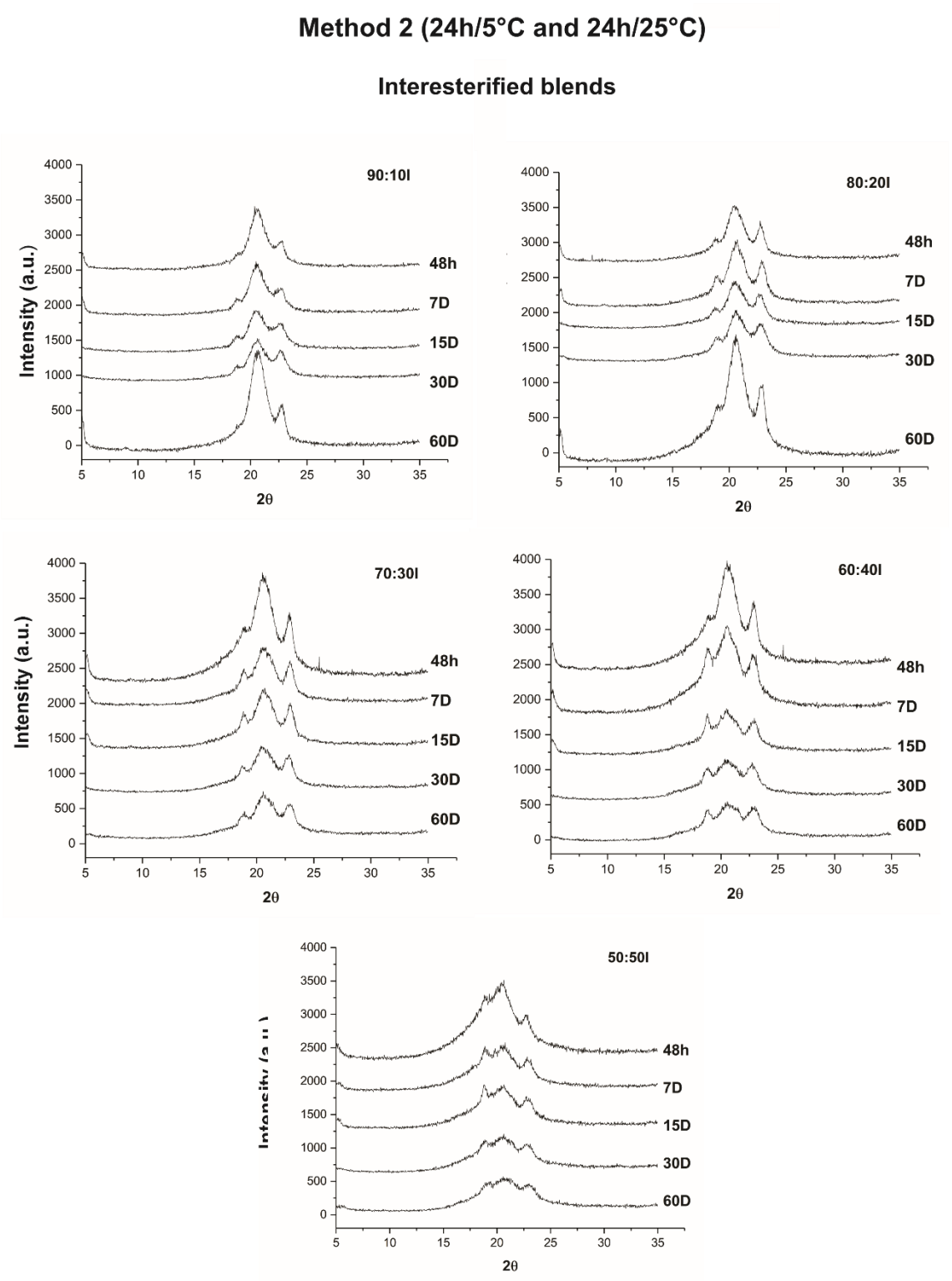

Table 3. Polymorphic forms of the simple (S) and interesterified (I) blends in the respective proportions (FHMO/SO w:w): 90:10, 80:20, 70:30, 60:40, 50:50 stabilized by Method 1 (24h/25°C).

Method 1 (24h/25°C)					
	24 hours	**7 days**	**15 days**	**30 days**	**60 days**
90:10S	β	β	β	β	β
90:10I	β'	β'	β’	β’	β’
80:20S	β	β	β	β	β
80:20I	β + β’	β + β’	β + β’	β + β’	β + β’
70:30S	β	β	β	β	β
70:30I	β’	β’	β’	β’	β
60:40S	β	β	β	β	β
60:40I	β’	β’	β’	β’	β’
50:50S	β	β	β	β + β’	β + β’
50:50I	β’	β’	β’	β’	β’

Table 4. Polymorphic forms of the simple (S) and interesterified (I) mixtures in the respective proportions (FHMO/SO w:w): 90:10, 80:20, 70:30, 60:40, 50:50 stabilized by Method 2 (24h/5°C e 24h/25°C).

Method 2 (24h/5°C and 24h/25°C)					
	48 hours	**7 days**	**15 days**	**30 days**	**60 days**
90:10S	β	β	β + β’	β	β
90:10I	β'	β'	β +β’	β+ β’	β + β’
80:20S	β	β + β’	β + β’	β	β
80:20I	β'	β +β’	β +β’	β + β’	β +β’
70:30S	β	β	β + β’	β	β
70:30I	β'	β +β’	β +β’	β +β’	β +β’
60:40S	β	β	β	β + β’	β
60:40I	β +β’	β +β’	β +β’	β +β’	β +β’
50:50S	β	β	β	β +β’	β + β’
50:50I	β’	β +β’	β +β’	β +β’	β +β’

The characterization of the raw materials alone showed the presence of polymorphic α habit in FHMO, which is characteristic of fully hydrogenated oils in the early crystallization stages, with an intense peak at 4.12 Å (Ribeiro et al., 2017). The SO was not evaluated for its polymorphic form because there was no crystalline phase at the temperatures studied; however, previous studies have

shown that it is characterized by the polymorphic β form (Demodaran et al., 2010; O'Brien, 2009)

With respect to the first crystallization protocol, with the blends kept at 25 °C for slow crystallization (method 1) (Figure 2 and 3; Table 3), the polymorphic form β was observed in all simple blends with concomitant presence of β' in the blend 50:50S after 60 days of storage, while the blends 90:10I, 60:40I, and 50:50I showed the polymorphic β' habit indefinitely and in isolated form, as well as the blend 80:20I showed both β' and β and forms simultaneously throughout the evaluation time. Only the blend 70:30I showed a change from β' to β form after 60 days of storage. Concerning the peak intensity, the interesterified blends showed β' form (with peaks mostly at 4.3 and 3.8Å) and the simple blends showed a polymorphic β form (peak at 4.55Å), with maintenance of peak intensity throughout the evaluation time. Only the interesterified blend 80:20I exhibited the concomitant polymorphic β form, in a small proportion. This result confirming the crystalline targeting ability of the interesterification reaction.

After 30 days, the β' form appeared in the simple blend 50:50S probably due to the joint and delayed crystallization of more unsaturated TAG fractions naturally present in OS. Furthermore, specific crystallization and storage conditions are considered decisive for the formation of crystal network, and the presence of β' and β polymorphs in a joint form is common in the interesterified blends, which is more favorable in blends containing high StStSt contents that remain even after interesterification, despite the increase in S2U (Chong et al., 2007).

These findings are due to the high content of S_3 TAGs such as StStSt and PStSt in the simple blends with increasing FHMO. Thus, despite the high levels of homogeneous TAGs such as StStSt, the FHMO:SO blends showed preferentially β' polymorphic habit after interesterification. As reported by Bouzidi & Narine (2012), the homogeneity of StStSt TAG guides the fat to the polymorphic β habit. However, upon randomization of fatty acids in the glycerol molecule, the interesterification reaction promotes greater TAG heterogeneity in the final fat, which results in an indefinitely polymorphic β' habit. Therefore, even though they contained considerable StStSt levels, the interesterified blends showed polymorphic β' habit throughout the evaluation time, indefinitely until the 60 days of storage at 25 °C. This result suggests that the effect of randomization

overlapped with the effect of the presence of high saturated TAG of the raw material, guiding the final polymorphic form of the lipid system toward β'. Those authors also reported that StStSt TAGs crystallize preferentially in the polymorphic β form, while PStSt crystallizes in the β' form, therefore, the coexistence of β and β' forms can be due to the majority presence of these TAGs.

The quick crystallization method (24h at 5°C and 24h at 25°C - method 2) (Figure 4 and 5; Table 4) showed a predominance of the β' form in the interesterified blends and β form in the simple blends after 48 hours of storage, which changed after 7 days, with the appearance of the β form in the interesterified blends 70:30I, 60:40I, and 50:50I. Interestingly, after 15 days, there was coexistence of the polymorphic β and β' forms in all simple and interesterified blends, except for the blends 50:50S and 60:40S, which maintained only the β form. Probably this result is due to the late crystallization of more unsaturated fractions that are in bigger quantity compared with the others proportions.

Although these effects are due to the TAG composition, they are driven by the stabilization method. The late appearance of β' form and disappearance of β form with time may be due to the possible formation of brittle crystal network, which melted with increasing the temperature at 25 °C. This event may favor a possible recrystallization, with appearance of new crystals presenting new polymorphic forms, as observed for the blends 90:10S and 90:10I, and the blends 80:20S, 70:30S, 60:40S and 50:50S, which presented a late appearance of polymorphic β' form.

In turn, under slow stabilization conditions, with maintenance at 25 °C (method 1), there was no melting or recrystallization during storage, with the formation of preferential crystals according to the TAG composition, more slowly and with monotropic transition over time, as observed for the blend 70:30I, which had a polymorphic β' habit until 30 days of evaluation followed by transition to the β form on day 60 of storage.

Therefore, in addition to randomization, the fat stabilization by method 2 also favored the appearance of β' form over time despite guiding the formation of polymorphic β habit, which was able to modify the crystal polymorphism; while the crystallization method 1 had little effect on modifying the polymorphic habit, essentially directed by the TAG composition, once the slowly crystallized simple blends presented predominant polymorphic β habit, with a preferential

appearance of polymorphic β' habit after randomization due to the greater heterogeneity of TAGs.

Ribeiro et al. (2017), Narine & Humphrey (2004), Rashid et al. (2016); Ribeiro, et al. (2009a), and Zhu et al. (2019) reported that oil and hardfat blends produced peaks of strong intensity characterizing the β-form with the concomitant presence of the β′ polymorph at lower intensity before randomization, while two peaks of varying intensity were observed after the reaction, corresponding only to the β' polymorph. According to some authors, this result may be due to the crystal formation favored by the TAG composition and the crystallization protocol used. This event is usually observed during supercooling, as evaluated in method 2, with the simultaneous presence of the polymorphic β and β' forms even in simple blends, which tend to stabilize in the β form (Metin & Hartel, 2005). As reported by Ribeiro et al. (2017), and Zhang et al. (2019), the dominance of the β polymorph in simple blends is probably due to the content of fully hydrogenated oil added, as also stated by Marangoni and Rosseau (2002).

The crystal structure of lipid bases is important factor in formulating fats for application in various products since each crystalline form presents properties related to plasticity, texture, solubility, and aeration (O'Brien, 2004). Fats crystallized in the β′ form ensure good aeration properties, while those presenting the β form have low aeration capacity and can cause a sandy perception in products due to the larger crystal size (Takeuchi et al., 2002). Therefore, considering only the polymorphic habit, interesterified blends with a predominance of the β′ polymorphic habit have greater applicability, with aeration capacity for use in fatty products such as confectionery and bakery goods (Oh et al., 2005).

3.5. Microstructure

The crystallization process occurs through the spontaneous ordering of lipid systems, characterized by total or partial restriction of movement caused by chemical or physical bonds between the triacylglycerol molecules. Thus, some factors such as lipid composition, crystallization conditions, and storage time can influence the crystal habit as well as the packing or aggregation of molecules, characterizing the fat crystal network microstructure (Wright et al., 2001).

In the present study, microscopic images were evaluated through the identification of morphology, size and total number of crystals, mean crystal diameter, and crystallized area (Tables 5 and 6). The comparison of parameters before and after randomization allows determining the effectiveness of the reaction since randomization can lead to morphological changes in crystals, including smaller crystal size, and higher crystal density (Campos, 2005; Rosseau & Marangoni, 2002).

Table 5. Microstructure parameters (Maximum diameter, mean diameter and crystallized area) of all mixtures (90:10, 80:20, 70:30, 60:40 and 50:50 (FHMO/SO w:w) in Crystallization Method 1 (slow crystallization at 25°C for 24 hours).

Method 1 (24h/25°C)					
Maximum diameter (µm)					
Blends	**24 hours**	**7 days**	**15 days**	**30 days**	**60 days**
90:10S	32.66±3.41Aa	30.25±3.11Aa	29.43±3.13Aa	30.84±2.65Aab	27.85±0.57Aa
90:10I	24.43±1.91Abc	20.62±3.20Ab	20.59±2.20Ab	21.13±3.42Aab	20.12±1.20Abc
80:20S	21.15±0.26Abc	19.05±0.28Ab	19.08±1.90Ab	18.71±1.32Ab	18.49±0.66Abc
80:20I	22.38±4.26Abc	22.30±1.01Ab	23.23±1.12Ab	24.12±1.04Aab	22.03±1.69Aab
70:30S	28.50±0.63Aab	25.76±0.63Aab	24.73±1.75Bab	25.98±1.87Aa	23.49±1.03Bab
70:30I	26.88±1.85Aabc	24.96±3.13Aab	23.88±3.72Aab	26.49±1.71Aa	25.93±4.64Aabc
60:40S	26.15±6.32Aabc	25.55±5.91Aab	22.24±0.47Ab	21.79±0.28Aab	20.65±0.23Aab
60:40I	20.09±0.84Bc	22.66±0.76Ab	21.53±0.32ABb	21.29±0.30ABab	23.40±1.47Aab
50:50S	24.03±0.79Abc	23.68±0.96ABab	23.35±0.98ABb	24.00±0.39Aab	21.80±0.83Bab
50:50I	21.38±1.23Abc	20.83±0.79Ab	19.71±1.39Ab	21.41±0.27Aab	23.40±5.59Ac
Mean diameter (µm)					
90:10S	18.91±1.19Aa	13.66±0.79Aa	17.35±0.80Aa	17.82±1.22Aa	16.40±0.31Aa
90:10I	14.89±0.68Aabc	17.81±0.97Ab	13.52±1.18Ab	13.84±1.83A	13.32±0.72Aab
80:20S	13.47±0.15Abc	13.54±1.79Aab	12.25±0.88ABb	12.18±0.79ABb	11.92±0.13Bb
80:20I	13.96±2.22Abc	12.13±0.31Aab	14.93±0.64Aab	15.48±0.65Aab	14.07±0.92Aab
70:30S	17.49±0.25Aab	14.38±0.62Bab	15.16±0.69Bab	15.86±1.09ABab	14.42±0.60Bab
70:30I	16.55±0.94Aabc	15.37±0.46Aab	15.13±2.30Aab	17.01±1.03Aab	16.68±2.76Aa
60:40S	15.94±3.46Aabc	15.94±1.83Aab	13.69±0.26Ab	13.54±0.10Ab	13.00±0.13Aab
60:40I	12.55±0.49Bc	15.50±3.35Aab	13.66±0.31ABb	13.75±0.51AB	15.23±1.15Aab
50:50S	14.67±0.33Abc	14.37±0.75Aab	14.10±0.55ABb	14.49±0.18Ab	13.24±0.36Bab
50:50I	13.66±0.64Ac	14.41±0.53Ab	12.88±0.79Ab	13.81±0.42A	15.27±3.38Aab
Crystallized área (%)					
90:10S	43.24±3.14Aa	43.51±7.35Aa	37.55±3.65Aba	41.16±4.70ABa	30.99±1.95Ba

90:10I	41.00±9.03Aa	28.87±9.16ABab	30.31±9.83ª87ab	30.55±7.66ABabcd	28.47±5.02ABa
80:20S	31.35±3.36Aab	19.23±4.06b	22.82±1.34Aab	21.95±5.41Acd	22.27±2.01Aa
80:20I	37.12±13.13Aab	32.34±3.51Aab	34.11±2.63Aa	37.07±3.03Aab	33.89±4.01Aa
70:30S	29.07±1.31Aab	28.54±2.51Aab	25.54±1.56Aab	28.77±4.82Aacd	23.06±2.12Aa
70:30I	43.36±1.18Aa	30.63±11.06Aab	26.44±13.11Aab	33.08±5.05Aabc	29.86±10.08Aa
60:40S	27.01±13.72Aab	28.15±10.39Aab	22.87±2.50Aab	21.24±0.34Acd	22.25±0.31Aa
60:40I	30.63±5.45Aab	17.55±5.14Aab	16.11±4.87Ab	17.33±4.83Ad	19.75±8.53Aa
50:50S	19.40±3.89Aab	20.40±3.06Ab	25.08±2.37Aab	24.80±0.69Acd	23.70±3.19Aa
50:50I	27.92±4.04Ab	15.86±3.05Aab	15.89±0.86A	17.28±4.91Ad	19.68±9.17Aa

FHMO: Fully hydrogenated microalgae oil; SO: soybean oil.

Table 6. Microstructure parameters (Maximum diameter, mean diameter and crystallized area) of all mixtures (90:10, 80:20, 70:30, 60:40, and 50:50 (FHMO/SO w:w) in Crystallization Method 2 (quick crystallization at 5°C for 24 hours and 25°C for 24 hours).

Method 2 (24h/5°C and 24h/25°C)					
			Maximum diameter (µm)		
Blends	**48 hours**	**7 days**	**15 days**	**30 days**	**60 days**
90:10S	33.89±4.13Ab	30.23±4.07Ac	20.09±0.13ABa	31.67±0.13Aab	25.36±1.47ABa
90:10I	23.01±1.29Ac	32.68±5.77Ac	22.69±2.79Abcd	23.34±2.79Aab	19.88±0.20Aa
80:20S	28.76±2.10Abc	23.42±1.88Bc	27.46±0.87ABab	26.33±0.87ABab	25.36±1.47Ba
80:20I	22.85±1.09Ac	19.64±0.60Bc	20.09±0.13Bd	18.86±0.13Ba	17.00±1.99Ba
70:30S	27.70±0.73Aab	26.43±0.71Bc	26.30±1.29Babc	24.60±1.29Bab	24.81±0.78Ba
70:30I	29.97±0.58Abc	27.86±3.95Ba	27.15±3.95Bab	23.35±9.80Bab	23.43±2.85Ba
60:40S	28.23±1.87Abc	21.49±1.49Bc	21.72±1.49Bd	20.98±1.51Bab	23.43±1.47Ba
60:40I	26.12±0.34Ac	20.73±1.13Ba	21.72±1.13Bd	19.65±1.51Bb	20.23±0.17Ba
50:50S	25.88±3.08Ac	20.24±0.51Ba	19.07±0.51Bd	23.34±0.13Bab	20.16±0.96Ba
50:50I	24.04±1.01Bc	30.23±3.74Aa	20.09±3.74Bd	19.87±0.13ABa	19.82±0.52Ba
			Mean diameter (µm)		
90:10S	19.63±1.10Aa	17.78±0.98Aa	13.22±0.04ABa	18.65±1.53Aa	15.05±0.48Bab
90:10I	14.22±0.50Ad	30.23±4.07Abc	14.14±1.38Abc	17.90±6.16Acd	12.57±0.18Abc
80:20S	17.06±1.07Abc	23.42±1.88Bbc	16.35±0.53ABab	15.98±0.57Babc	15.05±0.48Babc
80:20I	14.22±0.50ABd	12.54±0.21ABc	13.22±0.04Bc	12.21±0.07ABd	10.99±1.22Aabc
70:30S	16.97±0.44Abc	15.88±0.35ABab	16.02±0.70ABab	15.29±0.71Bbcd	15.16±0.52Ba
70:30I	17.93±0.32Aab	17.16±1.90Aa	16.75±2.21Aab	13.54±2.52Aab	14.39±1.39Aabc
60:40S	16.83±0.91Abc	13.21±0.75Bbc	13.19±0.58Bc	12.93±0.86Bcd	14.39±1.59Babc
60:40I	15.42±0.22Acd	13.38±0.63Bbc	13.19±0.78Bc	12.47±0.46Bd	12.82±0.12Babc
50:50S	15.46±1.46Acd	12.54±0.28Bc	11.77±0.04Bc	14.82±1.50Bcd	12.55±0.49Bbc
50:50I	14.45±0.44Ad	17.78±0.98ABbc	13.22±0.04BCc	13.00±0.39BCcd	12.50±0.30Cc

			Crystallized área (%)		
90:10S	44.24±4.75ABa	40.09±2.16ABb	40.74±2.42ABab	45.27±3.06Aa	36.23±1.55Ba
90:10I	42.53±4.40Aab	35.71±7.67Aabc	34.80±11.13Aabc	37.42±7.60Aab	27.71±0.37Aabd
80:20S	40.97±2.79Aab	30.48±4.78Bb	35.70±1.68ABbcd	35.70±1.68ABabc	30.48±5.86Babd
80:20I	41.48±3.45Aab	24.82±6.00B	22.83±1.58Bcde	19.57±6.08Bcd	23.77±6.91Babd
70:30S	30.57±1.33ABc	31.59±0.16Aab	27.37±3.24ABabcd	24.82±1.43Bbcd	29.09±2.96ABabd
70:30I	47.88±0.93Aa	44.01±5.30Aa	39.36±9.34Aa	46.07±8.11Aa	33.78±7.33Aab
60:40S	31.02±1.56ABc	18.62±6.07AB	20.41±4.89ABde	14.50±4.50Bd	20.82±5.99ABbd
60:40I	45.92±0.74Aa	25.12±1.06B	19.66±0.76BCcde	14.36±3.40Cd	25.30±1.90BCbd
50:50S	35.33±2.87Abc	15.79±2.73BC	11.36±1.08Ce	21.50±3.25Bcd	19.78±1.24Bbd
50:50I	42.08±2.73Aab	24.82±2.41B	16.02±0.37Ccde	15.59±2.74Cd	23.38±1.25Bad

FHMO: Fully hydrogenated microalgae oil; SO: soybean oil. melting enthalpy. Uppercase letters in lines indicate the statistical differences, and lowercase letters in columns indicate the statistical differences by Tukey`s test ($P<0.05$); Similar letters no show statistical differences between them.

The microstructure of the simple and interesterified blends were evaluated in different static crystallization conditions, as follows: slow crystallization at 25 °C for 24 hours (Method 1 – Figure 6), and quick crystallization at 5 °C (Method 2 – Figure 7) for 24 hours, with subsequent storage at room temperature (25 °C) for 60 days. The crystallization method 1 showed a decrease in the maximum and mean crystal diameter and crystallized area for all blends over time. However, the mean and maximum crystal diameter was higher before randomization, possibly due to the more frequent presence of β-type crystals in the simple blends, which can reach larger diameters, on average 30 μm (Miskandar et al., 2005).

Regarding the proportion of FHMO used, the crystal diameters and crystallized area were proportional to the FHMO concentration, i.e., the more FHMO, the larger the crystal diameter and crystallized area due to the increase in TAG S_3, which favored the formation of more stable and larger β-crystals (Figure 2).

Figure 6. Comparison between the initial and end time to evaluate the microstructure of simple and interesterified blends crystallized according to the Method 1 (slow crystallization).

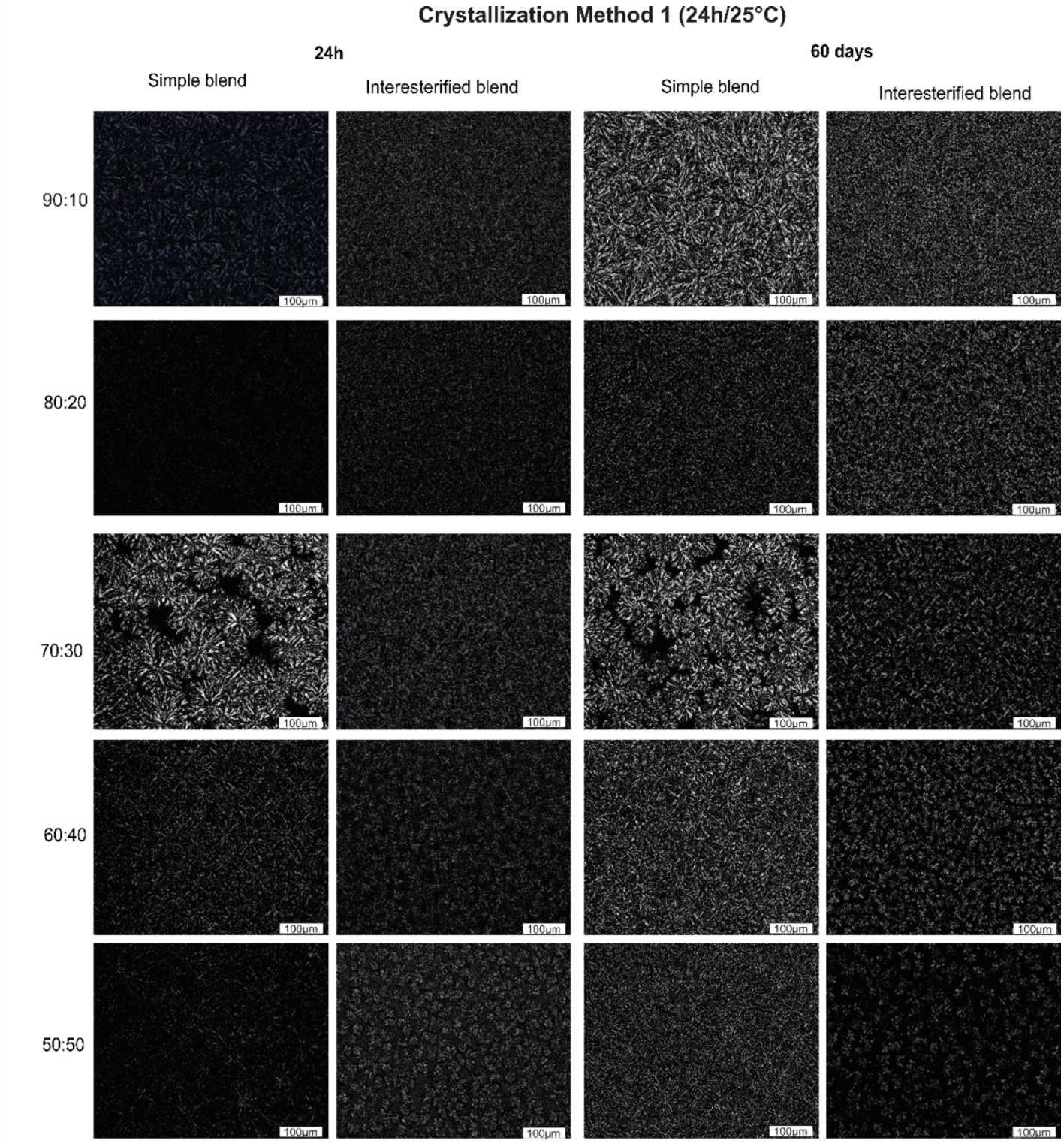

Figure 7. Comparison between the initial and end time to evaluate the microstructure of simple and interesterified blends crystallized according to the Method 2 (quick crystallization).

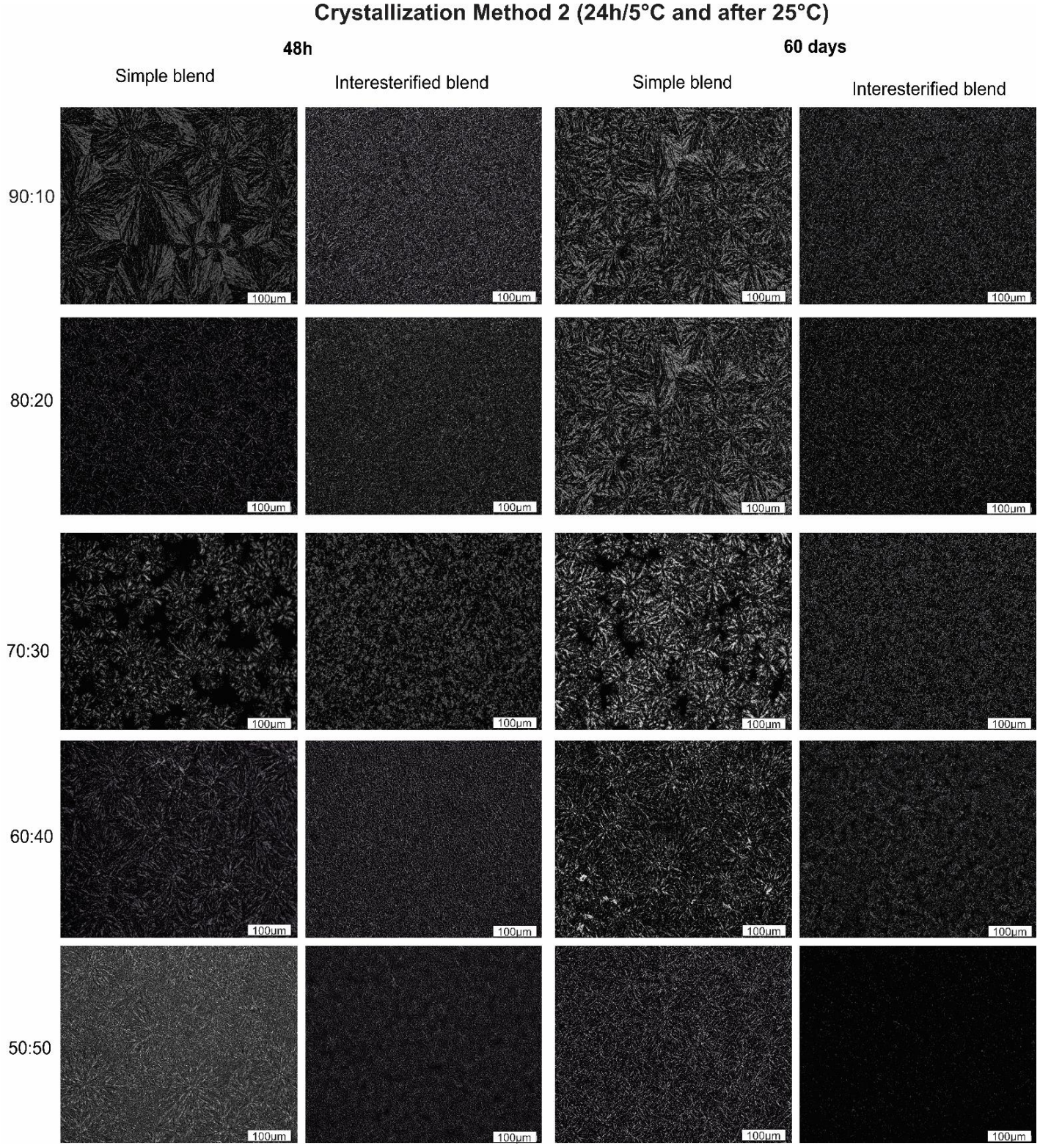

The blend 90:10S, subjected to the crystallization method 1, showed a maximum crystal diameter of 32.66 μm after 24 hours, with a non-significant reduction to 27.85 μm over time. Values above 30μm are considered sensory perceptible and undesirable for food application (Herrera & Marquez Rocha, 1996). The blends 90:10I, 80:20S, 80:20I, 70:30I, 60:40S, and 50:50I also showed a non-significant reduction in the maximum diameter over time, while the other blends (70:30S, 60:40I, 50:50S) had a significant decrease. Although a similar crystallization profile was observed in the crystallization method 2, all blends had a significant reduction in maximum crystal diameter after at least 7 days. Similar tendency was observed for mean diameter of the crystals, with a decrease over time for all blends, with statistical significance mainly in method 2. This result had a direct impact on the crystallized area, with a decrease in the total crystallized area over time.

These findings can be confirmed by the microstructure images under polarized light, in which the simple blends showed larger and disk-shaped crystals, while the interesterified blends showed smaller disk-shaped crystals (ratios 70:30I, 60:40I and 50:50I) or modification of the morphology from disk to needle (90:10I and 80:20I). Although a quantitative analysis through microstructure images becomes difficult over time due to the high crystallinity of the system, slight changes were observed in the images of the blends containing lower FHMO concentrations (60:40 and 50:50).

Similar results were found by De Graef et al. (2012), who reported that lower static crystallization temperatures (15 °C) led to rapid crystal growth, with formation of a dense structure, which prevented a clear definition of the crystal structure. Therefore, little changes in the microstructure were visualized during storage. At the highest crystallization temperature (25 °C), the nucleation rate was slower, with greater differences in the microstructure immediately after crystallization.

Ribeiro et al. (2017) used the slow crystallization method (25°C/24h) and microstructure analysis in simple and chemically interesterified matrices, reported a considerable change in crystal distribution. Before the reaction, high oleic sunflower oil and fully hydrogenated crambe oil blends showed needle-shaped crystals with compact and radially distributed nuclei, which changed to a less compact needle shape after the reaction, with a decrease in crystal size.

Regarding the quick crystallization method (Method 2), as expected, lower crystal diameters and larger crystallized area were observed when compared to the slow crystallization (Method 1) for all blends. The quick crystallization method prevents crystal growth, but allows the rapid formation of a larger number of crystals as a direct effect of nucleation, while a smaller number of crystals with larger dimensions are formed at higher temperatures (25 °C) (Lawler & Dimick, 2002; Tang & Marangoni, 2006).

Similarly to Method 1, a decrease in the maximum and mean crystal diameter and crystallized area was observed over time, and the crystal diameters were proportional to the addition of FHMO. Regarding the crystal morphology, there was a change from large disk-shaped crystals before randomization to small needle-shaped crystals after randomization, as well as a reduction in the crystallized area over time, as shown by the quantitative parameters. Concerning the crystal distribution, both crystallization methods provided a higher number of single crystals rather than crystalline clusters.

The slow crystallization (Method 1) allowed maintaining the number of clusters and isolated crystals throughout the storage at 25 °C for the blends 90:10S, 90:10I, 80:20S, 80:20I, 70:30S and 70:30I (Figure 8). There was an increase in the number of clusters and isolated crystals in the simple blends (60:40S and 50:50S), with a reduction for the interesterified blends (60:40I and 50:50I). When comparing the simple and interesterified fractions, higher numbers of isolated crystals and lower numbers of clusters were identified for the interesterified blends. This behavior may be due to the slower nucleation and subsequent growth of these crystals after interesterification. The larger surface area of slowly formed crystals may lead to an increase in the crystallized area over time, as observed in this study, with no formation of clusters.

Figure 8. Quantities of clusters and single crystals quantified in all mixtures (90:10, 80:20, 70:30, 60:40 and 50:50 (FHMO/SO w:w) in the Crystallization Method 1: slow crystallization at 25°C for 24 hours until 60 days and Crystallization Method 2: quick crystallization at 5°C/24 hours and both will be storage at 25°C until 60 days.

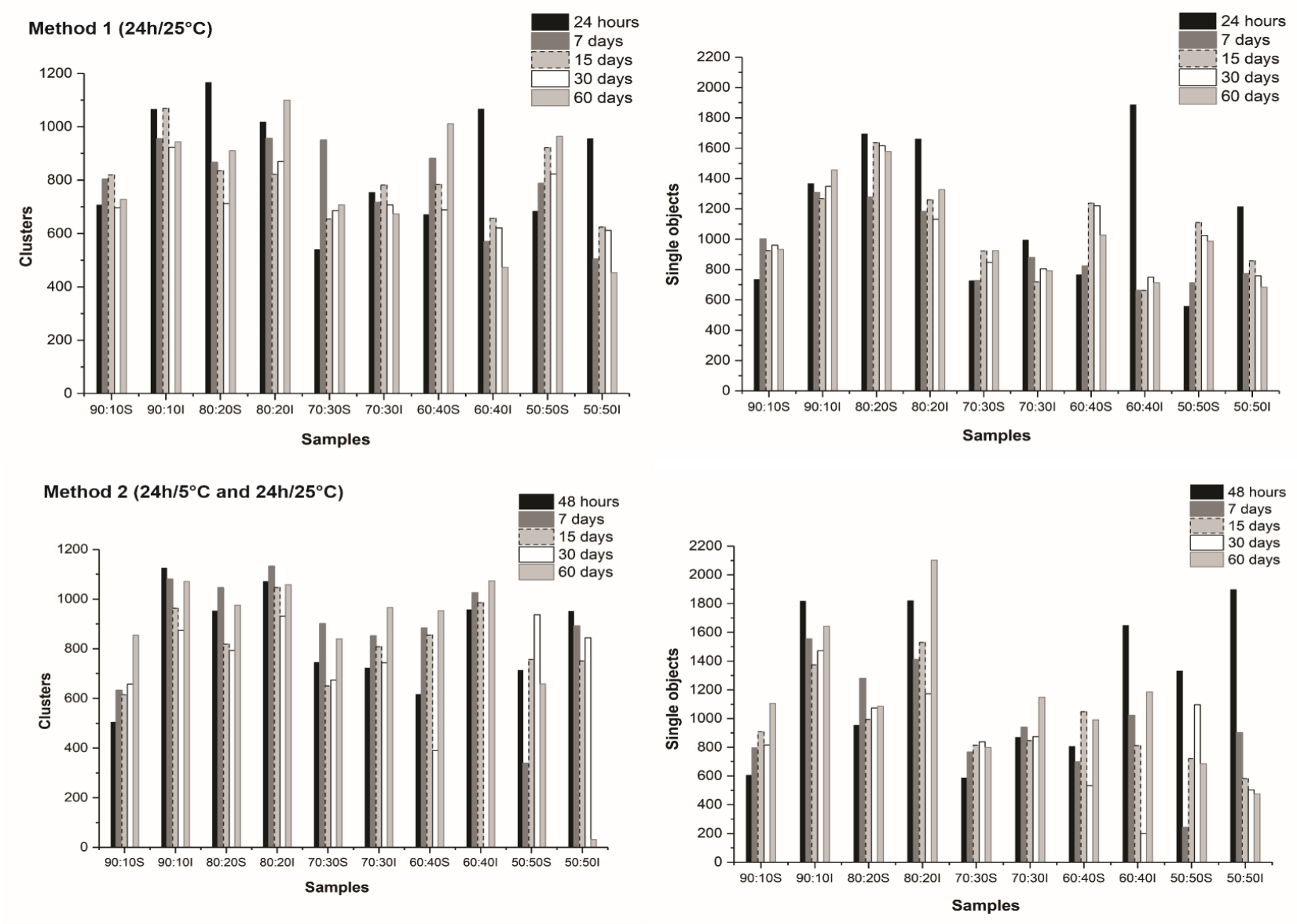

In turn, the quick crystallization (Method 2) identified a higher number of clusters when compared to Method 1. This result may be due to the immediate formation of small crystal nuclei under static crystallization at low temperature (5 °C), with a smaller surface area, which increases the tendency to agglomerate. A greater number of clusters were observed in the interesterified blends when compared to the simple blends, except for the blends 60:40I and 50:50I, possibly due to the smaller crystal diameter. In contrast, the blends 90:10S and 80:20S had higher number of clusters and single crystals when compared to their interesterified fractions. This finding shows the greater impact of the FHMO concentration on crystal formation in the single blends.

All these results may be associated with the same hypotheses raised during the polymorphism analysis, which showed a delayed appearance of polymorphic β' form and disappearance of β form. This effect may lead to a reduction in the number of single crystals and crystallized area over time, with an increase only after 60 days of storage. This event is so-called ripening of the crystals, in which a decrease in the total number of crystals is observed over time, while the number of β' crystals that appear late is not as expressive as the number of β crystals observed earlier (Himawan et al., 2006).

Thus, the decrease in the mean and maximum crystal diameters over time may be due to the melting of larger and unstable β crystals, initially formed in the crystallization Method 2, which melted with the increase in temperature. In addition, smaller crystals appear subsequently with the appearance of the polymorphic β' form, which directly affects the maximum and mean crystal diameters and the amount of isolated crystals at 60 days of storage.

The intensity of the decrease in crystal diameters in Method 2 is probably due to the simultaneous effect of two phenomena: appearance of β' crystals and reduction crystals by melting. The occurrence of the Ostwald ripening phenomenon is another possible hypothesis that may cause a decrease in the crystallized area, and the mean crystal size (Himawan et al., 2006). This phenomenon is a post-crystallization process that includes nucleation of new crystals, with dissolution of smaller crystals that solubilize in the dispersed phase, with concomitant growth of larger crystals. The late nucleation of β' type crystals and the disappearance of β type crystals mainly in crystallization Method 2 can lead to the solubilization of crystals in the dispersed phase over time, according

to the Oswald ripening effect, mainly for the blends containing higher contents of dispersed phase (SO). Moreover, there may be agglomeration of crystals, increasing the number of clusters and decreasing the amount of isolated crystals in both phenomena.

All these effects can lead to a reduction of the crystallized area over time since the dissolution of smaller and more brittle crystals leads to the formation of more dispersed phase and less crystalline phase (Bouzidi & Narine, 2012; da Silva et al., 2022; McClements, 2016).

Zhu et al. (2019) reported that the differences in SFC, polymorphism, nucleation mechanism, and crystal growth of fats indicate significant differences in the crystal morphology in matrices before and after interesterification. The authors observed large rod-shaped crystals throughout the crystal network before the interesterification, and decreased crystal size after the reaction. These results again suggested that StStSt may act as a crystallization inducer, driving the formation of dense three-dimensional network, as verified in this study, with a large number of single crystals, especially at higher FHMO concentrations (90:10S and 80:20S).

The crystallization parameters, mainly the quick crystallization, have been discussed by Metin & Hartel (2005), who stated that static crystallization conditions induce the formation of spherical particles. Also, De Graef et al. (2012) observed a larger number of crystals in the crystallization at lower temperatures, generating a dense crystalline structure, i.e., with a larger crystallized area, as observed in the present study.

The reduced crystal size observed in interesterified blends is considered a positive factor for the application of fats in foods. Small crystals ensure greater firmness and better texture at the time of consumption, while large crystals can promote soft fats, but with a sandy mouthfeel (Pande & Akoh, 2013). This result corroborates with the polymorphism results, once the interesterification process modified the crystal habit of the fats studied, with a predominance of the β′ polymorph. The β′ crystals are small, with desirable plasticity characteristics in products such as margarines and fats for bakery and confectionery products. On the other hand, polymorphic β crystals tend to produce broad granular crystals, resulting in products with low aeration potential, which can impair the macroscopic properties of some foods (Shi et al., 2005). In addition, the storage

time at 25 °C contributed to such characteristics, with a decrease in crystal diameters of the blends before and after randomization, favoring the formation of clusters, which can reinforce the crystal network formed while maintaining the crystal size.

Ribeiro et al. (2009a) reported that the crystal morphology was totally modified after randomization of interesterified fats from a large spherulite in the simple blends to a small disk with granular crystal structure. In turn, Ahmadi et al. (2008), Rashid, et al. (2016), and Ribeiro et al. (2018) reported that besides altering the polymorphism of the blends, the chemical interesterification affected the crystal morphology, changing the crystals from disk-shaped, associated with the polymorphic β-form, to needle-shaped, associated with the β' form with lower crystal density. These results may be due to the regiospecific distribution since a significant reduction of TAG S_3 and increase of SU_2 was observed after the reaction.

Ahmadi et al. (2008) evaluated the effect of the crystallization temperature on fat morphology of different lipid blends under isothermal crystallization at 20, 30, 40, and 50 °C for 24 h. The authors reported that the higher crystallization temperature, the lower the percentage of crystallized area. No changes in crystal morphology were observed as a function of storage time, even after 100 days of storage. De Graef et al. (2012) reported little change in the microstructure of the simple blends, with the appearance of large spherulites between small crystals after 24 hours, which grew to form large spherulites after 30 days. This result was probably due to initial crystallization with formation of a brittle network, followed by nucleation of a more stable polymorph due to the great presence of StStSt, similar to the present study.

Therefore, the interesterified blends, independent of the crystallization method showed more tendency to form a β’ crystals. Over time, the study showed that these crystals continue to the monotropic transformation when the Method 1 was used, increasing the β crystals over time. When the Method 2 was used, the crystals were formed quickly and this behavior results in fragile crystals in β and β’ forms concomitant. Over time, this condition tends to change due to the Oswald Ripening phenomenon and the new β’ crystals formation, besides the maintenance of β crystals content. So, the Method 2 could be the most suitable

for food applications, once they promoted the formation of crystals with smaller diameter, less monotropic transitions, denser crystal network when forming clusters, and larger crystallized area, specific characteristics of the polymorphic β' form, which tend to the formation of aerated products, with increased applicability. Again, the results have shown that the esterification was more effective than the homogeneous composition of TAGs such as tristearin, even in significant amounts after the interesterification reaction.

4. Conclusion

The present study evaluated blends made with fully hydrogenated microalgae oil (FHMO) and soybean oil (SO) in the ratios 90:10, 80:20, 70:30, 60:40, and 50:50 before and after the chemical interesterification, for the chemical and crystallization characteristics (slow or quick crystallization) during storage for 60 days. A predominance of tristearine triacylglycerol in both the simple and interesterified blends was observed in a triacylglycerol distribution, due to the fatty acid composition of FHMO and SO raw materials. The randomization led to a reduction of trisaturated triacylglycerols with simultaneous increase in disaturated TAGs, modifying the crystal morphology and the physical properties of the blends. In the simple blends, large disk-shaped crystals were identified, with formation of small needle-shaped crystals after randomization towards the β' crystalline configuration. The quick crystallization methodology (24h/5°C and after at 25°C) showed a higher crystal density after 48 hours, with crystals of smaller mean and maximum diameter and larger crystallized area when compared to the slow crystallization method (24h/25°C). In addition, the quick crystallization resulted in a β and β’ polymorphic habits simultaneously probably due to melting of brittle crystals rapidly formed, with subsequent recrystallization into a new polymorphic form (β'). The Ostwald ripening may also have favored the dissolution of smaller crystals reducing the crystallized area over the time. On the other hand, the slow crystallization (24h/25°C) resulted in a more stable crystal network, with late appearance of polymorphic β' form and stabilization mostly in polymorphic β form even in the interesterified blends and following the tradition monotropic changes during the time. Thus, the present study pointed out that the quick crystallization (5°C/24h and 24h/25°C) can be effective for food

applications by guiding the fats to the polymorphic β' form and maintenance of this amount over time, with smaller diameter mainly in the interesterified blends, avoiding the bigger crystals and expanding the possibilities of application in products that require aeration such as margarines, bakery products, and confectionery.

5. Appendix

Appendix 1. Fatty acid composition (%) of raw materials (SO and FHMO) and the respective mixtures.

Fatty acids (%)	FHMO	SO	90:10 (w:w)	80:20 (w:w)	70:30 (w:w)	60:40 (w:w)	50:50 (w:w)
C 12:0 – Lauric acid	0.15±0.02	0.02±0.01	0.14±0.01	0.13±0.01	0.11±0.01	0.10±0.01	0.09±0.01
C14:0 – Miríst ic acid	0.47±0.01	0.10±0.02	0.43±0.00	0.39±0.00	0.35±0.00	0.32±0.01	0.28±0.01
C16:0- Palmític acid	5.52±0.01	11.10±0.24	6.06±0.03	6.62±0.05	7.18±0.07	7.74±0.10	8.29±0.12
C 16:1 – Palmitoleic acid	-	-	0.01±0.00	0.02±0.00	0.03±0.00	0.04±0.00	0.05±0.01
C 17:0 – Margaric acid	0.09±0.01	0.09±0.01	0.09±0.01	0.09±0.01	0.09±0.01	0.09±0.01	0.09±0.01
C18:0 – Stearic acid	92.85±0.10	3.74±0.35	83.71±0.08	74.83±0.04	65.94±0.04	57.06±0.07	48.18±0.12
C18:1 – Oleic acid	-	24.53±2.28	2.60±0.32	5.03±0.54	7.47±0.76	9.90±0.97	12.34±1.19
C18:2 – Linoleic acid	0.12±0.01	52.70±2.15	5.37±0.21	10.62±0.43	15.87±0.64	21.12±0.86	26.37±1.07
C18:3 – Linolenic acid	-	6.39±0.50	0.63±0.05	1.28±0.10	1.91±0.15	2.56±0.20	3.19±0.26
C20:0 – Araquidic acid	0.95±0.01	0.48±0.10	0.90±0.01	0.86±0.02	0.81±0.03	0.76±0.04	0.72±0.05
C20:1 – Eicosenoic acid	-	0.23±0.02	0.02±0.00	0.05±0.00	0.07±0.01	0.09±0.01	0.11±0.00
C22:0 – Behenic acid	-	0.51±0.03	0.10±0.02	0.15±0.02	0.19±0.02	0.24±0.02	0.28±0.02
C24:0 – Lignoceric acid	-	0.20±0.02	0.02±0.00	0.04±0.01	0.06±0.01	0.08±0.01	0.10±0.01
∑ Saturated	99.94±0.10	16.14±0.76	91.36±0.12	83.01±0.14	74.65±0.16	66.30±0.18	57.94±0.02
∑ Monounsaturated	-	24.77±2.31	2.63±0.01	5.10±0.02	7.56±0.04	10.03±0.05	12.49±0.07
∑ Polyunsaturated	0.12±0.1	59.09±2.62	6.01±0.04	11.90±0.08	17.78±0.11	23.67±0.15	29.57±0.18
S. I.	190±5.44	193±42.66	-	-	-	-	-
I.I. (I_2/100g)	129±2.64	0.33± 0.07	-	-	-	-	-

FHMO: Fully hydrogenated microalgae oil; SO: soybean oil; S.I: Saponification Index; I.I.: Iodine Index.

Appendix 2. Triacylglycerols composition (%) of raw materials (SO and FHMO) and the respective mixtures

TAG	NC	FHMO	SO	90:10S	90:10I	80:20S	80:20I	70:30S	70:30I	60:40S	60:40I	50:50S	50:50I
PPP	48	0.69±0.12	-	0.55±0.10	0.94±0.15	0.20±0.10	1.06±0.17	0,28±0,24	1.01±0.19	0.66±0.24	0.75±0.21	0.68±0.14	0.65±0.12
POP		-	1,07±0.34	-	-	0.22±0.10	-	1.08±1.08	-	1.12±0.07	-	0.28±0.12	-
PLP	50	-	2,11±0.34	-	-	0.88±0.22	-	0.42±0.17	-	-	-	7.68±1.40	-
PPS		3.79±0.39	-	3.01±0.30	2.62±0.19	2.94±0.22	2.36±0.03	2.07±1.27	2.19±0.12	2.56±0.42	2.45±0.19	1.41±0.16	2.46±0.41
POO		-	5,71±0.90	2.42±0.93	-	2.75±0.18	-	1.42±1.34	-	2.97±0.25	-	4.32±0.46	-
PPO		-	-	-	0.17±0.02	-	0.49±0.16	-	0.70±0.23	-	0.81±0.14	-	1.29±0.32
PLO	52	-	10,62±1.22	-	-	4.09±1.82	-	3.40±1.30±	-	3.16±1.49	-	5.89±0.06	-
PLL		-	12,57±0.70	0.34±0.30	-	-	-	3.59±1.25	-	4.35±1.39	-	0.62±0.25	-
PLnL		-	2,09±0.45	-	-	-	-	1.24±1.25	-	-	-	-	-
PSS		15.45±0.43	-	11.35±1.37	16.46±0.51	13.36±1.15	13.98±1.14	8.44±1.28	12.96±1.47	8.61±1.18	13.48±0.01	1.88±0.58	10.59±1.91
PSO			-	-	1.66±0.14	-	4.47±0.47	-	6.66±1.22	-	6.83±0.07	-	9.25±0.39
OOO		-	8,75±1.04	-	-	3.43±1.08	-	3.06±1.27	-	4.8±1.04	-	6.45±2.11	-
OLO		-	14,20±0.90	-	-	4.36±1.35	-	3.90±1.28	-	2.77±2.17	-	8.07±0.08	-
OLL		-	19,05±1.22	-	-	2.42±1.33	-	3.09±1.43	-	4.87±3.76	-	10.30±1.15	-
LLL		-	18,48±1.07	-	-	2.34±0.47	-	2.84±1.51	-	6.01±4.24	-	6.16±0.66	-
LLnL		-	5,35±0.99	-	-	1.55±0.58	-	1.26±1.23	-	-	-	-	-
PSL		-	0.91±0.14	-	-	-	0.62±0.26	-	1.02±0.04	-	1.69±0.32	-	3.16±1.37
SSO	54	-	-	-	8.17±0.87	-	15.02±0.03	-	21.98±1.36	-	23.52±0.84	-	23.58±3.51
SSL		-	-	-	1.6±0.14	-	2.55±0.07	-	4.10±0.70	-	8.5±1.66	-	12.07±2.25
SSLn		-	-	-	-	-	0.84±0.01	-	1.49±0.06	-	2.82±0.15	-	4.66±2.71
SLLn		-	-	-	0.62±0.18	-	0.62±0.36	-	1.49±0.06	-	1.11±0.10	-	-
SLL		-	-	-	2.08±0.34	-	1.83±0.21	-	1.80±0.19	-	2.20±1.60	-	2.21±1.78
SLLn		-	-	-	-	-	-	-	-	-	-	-	1.36±0.76
SLnLn		-	-	-	0.42±0.15	-	-	-	0.51±0.06	-	-	-	-
LLL		-	-	-	0.51±0.16	-	0.59±0.58	-	0.37±0.22	-	0.90±0.44	-	0.90±0.39

LLLn		-	-	-	0.24±0.16	-	0.29±0.23	-	0.35±0.02	-	0.65±0.24	-	0.69±0.22
LLnLn		-	-	-	-	-	0.15±0.06	-	0.19±0.04	2.46±2.54	0.42±0.08	-	0.50±0.09
SSS		78.38±0.45	-	48.41±2.75	63.45±0.96	60.58±4.87	54.85±0.59	63.51±1.18	44.66±0.17	55.96±7.30	33.80±0.41	48.41±2.75	23.08±3.86
SSA	56	1.68±0.24	-	-	0.16±0.09	0.94±0.51	-	0.40±0.05	-		-	-	0.56±0.26
ΣS_3		98.32±0.24	-	88.48±0.87	83.47±1.28	77.08±0.66	72.26±1.54	74.30±2.14	61.93±1.57	67.81±7.36	50.77±0.37	54.18±2.17	36.85±6.11
ΣS_2U		1.68±0.24	3.19±0.60	1.99±0.67	12.67±1.13	1.90±0.11	23.98±0.28	1.89±0.66	34.47±2.10	1.12±0.46	45.66±2.06	7.97±1.44	57.59±7,08
ΣSU_2		-	30.99±0.93	4.39±1.21	3.12±0.64	8.40±0.05	2.45±0.57	9.66±1.13	2.49±0.25	10.48±3.58	2.09±1.71	6.52±0.31	3.55±1.05
ΣU_3		-	65.82±0.70	5.18±0.27	0.75±0.21	12.56±0.83	1.32±0.68	14.15±0.86	1.11±0.28	20.89±4.68	2.51±	27.01±3.88	2.01±0.22

Simple (S) and Interesterified (I) blends of fully hydrogenated microalgae oil (FHMO) and soybean oil (SO) in the respective proportions (w:w): 90:10, 80:20, 70:30, 60:40 e 50:50; Triacylglycerols (TAG); Number of carbons (NC); Trisaturated (S3), Disaturated-monounsaturated (S2U); monosaturated-diunsaturated (SU2), triunsaturated (U3). Mean between sample injection triplicates.

Simple (S) and Interesterified (I) blends of fully hydrogenated microalgae oil (FHMO) and soybean oil (SO) in the respective proportions (w:w): 90:10, 80:20, 70:30, 60:40 e 50:50; Triacylglycerols (TAG); Number of carbons (NC); Trisaturated (S3), Disaturated-monounsaturated (S2U); monosaturated-diunsaturated (SU2), triunsaturated (U3). Mean between sample injection triplicates.

CRediT authorship contribution statement

Kamila Ramponi Rodrigues de Godoi Fernandes: Conceptualization, Methodology, Investigation, Formal analysis, Writing – original draft. Mayanny Gomes da Silva: Methodology, Formal analysis, Review. Lisandro Pavie Cardoso: Supervision, Resources. Ana Paula Badan Ribeiro: Conceptualization, Writing – review & editing, Supervision, Funding acquisition, Resources, Project administration.

Declaration of Competing Interest

The authors declare that they have no known competing financial interests or personal relationships that could have appeared to influence the work reported in this paper.

Acknowledgments

Ana Paula Badan Ribeiro thank CNPq (303429/2018-6) for productivity grant and São Paulo Research Foundation-FAPESP (16/11261-8). Kamila Ramponi Rodrigues de Godoi Fernandes thank CNPq (140789/2017-0) for PhD scholarship grant. Lisandro Pavie Cardoso thank CNPq (302626/2016-6 and 307896/2019-6) for productivity grant. This study was financed in part by the “Coordenação de Aperfeiçoamento de Pessoal de Nível Superior - Brazil (CAPES)”–Finance Code 001.

References

Ahmadi, L., Wright, A. J., & Marangoni, A. G. (2008). *Chemical and enzymatic interesterification of tristearin / triolein-rich blends : Microstructure and polymorphism*. 1025–1034. https://doi.org/10.1002/ejlt.200800059

Antoniosi Filho, N. R., Mendes, O. L., & Lanças, F. M. (1995). Computer prediction of triacylglycerol composition of vegetable oils by HRGC. *Chromatographia*, *40*(9–10), 557–562. https://doi.org/10.1007/BF02290268

AOCS. (2009). *Official methods and recommended practices of the American Oil Chemists’ Society* (6th Edition). https://doi.org/http://dx.doi.org/10.1002/0471740039.vec0152

Asbridge, D. D. (2015). Soybeans vs.Other vegetable oils as a source of edible

oil products. In D. R. Erickson (Ed.), *Pratical Handbook and soybean processing and utilization* (pp. 1–9). AOCS Press.

Ballestra, D. (n.d.). *Produce trans-free fats - Interchem® Technology*. https://www.desmetballestra.com/oils-fats/fat-modification/interesterification/chemical-interesterification

Bouzidi, L., & Narine, S. S. (2012). Relationships between molecular structure and kinetic and thermodynamic controls in lipid systems. Part II: Phase behavior and transformation paths of SSS, PSS and PPS saturated triacylglycerols - Effect of chain length mismatch. *Chemistry and Physics of Lipids*, *165*(1), 77–88. https://doi.org/10.1016/j.chemphyslip.2011.11.005

Campos, R. (2005). Fat Crystal Networks. In *Fat Crystal Networks* (pp. 267–349). Marcell Dekker Inc.

Chong, C. L., Kamarudin, Z., Lesieur, P., Marangoni, A., Bourgaux, C., & Ollivon, M. (2007). Thermal and structural behaviour of crude palm oil: Crystallisation at very slow cooling rate. *European Journal of Lipid Science and Technology*, *109*(4), 410–421. https://doi.org/10.1002/ejlt.200600249

Chopin-Doroteo, M., Morales-Rueda, J. A., Dibildox-Alvarado, E., Charó-Alonso, M. A., de la Peña-Gil, A., & Toro-Vazquez, J. F. (2011). The Effect of Shearing in the Thermo-mechanical Properties of Candelilla Wax and Candelilla Wax-Tripalmitin Organogels. *Food Biophysics*, *6*(3), 359–376. https://doi.org/10.1007/s11483-011-9212-5

Dassanayake, L. S. K., Kodali, D. R., & Ueno, S. (2011). Formation of oleogels based on edible lipid materials. *Current Opinion in Colloid and Interface Science*, *16*(5), 432–439. https://doi.org/10.1016/j.cocis.2011.05.005

De Graef, V., Vereecken, J., Smith, K. W., Bhaggan, K., & Dewettinck, K. (2012). Effect of TAG composition on the solid fat content profile, microstructure, and hardness of model fat blends with identical saturated fatty acid content. *European Journal of Lipid Science and Technology*, *114*(5), 592–601. https://doi.org/10.1002/ejlt.201100215

Demodaran, S., Parkin, K. L., & Fennema, O. L. (2010). *Química de Alimentos de Fennema* (Forth edit). Editora Artmed.

Fageria, N. K., Baligar, V. C., & Jones, C. A. (2010). *Growth and Mineral Nutrition of Field Crops* (Third Edit, p. 551). CRC Press.

Grimaldi, R., Gonçalves, L. A. G., & Ando, M. Y. (2005). Otimização da reação

de interesterificaç ão química do óleo de palma. *Quimica Nova*, *28*(4), 633–636. https://doi.org/10.1590/s0100-40422005000400015

Guedes, A. M. M., Ming, C. C., Ribeiro, A. P. B., Silva, R. C., Gioielli, L. A., & Gonçalves, L. A. G. (2014). Physicochemical Properties of Interesterified Blends of Fully Hydrogenated Crambe abyssinica Oil and Soybean Oil. *Journal of American Oil Chemistry Society*, *91*(1), 111–123.

Hammond, E. G., Johnson, L. a, Su, C., Wang, T., & White, P. J. (2005). Soybean Oil. *Bailey's Industrial Oil and Fat Products*, *1*, 577–653. https://doi.org/10.1002/047167849X.bio041

Hartman, L., & Lago, R. C. A. (1973). Rapid preparation of fatty acid methyl esters from lipids. *Lab. Pract.*, *22*(January), 475-476,494.

Herrera, M. L., & Marquez Rocha, F. J. (1996). Effects of sucrose ester on the kinetics of polymorphic transition in hydrogenated sunflower oil. *Journal of the American Oil Chemists' Society*, *73*(3), 321–326. https://doi.org/10.1007/BF02523425

Himawan, C., Starov, V. M., & Stapley, A. G. F. (2006). Thermodynamic and kinetic aspects of fat crystallization. *Advances in Colloid and Interface Science*, *122*(1–3), 3–33. https://doi.org/10.1016/j.cis.2006.06.016

Ifeduba, E. A., Martini, S., & Akoh, C. C. (2016). Enzymatic Interesterification of High Oleic Sunflower Oil and Tripalmitin or Tristearin. *JAOCS, Journal of the American Oil Chemists' Society*, *93*(1), 61–67. https://doi.org/10.1007/s11746-015-2756-7

Lawler, P. J., & Dimick, P. S. (2002). Crystallization and Polymorphism of Fats. In *Food Lipids: Chemistry, Nutrition, and Biotechnology*.

Marangoni, A. G., & Rosseau, D. (2002). The effects of interesterification on the physical properties of fats. In A. G. Marangoni & S. S. Narine (Eds.), *Physical Properties of Lipids*. Marcell Dekker Inc.

McClements, D. J. (2016). *Food Emulsions*.

Mensink, R. P. (2005). Effects of stearic acid on plasma lipid and lipoproteins in humans. In *Lipids* (Vol. 40, Issue 12, pp. 1201–1205). https://doi.org/10.1007/s11745-005-1486-x

Metin, S., & Hartel, R. W. (2005). Fats and Oils. *Bailey's Industrial Oil and Fat Products*, 45–76.

Miskandar, M. S., Man, Y. C., Yusoff, M. S. A., & Rahman, R. A. (2005). Quality

of margarine: Fats selection and processing parameters. *Asia Pacific Journal of Clinical Nutrition*, *14*(4), 387–395.

Narine, S. S., & Humphrey, K. L. (2004). A comparison of lipid shortening functionality as a function of molecular ensemble and shear: Microstructure, polymorphism, solid fat content and texture. *Food Research International*, *37*(1), 28–38. https://doi.org/10.1016/j.foodres.2003.09.013

O'Brien, R. D. (2009a). Interesterification. In *Fats and Oils: Formulating and Processing for Applications* (pp. 122–132). CRC Press.

O'Brien, R.D. (2009b). Chapter 1 - Raw Materials. In *Fats and Oils: Formulating and Processing for Applications* (Third Edit, pp. 1–66). CRC Press.

O'Brien, Richard D. (2004). Fats and oils: formulating and processing for applications. In *New York*.

Oh, J. H., McCurdy, A. R., Clark, S., & Swanson, B. G. (2005). Stabilizing polymorphic transitions of tristearin using diacylglycerols and sucrose polyesters. *JAOCS, Journal of the American Oil Chemists' Society*, *82*(1), 13–19. https://doi.org/10.1007/s11746-005-1036-y

Pande, G., & Akoh, C. C. (2013). Enzymatic modification of lipids for trans-free margarine. *Lipid Technology*, *25*(2), 31–33. https://doi.org/10.1002/lite.201300253

Rashid, N. A., Kamarulzamana, N. A., & Omarb, Z. (2016). Effect of chemical and enzymatic interesterification on the physicochemical properties of palm oil and. Palm kernel oil blends. *Jurnal Teknologi*, *2*, 19–25. www.jurnalteknologi.utm.my

Rashid, N. A., Safuan, T. S. S. T., Kelana, A. T., Zuher, M. A., & Omar, Z. (2016). Effects of chemical interesterification on the physicochemical properties of palm stearin and rice bran oil blends. *Jurnal Teknologi*, *5*, 21–27.

Ribeiro, A. P. B., Basso, R. C., Grimaldi, R., Gioielli, L. A., dos Santos, A. O., Cardoso, L. P., & Guaraldo Gonçalves, L. A. (2009a). Influence of chemical interesterification on thermal behavior, microstructure, polymorphism and crystallization properties of canola oil and fully hydrogenated cottonseed oil blends. *Food Research International*, *42*(8), 1153–1162. https://doi.org/10.1016/j.foodres.2009.05.016

Ribeiro, A. P. B., Basso, R. C., Grimaldi, R., Gioielli, L. A., & Gonçalves, L. A.

G. (2009). Instrumental Methods for the Evaluation of Interesterified Fats. *Food Analytical Methods*, *2*(4), 281–302.

Ribeiro, M. D. M., Ming, C. C., Silvestre, I. M., Grimaldi, R., & Ap. G. Gonçalves, L. (2017). Comparison between enzymatic and chemical interesterification of high oleic sunflower oil and fully hydrogenated soybean oil. *European Journal of Lipid Science and Technology*, *119*(2), 1–9. https://doi.org/10.1002/ejlt.20150047

Ribeiro, A. P. B., Basso, R. C., Grimaldi, R., Gioielli, L. A., Gonçalves, L. A. G., Oliveira, P. D., Rodrigues, A. M. C., Bezerra, C. V., Silva, L. H. M., Morselli Ribeiro, M. D. M., Ming, C. C., Silvestre, I. M., Grimaldi, R., Ap. G. Gonçalves, L., Dunn, A. M., Hofmann, O. S., Waters, B., Witchel, E., Ramli, N; Mohd Sobani, S. Hrádková, I. (2017). Effects of chemical interesterification on the triacylglycerols, solid fat contents and crystallization kinetics of palm oil-based fats. *Proceedings of the 20th USENIX Security Symposium*, *2*(1), 369–376. https://doi.org/10.1016/j.foodres.2018.05.015

Ribeiro, A. P. B., Grimaldi, R., Gioielli, L. A., Dos Santos, A. O., Cardoso, L. P., & Gonçalves, L. A. G. (2009b). Thermal behavior, microstructure, polymorphism, and crystallization properties of zero trans fats from soybean oil and fully hydrogenated soybean oil. *Food Biophysics*, *4*(2), 106–118. https://doi.org/10.1007/s11483-009-9106-y

Ribeiro, A. P. B., Grimaldi, R., Gioielli, L. A., Dos Santos, A. O., Cardoso, L. P., & Gonçalves, L. A. G. (2009c). Thermal behavior, microstructure, polymorphism, and crystallization properties of zero trans fats from soybean oil and fully hydrogenated soybean oil. *Food Biophysics*, *4*(2), 106–118. https://doi.org/10.1007/s11483-009-9106-y

Ribeiro, M. D. M. M., Ming, C. C., Lopes, T. I. B., Grimaldi, R., Marsaioli, A. J., & Gonçalves, L. A. G. (2017). Synthesis of structured lipids containing behenic acid from fully hydrogenated Crambe abyssinica oil by enzymatic interesterification. *Journal of Food Science and Technology*, *54*(5), 1146–1157. https://doi.org/10.1007/s13197-017-2540-9

Ribeiro, M. D. M. M., Ming, C. C., Lopes, T. I. B., Grimaldi, R., Marsaioli, A. J., & Gonçalves, L. A. G. (2018). Enzymatic synthesis of structured lipids from liquid and fully hydrogenated high oleic sunflower oil. *International Journal*

of Food Properties, *21*(1), 702–716. https://doi.org/10.1080/10942912.2018.1454943

Rogers, M. A., Tang, D., Ahmadi, L., & Marangoni, A. G. (2008). Fat crystal networks. *Food Materials Science: Principles and Practice*, 369–414. https://doi.org/10.1007/978-0-387-71947-4_17

Rosseau, D., & Marangoni, A. G. (2002). Chemical Interesterification of Food Lipids: Theory and Practice. In C. C. Akoh & D. B. Min (Eds.), *Food Lipids : Chemistry, Nutrition, and Biotechnology* (Second Edi, p. 1014). Marcel Dekker, Inc.

Rousseau, D., & Marangoni, A. G. (1998). The effects of interesterification on physical and sensory attributes of butterfat and butterfat-canola oil spreads. *Food Research International*, *31*(5), 381–388. https://doi.org/10.1016/S0963-9969(98)00100-8

Rousseau, D., Marangoni, A. G., & Jeffrey, K. R. (1998). The influence of chemical interesterification on the physicochemical properties of complex fat systems. 2. morphology and polymorphism. *JAOCS, Journal of the American Oil Chemists' Society*, *75*(12), 1833–1839. https://doi.org/10.1007/s11746-998-0339-6

Sampath, H., & Ntambi, J. M. (2005). The fate and intermediary metabolism of stearic acid. *Lipids*, *40*(12), 1187–1191. https://doi.org/10.1007/s11745-005-1484-z

Sato, K., & Ueno, S. (2005). Polymorphism in fats and oils. *Bailey's Industrial Oil and Fat Products*, *1*, 77–120. http://onlinelibrary.wiley.com/doi/10.1002/047167849X.bio020/full

Silva, M. G., de Godoi, K. R. R., Gigante, M. L., Pavie Cardoso, L., & Paula Badan Ribeiro, A. (2022). Developed and characterization of nanostructured lipid carriers containing food-grade interesterified lipid phase for food application. *Food Research International*, *155*(October 2021), 111119. https://doi.org/10.1016/j.foodres.2022.111119

Speranza, P., Macedo, G., & Ribeiro, A. P. B. (2015). Lipase catalyzed interesterification of Amazonian patauá oil and palm stearin for preparation of specific-structured oils. *Journal of Food Science and Technology*, *52*, 8268–8275.

Takeuchi, M., Ueno, S., & Sato, K. (2002). Crystallization kinetics of

polymorphic forms of a molecular compound constructed by SOS (1,3-distearoyl-2-oleoyl-sn-glycerol) and SSO (1,2-distearoyl-3-oleoyl-rac-glycerol). *Food Research International*, *35*(10), 919–926. https://doi.org/10.1016/S0963-9969(02)00154-0

Tang, D., & Marangoni, A. G. (2006). Microstructure and fractal analysis of fat crystal networks. *JAOCS, Journal of the American Oil Chemists' Society*, *83*(5), 377–388. https://doi.org/10.1007/s11746-006-1216-9

Wright, a. J., Scanlon, M. G., Hartel, R. W., & Marangoni, a. G. (2001). Rheological Properties of Milkfat and Butter Concise Reviews in Food Science. *Journal of Food Science*, *66*(8), 1056–1071. https://doi.org/10.1111/j.1365-2621.2001.tb16082.x

Yap, P., Man, J. De, & Man, L. De. (1989). Polymorphism of palm oil and palm oil products. *Journal of the American Oil Chemist's Society*, *66*(5), 693–697. https://doi.org/10.1007/BF02669954

Zhang, Z., Lee, W. J., Zhou, H., & Wang, Y. (2019). Effects of chemical interesterification on the triacylglycerols, solid fat contents and crystallization kinetics of palm oil-based fats. *Food and Function*, *10*(11), 7553–7564. https://doi.org/10.1039/c9fo01648a

Zhu, T., Zhang, X., Wu, H., & Li, B. (2019). Comparative study on crystallization behaviors of physical blend- and interesterified blend-based special fats. *Journal of Food Engineering*, *241*(May 2018), 33–40. https://doi.org/10.1016/j.jfoodeng.2018.08.005

ARTIGO 3. SIMPLE AND INTERESTERIFIED LIPID BLENDS FOR FORMULATING FOOD-GRADE NANOSTRUCTURED LIPID CARRIERS

Kamila Ramponi Rodrigues de Godoi Fernandes[1], Mayanny Gomes da Silva[1], Lisandro Pavie Cardoso[2], Mirna Lucia Gigante[1], Ana Paula Badan Ribeiro[1]

[1]Department of Engineering and Food Technology, School of Food Engineering, University of Campinas, Brazil;

[4]Department of Applied Physics, Institute of Physics, University of Campinas, Brazil

Corresponding author: kamila.ramponi@hotmail.com

(Manuscrito a ser submetido ao Periódico *Colloids and surfaces A: Physicochemical and engineering aspects*)

Abstract: The nanostructured lipid carriers (NLCs) are delivery systems capable to incorporate a lot of bioactive compounds according to their physical characteristics and stability. The present study produced NLCs with new raw materials as lipid phase, as follows: simple and chemically interesterified blends of fully hydrogenated microalgae oil (FHMO) and soybean oil (SO) in different proportions (w:w): 90:10, 80:20, 70:30, and 60:40, by using hot high-pressure homogenization (HPH). The NLCs were evaluated according to melting behavior, recrystallization index (RI), solid fat content (SFC), polymorphism, droplet size, polydispersity index, zeta potential, and stability during 60 days of storage. The FHMO proportion in the NLCs directly affected the physical parameters while the interesterification reaction of the lipid phase influenced the stability of the NLCs. The NLCs composed of randomized lipid fractions showed lower thermal resistance, lower SFC, lower droplet size, and greater homogeneity when compared to the simple lipid fraction, and were more resistant to destabilization throughout the storage. Both NLCs lipid fractions showed lower RI and β polymorphic habit. Concerning the FHMO to SO ratios, the higher FHMO proportion had the opposite effect when compared to the interesterified blends, with higher thermal resistance, higher SFC, higher droplet size, and lower homogeneity of NLCs. The physical characteristics and the higher stability over time can provide the potential use of these NLCs containing randomized FHMO and SO blends as a delivery system of bioactive compounds, mainly for food enrichment, by incorporation in products such as spreads, margarine, and beverages.

Keywords: Nanoemulsion, Microalgae oil, Soybean oil, Lipid crystallization, Encapsulation.

1. Introduction

The use of nanocarriers as encapsulating agents of food ingredients can improve the stability and viability of bioactive compounds, protecting them from environmental factors such as heat, extreme pH values, enzyme action, oxygen, light, and heavy metals during food processing and gastrointestinal conditions (Ghanbarzadeh et al., 2019; Jafari et al., 2017). These nanocarriers can be encapsulation materials made of carbohydrates, protein, or lipid-based compounds (Katouzian et al., 2017).

The lipid nanoparticles combine the advantages of other carrier systems as higher physical and chemical stability and lower release rate of the encapsulated compound due to the more compact structure (Ghanbarzadeh et al., 2019). The lipid nanoparticles are classified according to the fatty acids composition and physical behavior at room temperature of these materials, as solid lipid nanoparticles (SLN) and nanostructured lipid carriers (NLC) (Ghanbarzadeh et al., 2019). SLN consists of a core of solid lipids due to the composition made up mostly of saturated fatty acids. In turn, NLC contains crystallized lipid droplets (solid phase) and an amorphous crystalline structure (liquid phase) due to the presence of fats and oils with different melting points (Mohammadi et al., 2019).

The presence of oil in NLCs promotes a more disordered system, leading to the minor release of bioactive compounds, thus with a low tendency toward undesirable changes in particle morphology, aggregation, and gelation (Huang et al., 2017). However, to present this characteristic, the selection of an appropriate lipid matrix has a crucial role. It is known that the preferential polymorphic habit of the lipid matrix can directly affect the physicochemical characteristics of NLCs, which can also the encapsulation capability (Jafari & Esfanjani, 2017).

In lipids, three specific types of polymorphs predominate such as α, β', and β. The α-form is metastable, with hexagonal chain packing. The β'-form has intermediate stability and orthorhombic perpendicular packing, whereas the β-form has greater stability and parallel triclinic packing. The melting temperature increases with increasing stability (α→β'→β), and the α and β' forms can transform into β form at a constant temperature as a function of time (Santos et al., 2019; Sato & Ueno, 2005). The solid lipids with β’ form and the polymorphic

transition phenomena to β form can favor the release of the bioactive compound from the nanoparticle. In general, the more diverse the structure of the triacylglycerol, the less the tendency to form β polymorph (Oh et al., 2005).

This study investigated an unprecedented proportions combination of lipid materials consisting of soybean oil (SO) and fully hydrogenated microalgae oil (FHMO) due to the beneficial fatty acids composition. SO is rich in essential fatty acids (linoleic fatty acid (55%) and linolenic fatty acid (7%)), while FHMO is composed of more than 90% (w:w) of stearic acid (Asbridge, 2015; Demodaran et al., 2010; Fageria et al., 2010; Hammond et al., 2005). SO has low cost and high availability, and the FHMO shows a positive nutritional profile due to the presence of stearic acid from the total hydrogenation of unsaturated fatty acids with 18 carbon atoms. In addition, FHMO does not cause adverse effects on the risk of cardiovascular disease and presents a neutral atherogenic effect (Crupkin & Zambelli, 2008; Ribeiro et al., 2017).

The use of fully hydrogenated oils in NLCs is still limited and the composition of these oils is different from the FHMO. Several authors have studied the addition of fully hydrogenated oil to NLC. Santos et al. (2019) and Santos et al. (2019) made NLCs composed of SO and fully hydrogenated soybean oil (FHSO) containing a maximum level of 87.11% stearic acid and 11.22% of palmitic acid; Kharat and McClements (2019) used FHSO as a solid lipid phase and the emulsifier quillaja saponin as a liquid phase; Zheng et al. (2013) used fully hydrogenated sunflower, fully hydrogenated rapeseed oil, and a blend of palm oil and palm stearin in blends made with SO. In the present study, besides exploring the potential and behavior of FHMO and SO blends, these blends were subjected to chemical interesterification too. This lipid modification process is a strategy that allows obtaining the polymorphic form β′ indefinitely due to the random redistribution of fatty acids in the glycerol backbone, affecting the polymorphism, solid fat content, melting point, thermal behavior, stability, and microstructure of the lipid system (Marangoni & Rosseau, 2002; Ribeiro et al., 2017; Ribeiro, Basso, Grimaldi, Gioielli, dos Santos, et al., 2009).

Therefore, besides using fully hydrogenated oil as a raw material to improve the thermal behavior of NLCs, the use of interesterified lipids is a promising alternative once it can guarantee a lower degree of the organization

due to the β′ form, which provides high stability and encapsulation efficiency for NLCs.

Recently, Leão et al. (2019) and Reis et al. (2020) obtained nanoemulsions composed of enzymatically interesterified and non-interesterified buriti oil and reported that the interesterified nanoemulsion presented smaller droplet size, higher stability during 30 days of storage, proper oxidative stability, and less susceptibility to droplet aggregation. Ji et al. (2020) used SO and coconut oil enzymatically interesterified blends and found adequate stability, high encapsulation efficiency, and improved bioavailability (from 8.12% to 54.02%) for NLCs composed of interesterified lipids to carry curcumin. Our study group has evaluated new NLCs containing free phytosterols using simple and chemical interesterified blends composed of soybean oil as liquid phase (unsaturated) and fully hydrogenated oils of palm or crambe oils as solid (saturated) lipids. All NLCs exhibited appropriate nanoscale size and physical stability during 30 days of storage, and the NLCs formulated with interesterified blends showed lower particle size, with less evidence of agglomeration, higher stability, and higher zeta potential values when compared to NLCs made with simple blends, leading to crystallinity decrease and a less structure organization.

Thus, to better understand the use of chemical interesterification to produce lipids to compose NLC, this study aimed to evaluate the crystallinity properties and the physical stability of NLC composed of fully hydrogenated microalgae oil (FHMO), an unexpected solid lipid, and soybean oil (SO) as liquid lipid in different proportions in the simple and chemically interesterified blends.

2. Material and methods

2.1. Material

The nanostructured lipid carriers (NLC) were made using fully hydrogenated microalgae oil (FHMO) and soybean oil (SO) blends as the lipid phase. The FHMO was kindly supplied by SGS (Brazil) and soybean oil (SO) was purchased in a local market. The fatty acid composition of FHMO consisted of 99.94% of saturated fatty acids, with 92.85% of stearic acid (C18:0) and 5.52% of palmitic acid (C16:0). SO showed 83.86% of unsaturated fatty acids, with

24.53% of oleic acid (C18:1), 52.70% of linoleic acid (C18:2), and 11.10% of palmitic acid (C16:0). The enzyme-modified soy lecithin (SL) (Solec® AEIP) obtained from DuPont™ (Wilmington, DE, USA) containing 16% (w:w) of phosphatidylcholine, 15% (w:w) of lysophosphatidylcholine, 14% (w:w) of phosphatidylethanolamine, and 37% (w:w) of triglycerides was used as an emulsifier. Sodium methoxide anhydrous powder (99% purity; Sigma-Aldrich, Brazil) was used in the chemical interesterification process. Double-distilled deionized water was used throughout the study. All other reagents and solvents used in the experiment were of analytical or chromatographic grade.

2.2. Methods

2.2.1. Preparation of lipid blends

2.2.1.1. Preparation of simple blends

The FHMO and SO, in mass proportions (FHMO:SO w:w) of 90:10, 80:20, 70:30, and 60:40, were heated until total melting and mixed under magnetic stirring, until complete homogenization.

2.2.1.2. Preparation of chemically interesterified blends

The reactions were performed using the FHMO and SO ratios described in Section 2.2.1.1 with optimization according to Grimaldi et al. (2005). For the chemical interesterification reaction, on a laboratory scale, each blend was placed in 500mL borosilicate-glass jacketed coupled to a model RE 212 recirculating thermostat bath (Lauda, Manheim, Germany) and heated until 100°C under magnetic stirring (500rpm) (Marconi, Piracicaba, Brazil) for 20 minutes under vacuum to remove the moisture. After, the dried blend was interesterified using 1.54% of sodium methoxide, according to the quantity of free fatty acids (0.03%) and peroxide value (10 mEq/g) of SO and FHMO (Gioielli, 1998). Sodium methoxide was added to the blends at 100 °C, under magnetic stirring (500rpm) for 20 minutes of reaction under vacuum. Then, citric acid

solution (5g/100mL) was added to stop the reaction. The interesterified samples were washed with distilled water (80 °C). For drying, the blends were heated until 100 °C under magnetic stirring for 20 min under vacuum to remove the soaps. After the reaction, free fatty acids (FFA) and partial acylglycerols (diacylglycerols and monoacylglycerols) were removed according to Marangoni and Rosseau (2002), with modifications. The interesterified blends were melted and mixed with an equal volume of 96% ethanol at 40–50 °C in a separatory funnel. The ethanol phase was then extracted, and the procedure was repeated three times. The samples were stored in glass vials under to the temperatures studied (25 or 5°C).

2.2.2. Production of nanoparticles

The NLCs were composed of 10% (w/w) of the total lipid phase and 90% (w/w) of the aqueous phase. The manufacture of NLCs was performed according to 4 steps, as follows: (i) melting of the lipid fraction, (ii) emulsion formation, (iii) nanoemulsification, and (iv) crystallization of the lipid phase (Santos, Braz, et al., 2019). In the first step, the lipid blends (FHMO:SO, in different proportions) were melted, and the aqueous phase (composed of distilled water and 2% of the enzymatically modified lecithin as an emulsifier) was heated to 85 °C. Then, the mixture was homogenized in Ultraturrax (IKA, Germany) for 3 minutes at 10000 rpm for emulsion formation (Souto et al., 2011; Yang et al., 2014). The samples were subjected to nanoemulsification with hot homogenization in High-Pressure Homogenizer (HPH) FBF Homolab (Italia) at 700 bar of pressure and 2 cycles of passage in the equipment. Sodium azide (0.02% w/w) was added to the NLCs to inhibit microbial growth. The nanoemulsions were crystallized at 5°C for 24 hours and stored at 25°C before analysis (Kumbhar & Pokharkar, 2013; Qian et al., 2013; Yang et al., 2014).

2.2.3. Physical characteristics and stability of the nanoparticles

The physical stability of the NLC dispersions at 25 °C was evaluated during 60 days of storage in absence of light after 48 hours (24h at 5 °C; and 24h at 25 °C), on days 7, 15, 30, and 60, according to the analytical methods described below.

2.2.3.1. Melting behavior and recrystallization index

The melting behavior was determined using a differential scanning calorimeter (DSC) TA Q2000 coupled to an RCS90 Refrigerated Cooling System (TA Instruments, Waters LLC, New Castle) according to the AOCS method Cj 1-94, with adaptations (AOCS, 2009) using Universal V4.7A for data processing (TA Instruments, Waters LLC, New Castle). Approximately 10 mg of sample were disposed of in the hermetic aluminum pans and evaluated under isothermal conditions (25 °C, 10 min), followed by heating to 25 °C at a rate of 10 °C/min until 100 °C (Wang et al., 2014). The following parameters were determined: initial melting temperature (T_i), peak melting temperatures (T_p), and melting enthalpy (ΔH) (Campos, 2005).

The recrystallization index (RI) indicates the degree of recrystallization of the lipid phase, which was calculated according to Equation 1 to evaluate the physical state of nanoparticles after crystallization (5 °C/24 h and 25 °C/24 h).

$$IR\ (\%) = \frac{\Delta Hnp}{\Delta Hfl \times Cfl} \times 100 \qquad \textbf{Equation 1}$$

Where: ∆Hnp (J/g) is the total melting enthalpy of the nanoparticles; ∆Hfl (J/g) is the total enthalpy of the lipid phase; and Cfl is the quantity of lipid phase in the nanoparticles (10%) (Kumbhar and Pokharkar. 2013; Wang et al.. 2014).

2.2.3.2. Solid fat content (SFC)

The SFC of NLCs was determined at 25 °C using a pc120 Minispec Nuclear Magnetic Resonance spectrometer (Bruker, Rheinstetten, Germany) with an E200 Ecoline-star edition circulator heater (Lauda) (Ribeiro, Basso, Grimaldi, Gioielli, & Gonçalves, 2009). All measurements were performed in triplicate, and the results were expressed as mean ± SD values.

2.2.3.3. Polymorphism

The polymorphic habit of the samples was determined by X-ray diffraction according to the AOCS method Cj 2-95 (AOCS, 2009) with modifications. The nanoemulsions were crystallized at 5 °C for 24 hours and stored at 25 °C for 60 days. The determinations were made at -25 °C in a Philips diffractometer (PW

1710) using Bragg-Bretano geometry (θ:2θ) with Cu-Kα radiation (λ = 1.54056Å, 40 KV, and 30 mA). The measurements were obtained with steps of 0.03 ° in 2θ and an acquisition time of 3 seconds, with scans from 2 to 40° (scale 2θ). The identification of the crystalline forms was carried out from the characteristic short spacings of the crystals (Dassanayake et al., 2011; Yap et al., 1989).

2.2.3.4. Droplet size, size distribution, and polydispersity index

The droplet size was analyzed by light scattering using the Mastersizer 2000 equipment (Malvern Instruments, Malvern, UK) in aqueous dispersion. The mean droplet size was characterized by D32 (mean surface diameter) according to Eq. 2, and the polydispersity index was determined by the Span value according to Eq. 3.

$$D_{32} = \frac{\Sigma n_i d_i^3}{\Sigma n_i d_i^2} \qquad \textbf{Equation 2}$$

$$Span = \frac{d_{90} - d_{10}}{d_{50}} \qquad \textbf{Equation 3}$$

where n_i is the number of particles with diameter d_i; d_{10}, d_{50}, and d_{90} represent 10, 50, and 90% of the cumulative volume of the droplets, respectively (Gomes et al., 2022). The results were expressed as mean ± standard deviation (SD).

2.2.3.5. Zeta potential

The zeta potential parameter was measured by Dynamic Light Scattering (DLS) using the equipment Zetasizer Nano-ZS (Malvern Instruments. Malvern. UK). For the measurements, the samples were diluted (100 µL) in 10 mL of ultrapurified water, the conductivity was adjusted (50 µS/cm), and the sample was placed in a DTS1060 capillary cell using an alternating voltage of ± 150 mV, water as a dispersant, and dielectric constant of 78.5. Each sample was measured at least in triplicate, and the results were expressed as mean ± standard deviation (SD) (Das et al., 2012; Souto et al., 2011).

2.2.3.6. Kinetic stability by Turbiscan measurements

The kinetic stability was determined using Turbiscan ASG equipment (Formulaction, l'Union, France) at 25 °C. Immediately after preparation, the nanoemulsions were placed in cylindrical glass tubes with a flat bottom (40 mm in height and 16 mm in diameter). The stability of the systems was analyzed using the backscattering profiles (BS), with scans at 880 nm in length at different heights (mm). The initial height of the sample (H = 0 mm) was considered the lower part of the measuring cell. The creaming index was detected by varying the particle concentration between the top and bottom of the tubes. When creaming takes place in a nanoemulsion, the DBS curves show a peak at heights between 0 and 20 mm. The variation of the peak width over time may be due to the migration kinetics of small particles (Huck-Iriart et al., 2013). The TSI (Turbiscan Stability Index) was calculated (Eq. 4) to compare the stability of the samples. This parameter shows the variations in the system over time and was calculated according to backscattering changes that indicate the particle aggregation and dynamic migration by Turbisoft 2.0. The kinetics is based on Eq. 4, in which each scan is compared to the previous one, on the selected height, and the result is divided by the total height selected to obtain a result that does not depend on the quantity of product in the measuring cell (Queirós et al., 2020; Llinares et al., 2018; Trujillo-Cayado et al., 2018).

$$TSI = \sqrt{\frac{\sum_{i-1}^{n} (x_i - x_{BS})^2}{n-1}} \qquad \textbf{Equation 4}$$

where x_i is the average value of the scattered light intensity at each time, x_{BS} is the average of x_i and n is the number of scanning. TSI values range from 0 (i.e., a highly stable dispersion) to 100 (i.e., a highly unstable dispersion).

2.2.4. Statistical analysis

The results were subjected to analysis of variance (ANOVA) using the software STATISTICA Version 8 (StatSoft Inc., Tulsa, OK). Tukey tests were applied for comparisons of means, at a 5% significance level ($p<0.05$).

3. Results and discussion

3.1. Physical characteristics of nanoparticles

3.1.1. Melting Behavior and Recrystallization index

The determination of the melting parameters is an important approach to studying nanoemulsions once they provide data on the possible loss of structure of NLCs due to temperature (Dehnad et al., 2014; Jafari et al., 2015). The thermal parameters evaluated were onset melting temperature (Ti), enthalpy (ΔH), peak temperature (Tp), and final melting temperature (Tf). The NLCs made with interesterified blends showed lower Ti and Tf values when compared to the simple blends (Table 1). This effect was also observed for the lipid fractions in their bulk phase, in which the reorganization of fatty acids in the glycerol molecule after the randomization reaction led to a reduction of the onset and final crystallization temperature in the interesterified blends when compared to the simple fractions (GODOI-FERNANDES et al., 2023).

Table 1. Melting behavior parameters of NLCs composed by FHMO:SO (w:w) in simple and interesterified blends in the proportions 90:10, 80:20, 70:30 and 60:40 (w:w) during 60 days of storage at 25°C.

NLC	48H	7D	15D	30D	60D
			T_i (°C)		
90:10S	58.77±2.13^{aA}	51.67±5.72^{abcA}	55.24±0.59^{aA}	56.26±0.35^{aA}	54.31±0.33^{aA}
90:10I	43.40±0.93^{bA}	42.46±0.35^{cdeA}	44.49±0.82^{dA}	42.82±1.34^{bcdA}	44.08±0.18^{bA}
80:20S	57.15±1.26^{aA}	49.44±2.58^{abcB}	54.27±0.57^{abA}	39.54±10.68^{abcB}	55.65±1.88^{aA}
80:20I	38.29±1.18^{bcA}	43.62±2.76^{bceA}	39.50±1.34^{eB}	40.32±0.93^{cdB}	40.61±0.23^{bcB}
70:30S	57.54±0.01^{aA}	53.80±0.58^{abA}	53.56±0.50^{abA}	52.19±1.93^{abA}	54.10±0.58^{cdA}
70:30I	34.70±1.56^{bcA}	35.45±1.16^{deA}	34.32±1.11^{fA}	38.19±0.46^{cdA}	37.41±1.96^{cdA}
60:40S	51.15±2.41^{aA}	52.97±0.98^{abA}	51.98±1.04^{bB}	52.52±0.56^{abA}	52.16±1.93^{aA}
60:40I	33.79±0.69^{cA}	33.46±1.07^{dA}	33.57±0.39^{fA}	33.86±0.29^{bdA}	34.92±0.04^{dA}
			T_p(°C)		
90:10S	67.98±0.17^{aA}	67.23±8.80^{aA}	67.45±0.03^{aA}	67.25±0.04^{aA}	67.48±0.03^{aA}
90:10I	63.15±0.09^{eA}	62.96±0.09^{aA}	62.82±0.05^{eB}	62.83±0.01^{eB}	62.93±0.01^{eA}
80:20S	67.11±0.01^{bA}	63.58±3.13^{aB}	66.83±0.05^{bA}	44.52±12.85^{bB}	66.85±0.15^{bB}
80:20I	61.25±0.03^{fA}	60.90±0.15^{aB}	61.22±0.04^{fA}	61.15±0.05^{fAB}	63.02±1.05^{fA}
70:30S	66.83±0.02^{cA}	66.38±0.03^{aB}	66.25±0.05^{cC}	66.31±0.05^{cD}	66.44±0.05^{cB}
70:30I	59.86±0.03^{gA}	59.63±0.10^{aA}	59.69±0.36^{gA}	59.84±0.04^{gA}	59.80±0.08^{gA}
60:40S	65.65±0.12^{dA}	65.45±0.02^{aBC}	65.58±0.01^{dAB}	65.42±0.02^{dC}	65.41±0.03^{dC}
60:40I	57.76±0.17^{hA}	57.68±0.11^{aA}	57.46±0.06^{hA}	57.59±0.03^{hA}	57.42±0.18^{hA}
			ΔH (J/g)		
90:10S	12.05±0.55^{aA}	38.57±92.42^{aB}	12.78±0.14^{abA}	11.86±0.13^{aA}	13.19±0.17^{aA}
90:10I	9.64±0.10^{bB}	11.02±0.25^{bA}	7.06±1.43^{bcB}	10.62±0.33^{bA}	11.20±0.16^{abA}
80:20S	9.81±0.18^{bA}	7.37±3.82^{bA}	10.82±0.23^{abA}	7.25±2.09^{abA}	9.93±1.51^{bcA}
80:20I	7.03±0.22^{dBC}	5.89±0.28^{bC}	7.09±0.26^{bcBC}	6.57±0.54^{dA}	7.91±0.02^{cdeB}

70:30S	8.14±0.01^{cB}	10.05±0.26^{bA}	10.35±0.27^{abB}	10.37±0.25^{bA}	9.21±0.42^{bcAB}
70:30I	5.42±0.62^{eA}	5.06±0.38^{bA}	6.09±0.94^{cA}	5.14±0.34^{eA}	5.53±0.97^{eA}
60:40S	8.45±0.05^{cA}	8.24±0.33^{bA}	8.62±0.32^{abcA}	8.32±0.16^{cA}	8.37±0.07^{cdA}
60:40I	4.38±0.30^{fA}	5.10±0.26^{bA}	4.40±0.53^{cA}	4.12±0.21^{eA}	6.28±0.18^{deA}
			T_F(°C)		
90:10S	76.17±2.80^{aA}	83.14±3.48^{aA}	75.09±0.35^{aA}	74.09±0.01^{aA}	75.39±0.04^{aA}
90:10I	68.43±1.43^{bA}	63.90±8.98^{bA}	68.24±0.79^{cA}	69.02±0.02^{cA}	69.93±0.81^{dA}
80:20S	72.75±0.40^{aA}	72.66±5.30^{aA}	74.13±0.11^{abA}	48.90±14.13^{dA}	74.15±1.63^{abA}
80:20I	67.33±0.76^{bcAB}	67.81±0.95^{bA}	65.88±0.19^{dB}	66.63±0.50^{aAB}	67.20±0.39^{eAB}
70:30S	73.31±0.12^{aA}	73.67±0.78^{aA}	73.13±0.35^{bA}	73.89±0.19^{aA}	73.85±0.04^{bcA}
70:30I	64.29±0.81^{cdA}	63.64±0.51^{bB}	64.93±0.70^{dB}	64.72±0.24^{eB}	64.15±0.86^{fA}
60:40S	73.88±1.20^{aA}	72.18±0.50^{aB}	73.07±0.35^{bAB}	71.99±0.39^{bB}	71.91±0.10^{cdB}
60:40I	62.49±0.64^{dA}	61.28±1.03^{bA}	62.70±0.60^{eA}	62.06±0.40^{fA}	61.98±0.18^{gA}

NLC: Nanostructured lipid carrier; S: simple; I: interesterified; T_i: Initial temperature of melting; T_p: Peak temperature of melting; T_f: Final temperature of melting; ΔH: . D: days. The capital letters in lines indicates the statistical differences and the small letters in columns indicates the statistical differences by the Tukey test (P<0,05); Same letters did not show statistical differences between them.

The melting parameters Tp and ∆H were also evaluated. Similar to the other temperatures, the use of randomized fractions as lipid phase led to a decrease in Tp for the NLCs formulated with the interesterified fractions. This effect was also observed by Godoi-Fernandes et al. (2023) for the bulk phase, which was expected in the present study once chemical interesterification modifies the triacylglycerol composition of the lipid matrices, leading to changes in the thermal behavior (Ribeiro et al., 2009; Rosseau & Marangoni, 2002).

Concerning ∆H, i.e., the energy required to change the phase of the system, the NLCs containing interesterified fractions showed lower enthalpy, which is compatible with the lower Tp, Ti, and Tf observed in both the bulk phase (GODOI-FERNANDES et al., 2023) and the NLCs. In fats, randomization can

reduce the enthalpy of existing peaks, requiring less energy to crystallize or melt the randomized system, due to less variation and distribution of polymorphic forms (Zeitoun et al., 1993). These results indicate that NLCs from simple blends can be considered more thermally resistant when compared to those from interesterified blends.

The decrease in the FHMO ratio in the fractions led to a reduction in all melting parameters (Tp, Ti, Tf, and ΔH) of the NLCs, as a function of the saturated fatty acid contents. In the bulk lipid phase, the predominant fatty acids in the raw materials define the melting point and crystallization of the fats. For FHMO and SO blends, the main fatty acid present is stearic acid, which has a melting point of 70.1°C (Inoue et al., 2004; Scrimgeour, 2005). A similar result was observed by Godoi-Fernandes et al. (2023), with a reduction of the melting parameter inversely proportional to the SO concentration in the blend, i.e., the higher the SO content, the lower the enthalpy and melting temperatures. This behavior was also observed for the NLCs, which showed a reduction of Ti, Tp, and Tf with increasing SO concentration regardless of the bulk or randomized lipid fraction. Higher temperatures were observed for the ratio 90:10, while the ratio 60:40 showed lower temperatures, as well as the melting enthalpy. Again, this result corroborates the findings of the bulk phase of the lipid blends (GODOI-FERNANDES et al., 2023), despite the differences in crystallization and melting parameters of NLCs with the addition of 10% lipid fractions when compared to the bulk phase. Although they can affect thermal behavior, they may also be influenced by the addition of water and emulsifier in the system (McClements, 2012).

In this sense, the NLCs showed lower enthalpy values than those observed for the bulk phase (GODOI-FERNANDES, et al., 2023), with no changes for Tp. This effect has been reported in previous studies and is related to the nanometer scale of the particles in suspension in the nanoemulsion, as well as the larger surface area, which facilitates the loss or absorption of energy required for the phase change (MCCLEMENTS, 2012). Regarding the crystallization of nanoemulsions, Montenegro and Landfester (2003) reported that the cooling required for the crystallization of droplets is significantly higher than that required for the bulk material, due to the different nucleation mechanisms. For the even alkanes (C18-C24), there was a change in structure

from the triclinic form in the bulk material to an orthorhombic structure in nanoemulsions (100 nm) possibly due to the confinement of the lipid phase within the droplets. However, although the impact on crystallization was quite significant, the melting point decreased only slightly (0.7°C), which also occurred in the present study.

There was no variation in the thermal parameters regardless of the ratio of FHMO:SO or randomization of the lipid phase in the NLCs over the 60 days of storage, which suggests that time does not modify the thermal behavior of the nanoemulsions. This result is possibly due to the configuration of the nanoemulsion system, with the addition of small proportions of the lipid fraction (10%) and the confinement of the lipid phase in suspension in the aqueous phase, leaving it less susceptible to the effects of storage time and environment.

The analysis of the melting parameters allowed the evaluation of the recrystallization index (RI) of the lipid phase in the nanoemulsions (Table 2). This analysis was performed only after the static crystallization time of 48 hours (24h at 5°C and 24h at 25°C).

Table 2. Recrystallization index (RI) parameters of NLCs composed by FHMO:SO (w:w) in simple and interesterified blends after crystallization (24h at 5°C and 24h at 25°C).

90:10S	**90:10I**	**80:20S**	**80:20I**	**70:30S**	**70:30I**	**60:40S**	**60:40I**
0.78±0.26^{A}	1.04±0.10^{A}	0.88±0.00^{A}	1.46±0.15^{A}	0.87±0.05^{A}	0.69±0.12^{A}	0.99±0.18^{A}	1.11±0.07^{A}

The capital letters in line indicates the statistical differences by the Tukey test (P<0,05); Same letters did not show statistical differences between them.

The calculated RI parameter may involve some uncertainty, as it is related to the polymorphs present in the lipid phase. Therefore, the RI is calculated to obtain a measure of comparative crystallinity between formulations, defining them as more or less crystalline (Kovačević et al., 2014a). However, the RI of the NLCs was low (between 0.78% and 1.46%), with no significant difference between the blends.

Studies have shown that RI can be affected by the lipid matrix used and the storage temperature, and the use of lecithin as an emulsifier at a proportion of 2% favors lower recrystallization rates for NLCs (Siekmann & Westesen, 1994). Salminen et al. (2013) evaluated different types of lecithin as an emulsifier

in NLCs containing large amounts of triestearin, similarly to the present study, and reported that the interaction between the emulsifier and the lipid fraction can guide various aspects of the crystallization of the nanoemulsified system. During cooling, the use of high melting point lecithin in NLCs acted as a core for the crystallization of triestearin, resulting in a heterogeneous crystallization parallel to the surface, with liquid lipids inside the particle, whereas low melting point lecithin is not able to induce crystallization, which leads to the formation of disordered crystals by the liquid and solid lipids, which are randomly organized in any region of the particle. Therefore, despite the satisfactory performance as an emulsifier in the NLCs system, the enzymatically modified lecithin did not induce crystallization of the system, thus it may have favored low RI.

This effect of more disordered crystallization associated with low recrystallization rates may affect the ability to incorporate bioactive compounds inside the nanoparticle since high crystallinity rates can limit the space for the accommodation of the compounds of interest, as well as lead to their release during crystal modifications over time (Kovačević et al., 2014b; Tamjidi et al., 2013). Therefore, due to the low IR, there is no high crystal density in the nanoparticles, making them suitable for incorporation and protection of compounds, as reported by Silva et al. (2022) and Queirós et al. (2022).

In general, NLCs containing the randomized lipid fractions showed higher RI, probably due to the higher heterogeneity of TAG composition after interesterification. Regarding the saturated fatty acid content and FHMO:SO ratios, there was no significant difference between the NLCs. Although it was expected that a higher FHMO content would promote crystallization induction due to the large amount of triestearin, especially in the simple fraction, effect not observed in the NLCs.

3.1.2. Solid fat content (SFC)

The SFC of nanoemulsions can indicate modifications in the crystallization of NLCs during prolonged storage because it gives the percentage of fat in the solid state at a given temperature (Chiu & Gioielli, 2002). Analysis of the SFC of NLCs was performed at 25°C throughout 60 days of storage to evaluate the effect of storage time and the different lipid fractions (Figure 1).

Figure 1. Solid fat content (SFC) of NLCs composed by FHMO:SO (w:w) in simple and interesterified blends during 60 days of storage at 25°C.

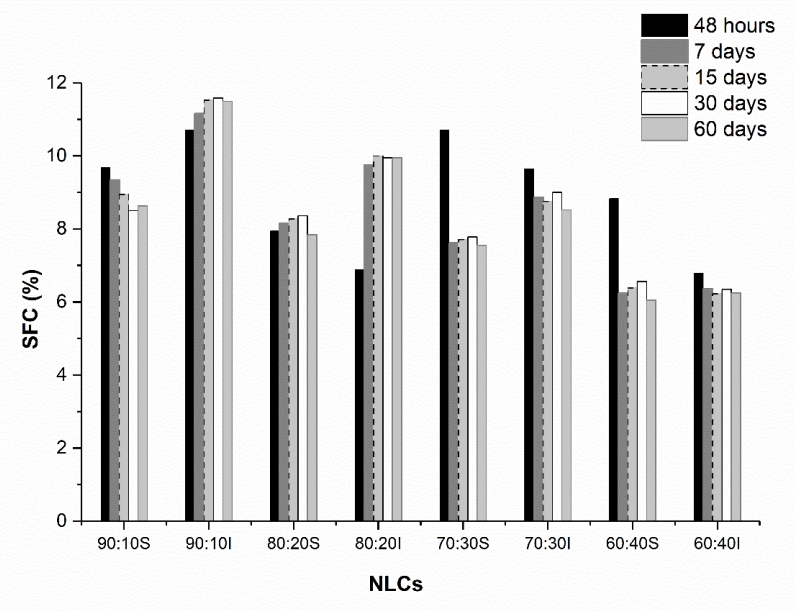

To properly evaluate this parameter in NLCs, it is important to consider the changes due to the interesterification reaction and its impact on lipid crystallization and the NLC system. For the simple blends with higher FHMO contents (90:10 and 80:20) there was an increase in SFC after static crystallization (48h), with the maintenance of SFC until 60 days of storage at 25 °C. In turn, NLCs containing blends in the ratios 70:30S and 60:40S exhibited higher initial SFC (after the first 48 hours of storage) with subsequent reduction of the parameter.

The behavior of NLCs containing interesterified blends, in turn, proved to be different. For the ratios 90:10I and 80:20I an increase in SFC was observed over time, while the ratios 70:30I and 60:40I had a slight reduction in SFC until 60 days of storage at 25°C. This reduction may be associated with the melting Ti of these NLCs, which is 34 °C and 33 °C, respectively, closer to the storage temperature after 48h (25°C) in a lipid matrix that contained significant quantities of unsaturated lipid.

These characteristics are associated with the chemical properties of the lipid blends before and after randomization. There was a predominance of trisaturated triacylglycerols (TAG) (S3), especially triestearin (SSS) in all blends, regardless of the interesterification reaction, due to the expressive stearic acid content of

FHMO observed in the fatty acid composition. After the interesterification reaction, although the SSS levels were still high, there was modulation of the triacylglycerol composition, with the reduction in the contents of S3, monounsaturated (U2S) and triunsaturated (U3) TAGs, and formation of new disaturated triacylglycerols (S_2U) (GODOI-FERNANDES, et al. 2023).

An increase in SFC was observed in the blends with a higher saturated fatty acid content, with the formation of more stable lipid crystals belonging to S3 TAGs, which have a higher melting point at storage temperature (25°C). In addition, previous studies have shown that the association between a highly unsaturated matrix such as soybean oil and a fully hydrogenated oil can delay the crystallization of the system, resulting in an increase in SFC over the storage at 25 °C (Braipson-Danthine & Deroanne, 2004; Godoi et al., 2019). This effect may be due to the presence of TAG S2U, which crystallizes at a temperature near 25 °C.

The nanoemulsions containing simple and interesterified fractions made from blends with lower FHMO contents (70:30 and 60:40) showed a decrease in SFC over time. In these NLCs, there was an immediate presence of a higher number of crystals when subjected to refrigeration temperature (5°C) for 24 hours. At low temperatures, crystals formed by S3 TAGs crystallize faster, allowing the initiation of crystallization of fractions composed by S2U TAGs, which have a melting temperature of around 25°C (Martini et al., 2002; Ribeiro, et al. 2009). Thus, maintaining the system at 5°C for 24 hours may result in a greater amount of crystals formed. After this period, by submitting the NLCs to room temperature (25°C), the crystals formed mostly by S3 TAGs, of high melting point and more thermo resistant, remain in the system. Those composed mainly of S2U or SU2 TAGs that may have formed at 5°C can melt when stored at 25°C for a prolonged time, leading to reduced SFC.

These losses and gains of SFC over time may also be associated with the low enthalpy energy values of NLCs, especially for those with lower FHMO contents and containing interesterified fractions. Thus, when raising the temperature to 25 °C, NLCs easily change their physical state.

3.1.3. Polymorphism

The effectiveness of nanostructured lipid systems is determined by modifications of the crystalline network characteristic of a specific set of triacylglycerols (Helgason et al., 2009b). The relationship between crystal modification and encapsulation also affects the interactions between the lipid matrix and the emulsifiers used. In general, lipid crystals exhibit higher mobility in thermodynamically unstable configurations. Therefore, these configurations have lower crystal density, and thus a greater capacity for incorporation of external molecules (Salvia-Trujillo et al., 2017).

During storage, rearrangement of the crystalline network can occur towards the most stable state, and these transitions are usually associated with the expulsion of a fraction of the encapsulated compound. The occurrence of polymorphic transformations is usually accompanied by changes in particle morphology from spherical to flattened shapes (Berton-Carabin et al., 2013). Therefore, the analysis of polymorphic forms is essential for the evaluation of NLC, since their crystallization characteristics influence the ability to incorporate compounds inside the nanoparticle.

As shown in the diffractograms in Figure 2, it was possible to distinguish most of the polymorphic shapes present in the NLCs. Such identification was quite difficult due to the water content of the formulations because the crystallization of water at the analysis temperature (-60°C) leads to the formation of a broad peak together with the peaks of the lipid phase, which hides them in the diffractogram. As observed by Bernal & Fowler (1933) and by the additional analysis performed by our research group, the 3 crystalline ice peaks at -60°C appear at 2θ values of 25, 40, and 48 with high intensity (up to 10,000 a.u.), while the conventional fat peaks have about 10x lower intensity and very similar location, commonly between 20 and 35 at 2θ.

The effect of the water peak was mainly observed in the blends 80:20I after 48 hours and the blends 70:30I after 7 and 15 days since there was great difficulty in visualizing the lipid peaks. Additionally, in some NLCs (90:10S, 90:10I, 70:30I, and 60:40I) there was the late appearance of the polymorphic β' form, less stable, possibly due to the late crystallization of unsaturated fraction or the effect of interesterification, which can direct the lipid system indefinitely to the polymorphic

β' form because the more diverse the TAG structure, the lower the tendency to form β-type polymorphs (Oh et al., 2005). These results observed by Godoi-Fernandes et al. (2023) for the same pure blends showed the concomitant presence of the β-polymorph, attributed to the stabilization methodology (5°C/24h and 24h/25°C). Furthermore, the triacylglycerol composition showed a predominance of TAG SSS even after the interesterification reaction, which may also direct lipid systems towards the polymorphic β-form. Therefore, the behavior of the lipid material at the macro and nanoscale were quite similar, which may be due to the stabilization methodology and the triacylglycerol composition after the interesterification reaction.

Figure 2. Diffractions peak showing the polymorphic habit of nanoemulsions containing simple and interesterified lipid matrices in different proportions of FHMO:SO (90:10S, 90:10I, 80:20S, 80:20I, 70:30S, 70:30I, 60:40S, 60:40I w:w) during 60 days of stabilization at 25°C.

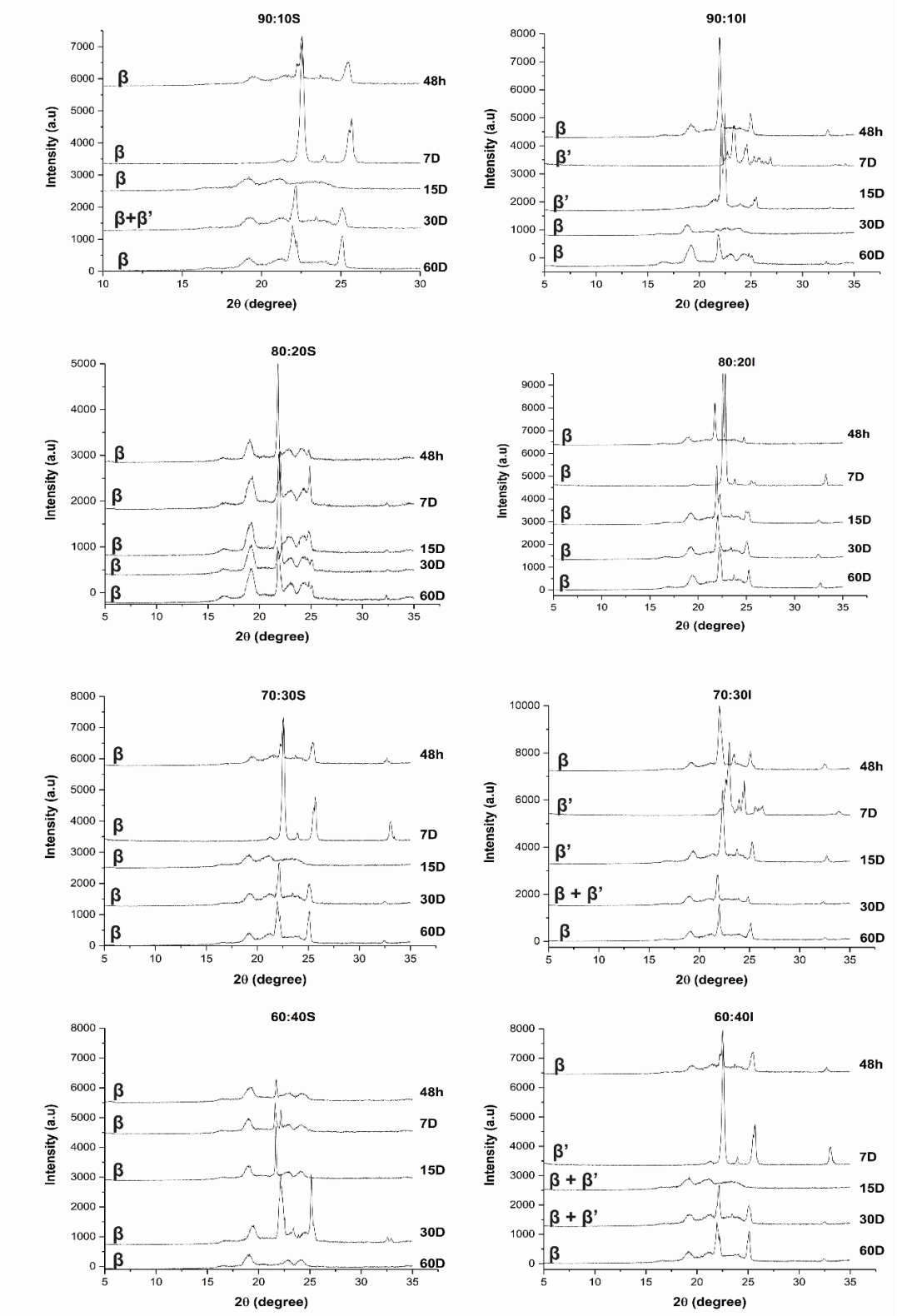

FHMO: Fully hydrogenated microalgae oil, SO: soybean oil.

However, because it is the most stable form, it is inconsistent that the β form was not detected in the NLCs that were initially characterized by this polymorph. Therefore, it is likely that the polymorphic β form was still present in the blends 90:10I at 7 and 15 days, and the blends 70:30I and 60:40I at 7 days of analysis, but was covered up by the intense peak of the water molecule in the diffractograms.

The predominance of the polymorphic β form was also observed in NLCs composed of SO and fully hydrogenated soybean oil (Santos, Koji Miyasaki, et al., 2019)

3.2. Stability of nanoparticles

3.2.1. Droplet size, size distribution, polydispersity index, and zeta potential

The size of nanoparticles can influence their physicochemical properties and functional performance, as well as stability, optical properties, biological characteristics, and release mechanism (Jafari & Esfanjani, 2017; Luykx et al., 2008). The size of the nanoparticles is designated as a particle size distribution represented by the mean surface area (D 3,2) and width of the distribution or polydispersity index (SPAN). The zeta potential is as important as particle size and is used as an indicator of emulsion stability, with the higher the potential value (in modulus), the more stable the colloidal dispersion, indicating high repulsion between particles and low tendency to flocculate or aggregate (Jafari & Esfanjani, 2017).

As can be seen in Table 3, no changes were observed for the parameter D3,2 as a function of time, with no differences for NLCs made with single or randomized blends, despite the slight increase inversely proportional to the FHMO concentration. The mean nanoparticle diameter ranged from 176nm (nanoemulsion with 90:10S lipid fraction) to 311nm (nanoemulsion with 60:40S fraction). Smaller nanoparticle sizes (<200 nm) are desirable for food consumption, as they remain longer in the gastrointestinal tract and promote greater solubility and reactivity (Luo et al., 2012).

Table 3. Particle size parameters of NLCs composed by FHMO:SO (w:w) in simple and interesterified blends during the 60 days of storage at 25°C.

NLC	48 hours	7 days	15 days	30 days	60 days
			$D_{3,2}$(nm)		
90:10 S	176±0.19^{bC}	190±3^{dAB}	198±2^{cA}	181±6^{cBC}	199±1.1^{cA}
90:10 I	254±13^{eA}	228±5^{eB}	219±4^{bBC}	214±5^{bC}	229±0.3^{bB}
80:20 S	218±8^{aBC}	230±6^{eB}	218±4^{bBC}	206±6^{bC}	251±3.2^{eA}
80:20 I	234±5^{dA}	207±2^{dC}	201±5^{cC}	193±1^{cD}	216±3^{cdB}
70:30 S	287±1,4^{cA}	279±6^{bAB}	265±8^{dAB}	259±0.8^{dB}	277±1.4^{adAB}
70:30 I	261±0.2^{eAB}	238±7^{eC}	252±6^{dB}	255±0.06^{dAB}	264±4^{deA}
60:40 S	299±14^{cAB}	311±2^{aA}	303±9^{aAB}	275±0.2^{aC}	275±0.4^{aB}
60:40 I	247±15^{deB}	256±3^{cAB}	261±3^{dA}	259±0.2^{dA}	266±1.1^{deA}
			Polidispersity index (SPAN)		
90:10 S	2.700±0.149^{bAB}	2.658±0.070^{bB}	3.012±0.156^{aA}	2.769±0.159^{aAB}	2.859±0.060^{aAB}
90:10 I	2.327±0.008^{bC}	2.582±0.010^{bcA}	2.483±0.067^{cAB}	2.531±0.029^{bA}	2.407±0.048^{cBC}
80:20 S	2.665±0.019^{bA}	2.352±0.091^{adB}	2.731±0.035^{bA}	2.737±0.029^{aA}	2.371±0.029^{cdB}
80:20 I	2.370±0.014^{bC}	2.587±0.011^{bcA}	2.449±0.500^{cB}	2.367±0.011^{bcC}	2.273±0.027^{deD}
70:30 S	2.315±0.050^{bA}	2.261±0.027^{deA}	2.154±0.024^{deB}	2.133±0.024^{deB}	2.054±0.024^{gB}
70:30 I	2.376±0.037^{aB}	2.474±0.021^{acdA}	2.334±0.047^{cdBC}	2.275±0.047^{cdC}	2.115±0.011^{fgD}
60:40 S	2.236±0.029^{aA}	2.167±0.010^{eB}	2.106±0.016^{eC}	2.073±0.024^{eC}	2.073±0.017^{bD}
60:40 I	2.358±0.041^{aA}	2.289±0.028^{eAB}	2.225±0.031^{deBC}	2.211±0.004^{cdeBC}	2.176±0.032^{efC}

The capital letters in lines indicates the statistical differences and the small letters in columns indicates the statistical differences by the Tukey test (P<0,05); Same letters did not show statistical differences between them.

The polydispersity index (PDI) provides information about the degree of homogeneity of the sample. The lower its value, the greater the homogeneity of the particle diameter in the system, and vice versa (Liu & Wu, 2010). According to Tamjidi et al. (2013), to classify a dispersion as stable over time, the PDI values should be in the range 0.1 to 0.25, while values above 0.5 indicate a very wide particle size distribution, leading to low physical stability over time. In the present study, nanoemulsions composed of interesterified blends gave rise to more homogeneous systems, even with low absolute values of NLCs, ranging from 2 to 3, with higher values for nanoemulsions composed of simple blends and with a higher proportion of FHMO.

This profile may be associated with the preferential polymorphism of the lipid fraction since β' crystals were visualized only in the 90:10S, 90:10I, 70:30I,

and 60:40I matrices, i.e., in the interesterified blends and the blend with higher FHMO concentration. Possibly, the difficulty in visualizing the peaks of the polymorphic forms due to the presence of water may have prevented the detection of this polymorphic form also in the 80:20I blend.

The parameter D3,2 remained stable as a function of time, which corroborated the bimodal distribution of particle sizes, with no significant changes over time.

Regarding the zeta potential, a decrease of this parameter was observed in all nanoemulsions over time, regardless of the lipid raw material used. Comparatively, the NLCs formulated with interesterified blends and with lower FHMO content showed higher zeta potential values, thus they can be considered more stable (Figure 3).

Figure 3. Zeta potential (in modulus) of NLCs composed by FHMO:SO (w:w) in simple and interesterified blends during the 60 days of storage.

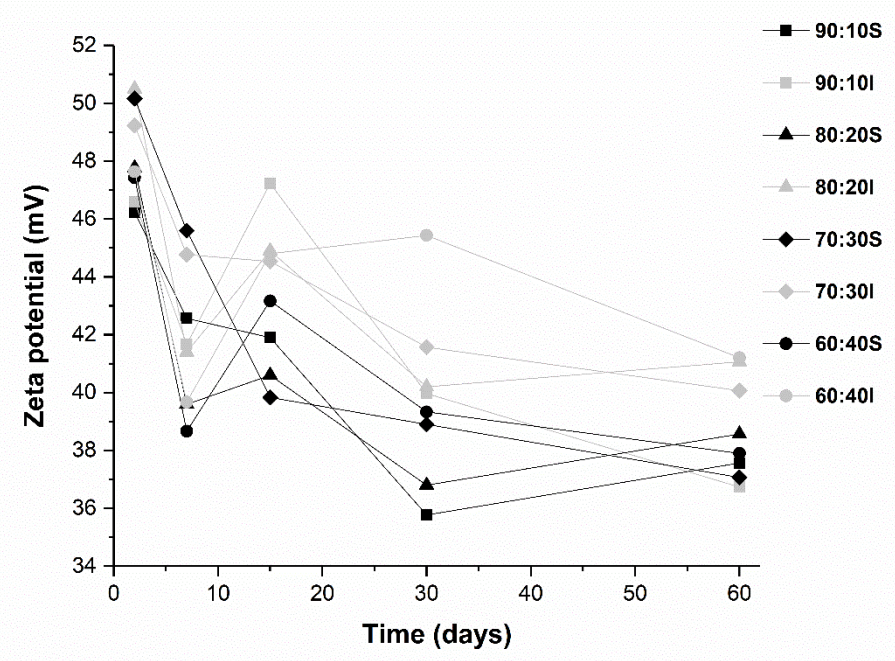

Previous studies have shown that changes in zeta potential over time may indicate destabilization of the system, with consequent expulsion of the incorporated bioactive compounds during the storage. This reduction may be due to the predominant polymorphism in the NLCs and possible late crystallization or recrystallization of the lipid matrices. On a macro scale, the late formation of β'

crystals may alter the charges of the NLCs due to the presence of a new polymorph, which may present a new ratio of differently charged crystal surfaces, leading to changes in zeta potential (Araújo et al., 2011).

However, zeta potential values of around 30 mV characterize colloidal systems with adequate stability, while values around 60 mV are considered optimal, thus the values can still be classified as satisfactory even with the reduction of ZP values over time (Badea et al., 2015; Madureira et al., 2015; Shah et al., 2015). Therefore, the NLCs obtained with randomized blends were less prone to destabilization (as observed in Figure 2) since they showed high zeta potential. Moreover, the storage time may favor the destabilization of the NLCs.

Silva et al. (2022) reported similar behavior, with the reduction of ZP over time for NLCs made from simple and interesterified lipid matrices.

3.2.2. Physical stability by Turbiscan measurements

Some common destabilization phenomena in emulsions can be detected by turbidimetry analysis. Light backscatter shows modifications across the length of the sample storage tube, and fluctuations in particle volume and size can represent migration (creaming and sedimentation) and/or particle aggregation (coalescence, flocculation). Particle migration is considered reversible, as particles can be easily redispersed by mechanical agitation, whereas particle aggregation is generally irreversible, with modifications seen at the ends of the tube (Shah et al., 2015; Silva et al., 2011).

Figure 4. Variation in the backscattering profile (BS) of NLCs composed by FHMO:SO (w:w) in simple and interesterified blends during 60 days of storage at 25°C.

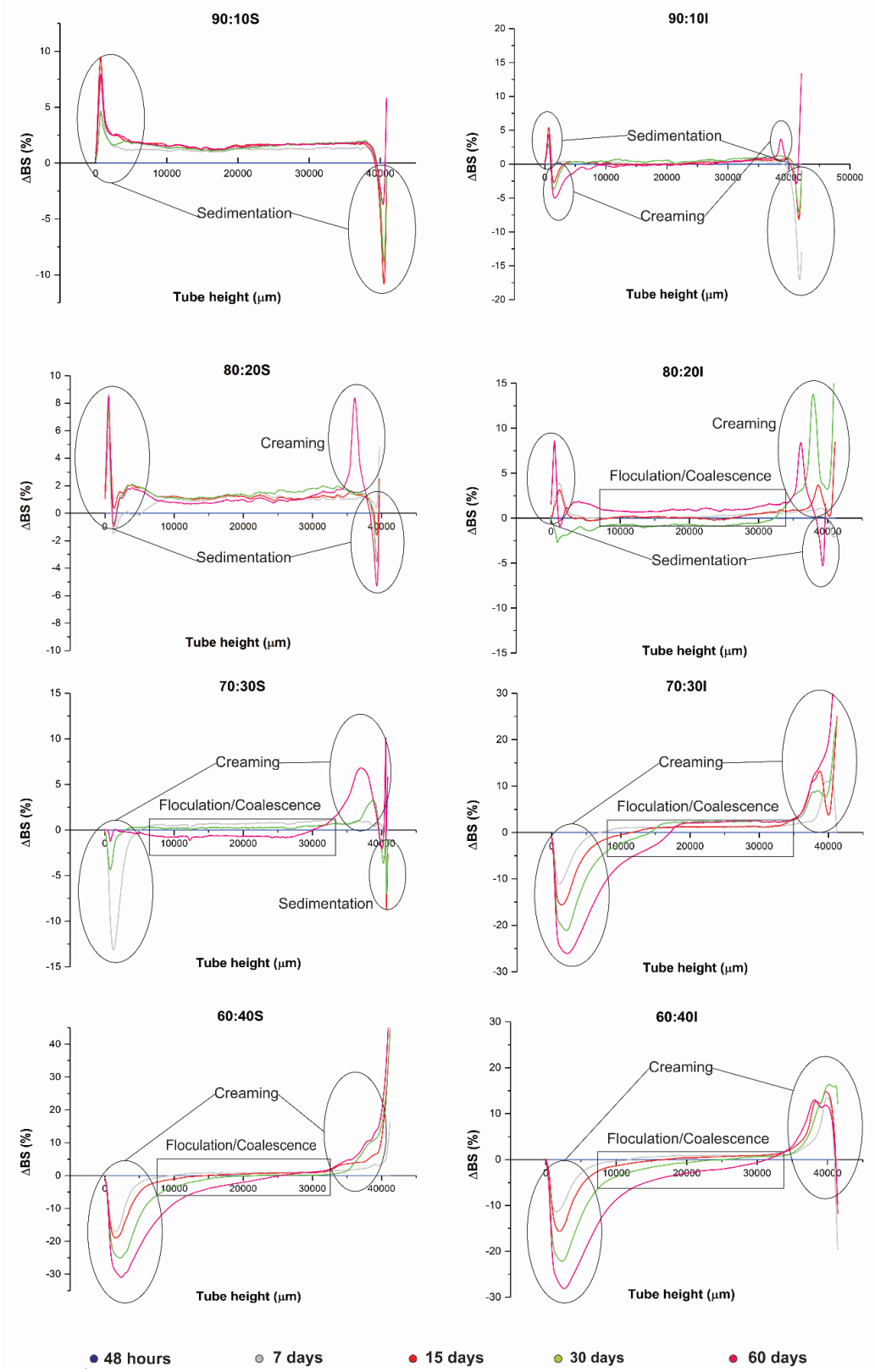

FHMO: Fully hydrogenated microalgae oil, SO: soybean oil, NLCs: Nanostructured lipid carriers.

As shown in Figure 4, the NLCs made with the blend 90:10 presented sedimentation, which became more pronounced over time, and the randomized fraction also presented creaming at 60 days of storage. Concerning the lipid fraction 80:20, sedimentation and creaming were observed after 60 days in the simple blend and after 15 days in the randomized blend. The blend 70:30 showed the creaming phenomenon, and the simple blend showed flocculation/coalescence characteristics concomitantly after 60 days of storage. Finally, the NLCs made with the blends 60:40 before and after randomization showed characteristics of creaming, and flocculation/coalescence, without expressive changes over time. Therefore, all NLCs showed destabilization over time, especially after 60 days of storage, regardless of randomization or proportion of lipid blends used.

TSI (Turbiscan Stability Index) is another parameter that indicates the colloidal stability of the dispersion (nanoemulsion) (Teng et al., 2019), and the higher the TSI value, the greater the destabilization of the sample (Xu et al., 2013). In this study, NLCs were evaluated as a function of time and the addition of lipid phases. As shown in Figure 5, the NLCs containing lipid phases with lower FHMO contents presented higher TSI, indicating greater destabilization, which increased over time, as observed by the backscattering profile and zeta potential. The other samples were more stable, with less variation in TSI over time, and the NLCs with higher FHMO content were considered the most stable.

Figure 5. TSI (Turbiscan Stability Index) curves of NLCs composed by FHMO:SO (w:w) in simple and interesterified blends during 60 days of storage at 25°C.

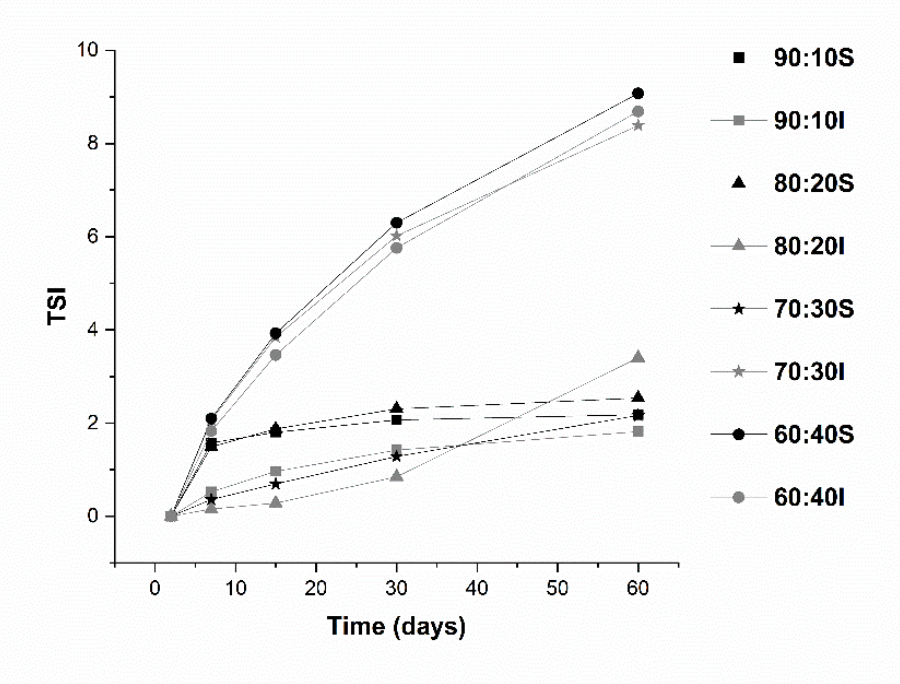

FHMO: Fully hydrogenated microalgae oil, SO: soybean oil, NLCs: Nanostructured lipid carriers.

The other stability determinations showed that the mean diameter of nanoparticles ranged from 176 nm (nanoemulsion with 90:10S lipid fraction) to 311 nm (nanoemulsion with 60:40S fraction) and the nanoemulsions with higher FHMO content showed smaller particle size, higher polydispersity index, and lower zeta potential values. The NLCs made with the interesterified fractions showed larger particle size, lower polydispersity index, and higher zeta potential when compared to NLCs containing simple blends in the same proportion. Thus, NLCs with interesterified blends were less prone to destabilization, as well as those containing lower FHMO contents. It was expected that the Turbiscan analysis confirmed these statements macroscopically for the nanoemulsion.

Differently from the nano-level evaluations, the Turbiscan analysis showed that the nanoemulsion 90:10S presented only destabilization and sedimentation, while the nanoemulsion 90:10I showed sedimentation along with creaming, as also observed for the 80:20S fraction. The other NLCs showed important destabilization, with concomitant existence of sedimentation, creaming, and flocculation, both in simple and interesterified fractions. Therefore, the Turbiscan analysis showed some destabilization for all nanoemulsions, and the NLCs with lower FHMO contents and interesterified fractions were more unstable.

Similar findings were reported by Silva et al.(2022). These controversial effects may be due to two main factors: the sensitivity of the analysis and the final physicochemical aspects of the nanoemulsion components. After the interesterification reaction, the redistribution of fatty acids in the glycerol molecule modifies the thermal parameters and, consequently, the final physical characteristics of the lipid system, reducing the viscosity with increasing S2U and SU2 TAGs contents. The reduction in the viscosity of the lipid fractions may affect the nanoemulsion formation and favor the creaming phenomenon, which was observed for all NLCs containing interesterified blends. The interesterification process may also generate minority lipids such as diacylglycerols, monoacylglycerols, and free fatty acids, which may have contributed to an accelerated destabilization.

On the other hand, it is known that unlike particle size and zeta potential measurements, the turbidity analysis does not require dilution of NLCs, which can provide more sensitive results about the physical characteristics and stability of nanoemulsions, explaining the difference between the different measurements (Badea et al., 2015; McClements, 2016).

However, considering that nanoemulsions can be used in complex food matrices, the physical characteristics should be evaluated mainly in the final product. Therefore, the results at the nano-level contribute to guiding the conclusions about nanoemulsions. In this sense, the interesterification and the use of lower saturated fatty acids contents provided better stability for the NLCs, thus they may be more indicated for applications in food matrices.

4. Conclusion

The analysis of the parameters in the NLCs showed that the characteristics of nanoemulsions were dependent on the FHMO concentrations since the increase in the concentration of fully hydrogenated oil led to increased thermal resistance, SFC, and particle size, in addition to lower zeta potential values, with greater susceptibility to particle aggregation and destabilization of the system, but what was not proved by Turbiscan measurements. Concerning the treatment with lipid phases, the NLCs made with randomized fractions showed lower thermal resistance, as well as higher SFC, homogeneity of distribution in particle

diameters and a lower tendency to aggregation and destabilization of the system. These characteristics are due to the physicochemical modifications of the lipid phase since the rearrangement of fatty acids in the glycerol molecule drives the polymorphic habit to the β' form indefinitely, reducing the values of the thermal parameters and the viscosity of the lipid system. These modifications had a direct impact on the characteristics of the nanoemulsions. For the NLCs, all nanoemulsions showed predominantly polymorphic β habit. However, the visualization of the lipid peaks was impaired by the crystallized water, which may have hidden the β' type crystal peaks. Overall, all NLCs showed a low recrystallization rate. Over the storage time, all NLCs showed physical destabilization measured by Turbiscan analysis. However, the macroscopic physical stability should be evaluated in the final product since the NLCs will be used in complex food matrices. Then, the NLCs made from randomized blends and lower FHMO concentrations proved to be more stable, with the delayed occurrence of instability during storage at 25 °C, with promising characteristics for incorporation of bioactive lipid compounds in foods.

CRediT authorship contribution statement

Kamila Ramponi Rodrigues de Godoi Fernandes: Conceptualization, Methodology, Investigation, Formal analysis, Writing – original draft. Mayanny Gomes da Silva: Methodology, Formal analysis, Review. Lisandro Pavie Cardoso and Mirna Lucia Gigante: Supervision, Resources. Ana Paula Badan Ribeiro: Conceptualization, Writing – review & editing, Supervision, Funding acquisition, Resources, Project administration.

Declaration of Competing Interest

The authors declare that they have no known competing financial interests or personal relationships that could have appeared to influence the work reported in this paper.

Acknowledgments

Ana Paula Badan Ribeiro thank CNPq (303429/2018-6) for productivity grant and São Paulo Research Foundation-FAPESP (16/11261-8). Kamila Ramponi Rodrigues de Godoi Fernandes thank CNPq (140789/2017-0) for PhD

scholarship grant. Lisandro Pavie Cardoso thank CNPq (302626/2016-6 and 307896/2019-6) for productivity grant. This study was financed in part by the “Coordenação de Aperfeiçoamento de Pessoal de Nível Superior - Brazil (CAPES)”–Finance Code 001.

References

AOCS. (2009). *Official methods and recommended practices of the American Oil Chemists’ Society* (6th Editio). https://doi.org/http://dx.doi.org/10.1002/0471740039.vec0152

Araújo, J., Nikolic, S., Egea, M. A., Souto, E. B., & Garcia, M. L. (2011). Nanostructured lipid carriers for triamcinolone acetonide delivery to the posterior segment of the eye. *Colloids and Surfaces B: Biointerfaces*, *88*(1), 150–157. https://doi.org/10.1016/j.colsurfb.2011.06.025

Asbridge, D. D. (2015). Soybeans vs.Other vegetable oils as a source of edible oil products. In D. R. Erickson (Ed.), *Pratical Handbook and soybean processing and utilization* (pp. 1–9). AOCS Press.

Badea, G., Lăcătuşu, I., Badea, N., Ott, C., & Meghea, A. (2015). Use of various vegetable oils in designing photoprotective nanostructured formulations for UV protection and antioxidant activity. *Industrial Crops and Products*, *67*, 18–24. https://doi.org/10.1016/j.indcrop.2014.12.049

Bernal, D. J., & Fowler, R. H. (1933). A Theory of Water and Ionic Solution, with Particular Reference to Hydrogen and Hydroxyl Ions. *The Journal of Chemical Physics*, *1*(8).

Berton-Carabin, C. C., Coupland, J. N., & Elias, R. J. (2013). Effect of the lipophilicity of model ingredients on their location and reactivity in emulsions and solid lipid nanoparticles. *Colloids and Surfaces A: Physicochemical and Engineering Aspects*, *431*, 9–17. https://doi.org/10.1016/j.colsurfa.2013.04.016

Braipson-Danthine, S., & Deroanne, C. (2004). Influence of SFC, microstructure and polymorphism on texture (hardness) of binary blends of fats involved in the preparation of industrial shortenings. *Food Research International*, *37*(10), 941–948. https://doi.org/10.1016/j.foodres.2004.06.003

Campos, R. (2005). Fat Crystal Networks. In *Fat Crystal Networks* (pp. 267–

349). Marcell Dekker Inc.

Chiu, M. C., & Gioielli, L. A. (2002). Conteúdo De Gordura Sólida Da Gordura Abdominal De Frango , De. *Ciênc. Tecnol. Aliment.*, *22*(2), 151–157.

Chopin-Doroteo, M., Morales-Rueda, J. A., Dibildox-Alvarado, E., Charó-Alonso, M. A., de la Peña-Gil, A., & Toro-Vazquez, J. F. (2011). The Effect of Shearing in the Thermo-mechanical Properties of Candelilla Wax and Candelilla Wax-Tripalmitin Organogels. *Food Biophysics*, *6*(3), 359–376. https://doi.org/10.1007/s11483-011-9212-5

Crupkin, M., & Zambelli, A. (2008). Detrimental impact of trans fats on human health: Stearic acid-rich fats as possible substitutes. *Comprehensive Reviews in Food Science and Food Safety*, *7*(3), 271–279. https://doi.org/10.1111/j.1541-4337.2008.00045.x

Das, S., Ng, W. K., & Tan, R. B. H. (2012). Are nanostructured lipid carriers (NLCs) better than solid lipid nanoparticles (SLNs): Development, characterizations and comparative evaluations of clotrimazole-loaded SLNs and NLCs? *European Journal of Pharmaceutical Sciences*, *47*(1), 139–151. https://doi.org/10.1016/j.ejps.2012.05.010

Dassanayake, L. S. K., Kodali, D. R., & Ueno, S. (2011). Formation of oleogels based on edible lipid materials. *Current Opinion in Colloid and Interface Science*, *16*(5), 432–439. https://doi.org/10.1016/j.cocis.2011.05.005

Dehnad, D., Mirzaei, H., Emam-Djomeh, Z., Jafari, S. M., & Dadashi, S. (2014). Thermal and antimicrobial properties of chitosan-nanocellulose films for extending shelf life of ground meat. *Carbohydrate Polymers*, *109*, 148–154. https://doi.org/10.1016/j.carbpol.2014.03.063

Demodaran, S., Parkin, K. L., & Fennema, O. L. (2010). *Química de Alimentos de Fennema* (Forth edit). Editora Artmed.

Fageria, N. K., Baligar, V. C., & Jones, C. A. (2010). *Growth and Mineral Nutrition of Field Crops* (Third Edit, p. 551). CRC Press.

Ghanbarzadeh, B., Keivani, F., & Mohammadi, M. (2019). Encapsulation of food ingredients by solid lipid nanoparticles (SLNs). In *Lipid-Based Nanostructures for Food Encapsulation Purposes*. Elsevier Inc. https://doi.org/10.1016/b978-0-12-815673-5.00006-4

Godoi, K. R. R. de, Basso, R. C., Ming, C. C., Silva, V. M. da, Cunha, R. L. da, Barrera-Arellano, D., & Ribeiro, A. P. B. (2019). Physicochemical and

rheological properties of soybean organogels: Interactions between different structuring agents. *Food Research International*, *124*. https://doi.org/10.1016/j.foodres.2019.05.023

Godoi-Fernandes, K. R. R. de, Silva, M. G., Cardoso, L.P., & Ribeiro, A. P. B. (2023). Effect of chemical interesterification on physico-chemical properties of soybean oil and fully hydrogenated microalgae oil blends. *Food Research International*,*submitted but not published yet.

Grimaldi, R., Gonçalves, L. A. G., & Ando, M. Y. (2005). Otimização da reação de interesterificaç ão química do óleo de palma. *Quimica Nova*, *28*(4), 633–636. https://doi.org/10.1590/s0100-40422005000400015

Hammond, E. G., Johnson, L. a, Su, C., Wang, T., & White, P. J. (2005). Soybean Oil. *Bailey's Industrial Oil and Fat Products*, *1*, 577–653. https://doi.org/10.1002/047167849X.bio041

Huang, J., Wang, Q., Li, T., Xia, N., & Xia, Q. (2017). Nanostructured lipid carrier (NLC) as a strategy for encapsulation of quercetin and linseed oil: Preparation and in vitro characterization studies. *Journal of Food Engineering*, *215*, 1–12. https://doi.org/10.1016/j.jfoodeng.2017.07.002

Huck-Iriart, C., Pizones Ruiz-Henestrosa, V. M., Candal, R. J., & Herrera, M. L. (2013). Effect of Aqueous Phase Composition on Stability of Sodium Caseinate/Sunflower oil Emulsions. *Food and Bioprocess Technology*, *6*(9), 2406–2418. https://doi.org/10.1007/s11947-012-0901-y

Inoue, T., Hisatsugu, Y., Ishikawa, R., & Suzuki, M. (2004). Solid-liquid phase behavior of binary fatty acid mixtures: 2. Mixtures of oleic acid with lauric acid, myristic acid, and palmitic acid. *Chemistry and Physics of Lipids*, *127*(2), 161–173. https://doi.org/10.1016/j.chemphyslip.2003.10.013

Jafari, S. M., & Esfanjani, A. F. (2017). Instrumental analysis and characterization of nanocapsules. In *Nanoencapsulation Technologies for the Food and Nutraceutical Industries* (pp. 524–544). Elsevier Inc. https://doi.org/10.1016/B978-0-12-809436-5/00014-8

Jafari, S. M., Khanzadi, M., Mirzaei, H., Dehnad, D., Chegini, F. K., & Maghsoudlou, Y. (2015). Hydrophobicity, thermal and micro-structural properties of whey protein concentrate-pullulan-beeswax films. *International Journal of Biological Macromolecules*, *80*, 506–511. https://doi.org/10.1016/j.ijbiomac.2015.07.017

Jafari, S. M., Paximada, P., Mandala, I., Assadpour, E., & Mehrnia, M. A. (2017). Encapsulation by nanoemulsions. In *Nanoencapsulation Technologies for the Food and Nutraceutical Industries*. Elsevier Inc. https://doi.org/10.1016/B978-0-12-809436-5.00002-1

Ji, S., Wu, J., Xu, F., Wu, Y., Xu, X., Gao, H., Ju, X., Xiong, W., & Wang, L. (2020). Synthesis, Purification, and Characterization of a Structured Lipid Based on Soybean Oil and Coconut Oil and Its Applications in Curcumin-Loaded Nanoemulsions. *European Journal of Lipid Science and Technology*, *122*(10), 1–10. https://doi.org/10.1002/ejlt.202000086

Katouzian, I., Faridi Esfanjani, A., Jafari, S. M., & Akhavan, S. (2017). Formulation and application of a new generation of lipid nano-carriers for the food bioactive ingredients. *Trends in Food Science and Technology*, *68*, 14–25. https://doi.org/10.1016/j.tifs.2017.07.017

Kharat, M., & McClements, D. J. (2019). Fabrication and characterization of nanostructured lipid carriers (NLC) using a plant-based emulsifier: Quillaja saponin. *Food Research International*, *126*(July), 108601. https://doi.org/10.1016/j.foodres.2019.108601

Kovačević, A. B., Müller, R. H., Savić, S. D., Vuleta, G. M., & Keck, C. M. (2014a). Solid lipid nanoparticles (SLN) stabilized with polyhydroxy surfactants: Preparation, characterization and physical stability investigation. *Colloids and Surfaces A: Physicochemical and Engineering Aspects*, *444*, 15–25. https://doi.org/10.1016/j.colsurfa.2013.12.023

Kovačević, A. B., Müller, R. H., Savić, S. D., Vuleta, G. M., & Keck, C. M. (2014b). Solid lipid nanoparticles (SLN) stabilized with polyhydroxy surfactants: Preparation, characterization and physical stability investigation. *Colloids and Surfaces A: Physicochemical and Engineering Aspects*, *444*, 15–25. https://doi.org/10.1016/j.colsurfa.2013.12.023

Kumbhar, D. D., & Pokharkar, V. B. (2013). Engineering of a nanostructured lipid carrier for the poorly water-soluble drug, bicalutamide: Physicochemical investigations. *Colloids and Surfaces A: Physicochemical and Engineering Aspects*, *416*(1), 32–42. https://doi.org/10.1016/j.colsurfa.2012.10.031

Leão, K. M. M., Reis, L. V. C., Speranza, P., Rodrigues, A. P., Ribeiro, A. P. B., Macedo, J. A., & Macedo, G. A. (2019). Physicochemical characterization

and antimicrobial activity in novel systems containing buriti oil and structured lipids nanoemulsions. *Biotechnology Reports*, *24*. https://doi.org/10.1016/j.btre.2019.e00365

Liu, C. H., & Wu, C. T. (2010). Optimization of nanostructured lipid carriers for lutein delivery. *Colloids and Surfaces A: Physicochemical and Engineering Aspects*, *353*(2–3), 149–156. https://doi.org/10.1016/j.colsurfa.2009.11.006

Llinares, R., Ramírez, P., Carmona, J., Carrillo, F., & Munñoz, J. (2018). Formulation and optimization of emulsions based on bitter fennel essential oil and EO/BO block copolymer surfactant. *Colloids and Surfaces A: Physicochemical and Engineering Aspects*, *536*(July 2017), 142–147. https://doi.org/10.1016/j.colsurfa.2017.07.027

Luo, Y., Teng, Z., & Wang, Q. (2012). Development of zein nanoparticles coated with carboxymethyl chitosan for encapsulation and controlled release of vitamin D3. *Journal of Agricultural and Food Chemistry*, *60*(3), 836–843. https://doi.org/10.1021/jf204194z

Luykx, D. M., Peters, R. J., van Ruth, S. M., & Bouwmeester, H. (2008). A review of analytical methods for the identification and characterization of nano delivery systems in food. *J Agric Food Chem*, *56*(18), 8231–8247. https://doi.org/10.1021/jf8013926 [doi]

Madureira, A. R., Campos, D. A., Fonte, P., Nunes, S., Reis, F., Gomes, A. M., Sarmento, B., & Pintado, M. M. (2015). Characterization of solid lipid nanoparticles produced with carnauba wax for rosmarinic acid oral delivery. *RSC Advances*, *5*(29), 22665–22673. https://doi.org/10.1039/c4ra15802d

Marangoni, A. G., & Rosseau, D. (2002). The effects of interesterification on the physical properties of fats. In A. G. Marangoni & S. S. Narine (Eds.), *Physical Properties of Lipids*. Marcell Dekker Inc.

Martini, S., Herrera, M. L., & Hartel, R. W. (2002). Effect of cooling rate on crystallization behavior of milk fat fraction/sunflower oil blends. *JAOCS, Journal of the American Oil Chemists' Society*, *79*(11), 1055–1062. https://doi.org/10.1007/s11746-002-0603-6

McClements, D. J. (2012). Crystals and crystallization in oil-in-water emulsions: Implications for emulsion-based delivery systems. *Advances in Colloid and Interface Science*, *174*, 1–30. https://doi.org/10.1016/j.cis.2012.03.002

McClements, D. J. (2016). *Food Emulsions*.

Mohammadi, M., Assadpour, E., & Jafari, S. M. (2019). Encapsulation of food ingredients by nanostructured lipid carriers (NLCs). In *Lipid-Based Nanostructures for Food Encapsulation Purposes*. Elsevier Inc. https://doi.org/10.1016/b978-0-12-815673-5.00007-6

Montenegro, R., & Landfester, K. (2003). Metastable and stable morphologies during crystallization of alkanes in miniemulsion droplets. *Langmuir*, *19*(15), 5996–6003. https://doi.org/10.1021/la027019v

Oh, J. H., McCurdy, A. R., Clark, S., & Swanson, B. G. (2005). Stabilizing polymorphic transitions of tristearin using diacylglycerols and sucrose polyesters. *JAOCS, Journal of the American Oil Chemists' Society*, *82*(1), 13–19. https://doi.org/10.1007/s11746-005-1036-y

Qian, C., Decker, E. A., Xiao, H., & McClements, D. J. (2013). Impact of lipid nanoparticle physical state on particle aggregation and β-carotene degradation: Potential limitations of solid lipid nanoparticles. *Food Research International*, *52*(1), 342–349. https://doi.org/10.1016/j.foodres.2013.03.035

Queirós, M.S., Viriato, R. L. S., Vega, D. A., Ribeiro, A. P. B., & Gigante, M. L. (2020). Milk fat nanoemulsions stabilized by dairy proteins. *Journal of Food Science and Technology*, *57*(9), 3295–3304. https://doi.org/10.1007/s13197-020-04362-0

Queirós, M. de S., Soares Viriato, R. L., Ribeiro, A. P. B., & Gigante, M. L. (2022). Development of solid lipid nanoparticle and nanostructured lipid carrier with dairy ingredients. *International Dairy Journal*, *130*. https://doi.org/10.1016/j.idairyj.2021.105186

Reis, L. V. de C., Leão, K. M., Speranza, P., Ribeiro, A. P. B., Macedo, G. A., & Macedo, J. A. (2020). Evaluation of nanostructured lipid carriers produced with interesterified buriti oil. *Food Technology and Biotechnology*, *58*(3), 284–294. https://doi.org/10.17113/ftb.58.03.20.6195

Ribeiro, A. P. B., Basso, R. C., Grimaldi, R., Gioielli, L. A., dos Santos, A. O., Cardoso, L. P., & Guaraldo Gonçalves, L. A. (2009). Influence of chemical interesterification on thermal behavior, microstructure, polymorphism and crystallization properties of canola oil and fully hydrogenated cottonseed oil blends. *Food Research International*, *42*(8), 1153–1162. https://doi.org/10.1016/j.foodres.2009.05.016

Ribeiro, A. P. B., Basso, R. C., Grimaldi, R., Gioielli, L. A., & Gonçalves, L. A. G. (2009). Instrumental Methods for the Evaluation of Interesterified Fats. *Food Analytical Methods*, *2*(4), 281–302.

Ribeiro, A. P. B., Basso, R. C., Grimaldi, R., Gioielli, L. A., Gonçalves, L. A. G., Oliveira, P. D., Rodrigues, A. M. C., Bezerra, C. V., Silva, L. H. M., Morselli Ribeiro, M. D. M., Ming, C. C., Silvestre, I. M., Grimaldi, R., Ap. G. Gonçalves, L., Dunn, A. M., Hofmann, O. S., Waters, B., Witchel, E., Ramli, N; Mohd Sobani, S. S. ., … Hrádková, I. (2017). Effects of chemical interesterification on the triacylglycerols, solid fat contents and crystallization kinetics of palm oil-based fats. *Proceedings of the 20th USENIX Security Symposium*, *2*(1), 369–376. https://doi.org/10.1016/j.foodres.2018.05.015

Rocha, J. C. B., Lopes, J. D., Mascarenhas, M. C. N., Arellano, D. B., Guerreiro, L. M. R., & da Cunha, R. L. (2013). Thermal and rheological properties of organogels formed by sugarcane or candelilla wax in soybean oil. *Food Research International*, *50*(1), 318–323. https://doi.org/10.1016/j.foodres.2012.10.043

Rosseau, D., & Marangoni, A. G. (2002). Chemical Interesterification of Food Lipids: Theory and Practice. In C. C. Akoh & D. B. Min (Eds.), *Food Lipids : Chemistry, Nutrition, and Biotechnology* (Second Edi, p. 1014). Marcel Dekker, Inc.

Salminen, H., Helgason, T., Kristinsson, B., Kristbergsson, K., & Weiss, J. (2013). Formation of solid shell nanoparticles with liquid ω-3 fatty acid core. *Food Chemistry*, *141*(3), 2934–2943. https://doi.org/10.1016/j.foodchem.2013.05.120

Salvia-Trujillo, L., Soliva-Fortuny, R., Rojas-Graü, M. A., McClements, D. J., & Martín-Belloso, O. (2017). Edible Nanoemulsions as Carriers of Active Ingredients: A Review. *Annual Review of Food Science and Technology*, *8*(1), 439–466. https://doi.org/10.1146/annurev-food-030216-025908

Santos, V. S, Ribeiro, A. P. B., & Santana, M. H. A. (2019). Solid lipid nanoparticles as carriers for lipophilic compounds for applications in foods. *Food Research International*, *122*(September 2017), 610–626. https://doi.org/10.1016/j.foodres.2019.01.032

Santos, V. da S., Braz, B. B., Silva, A. Á., Cardoso, L. P., Ribeiro, A. P. B., &

Santana, M. H. A. (2019). Nanostructured lipid carriers loaded with free phytosterols for food applications. *Food Chemistry*, *298*(May), 125053. https://doi.org/10.1016/j.foodchem.2019.125053

Santos, V. da S., Koji Miyasaki, E., Cardoso, L. P., Badan Ribeiro, A. P., & Andrade Santana, M. H. (2019). Crystallization, Polymorphism and Stability of Nanostructured Lipid Carriers Developed with Soybean Oil, Fully Hydrogenated Soybean Oil and Free Phytosterols for Food Applications. *Journal of Nanotechnology Research*, *01*(01), 1–22. https://doi.org/10.26502/jnr.2688-8521001

Sato, K., & Ueno, S. (2005). Polymorphism in fats and oils. *Bailey's Industrial Oil and Fat Products*, *1*, 77–120. http://onlinelibrary.wiley.com/doi/10.1002/047167849X.bio020/full

Scrimgeour, C. (2005). Chemistry of Fatty Acids. *Bailey's Industrial Oil and Fat Products*, 1–43. https://doi.org/10.1002/047167849X.bio005

Shah, R., Eldridge, D., Palombo, E., & Harding, I. (2015). *Production Techniques*. https://doi.org/10.1007/978-3-319-10711-0_3

Siekmann, B., & Westesen, K. (1994). Thermoanalysis of the recrystallization process of melt-homogenized glyceride nanoparticles. *Colloids and Surfaces B: Biointerfaces*, *3*(3), 159–175. https://doi.org/10.1016/0927-7765(94)80063-4

Silva, A. C., González-Mira, E., García, M. L., Egea, M. A., Fonseca, J., Silva, R., Santos, D., Souto, E. B., & Ferreira, D. (2011). Preparation, characterization and biocompatibility studies on risperidone-loaded solid lipid nanoparticles (SLN): High pressure homogenization versus ultrasound. *Colloids and Surfaces B: Biointerfaces*, *86*(1), 158–165. https://doi.org/10.1016/j.colsurfb.2011.03.035

Silva, M. G., de Godoi, K. R. R., Gigante, M. L., Pavie Cardoso, L., & Paula Badan Ribeiro, A. (2022a). Developed and characterization of nanostructured lipid carriers containing food-grade interesterified lipid phase for food application. *Food Research International*, *155*(October 2021), 111119. https://doi.org/10.1016/j.foodres.2022.111119

Silva, M. G., Godoi, K. R. R., Gigante, M. L., Cardoso, L. P., & Ribeiro, A. P. B. (2022b). Nanostructured lipid carriers for delivery of free phytosterols: Effect of lipid composition and chemical interesterification on physical

stability. *Colloids and Surfaces A: Physicochemical and Engineering Aspects*, *640*(January), 128425. https://doi.org/10.1016/j.colsurfa.2022.128425

Souto, E., Severino, P., Santana, M. H., & Pinho, S. (2011). Nanopartículas de lipídios sólidos: métodos clássicos de produção laboratorial. *Quimica Nova*, *34*(8), 1323–1327.

Tamjidi, F., Shahedi, M., Varshosaz, J., & Nasirpour, A. (2013). Nanostructured lipid carriers (NLC): A potential delivery system for bioactive food molecules. *Innovative Food Science and Emerging Technologies*, *19*, 29–43. https://doi.org/10.1016/j.ifset.2013.03.002

Teng, W., Zhao, L., Yang, S., Zhang, C., Liu, M., Luo, J., Jin, J., Zhang, M., Bao, C., Li, D., Xiong, W., Li, Y., & Ren, F. (2019). The hepatic-targeted, resveratrol loaded nanoparticles for relief of high fat diet-induced nonalcoholic fatty liver disease. *Journal of Controlled Release*, *307*(April), 139–149. https://doi.org/10.1016/j.jconrel.2019.06.023

Trujillo-Cayado, L. A., Alfaro, M. C., & Muñoz, J. (2018). Effects of ethoxylated fatty acid alkanolamide concentration and processing on D-limonene emulsions. *Colloids and Surfaces A: Physicochemical and Engineering Aspects*, *536*(June 2017), 198–203. https://doi.org/10.1016/j.colsurfa.2017.06.010

Wang, J. L., Dong, X. Y., Wei, F., Zhong, J., Liu, B., Yao, M. H., Yang, M., Zheng, C., Quek, S. Y., & Chen, H. (2014). Preparation and characterization of novel lipid carriers containing microalgae oil for food applications. *Journal of Food Science*, *79*(2). https://doi.org/10.1111/1750-3841.12334

Xu, B., Kang, W., Meng, L., Yang, R., Liu, S., & Zhang, L. (2013). Synthesis, aggregation behavior and emulsification characteristic of a multi-sticker amphiphilic polymer. *Journal of Macromolecular Science, Part A: Pure and Applied Chemistry*, *50*(3), 302–309. https://doi.org/10.1080/10601325.2013.755855

Yang, Y., Corona, A., Schubert, B., Reeder, R., & Henson, M. A. (2014). The effect of oil type on the aggregation stability of nanostructured lipid carriers. *Journal of Colloid and Interface Science*, *418*, 261–272. https://doi.org/10.1016/j.jcis.2013.12.024

Yap, P., Man, J. De, & Man, L. De. (1989). Polymorphism of palm oil and palm oil products. *Journal of the American Oil Chemist's Society*, *66*(5), 693–697. https://doi.org/10.1007/BF02669954

Zeitoun, M. A. M., Neff, W. E., List, G. R., & Mounts, T. L. (1993). Physical properties of interesterified fat blends. *Journal of the American Oil Chemists' Society*, *70*(5), 467–471. https://doi.org/10.1007/BF02542577

Zheng, M., Falkeborg, M., Zheng, Y., Yang, T., & Xu, X. (2013). Formulation and characterization of nanostructured lipid carriers containing a mixed lipids core. *Colloids and Surfaces A: Physicochemical and Engineering Aspects*, *430*, 76–84. https://doi.org/10.1016/j.colsurfa.2013.03.070

ARTIGO 4. INCORPORATION OF OMEGA-3 FATTY ACIDS IN NANOSTRUCTURED LIPID CARRIERS BASED ON SOYBEAN OIL AND FULLY HYDROGENATED MICROALGAE OIL: EFFECT OF SATURATED FATTY ACID CONTENT AND TRIACYLGLYCEROL COMPOSITION

Kamila Ramponi Rodrigues de Godoi Fernandes[1], Mayanny Gomes da Silva[1], Mirna Lucia Gigante[1], Ana Paula Badan Ribeiro[1]

[1]Department of Engineering and Food Technology, School of Food Engineering, University of Campinas, Brazil

Corresponding author: kamila.ramponi@hotmail.com

(Manuscrito a ser submetido ao Periódico *Colloids and surfaces A: Physicochemical and engineering aspects*)

Abstract: The potential of nanostructured lipid carriers (NLCs) to incorporate bioactive compounds has been studied in recent years. This study aimed to evaluate the incorporation of fish oil rich in omega-3 fatty acids in NLCs composed of 88% of aqueous phase (distilled water), 2% of emulsifier (enzymatically modified soybean lecithin), and 10% of lipid phase (simple and chemically interesterified blends of fully hydrogenated microalgae oil (FHMO) and soybean oil (SO) in the proportions of 60:40 and 70:30 (w/w), respectively). The NLCs were produced by hot high-pressure homogenization (HPH) and characterized for thermal behavior, solid fat content (SFC), particle size, polydispersity (PDI), zeta potential (ZP), physical stability by Turbiscan, encapsulation efficiency, and oxidative stability by peroxide value (PV) during 30 days at 25 °C. The combination between FHMO and SO as lipid phase in NLCs was adequate to encapsulate fish oil. The highest encapsulation efficiency was 100%, with a reduction as a function of time. The NLCs composed of lower FHMO concentration with interesterified blend showed lower thermal resistance and SFC at 25 °C. In general, the particle size of all NLCs was approximately 300 nm and PDI approximately 1, with higher particle size and higher PDI observed for the NLCs made with interesterified blends, while similar zeta potential values between -38 and -54v were observed for all NLCs. The physical stability assessed by Turbiscan measurements indicated destabilization of NLCs after 7 days of storage at 25 °C. All NLCs presented creaming, while the NLC 60:40I also presented the flocculation/coalescence phenomena. All lipid matrices showed similar oil encapsulation capacity and peroxide indices. Over time, a reduction in the physical and oxidative stability of the particles was observed. The NLCs made with simple and interesterified blends were adequate for the encapsulation of fish oil with low melting points and crystallinity. However, specific thermal behavior characteristics and low crystalline organization are recommended for the encapsulation of bioactive compounds with a high melting point to be used in foods including spreads, margarine, and beverages, without conferring undesirable flavor, thus increasing the intake of bioactive compounds.

1. Introduction

Bioactive compounds can have a limited application in foods due to their lower stability and undesirable flavor. However, the health benefits associated with the use of these compounds such as carotenoids, oils rich in essential fatty acids, phenolic compounds, vitamins, and antioxidants, have raised interest in the food industry (Zardini et al., 2018; Esfanjani et al., 2018; Pezeshki et al., 2019).

To solve the limitations of the application of bioactive compounds in processed foods, nanoencapsulation has emerged as an alternative to increasing the stability and viability of bioactive compounds, besides allowing other applications to improve food quality (Katouzian et al., 2017). Lipids are considered adequate raw materials for incorporation into nanoparticles, leading to the formation of lipid nanoparticles (LN) that are colloidal systems containing a lipid phase, an aqueous phase, and emulsifiers to encapsulate bioactive compounds. These LN can be classified as solid lipid nanoparticles (SLN) or nanostructured lipid carriers (NLC), distinguished by the lipid phase's composition. The SLN has only high saturated fat as a lipid phase that is solid at room temperature resulting in a highly ordered crystalline structure. This characteristic can cause a negative impact over time due to the risk of the release of bioactive compounds from the particles when the crystallization happens. In turn, NLCs are lipid nanostructures that contain crystallized lipid droplets and an amorphous crystalline structure represented by oil, and a crystalized phase represented by hardfats, which allows the equilibrium between saturated and unsaturated fatty acids and favors adequate crystallization and incorporation of bioactive lipophilic compounds (Mohammadi et al., 2019)

Searching for the most stable NLC with a greater ability to incorporate lipophilic compounds the crystallization behavior of the lipid phase is important. In lipids, the β'-form has intermediate stability and small crystal size, which is beneficial to the NLC, once the low lipid crystallinity can favor the incorporation of bioactive compounds (Santos et al., 2019; Sato & Ueno, 2005).

In this context, studies have shown the use of chemical interesterified fats for this application (Silva et al., 2022). Chemical interesterification is a lipid modification process capable to stabilize the crystal fats in the β′ polymorphic

form indefinitely, once it promotes the randomization of fatty acids in triacylglycerols, which become more heterogeneous, forming crystals lattices of lower density (Ribeiro et al., 2009).

Soybean oil (SO) was used as a raw material to formulate NLCs in this study due to low cost and high availability, besides having desirable nutritional characteristics rich in linoleic fatty acid (55%) and linolenic fatty acid (7%) (Asbridge, 2015; Demodaran et al., 2010; Fageria et al., 2010; Hammond et al., 2005). Fully hydrogenated microalgae oil (FHMO) composed of approximately 92% stearic acid was used as a solid lipid phase, which is an unexpected raw material for the composition of NLC. Godoi-Fernandes (2023a) investigated the most promising combination between SO and FHMO in simple and chemical interesterified blends for NLC application.

The use of high shear processes as hot high-pressure homogenization shows a good potential to encapsulate lipophilic compounds has been confirmed by recent studies (Huang et al., 2017; Munin & Edwards-Lévy, 2011; Patra & Baek, 2014), with satisfactory results to incorporate carotenoids (Pezeshki et al., 2019), resveratrol (Poonia et al., 2019), curcumin (Behbahani et al., 2019), rutin (Babazadeh et al., 2016), lycopene (Zardini et al., 2018), conjugated linoleic acid (Hashemi et al., 2020), astaxanthin (Tamjidi et al., 2014), phenolic compounds (Esfanjani et al., 2018), phytosterols (Silva et al., 2022) and liposoluble vitamins (Ying Yang & McClements, 2013), and oils rich in essential fatty acids, as linseed and fish oils (Assadpour & Mahdi Jafari, 2019; Huang et al., 2017; Shahparast et al., 2019).

Fish oil is a bioactive compound with health benefits due to its rich composition in the essential fatty acids eicosapentaenoic acid (EPA), docosapentaenoic acid, and docosahexaenoic acid (DHA), known as omega-3 (ω-3) (Awad et al., 2009). These essential fatty acids play important roles in conception, pregnancy, infancy, and throughout life (Vellido-Perez et al., 2021). The adequate intake of these essential fatty acids has shown improvements concerning chronic diseases, controlling inflammation levels, preventing diseases such as metabolic syndrome (type 2 diabetes and obesity), acting in mental health, and decreasing the risk of cancer (Lalia & Lanza, 2016; Perica & Delaš, 2011; Sulciner et al., 2018).

Therefore, knowledge about the therapeutic properties associated with the ω-3 fatty acids can allow the enrichment of food products to increase their consumption. However, the protection and maintenance of bioavailable ω-3 fatty acids is a challenge due to the high unsaturated chemical composition, which makes them highly susceptible to oxidation, and the unpleasant aroma and flavor of seafood (Vellido-Perez et al., 2021).

In this sense, several studies have shown novel methods and strategies to obtain systems capable to maintain the stability and availability of ω-3 fatty acids. The most efficient and common system to protect and release the ω-3 fatty acids includes oil in water emulsions (O/W), and oils containing ω-3 fatty acids have been used in nanoemulsions. Liu et al. (2016) studied fish oil-in-water emulsions using two natural emulsifiers (quillaja saponins and rhamnolipids) and a synthetic emulsifier (Tween-80) with proper oxidative stability; Ojagh & Hasani (2018) studied nanoliposomes of fish oil in bread with high texture quality and sensory acceptability; Venugopalan et al. (2021) investigated the encapsulation of fish oils into colloidal particles to improve the dispersibility, stability, and bioavailability of ω-3 fatty acids; Esfahani et al. (2019) studied the nanoencapsulation of ω3 fatty acids by gelatin-gum arabic complexes and reported high impact of the homogenization rate on the particle size. As reported by Salminen et al. (2016), the encapsulation of hydrophobic liquid lipids, such as ω-3 fish oils, can lead to the formation of structures that allow the presence of oil either in the core or on the surface, as a function of the surfactant used.

Thus, based on the literature background, this study aimed to produce and evaluate the ability of NLCs composed of simple and interesterified blends of fully hydrogenated microalgae oil (FHMO) and soybean oil (SO) in the proportions 60:40 and 70:30 (w/w) to encapsulate fish oil rich in ω-3 fatty acids.

2. Material and methods

2.1. Material

The nanostructured lipid carriers (NLC) were formulated using fully hydrogenated microalgae oil (FHMO) and soybean oil (SO) as lipid phases. The FHMO was kindly supplied by SGS (Brazil) and soybean oil (SO) was purchased

in a local market. The enzyme-modified soy lecithin (SL) (Solec® AEIP) used as emulsifier was supplied by DuPont™ (Wilmington, DE, USA). and containing 16% (w/w) of phosphatidylcholine, 15% (w/w) of lysophosphatidylcholine, 14% (w/w) of phosphatidylethanolamine, and 37% (w/w) of triglycerides. Sodium methoxide anhydrous powder (99% purity; Sigma-Aldrich, Brazil) was used for the chemical interesterification process. All other reagents and solvents used in this study were of analytical or chromatographic grade. Fish oil rich in ω-3 supplied by AQIA Industrial Chemistry (Brazil) with 73.66% of docosahexaenoic acid (C22:6), 6.72% of docosapentaenoic acid (C22:5), 4.15% of oleic acid (C18:1), and 4.08% of acid eicosapentaenoic (C20:5).

2.2. Production of the lipid matrices

2.2.1. Simple blends

The FHMO and SO in the proportions (FHMO: SO w/w) of 60:40 and 70:30 were heated until total melting and mixed under magnetic stirring until complete homogenization.

2.2.2. Chemically interesterified blends

The reactions were performed using the FHMO and SO ratios in Section 2.1.1.1, with optimization according to Grimaldi et al. (2005). For the chemical interesterification reaction, on a laboratory scale, each blend was placed in a 500mL borosilicate-glass jacket coupled to a model RE 212 recirculating thermostat bath (Lauda, Manheim, Germany) and heated until 100°C under magnetic stirring (500rpm) (Marconi, Piracicaba, Brazil) for 20 minutes under vacuum to remove the moisture. After, each dried blend was interesterified using 1.54% of sodium methoxide, according to the calculated quantity of free fatty acids (0.03%) and peroxide value (10 mEq/g) of SO and FHMO (Gioielli, 1998). Sodium methoxide was added to the dried blends at 100 °C, under magnetic stirring (500rpm) for 20 min of reaction under vacuum. Then, citric acid solution (5g/100mL) was added to stop the reaction. The interesterified samples were washed with distilled water (80°C) to remove soaps. For drying, the blends were

heated until 100 °C under magnetic stirring for 20 min under vacuum. After the reaction, FFA and the partial acylglycerols (diacylglycerols and monoacylglycerols) were removed according to Marangoni and Rosseau (2002), with modifications. The interesterified blends were melted and mixed with an equal volume of 96% ethanol at 40–50 °C in a separatory funnel. The ethanol phase was then extracted, and the procedure was repeated three times. The samples were stored in glass vials under refrigeration according to each analysis (25 or 5°C).

2.3. Characterization of lipid matrices

2.3.1. Fatty acid composition

The fatty acid composition of SO, FHMO, lipid blends (70:30 and 60:40 (w/w) FHMO:SO) and fish oil were determined using a gas chromatograph CGC Agilent Series 6850 (Santa Clara, California, USA) with an FID detector, after esterification, as reported by Hartman & Lago (1973). The methyl esters were separated according to AOCS Cf 1-96 (AOCS, 2009) in capillary column Agilent-DB-23 (50% cyanopropyl – methylpolysiloxane), length 60 m, internal diameter 0.25 mm, and film thickness 0.25 µm.; The operation conditions were a flow rate of 1.0 ml/min; linear velocity of 24 cm/s; injector temperature of 250 °C; detector temperature of 280 °C/min; oven temperature of 110 °C for 5 min, 110 - 215 °C at 5 °C/min, 215 °C for 34 min; helium as a carrier gas; injected volume of 1.0 µL/min, and split ratio of 1:50. The individual fatty acid methyl esters were identified by comparison of retention times to commercial standards, and quantified based on relative peak areas. The fatty acid composition of the blends was calculated by comparing them with their respective mass fractions in the blends.

2.3.2. Triacylglycerol composition

Triacylglycerol composition was determined using a gas chromatograph CGC Agilent 6850 Series GC System (Santa Clara, California, USA). A capillary column Agilent - DB-17 HT (50% phenyl- 50% methylpolysiloxane) with a length of 15 m, an internal diameter of 0.25 mm, and a film thickness of 0.15 µm was

used. The operation conditions were injector temperature of 360 °C; detector temperature of 375 °C/min; oven temperature from 250°C to 350 °C at 5 °C/min, 350 °C for 20 min; helium as a carrier gas; injected volume of 1.0 µL/min, and split ratio of 1:100. Triacylglycerols were identified by comparison of retention times and quantified based on relative peak areas (Filho et al., 1995) The triacylglycerol composition of the blends was calculated by comparing the composition of SO and FHMO with their respective mass fractions in the blends for trissaturated (S3), dissaturated (S2U), monossaturated (SU2), and triunsaturated (U3) triacylglycerols.

2.3.3. Fatty acid regiospecific distribution

Proton-decoupled 13C NMR (Nuclear Magnetic Resonance) was used to analyze the positional distribution of classes of fatty acids on the triacylglycerol (TAG) backbone. Lipid samples were dissolved in deuterated chloroform in NMR tubes, and NMR spectra were recorded on a Bruker Advance DPX spectrometer operating at 300 MHz. The determination of 13C was performed at a frequency of 75.8 MHz, with a 5 mm multinuclear probe operating at 30°C (Vlahov, 1998).

2.4. Production of the nanoparticles

The NLCs were made with 10% (w/w) of the total lipid phase and 90% (w:w) of the aqueous phase. The production of the NLCs was performed according to 4 steps, as follows: (i) melting of the lipid fraction, (ii) formation of the emulsion, (iii) nanoemulsification, and (iv) crystallization of the lipid phase (Santos et al., 2019). In the first step, the lipid blends (9.5%,w/w) composed of 60:40 or 70:30 (w/w) (FHMO: SO) in chemical interesterified or simple blends were melted. The fish oil (0.5%, w:w) was mixed with the melted lipid phase with magnetic stirring until the complete homogenization, not exceeding 3 min to prevent degradation of the bioactive compound. The aqueous phase (composed of distilled water and 2% of the enzymatically modified lecithin as an emulsifier) was heated to 85 °C and mixed with the lipid phase. After, both phases were homogenized to form the pre-emulsion through continuous agitation in Ultraturrax (IKA, Alemanha) for 3 minutes at 10000 rpm (Souto et al., 2011; Yihui Yang et

al., 2014). Then, the samples were subjected to nano emulsification by hot homogenization in a high-pressure homogenizer (HPH) FBF Homolab (Italia) using 700 bar of pressure and 2 cycles of passage in the equipment (Ludtke et al., 2017). Sodium azide (0.02% w/w) was added to the NLCs to inhibit microbial growth. The resulting nanoemulsions were crystallized at 5 °C for 24 hours and stored at 25 °C for the period of study (Kumbhar & Pokharkar, 2013; Qian et al., 2013; Yihui Yang et al., 2014).

2.4.1. Physical characteristics and stability of the nanoparticles

The physical stability of the NLCs containing fish oil was evaluated during 30 days in absence of light, after 2 days (24h at 5°C for crystallization and 24h at 25°C) and 7, 15 and 30 days at 25°C according to the analytical methods described below.

2.4.2. Physical characteristics of nanoparticles

2.4.2.1. Melting Behavior

The melting behavior was determined using a differential scanning calorimeter (DSC) TA Q2000 coupled to an RCS90 Refrigerated Cooling System (TA Instruments, Waters LLC, New Castle) according to the AOCS method Cj 1-94, with adaptations (AOCS, 2009) using Universal V4.7A for data processing (TA Instruments, Waters LLC, New Castle). Approximately 10 mg of sample were disposed of in the hermetic aluminum pans and evaluated under isothermal conditions (at 25 °C and for 10 min), followed by heating to 25 °C at a rate of 10 °C/min until 100°C (Wang et al., 2014). The results were evaluated for the following parameters: onset melting temperature (T_i), peak melting temperature (T_p), and melting enthalpy (ΔH) (Campos, 2005).

2.4.2.2. Solid fat content (SFC)

The SFC of NLCs was determined at 25°C using a pc120 Minispec Nuclear Magnetic Resonance spectrometer (Bruker, Rheinstetten, Germany) with an

E200 Ecoline-star circulation heater (Lauda) (Ribeiro et al., 2009). All measurements were performed in triplicate, and the results were expressed as mean ± SD values.

2.5. Stability of nanoparticles

2.5.1. Droplet size, size distribution, and polydispersity index

The droplet size was analyzed by light scattering using the Mastersizer 2000 equipment (Malvern Instruments, Malvern, UK) in aqueous dispersion. The mean droplet size was characterized for the D3,2 (mean surface diameter) according to Eq. 2, and the polydispersity index was obtained by Span calculation, according to Eq. 3.

$$D_{32} = \frac{\Sigma n_i d_i^3}{\Sigma n_i d_i^2} \qquad \textbf{Equation 2}$$

$$Span = \frac{d_{90} - d_{10}}{d_{50}} \qquad \textbf{Equation 3}$$

where n_i is the number of particles with diameter d_i; and d_{10}, d_{50}, and d_{90} represent 10, 50, and 90% of the cumulative volume of the droplets, respectively (Gomes et al., 2022). The results were expressed as mean ± standard deviation (SD) values.

2.5.2. Zeta potential

The zeta potential of the samples was determined by Dynamic Light Scattering (DLS) using the equipment Zetasizer Nano-ZS (Malvern Instruments. Malvern. UK). For the measurements, the samples were properly diluted (100 µL) in 10 mL of ultra-purified water, the conductivity was adjusted (50 µS/cm), and the samples were placed in a DTS1060 folded capillary cell with an alternating voltage of ± 150 mV, using a dispersant (water) dielectric constant of 78.5. Each

value was measured at least in triplicate. The results were expressed as mean ± standard deviation (SD) (Das et al., 2012; Souto et al., 2011).

2.5.3. Kinetic stability by Turbiscan measurements

The kinetic stability was monitored using a Turbiscan ASG equipment (Formulaction, l'Union, France) at 25°C. Immediately after preparation, the nanoemulsions were placed in cylindrical glass tubes with a flat bottom (40 mm in height and 16 mm in diameter). The stability of the systems was analyzed using the backscattering profiles (BS), with scans at 880 nm in length at different heights (mm). The initial height of the sample (H = 0 mm) was considered the lower part of the measuring cell. The creaming index was detected by varying the particle concentration between the top and bottom of the tubes. When creaming takes place in a nanoemulsion, the DBS curves show a peak at heights between 0 and 20 mm. The variation of the peak width over time may be related to the migration kinetics of small particles (Huck-Iriart et al., 2013). To classify and compare the stability between the samples, the TSI (Turbiscan Stability Index) was calculated (Eq. 4), which shows the variations in the system over time. The TSI was calculated according to backscattering changes that indicate the particle aggregation and dynamic migration by Turbisoft 2.0. The kinetics are based on Equation 4, comparing every scan of a measurement to the previous one, on the selected height, and dividing the result by the total selected height to obtain a result that does not depend on the quantity of product in the measuring cell (Queirós et al., 2020; Llinares et al., 2018; Trujillo-Cayado et al., 2018).

$$TSI = \sqrt{\frac{\sum_{i-1}^{n} (x_i - x_{BS})^2}{n-1}} \qquad \textbf{Equation 4}$$

where x_i is the average value of the scattered light intensity at each time evaluated, x_{BS} is the average of x_i, and n is the number of scanning. TSI values range from 0 (i.e., a highly stable dispersion) to 100 (i.e., a highly unstable dispersion).

2.5.4. Peroxide value

To determine the peroxide value, the NLCs stored at 25 °C were submitted to the centrifugation in an ultracentrifuge (Beckman Coulter; Model Avanti J-26 XPI and Rotor JA-20) at 20 °C and 18000 rpm. The mechanical force leads to system destabilization sorting out the aqueous phase and the lipid phase. The aqueous phase was discarded and the lipid phase was evaluated. The lipid phase of each sample was weighed (1.0g) and mixed with 4g of high oleic sunflower oil (HOSO) - oil with good oxidative stability - in 250ml glass stoppered Erlenmeyer flasks. The peroxide value was determined according to the official method Cd 8b90 (AOCS, 2009) for each NLC mixed with HOSO, and HOSO alone to quantify the impact of the use of fish oil, according to Equation 5.

$$PV\omega\ (meq\ O2/kg) = PVm - PVh \qquad \textbf{Equation 5}$$

Where: *PVω* = Peroxide value of NLC loaded with fish oil; PVm = Peroxide value of the mixture of lipid phase of nanoemulsion and HOSO; PVh = Peroxide value of HOSO.

2.5.5. Encapsulation efficiency (EE)

The EE can be calculated after quantification of free or encapsulated bioactive compound. The unencapsulated free bioactive compound can dissolve in the aqueous phase, while the crystallized portion contains the amount of compound entrapped. The liquid (aqueous) and solid (lipid) phases were separated by ultracentrifugation of the nanoemulsions (Agrawal et al., 2010) for further analysis. For that, the NLCs stored at 25°C were submitted to the centrifugation in an ultracentrifuge (Beckman Coulter; Model Avanti J-26 XPI and Rotor JA-20) at 20°C and 18000 rpm. Then, the liquid phase was discarded and the solid phase was submitted to the fatty acid composition analysis using a gas chromatograph CGC Agilent Series 6850 (Santa Clara, California, USA) with FID detector, after esterification as reported by Hartman & Lago (1973b). The fatty acid methyl esters were separated according to AOCS Ce 2-66 method (AOCS, 2009) in a capillary column Agilent-DB-23 (50% cyanopropyl –

methylpolysiloxane), length 60 m, internal diameter 0.25 mm, and film thickness 0.25 µm.; The operation conditions were: flow rate of 1.0 ml/min; linear velocity of 24 cm/s; injector temperature of 250 °C; detector temperature of 280 °C/min; oven temperature of 110 °C for 5 min, 110 - 215 °C at 5 °C/min, 215 °C for 34 min; helium as a carrier gas; injected volume of 1.0 µL/min, and split ratio of 1:50. Individual fatty acid methyl esters were identified by comparison of retention times to commercial standards and quantified based on relative peak areas.

The fatty acid composition of the solid phase was calculated according to the fatty acid composition of the raw materials and ω-3 and compared to the result of each specific fatty acid from ω-3 concentrate (docosahexaenoic acid - C22:6; docosapentaenoic - C22:5; and acid eicosapentaenoic - C20:5). The quantity corresponded to the fish oil concentration entrapped in the solid (lipid) phase. The fatty acid composition of each fatty acid was calculated according to Equation 6.

$$FA\ total\ (\%) = (FR * 9.5\%) + (FB * 0.5\%) \qquad \textbf{Equation 6}$$

Where: FA total = total fatty acids of lipophilic compound added to lipid phase; FR = total fatty acids contained in the raw materials (FHMO and SO) proportionally of the amount added; FB = total fatty acids contained in the bioactive compound (Omega 3).

The encapsulation efficiency (EE) of the lipophilic compounds incorporated into NLC was calculated as reported by Nguyen et al.(2012) with modifications, according to Equation 7, considering the majority and specific omega 3 fatty acid (docosahexaenoic acid - C22:6) present in the lipid phase after 48h, 7, 15, and 30 days of storage.

$$EE\ (\%) = \frac{FA\ encapsulated}{FA\ total} \times 100 \qquad \textbf{Equation 6}$$

Where: EE = encapsulation efficiency in %; FA encapsulated = total fatty acids of lipophilic compound encapsulated; FA total = total fatty acids of lipophilic compound added to lipid phase.

2.5.6. Statistical analysis

The results were subjected to analysis of variance (ANOVA) using the software STATISTICA Version 8 (StatSoft Inc., Tulsa, OK). Tukey's test was used for statistical comparisons of means, at a 5% significance level ($p<0.05$).

3. Results and Discussion

3.1. Characterization of the lipid phase

As previously defined, the lipid phase of NLCs was composed of SO and FHMO. The predominant fatty acid composition of the SO is linoleic acid (52.70%), oleic acid (24.53%), palmitic acid (11.10%), and linolenic acid (6.39%), while the FHMO contains mainly 92.85% stearic acid and 5.52% palmitic acid (O'Brien. 2009a; GODOI-FERNANDES, et al. 2023a). Thus, when these raw materials were mixed as suggested in this study, the fatty acid composition changed proportionally to the ratios used, as shown in Table 1.

As expected, the lipid fractions presented similar composition before and after interesterification, with changes only in the distribution of the fatty acids in the triacylglycerol molecule. A modification in the triacylglycerol composition was observed after the interesterification reaction with a reduction in the contents of trisaturated (S3), monosaturated (U2S) and triunsaturated (U3) triacylglycerols (TAG), and a concomitant increase in disaturated triacylglycerols (S2U) for both ratios used, as shown in Table 2. In general, the chemical interesterification led to a decrease in the amount of saturated fatty acids of the blend 70:30 for all glycerol positions, while the blend 60:40 showed an increase of 12% in the sn 1-3 position. In turn, a decrease in the amount of saturated and an increase in unsaturated fatty acids was observed for the sn-2 position (Table 3).

Table 1. Fatty acid composition (%) of raw materials (SO and FHMO) and the respective blends.

Fatty acids (%)	70:30 (w:w) FHMO: SO	60:40 (w:w) FHMO: SO
C 12:0 – Lauric acid	0.11±0.01	0.10±0.01
C14:0 – Mirístic acid	0.35±0.00	0.32±0.01
C16:0- Palmític acid	7.18±0.07	7.74±0.10
C 16:1 – Palmitoleic acid	0.03±0.00	0.04±0.00
C 17:0 – Margaric acid	0.09±0.01	0.09±0.01
C18:0 – Stearic acid	65.94±0.04	57.06±0.07
C18:1 – Oleic acid	7.47±0.76	9.90±0.97
C18:2 – Linoleic acid	15.87±0.64	21.12±0.86
C18:3 – Linolenic acid	1.91±0.15	2.56±0.20
C20:0 – Araquidic acid	0.81±0.03	0.76±0.04
C20:1 – Eicosenoic acid	0.07±0.01	0.09±0.01
C22:0 – Behenic acid	0.19±0.02	0.24±0.02
C24:0 – Lignoceric acid	0.06±0.01	0.08±0.01
∑ **Saturated**	74.65±0.16	66.30±0.18
∑ **Monounsaturated**	7.56±0.04	10.03±0.05
∑ **Polyunsaturated**	17.78±0.11	23.67±0.15

FHMO: Fully hydrogenated microalgae oil; SO: soybean oil.

Table 2. Triacylglycerol classes (TAG) (%) of FHMO: SO for the simple (S) and interesterified blends (I).

Blends	S_3	S_2U	SU_2	U_3
70:30S	74.29±2.14%	1.89±0.66%	9.65±1.12%	14.15±0.85%
70:30I	61.93±1.56%	34.47±2.09%	2.49±0.25%	1.10±0.27%
60:40S	67.81±7.35%	1.11±0.46%	10.48±3.58%	20.88±3.58%
60:40I	50.52±0.39%	44.20±2.09%	3.30±1.71%	1.96±1.71%

Triacylglycerols: S3 (trisaturated), S2U (disaturated–monounsaturated), SU2 (monosaturated-diunsaturated), and U3 (triunsaturated). Mean between sample injection triplicates.

Table 3. Fatty acids distribution (%) at the sn-1,3 and sn-2 position on the TAG of fully hydrogenated microalgae oil (FHMO) and soybean oil (SO) for the simple (S) and interesterified blends (I) in the proportions 70:30 and 60:40 (FHMO:SO) (w/w).

Blends	sn-1,3		sn-2	
	Saturated	Unsaturated	Saturated	Unsaturated
70:30S	81,02 ± 0,72	18,98 ± 0,36	74,70 ± 0,77	25,30 ± 0,43
70:30I	80,82 ± 0,99	19,18 ± 0,34	63,06 ± 0,53	36,94 ± 0,11
60:40S	74,17 ± 0,65	25,83 ± 0,11	67,51 ± 0,44	32,49 ± 0,38
60:40I	87,77 ± 0,74	12,22 ± 0,22	59,06 ± 0,91	40,94 ± 0,33

FHMO: Fully hydrogenated microalgae oil; SO: soybean oil.

3.2. Physical characteristics of the nanoparticles

3.2.1. Melting Behavior

For the characterization of NLCs and their ability to incorporate the bioactive compounds, thermodynamic, mechanical, chemical, microscopic, spectroscopic, and chromatographic techniques are required (Demetzos, 2008).

Thermal melting analyses allows to evaluate the thermal resistance of NLCs and their ability to encapsulate fish oil in the lipid matrix. The thermal parameters studied were initial melting temperature (Ti), enthalpy (ΔH), peak temperature (Tp), and final melting temperature (Tf) during 30 days of storage at 25 °C (Table 4/Figure 1).

The storage time did not affect the thermal parameters studied, with no significant differences for the samples after 48 hours, 7, 15, or 30 days. In turn, the FHMO: SO ratio affected the melting parameters, and the NLCs with higher FHMO concentration (70:30) showed higher thermal parameters when compared to the NLCs made with the FHMO: SO ratio of 60:40. This result was expected due to the FHMO composition that has mostly saturated fatty acids (about 99.9%), and, consequently, allows the greater formation of S3 TAGs. Concerning the blends with FHMO, the large amount of stearic acid favored the formation of TAGs such as triestearin (StStSt), which is a homogeneous TAG, with a high melting point, around 73 °C, capable of conferring greater thermal resistance to the lipid system (Bertoni et al., 2021; Silva et al., 2016). These findings are in line with the triacylglycerol composition, once the chemical interesterification reduced

the amount of TAG S3 when compared to the same FHMO: SO ratios, with higher levels observed for the blend 70:30.

Table 4. Melting behavior parameters of NLCs composed by FHMO: SO (w/w) in simple and interesterified blends in the proportions 70:30 and 60:40 (w/w) for the encapsulation of fish oil during 30 days of storage at 25 °C.

NLC	48H	7D	15D	30D
			T_i (°C)	
70:30S	56.30±0.07^{aA}	54.70±0.51^{aA}	52.40±4.07^{aA}	55.25±0.68^{bA}
70:30I	41.20±0.02^{cA}	38.48±2.96^{bB}	39.05±0.87^{bB}	40.30±1.59^{bB}
60:40S	54.53±0.12^{dA}	54.18±0.70^{aA}	54.01±3.99^{aA}	53.23±1.57^{aA}
60:40I	36.73±0,69^{cA}	37.20±0.73^{bA}	39.26±3.67^{bA}	37.58±0.20^{bA}
			T_p (°C)	
70:30S	67.50±0.07^{aA}	67.52±0.23^{aA}	67.18±0.16^{aA}	67.14±0.13^{aB}
70:30I	58.40±0.02^{cA}	61.75±0.14^{cA}	60.29±0.68^{bA}	59.64±1.17^{bA}
60:40S	66.85±0.14^{dA}	66.79±0.28^{bA}	66.23±0.01^{bA}	66.39±0.07^{aB}
60:40I	59.86±0.12^{dA}	59.44±0.08^{dA}	58.33±0.06^{cA}	57.14±2.63^{bA}
			ΔH (J/g)	
70:30S	8.99±1.22^{aA}	9.96±0.55^{bA}	10.12±4.07^{aA}	8.85±0.33^{aA}
70:30I	5.02±0.01^{bA}	5.25±0.70^{bA}	10.10±2.47^{aA}	5.61±1.10^{cdA}
60:40S	7.81±0.33^{aA}	8,24±0,33^{bA}	6.40±1.73^{abcA}	6.90±0.27^{bcA}
60:40I	3.74±0.82^{bA}	5.06±0.49^{bA}	5.05±2.62^{aA}	5.36±0.32^{dA}
			T_f (°C)	
70:30S	75.09±2.21^{aA}	76.20±0.94^{aA}	73.55±0.36^{aA}	75.42±0.47^{aA}
70:30I	68.20±0.07^{bA}	67.46±0.81^{bAB}	66.02±0.68^{bB}	67.01±0.92^{bAB}
60:40S	74.90±0.27^{aA}	75.44±0.86^{aA}	72.62±2.81^{aA}	75.16±0.19^{aA}
60:40I	64.50±0.19^{cA}	66.99±1.22^{bA}	65.14±1.22^{bA}	65.57±0.60^{cA}

NLC: Nanostructured lipid carrier; S: simple; I: interesterified; T_i: initial melting temperature; T_p: peak melting temperature; T_f: final melting temperature; ΔH: peak melting enthalpy. Uppercase

letters in lines indicate the statistical differences and the lowercase letters in columns indicate the statistical differences by Tukey`s test (P<0.05); Similar letters show no statistical differences between them.

Figure 1. Melting behavior parameters of NLCs made with 60:40 and 70:30 FHMO: SO (w/w) in simple and interesterified blends with fish oil during 30 days of storage at 25 °C.

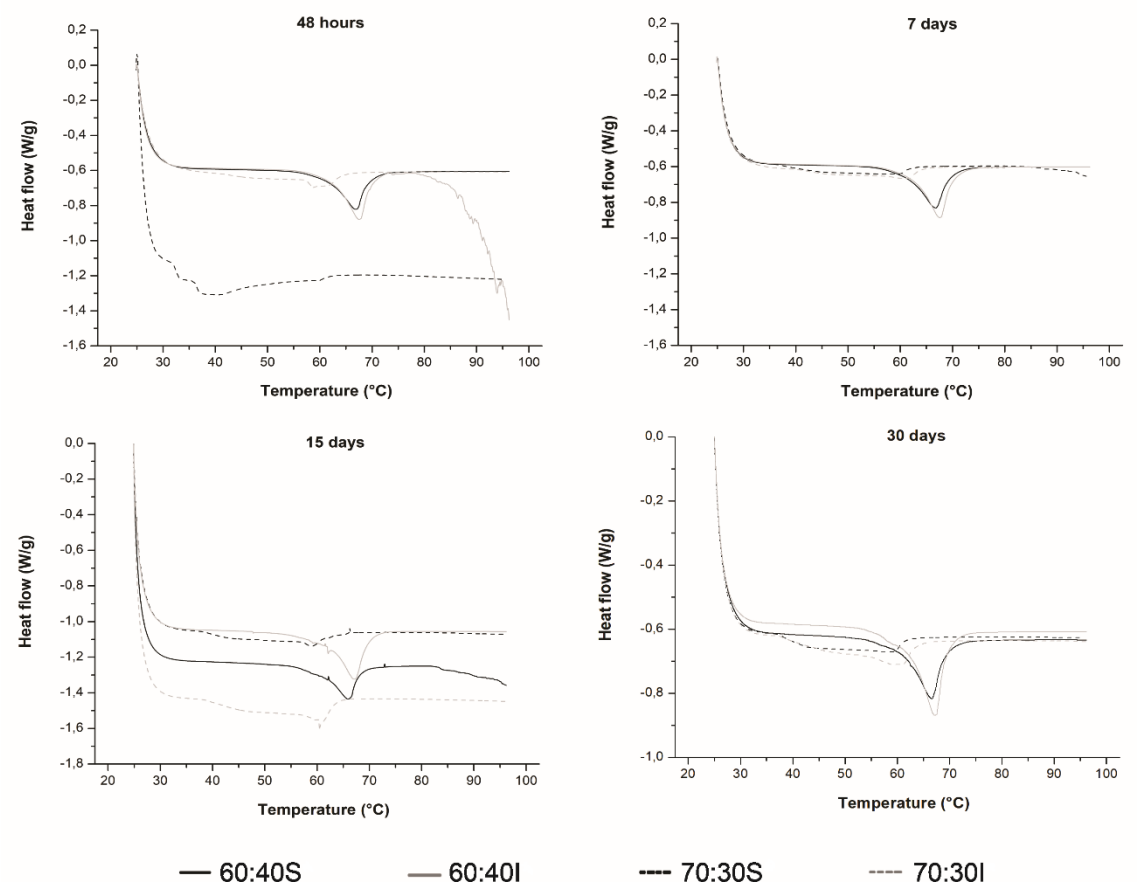

NLC: Nanostructured lipid carrier; T_i: initial melting temperature; T_p: peak melting temperature; T_f: final melting temperature; ΔH: peak melting enthalpy. Uppercase letters in lines indicate the statistical differences, and lowercase letters in columns indicate the statistical differences by Tukey`s test (P<0.05); Similar letters no show statistical differences between them.

Regarding the melting curves, they were similar when compared to the different proportions of lipid phase with similar fatty acid composition, i.e., comparing the proportions of simple blends and the interesterified fractions (Figure 1). In general, this similarity showed wider melting curves and lower height for the NLCs made with the interesterified lipid blends, which suggests an increase in liquid lipids content in the NLCs in the crystal network, which is desirable for improving the encapsulation ability, due to lower crystalline

organization or network defects within the lipid carriers. Silva et al. (2022), Wang et al. (2014), and Zheng et al. (2013) reported similar results with different raw materials, using blends of simple and interesterified oils and fats to produce NLCs. The authors reported that interesterification promoted broader melting peaks, lower melting temperatures, and lower enthalpy when compared to the NLCs made from simple blends.

Concerning the thermal parameters, the NLCs made with the lipid phase constituted by interesterified lipid matrices showed lower values when compared to the simple matrices for the same storage time and FHMO: SO ratio. This result is due to the interesterification reaction and the rearrangement of fatty acids in the glycerol molecule, increasing the levels of TAGs S2U and SU2 and decreasing S3, which modifies the physical and crystallization characteristics of the system. Importantly, despite the reduced levels of S3 TAGs after the reaction, they accelerated crystallization because they are composed of triestearin, a high melting point TAG, resulting in higher parameters for the ratio 70:30. These findings indicate that the chemical interesterification can prevent or delay the solid lipid recrystallization during the cooling process.

Similar results were reported by Godoi-Fernandes (2023c), who studied NLCs with the similar composition as those evaluated in the present study, without the addition of a bioactive compound. When comparing the results of the thermal parameters to those previously obtained by Godoi-Fernandes (2023c), the NLCs formulated from simple lipid matrices also showed higher Ti, ΔH, Tp, and Tf for all periods studied, confirming that the interesterification reaction tends to reduce the thermal resistance of the system by decreasing the proportion of S3 TAGs. However, when comparing the NLCs without the addition of the bioactive compound (GODOI-FERNANDES, 2023c) and with the addition of fish oil, no difference was observed in the thermal behavior between the matrices or as a function of storage time, with a slight perturbation of the thermal curve observed in the present study.

Lacatusu et al. (2013) evaluated the melting thermogram of NLCs loaded with fish oil as a carrier for lutein delivery. The results showed a peak located at approximately – 52 °C, considered specific for unsaturated ω-3 fatty acids, and an endothermic shoulder at approximately 45 °C corresponding to the saturated fatty acids from fish oil. Therefore, fish oil alone has quite distinct melting

parameters when compared to the lipid matrices used (FHMO and SO), besides exhibiting more than one endothermic effect. This result indicates that despite the differences in the melting curve, probably a large amount or all fish oil was trapped inside the NLCs since the difference in the thermal curve was extremely subtle, probably due to the less ordered crystalline structure caused by the presence of the bioactive compound rather than the mixture of this compound in the NLC matrix. An intense reduction of Ti, Tp, and Tf, and consequent increase of ΔH can occur when fish oil is not encapsulated, once fish oil requires a higher amount of energy to crystallize or melt due to its composition rich in polyunsaturated fatty acids (Awad et al., 2009; Ribeiro et al., 2015).

The present result highlights the importance of selecting adequate raw materials for the composition of NLCs. The nanoencapsulation with thermally resistant matrices can provide a physical barrier between the bioactive compound and adverse environmental conditions and/or food manufacturing, ensuring stability and preventing possible losses (Ye et al., 2018). In addition, the encapsulating agents must have viable characteristics for use in the food industry, such as good dissolution of the ingredients, and adequate resistance and protection properties for the formation of the nanoparticles (Ye et al., 2018).

In the present study, the combination of FHMO with TAGs of high melting point, and SO as a liquid lipid phase of high availability and low cost allowed for reaching adequate encapsulation characteristics, with the maintenance of the physical properties of NLCs even after the addition of fish oil.

As discussed earlier, the intrinsic characteristics of fish oil, rich in ω-3 fatty acids, make encapsulation a suitable alternative to protect this compound from oxidation. In addition, the important role of ω-3 as an essential fatty acid in fish oil products provides a great health appeal and a higher added value, which is increasingly demanded by consumers (Pathakoti et al., 2017).

3.2.2. Solid fat content (SFC)

The solid fat content determines the percentage of fat in a solid state at a given temperature, which can change as a function of the NLC composition and storage time (Chiu & Gioielli, 2002). The SFC analysis of fish oil containing NLCs was performed at 25 °C throughout 30 days of storage (Figure 2).

Figure 2. Solid fat content of NLCs made with 60:40 and 70:30 FHMO: SO (w/w) in simple and interesterified blends with fish oil during 30 days of storage at 25°C.

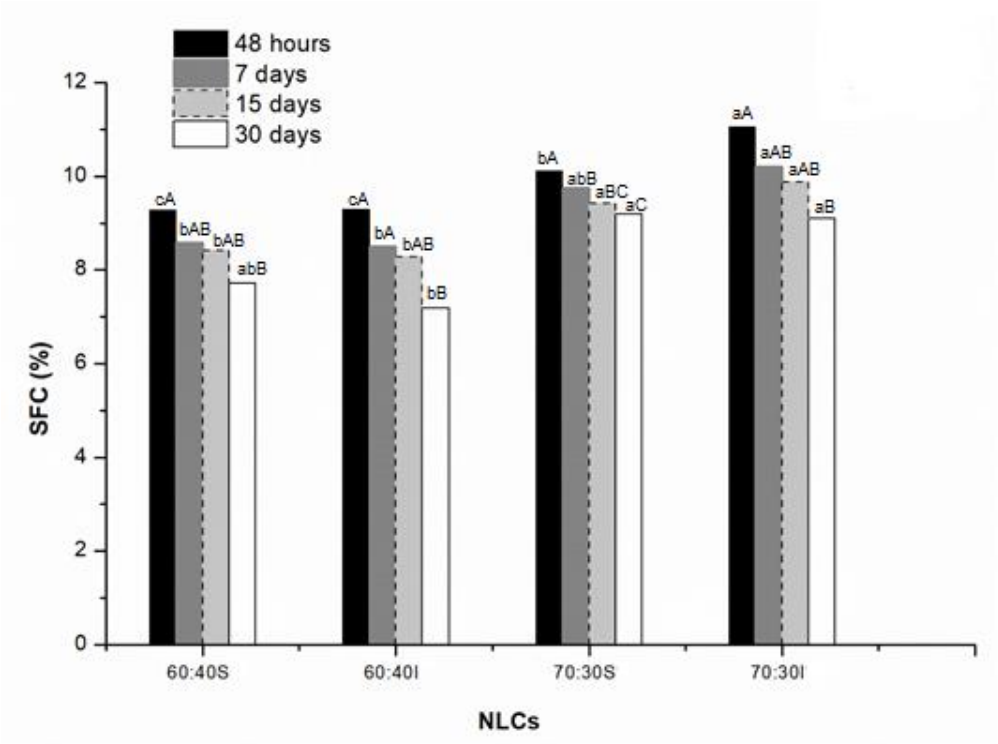

NLC: Nanostructured lipid carrier; SFC: Solid fat content; Uppercase letters indicate the statistical differences as a function of storage time, and lowercase letters indicate the statistical differences between the different samples in the same storage time by the Tukey`s test (P<0,05); Similar letters show no statistical differences between them.

In general, a decrease in SFC was observed as a function of time for all NLCs studied. When comparing NLCs made with simple and interesterified fractions, no significant difference was observed between NLCs composed of 60:30 lipid fraction before and after reaction, with a subtle difference for the NLCs made with 70:30 with higher SFC in the interesterified fraction. However, the SFC was mainly affected by the FHMO concentration, and the NLCs containing the 70:30 fraction as a lipid phase exhibited higher SFC when compared to the 60:40 NLCs, regardless of treatment. Therefore, the increase in the SFC was proportional to the amount of FHMO added. This result was expected since the inclusion and increase of fully hydrogenated oil in the simple or interesterified blends tends to increase the melting point due to its purely saturated fatty acid composition, as also observed in the thermal behavior of NLCs.

However, this result corroborates the melting behavior of NLCs, with a slight reduction in melting Ti over time for all NLCs. When comparing NLCs from simple and interesterified fractions, no difference was observed in the SFC of NLCs of the same lipid composition despite the reduction in melting behavior parameters. This may be related to the ability of high melting point TAGs, present in a majority form as S3 TAGs, mainly StStSt, to induce crystallization during cooling to 5°C and subsequent holding at 25°C since StStSt has fast crystallization and high melting point.

Silva et al. (2016) studied pure compounds and reported that StStSt took about 37 seconds to start crystal formation after cooling, with the first crystal at 53 °C. This high crystallization rate favors the formation of a larger number of crystals soon after cooling, usually in the physically unstable α-polymorphic form that is susceptible to melting or polymorphic transition over storage. This behavior was similar to the present study, in which induction of crystallization was observed during cooling mainly correlated to the FHMO concentration, which ensures high StStSt levels even after interesterification. Higher SFC was observed for NLCs 70:30I (11.06±0.25%) and 70:30S (10.12±0.05%), while lower SFC was observed for NLCs 60:40S (9.28±0.05%) and 60:40I (9.29±0.35%) immediately after the 48 hours of onset crystallization (24h/5°C and 24h/25°C).

Over time, the subtle reduction of SFC may be due to a possible dissolution of more unstable crystals, α type, which merged after temperature elevation and maintenance of NLCs at 25 °C, as well as the stabilization of the remaining crystals in more stable polymorphic forms, β and β'. This behavior is due to the use of liquid and solid lipids at storage temperature (25 °C) and the incorporation of hydrophobic compounds, which leads to imperfect crystallization and facilitates the incorporation of bioactive ingredients into the amorphous phase with more space for the compound and crystallization of the system (Katouzian et al., 2017).

These findings were similar to those reported by Godoi-Fernandes et al. (2023c) until the first 7 days of storage at 25 °C. The authors reported a decrease in SFC of NLCs made from blends with the same raw materials in simple and interesterified forms in 90:10, 80:20, 70:30, and 60:40 (w/w) FHMO: SO ratios until the 7th day of storage, with subsequent stabilization for up to 60 days at 25 °C. However, the SFC stabilization and reduction of the NLCs of the present study

containing fish oil as a bioactive compound may be due to the more intense disorganization of the system, promoted by the highly polyunsaturated compound, with reduced melting point (Ti approximately -77°C and Tf approximately -8°C), as observed in the melting behavior. In turn, the gradual decrease of SFC over time, which was not observed in NLCs without the addition of the compound after 7 days, may indicate incompatibility between the lipid matrices since significant differences were observed for the chemical and spatial structure (SO and FHMO blends with high saturated fatty acids and S3 TAGs), in addition to the high melting point (~ 70°C for 60:40S and 70:30S, and 65°C for 60:40I and 70:30I). In contrast, fish oil had high contents of unsaturated fatty acids and U3) and very low melting point.

3.3. Characterization of the nanoparticles

3.3.1. Droplet size, size distribution, polydispersity index, and zeta potential

The particle size and distribution of the nanoparticles can affect their properties and stability during storage. The average surface area (D3,2) and the polydispersity index (SPAN) are shown in Table 5.

According to D3,2, soon after the production (48h), only the NLC with lipid phase 60:40S was significantly smaller (366±0.04nm) than the other proportions. At 7 days, both NLC made with the 60:40S (359±0.04nm) and 60:40I (371±0.05nm) showed lower D3,2 when compared to the 70:30S (386±0.14nm) and 70:30I (394±0.03nm). At 15 days, different behavior was observed for all NLCs, with the 60:40S resulting in lower D3,2 (344±0.01nm), followed by 60:40I (365±0.01nm), 70:30S (373±0.02nm), and 70:30I (387±0.02nm). Finally, at 30 days of storage, the NLC with 60:40I (340±0.02nm) showed the lowest D3,2. These results indicate a greater effect of the saturated fatty acid contents and predominance of S3 TAGs on the parameter D3,2 rather than the interesterification reaction. This event became noticeable when comparing the ratio 60:40, which exhibited D3,2 significantly lower than the fraction 70:30 regardless of the occurrence of the interesterification reaction, which was also observed by Silva et al. (2022).

Table 5. Mean surface diameter (D 3,2) and polydispersity index (SPAN) of NLCs composed by 60:40 and 70:30 FHMO: SO (w/w) in simple and interesterified blends with fish oil during 30 days of storage at 25 °C.

NLC	48 horas	7 dias	15 dias	30 dias
		$D_{3,2}$(nm)		
60:40S	366±0.04bA	359±0.04cA	344±0.01dB	340±0.02cB
60:40I	388±0.03aA	371±0.05bcB	365±0.01cB	359±0.02abC
70:30S	393±0.06aA	386±0.14abAB	373±0.02bAB	369±0.010aB
70:30I	385±0.04aA	394±0.03aA	387±0.02aA	354±0.05bcB
		Polidispersity index (SPAN)		
60:40S	1.692±0.017 bA	1.639±0.09cB	1.560±0.05cB	1.528±0.011cC
60:40I	1.860±0.021aA	1.737±0.012bB	1.756±0.011aB	1.734±0.014aB
70:30S	1.778±0.053aA	1.727±0.041bAB	1.633±0.021bB	1.682±0.026bB
70:30I	1.808±0.027aAB	1.856±2.762aA	1.754±0.027aB	1.555±0.024cC

NLC: Nanostructured lipid carrier; S: simple blend; I: interesterified blend; FHMO: Fully hydrogenated microalgae oil; SO: Soybean oil. Uppercase letters indicate statistical differences as a function of the time of storage of the same sample; lowercase letters indicate statistical differences between different samples for the same time of storage by the Tukey's test (P<0,05); Similar letters show no statistical differences between them.

The higher D3,2 in NLCs with higher FHMO concentrations may be associated with the formation of a more viscous lipid phase due to the higher amount of saturated fraction (FHMO), capable of increasing the surface tension and generating larger particle size (Pinto et al., 2018). In addition, the increased melting point associated with FHMO in lipid blends can reduce the homogenization efficiency, resulting in larger particle size (Elmowafy et al., 2017)

There was a gradual decrease in D3,2 as a function of time for all NLCs when compared to the results immediately after the manufacture and at the end of the storage period (30 days). A reduction of D3,2 from 366±0.04 to 340±0.02, 388±0.03 to 359±0.02, 393±0.06 to 369±0.05, and 385±0.04 to 354±0.05 nm was observed for the NLCs 60:40S, 60:40I, 70:30S, and 70:30I, respectively. Silva et al.(2022) and Santos et al. (2019) studied the encapsulation of phytosterols and reported a similar reduction, probably due to a synergistic effect between the encapsulated compound and the emulsifier at the oil-water interface. This effect may be similar to that observed in the present study. Godoi-Fernandes et al. (2023c) evaluating NLCs with similar lipid composition, without the addition

of the bioactive compound, reported an absolute value of D3,2 inversely proportional to the FHMO concentration, with slightly smaller dimensions (approximately 200 nm) than those observed in the present study.

In contrast, considering only the lipid fraction, Godoi-Fernandes et al. (2023b) reported that FHMO: SO blends tend to transition to a more stable polymorphic form over time. In the simple fractions, there was an appearance of polymorphic β-type forms soon after rapid crystallization (24h/5 °C and 24h/25 °C) while a crystallization into the polymorphic β' form was observed for the interesterified fractions, with concomitance of polymorphic β' and β forms after 7 days of storage at 25 °C. For all cases, these polymorphic forms remained until the end of the storage, day 60. This polymorphic rearrangement to the most stable form over time is due to the triacylglycerol composition of the blends before and after randomization. The high FHMO concentration resulted in approximately 74 and 67% S3 TAGs, respectively, for the 70:30 and 60:40 ratios before randomization, with a slight reduction after the reaction, reaching 62 and 50%. Despite this result, a predominance of S3 TAGs was observed in the lipid fraction for both treatments. Therefore, the TAG S3 found in a majority form provides the stabilization of the polymorphic form to the more ordered form, allowing the system to become more compact, which may have led to the reduction of D3,2 over time.

The polydispersity index (SPAN) is also a very important parameter for evaluating the particle size distribution at the nanoscale, and the lower the value, the greater the homogeneity of the particle diameter of the system (Liu & Wu, 2010). In this sense, it is possible to directly correlate the SPAN value with D3,2, with a decrease in particle size and SPAN over the storage, indicating that the reduction in D3,2 led to greater homogenization of the system, favoring the physical stability.

Regarding the addition of the bioactive compound, Li et al. (2020) observed that the addition of fish oil to NLCs above 1.5% can significantly increase the particle size and SPAN, indicating insufficient wall material for encapsulation/coating, or adhesion of fish oil to the surface of the NLCs. When the addition of fish oil is below 1%, there is no increase in particle size, which may be an indication of proper encapsulation. Thus, the encapsulation efficiency should be evaluated in the present study because we observed a slight increase

in D3,2 for the NLCs with fish oil. However, the particle size range was in agreement with Ghorbanzade et al. (2017), who reported a small particle size range (300-500 nm) with distribution considered uniform for NLCs containing fish oil.

Previous studies have shown that the addition of fish oil was associated with increased particle size when compared to NLCs without the bioactive compound. In those studies, the size of the NLCs increased proportionally to the oil addition, possibly due to the difference in viscosity of the system caused by the fish oil (Mohammadi et al., 2017)

In the present study, NLCs with fish oil obtained from interesterified lipid fractions were higher than those made with simple fractions during the period studied (30 days) (Table 5). Concerning the FHMO concentration, a lower SPAN value was observed for NLCs made with the simple lipid fraction. Therefore, the higher D3,2 of NLCs from interesterified blends suggests a higher particle size diversity, which may be due to the distribution of TAGs after randomization since the reaction reduced TAG S3 and U3, and increased TAG S2U. This effect led to a higher content of TAG with an intermediate melting point (S2U), which guides the polymorphic form towards β'. Moreover, these contents remained majority after randomization due to the composition of FHMO almost entirely of saturated fatty acids and StStSt TAGs, leading to the concomitant appearance of β- and β' type crystals, which may affect the organization of the NLC system and confer greater variability in particle size.

A reduction of D3,2 and SPAN values was observed as a function of time, i.e., the reduction in particle diameter over time, demonstrated by D3,2, led to a lower size diversity of the NLCs in the suspension, which was also observed by Godoi-Fernandes (2023c) in NLC without the addition of the bioactive compound. Similarly, Queirós et al. (2020) evaluated the stability of nanoemulsions at 25 °C for 60 days and also reported that the composition of the nanoemulsion affected the mean particle diameter and SPAN, with no differences during the storage.

Although the production of NLCs with smaller particle sizes ensures greater gastrointestinal absorption and stability, it may also be associated with a greater tendency to destabilization and aggregation. In this context, the method of obtaining NLCs by high-pressure homogenization, as well as the number of cycles and the raw materials used (FHMO and SO) allowed for obtaining

appropriate particle diameters, which were smaller than those reported by other authors (up to 500 nm), but slightly above the dimensions required for a greater intestinal absorption (Salvia-Trujillo et al., 2021). Small nanoparticles (<200 nm) tend to remain longer in the gastrointestinal tract due to their greater solubility and reactivity, which may favor the absorption of the encapsulated compound (Jun-Xia et al., 2011). Thus, the NLCs of the present study may have their gastrointestinal absorption impaired due to the larger particle diameter, which can be further evaluated in digestibility trials.

Zeta potential (ZP) provides information about the emulsion stability, and the higher the ZP (in a module), the lower the tendency of particle aggregation. It is noteworthy that a zeta potential value of ± 30 mV is considered sufficient to provide stability to the nanoemulsion, while values around 60 mV are considered optimal (Mohammadi et al., 2017; Shah et al., 2015).

The NLCs of the present study showed ample and adequate stability, with values ranging from -53 to -48 mV after 48 hours of storage, and a slight reduction over time (Figure 3). When comparing the different fractions used to produce the NLCs, the fractions 60:40I (-53.4±2.17mV) and 70:30S (-53.66±1.74mV) showed the highest zeta potential values after 48 hours, with no significant differences, while lower ZP values were observed for the fractions 60:40S (48.1±1.98mv) and 70:30I (50.66±1.79mV). At 7 days, only the NLC 60:40I showed a significantly higher value (49.3±1.53mV). At 15 days, this characteristic remained for the fractions 60:40I (42.6±0.43mV) and 70:30S (43.63±1.53mV) with higher stability when compared to the others, with no differences among NLCs at 30 days of storage. Therefore, no tendency was observed between NLCs produced with simple and interesterified lipid fractions, and the 60:40S and 70:30I NLCs were more stable over time. However, it is known that the raw materials used to produce the NLC can affect the zeta potential, which is mainly impaired by the use of some emulsifiers (Hashemi et al., 2020).

Figure 3. Zeta potential of NLCs composed by 60:40 and 70:30 FHMO: SO (w/w) in simple and interesterified blends with fish oil during 30 days of storage at 25 °C.

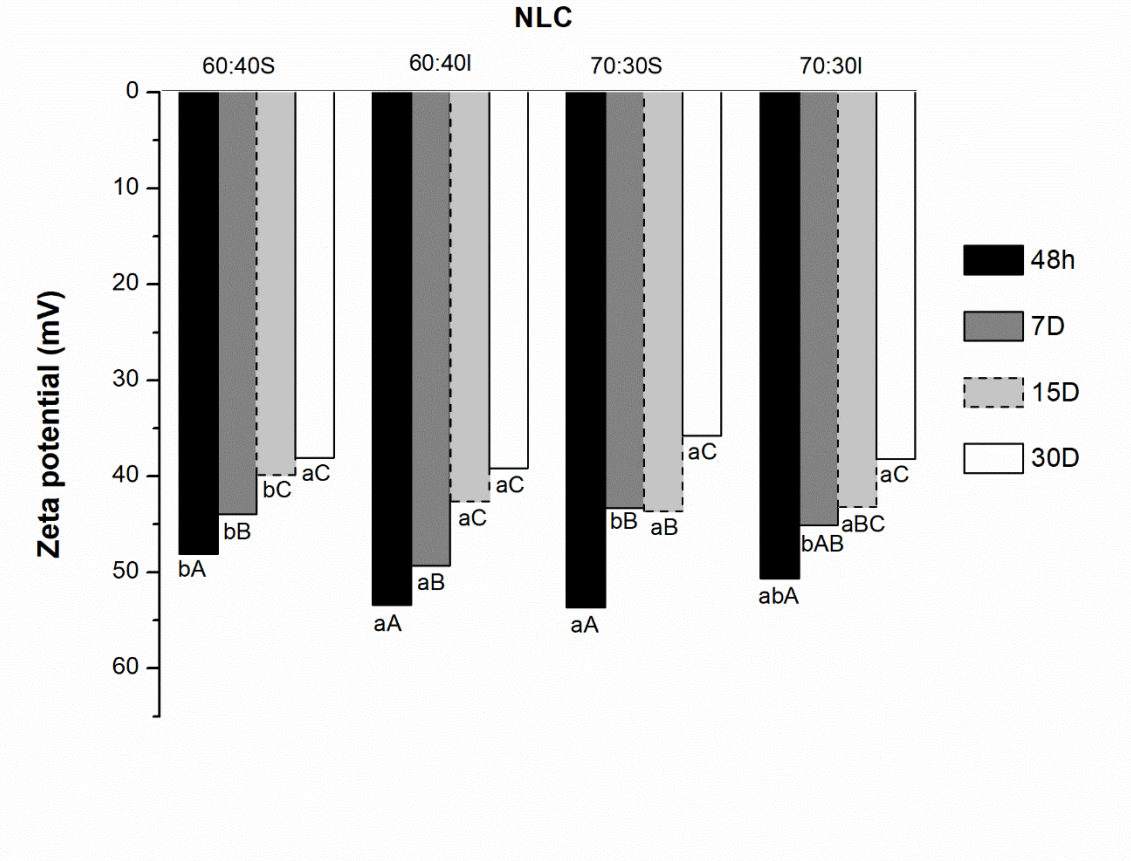

NLC: Nanostructured lipid carrier; S: simple blend; I: interesterified blend. Uppercase letters indicate statistical differences as a function of the time of storage of the same sample; lowercase letters indicate statistical differences between different samples for the same time of storage by the Tukey's test (P<0,05); Similar letters show no statistical differences between them.

The use of non-ionic emulsifiers is preferred for the production of NLCs due to their amphipathic characteristic and the formation of stable micelles in an aqueous medium. In turn, soy lecithin consists of a complex mixture of essentially hydrophobic phospholipids (HLB = 8), thus it is adequate for NLC stabilization only when combined with other emulsifiers (Vieira et al., 2020). However, the enzymatically modified soy lecithin used in this study has a higher amount of lysophosphatidylcholine, which makes it more hydrophilic and contributes directly to the characteristics of the nanoemulsion, and is associated with greater particle size and physical stability (McClements, 2004). For the zeta potential, negative charges were observed, probably due to the adsorption of OH species from water to the nanoemulsion interface, and the increase in the intensity of the parameter, possibly due to the steric repulsion of the emulsifier molecules, which is affected

by the ionic strength of the continuous phase and charge density on the water/oil surface. Therefore, the use of the more hydrophilic lecithin may favor the production of more stable NLCs, once it is an emulsion composed of a 90% aqueous phase (Artigas et al., 2018; Hashemi et al., 2020).

Other authors have also used soy lecithin and reported positive results in stabilizing NLCs, with a reduction of crystallization of the system and increased physical stability. The use of soy lectin has also protection advantages since studies have shown an antioxidant effect of lecithin, which is a poorly elucidated mechanism, besides being an ingredient of natural origin (Deng, 2021; Salminen et al., 2016; Thrandur et al., 2009).

When comparing the NLCs with encapsulated fish oil of the present study and the nanoparticles without the encapsulated fish oil evaluated by Godoi-Fernandes et al. (2023c), higher zeta potential was observed for the NLCs with the bioactive compound. This result indicates that, despite the higher particle size, there is greater stability over time and particle dispersion regardless of the lipid phase used in the NLC. This behavior may favor the supply of fish oil in nanoencapsulation form using the carriers of this study.

In general, despite the reduction of zeta potential over storage for all NLCs, the ZP values were always higher than 30mV. The negative charge was due to the use of enzymatically modified soy lecithin, which provides greater physical stability, and no clear tendency was observed for the randomization or the saturated fatty acids content present in the NLCs.

3.3.2. Physical stability by Turbiscan

Nanoemulsions are complex systems with stable physical characteristics, thus preventing the destabilization of the system. The turbidimetric analysis is used to evaluate the emulsion stability and destabilization effects. Light backscattering allows identify the destabilization phenomena such as migration (creaming and sedimentation) and/or particle aggregation (coalescence, flocculation) (Kang et al., 2012; Shah et al., 2015).

The backscattering profile of the NLCs of the present study showed that all NLCs loaded with fish oil showed destabilization as sedimentation, creaming, coalescence, or flocculation at 7 days of storage, which intensified over time (Figure 4).

Figure 4. Variation in the backscattering profile (BS) of NLCs with fish oil composed by 60:40 and 70:30 FHMO: SO (w/w) in simple and interesterified blends during 30 days of storage at 25°C.

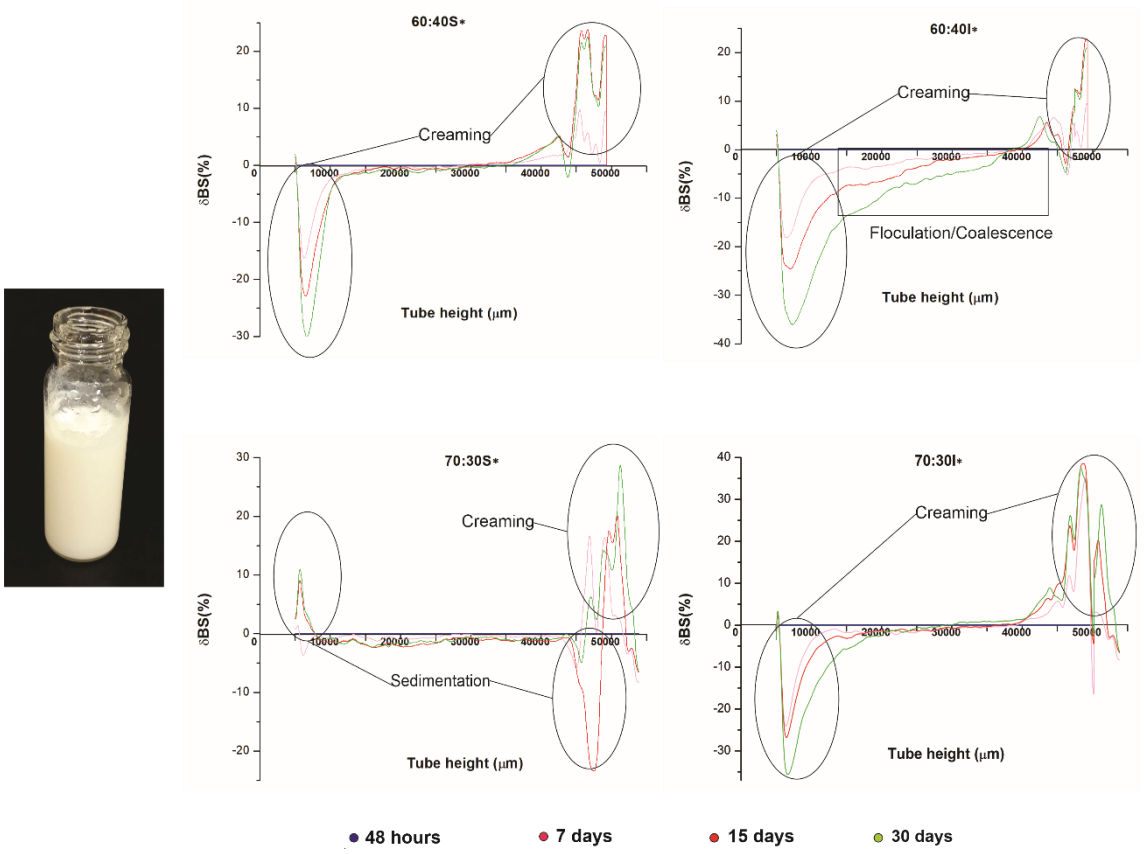

FHMO: Fully hydrogenated microalgae oil, SO: soybean oil, NLCs: Nanostructured lipid carriers; S: Simple; I: Interesterified.

The NLCs with interesterified blends (60:40I and 70:30I) presented the creaming phenomenon from 7 days of storage, while the fraction 60:40I presented concomitant flocculation and coalescence of the particles. In turn, the NLCs produced with simple blends (60:40S and 70:30S) as a lipid phase presented sedimentation over the storage time, besides the creaming phenomenon.

Creaming and sedimentation are caused by particle migration due to changes in density, while flocculation and coalescence are related to the changes in the diameter/ size of the droplets. Creaming was observed for all NLCs, occurring when the dispersed phase is less dense than the continuous phase, causing greater backscattering variations at the top of the measuring cell. In turn, sedimentation occurs with the migration of particles to the bottom of the measuring cell (Marhamati et al., 2021; McClements, 2004). These destabilization effects are directly related to the particle size parameters (D3,2). NLCs made with the fraction 60:40 were always larger when compared to the 70:30 NLCs. The 70:30S NLCs, in addition to creaming, also presented sedimentation, with deposition of the denser particles at the bottom of the measuring cell, while all the others presented creaming. This result may be due to the higher density of the 70:30S NLCs since it has a higher content of saturated fatty acids, which is associated with higher viscosity of the system.

Regarding the interesterification reactions, no effect of randomization was observed in D3,2, which affected the physical stability via Turbiscan, especially for the NLC with the 60:40I lipid phase, which exhibited flocculation and coalescence in addition to creaming. These effects are characterized by particle aggregation. Flocculation provides no destruction of individual particles, while coalescence corresponds to the complete melting of particles turning into a single, larger droplet (Nazarzadeh et al., 2013). Thus, in addition to the difference in density due to particle size, particle distribution is also of paramount importance. In this sense, the smaller the SPAN value, the more homogeneous the particle size distribution. The NLCs made with interesterified fractions exhibited higher SPAN values, which indicates a diversity of particle size and greater ease of flocculation and coalescence since smaller particles aggregate more easily to larger ones. This effect was not observed for the NLC with the fraction 70:30I, possibly due to the saturated fatty acid contents rather than the interesterification reaction, thus preventing the occurrence of other destabilizing events in the system.

One of the most important aspects to ensure the release of the bioactive compound is the maintenance of the physical structure of the NLC. A stable structure is achieved by forming a mechanical barrier between the oil droplets and the aqueous phase through the emulsifier and the electrostatic repulsion

forces between the NLCs (Marhamati et al., 2021). However, these forces decrease over time, which leads to intermediate instability scenarios before the complete separation of the aqueous and oil phases. Flocculation is characterized by the approximation of droplets and takes place when the attraction forces are greater than the repulsion forces; creaming and sedimentation occur purely due to the action of gravitational forces that make the particles move, while coalescence leads to the union of particles until the complete separation of the oil and water phases. Flocculation, creaming, and sedimentation are reversible events since agitation can recover the suspension by spreading the NLCs that have moved to the surface or bottom of the measuring cell. Therefore, although they are considered destabilization phenomena, each effect can have distinct consequences on the final product and compound release, and coalescence is the most worrisome instability process, as it may lead to the destruction of the emulsion (Bruxel et al., 2012; Tadros et al., 2004).

As reported by Godoi-Fernandes et al. (2023c), similar instability phenomena were observed in the NLCs produced without the addition of a bioactive compound, thus there is no effect of fish oil on the destabilization of the nanoemulsions.

The combined instability effect, as observed by light backscattering analysis, can also be evaluated by TSI (Turbiscan Stability Index), which provides the destabilization kinetics of the emulsions when subjected to light backscattering. Turbiscan values can range from 0 to 100, where 0 represents highly stable emulsions and 100 corresponds to highly unstable emulsions. Therefore, the higher the TSI value, the greater the destabilization of the nanoemulsion (Teng et al., 2019; Xu et al., 2013).

Opposite to that reported by Godoi-Fernandes (2023c), who observed no destabilization in NLCs made with the same lipid base without the bioactive compound, the present study showed that the fish oil-based NLCs exhibited a higher propensity to destabilize when the lipid phase was composed of interesterified bases, with no significant difference for the different FHMO ratios.

This effect may be due to the reaction towards the less stable polymorphic form β', caused by the interesterification, which may have intensified with the addition of the bioactive compound. This event contributes to the greater structural disorganization of the system, due to the low melting point and

preferential β' polymorphism. Fish oil has a low melting point, impairing the formation of crystals to the most stable form, the β' type, which may favor the structural disorganization of NLCs.

Figure 5. TSI (Turbiscan Stability Index) curves of NLCs with fish oil composed by 60:40 and 70:30 FHMO: SO (w/w) in simple and interesterified blends during 30 days of storage at 25 °C.

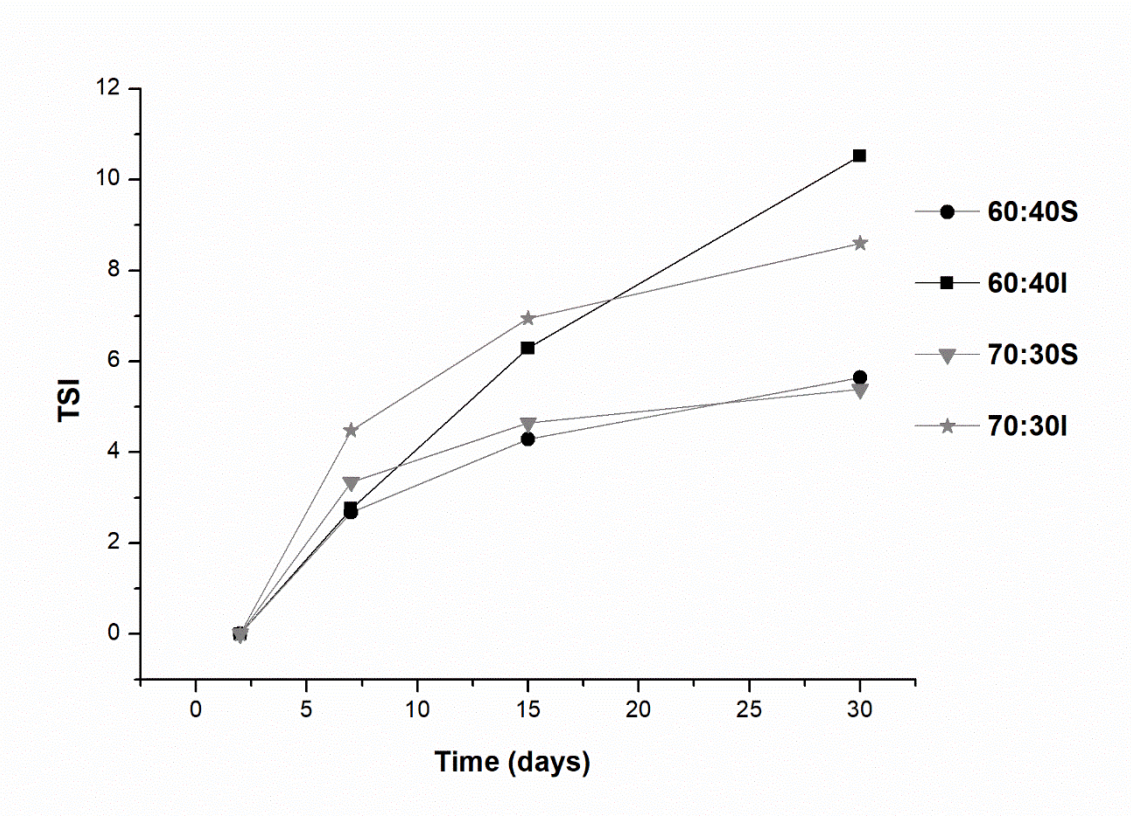

FHMO: Fully hydrogenated microalgae oil, SO: soybean oil, NLCs: Nanostructured lipid carriers; S: Simple; I: Interesterified.

For both cases, with or without the addition of fish oil, the destabilization phenomena may be due to the processing conditions to produce the NLCs, such as the number of cycles, high pressure, and high temperature, as well as the particle size and viscosity of the system.

Yuan et al. (2008) found that the emulsion stability decreases with increasing homogenization temperature and pressure, with a more pronounced destabilization above 70 °C, pressure close to 1000 bar, and application of more than 3 homogenization cycles. Probably, the increase in pressure, number of cycles, and temperature can favor the formation of a larger number of small

particles, more susceptible to collision and agglomeration. In the present study, there was no reduction in particle size despite the higher destabilization of the nanoemulsions over time.

According to the TSI parameter, the NLCs produced with the simple fractions 70:30S and 60:40S were the most stable nanoparticles. After 15 days, the difference in stability between NLCs with simple and interesterified fractions was greater, indicating a greater destabilization of NLCs, which was also observed by Silva et al. (2022). In the present study, the turbidimetric results were compared with the other parameters of the colloidal system, such as particle size, particle size distribution, and zeta potential.

The particle size of the NLCs made with interesterified blends presented higher D3,2, characterized by larger dimensions. Regarding the particle size distribution, higher SPAN values were observed for the interesterified blends, which indicates greater size heterogeneity. Concerning the zeta potential, similar ZP values ($p<0.05$) were observed for all NLCs. Thus, the NLC made with the 60:40I lipid phase presented the highest instability, as shown in the TSI, and flocculation/coalescence. This behavior was confirmed by other determinations, once the larger particle size and the heterogeneity of particle size distribution led to a greater destabilization of the final dispersion.

3.3.3 Encapsulation efficiency (EE)

Encapsulation efficiency (EE) is a very important parameter once it shows the amount of encapsulated material inside the NLCs, confirming the results of the thermal and physical analysis of the NLCs (Ghorbanzade et al., 2017). To ensure adequate intake and desired effect of the encapsulated compound, a sufficiently high concentration of the bioactive compound is required for an effective encapsulation (Tamjidi et al., 2013).

In the present study, a high and satisfactory EE was observed for the NLCs for all periods studied, regardless of the lipid phase used, ranging from 82.45±9.66 to 100% EE, i.e., at least 82% of fish oil was incorporated into the NLCs (Table 6). This high incorporation capacity of the NLCs may be due to the high compatibility between the wall materials, the encapsulated compound (lipophilic), and its low melting point, which does not affect a more intense crystallization.

Moreover, despite a small decrease in EE over time, this parameter was always above 80%, characterizing optimal encapsulation capacity.

Table 6. Encapsulation efficiency (EE) of NLCs composed by 60:40 and 70:30 FHMO: SO (w/w) in simple and interesterified blends with fish oil during 30 days of storage at 25°C.

	EE (%)				
NLC	**48 hours**	**7 days**	**15 days**	**30 days**	**Δ30 days**
60:40S	100,00±7,57aA	100,00±14,98aA	100,00±8,00aA	90,78±4,28aB	9.52
60:40I	100,00±2,94aA	100,00±0,12aA	99,96±10,28aA	82,45±9,66bB	17.55
70:30S	100,00±21,75aA	100,00±3,53aA	100,00±35,73aA	85,82±5,39abB	14.18
70:30I	93,90±2,61aA	95,06±10,55aA	96,66±27,17aA	89,03±4,36abB	4.18

NLC: Nanostructured lipid carrier; S: simple blend; I: interesterified blend; FHMO: Fully hydrogenated microalgae oil; SO: Soybean oil. Uppercase letters indicate statistical differences as a function of the time of storage of the same sample; lowercase letters indicate statistical differences between different samples for the same time of storage by the Tukey's test (P<0,05); Similar letters show no statistical differences between them.

Park et al. (2017) reported that besides the composition and affinity between the wall material and the bioactive compound, the EE was inversely proportional to the amount of bioactive used. A concentration of 30 mg/mL of vitamin D3 resulted in the highest EE (85.6%) while 100 mg/mL led to a lower EE (68.3%). Despite the efficiency of 60%, the authors considered the matrix effective for constituting the NLC, with an effective encapsulation of vitamin D3.

Similarly to the present study, Ghorbanzade et al. (2017) also studied the encapsulation of fish oil and reported high EE with sunflower oil and soy lecithin nano-liposomes, reaching 92.2%, probably due to the affinity of the materials used for the production of the encapsulating structures.

Concerning the SLNs, high EE values are difficult to reach because the lipid matrices with high melting points and extremely organized crystal structures provide little space for the entrapment of bioactive compounds, and a greater propensity to polymorphic transitions, leading to the compound release, especially during storage. The present study used blends of liquid vegetable oils and fully hydrogenated vegetable oils (solids), thus the crystal structure remained

sufficiently disorganized to minimize the release of fish oil from NLCs up to 30 days of storage. Furthermore, it is worth noting that this study used lipid matrices of food grade, and about 92% of the saturated fatty acids from FHMO correspond to stearic acid, which has a neutral atherogenic effect (Foster, 2004; O'Brien, 2009). When comparing NLCs and nanostructures made with synthetic materials, the use of conventional lipids common to human food may favor alignment with food regulations and lower production costs.

In general, storage time was the main variable that affected the EE of NLCs. The NLC made with the lipid fraction 60:40I exhibited the higher loss of bioactive compound, followed by the NLCs 70:30S, 60:40S, and 70:30I. Therefore, no clear impact of saturated fatty acid content and randomization on this parameter was observed. Considering the NLC with the lower EE, formulation 70:30I was the most stable for all periods studied. Thus, the interesterification reaction may provide the polymorphic form of the FHMO: SO blends to the most unstable form β', maintaining the system more disorganized and favoring the incorporation of fish oil into the NLC. The analysis of the bulk phase performed by Godoi-Fernandes et al. (2023a) showed that the interesterification reaction favored the formation of β' crystals, with no major impacts on the EE.

An important aspect of this study is the effect of the bioactive compound used for encapsulation. Godoi-Fernandes et al. (2023c) studied NLCs consisting of FHMO: SO in single and randomized fractions and reported that the use of lower FHMO concentrations and the interesterification reaction led to greater stability of the NLCs with delayed instability during storage at 25 °C. However, a different pattern was observed after the incorporation of fish oil into the NLC. Fish oil is an amorphous, liquid compound at storage temperature, thus it may adjust more easily to the structure of the NLC, favoring its incorporation into both simple and interesterified lipid matrices. Silva et al. (2022) investigated the incorporation of free phytosterols, which have high crystallinity and melting point, and found that the use of interesterified lipid matrices favored the solubility and maintenance of phytosterol in NLCs, providing lower release over time, with EE values reaching up to 75%.

Studies have shown that the content of liquid oil used for the encapsulation of bioactive compounds is the main factor that can affect the process. Pinto et al. (2018) evaluated the encapsulation of α tocopherol into NLCs made with pure

fatty acids (lauric, myristic, palmitic, and stearic) and oils from different sources and ratios. The authors reported that the higher concentrations of liquid oils led to a reduction of the particle size, and an increase in EE, reaching 97%. In the present study, this effect was not evident due to the lower concentration of liquid oil used (30 or 40% of lipid phase).

However, the encapsulation of liquid ingredients, such as fish oil, may favor higher incorporation, regardless of the characteristics of the NLCs. However, high melting point bioactive compounds, such as phytosterols, may have a favored encapsulation in more disorganized systems, with a greater effect of the interesterification reaction on the lipid phase of NLC, favoring a proper encapsulation.

3.3.1. Oxidative state

The fish oil used in the present study is highly susceptible to lipid oxidation due to its mostly polyunsaturated composition. The incorporation of fish oils into NLCs allows protect them from oxidation and promotes greater acceptability of the products. The encapsulation provides a lower sensory rejection due to unpleasant flavor or odor (Giorgio et al., 2019).

The peroxide value (PV) was determined to investigate how the addition of fish oil influenced the oxidative stability of the nanoemulsions. Lipid peroxidation is the chain of reactions of oxidative degradation of lipids, thus the peroxide value can provide information about the onset of deterioration or rancidity in the lipid fractions used as wall material in the nanoemulsions, as well as the encapsulation efficiency and the protection of the fish oil. In the present study, the NLCs were kept in amber flasks at 25 °C during the period of analysis.

As expected, the peroxide value increased during storage. Probably, the exposure of the lipid phase, considering the wall materials and the lipophilic bioactive compound, to high temperature during melting, incorporation, and production of the nanoemulsion by hot high-pressure homogenization may have favored the increase in the peroxide values in the first 48 hours of study. This effect may be greater for the interesterified matrices since there is the exposure of these matrices to high temperatures during the chemical interesterification, which takes place at 90 °C (Figure 7). However, the gradual increase of the

peroxide value over time may be due to the continuation of the chain reaction mechanism, typical of lipid oxidation. No significant differences were observed for the NLCs with similar composition, with and without the addition of fish oil. Furthermore, there was no significant difference when comparing the interesterified lipid fractions and the simple fractions or the different FHMO: SO ratios.

Figure 6. Peroxide value of NLCs with and without fish oil made with 60:40 and 70:30 FHMO: SO (w/w) in simple and interesterified blends during 30 days of storage at 25 °C.

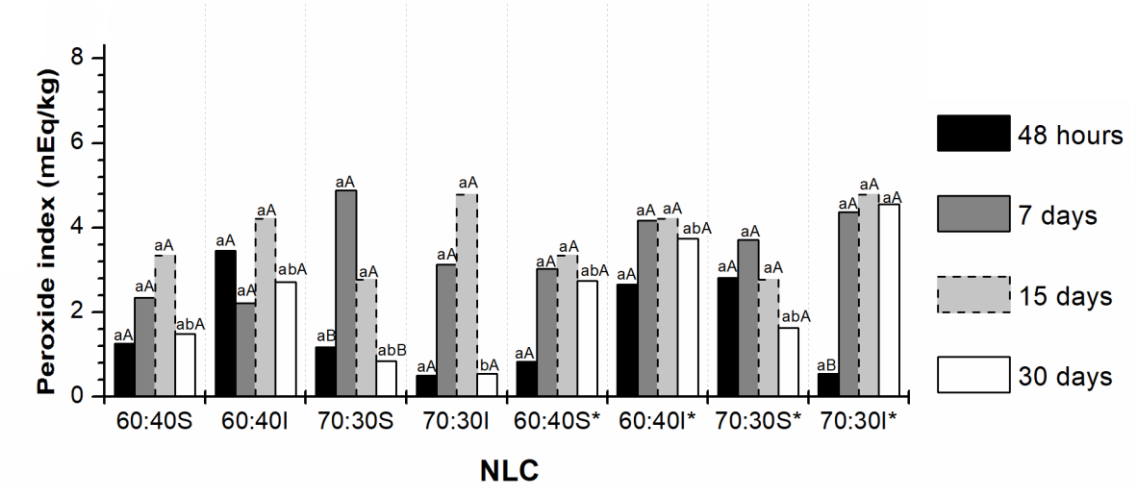

FHMO: Fully hydrogenated microalgae oil, SO: soybean oil, NLCs: Nanostructured lipid carriers; S: Simple; I: Interesterified; *: fish oil included. Uppercase letters indicate statistical differences as a function of time of storage for the same sample; lowercase letters indicate statistical differences between different samples for the same time of storage by the Tukey's test (P<0,05); Similar letters show no statistical differences between them.

The present results corroborate the EE values, with 100% of fish oil encapsulated in the NLCs with 60:40S, 60:40I, and 70:30S, while 93% of EE was observed for the NLC with 70:30I until 15 days of storage. The peroxide values showed an effective fish oil encapsulation, once the high susceptibility of the compound to oxidation may result in an expressive increase in PV when compared to NLCs without the bioactive compound.

According to the Codex Alimentarius, the peroxide value is considered a quality index and a regulatory parameter in the legislation of several countries, and the limit set by the Codex Alimentarius for refined edible oils is 10 mEq O2/kg (Stan, 2001). PV provides information about the processing conditions of vegetable oils, including the extraction and refining processes, as well as the

storage conditions. In the present study, no PV higher than 10mEq O2/kg was observed for the NLCs, thus they are considered suitable for use directly in food products. Concerning the application perspectives, food systems that allow the incorporation of NLCs, including dairy products, beverages, and others, can act as protectors of both NLCs and encapsulated fish oils.

4. Conclusion

Fish oil was effectively encapsulated in a nanostructured lipid carrier made with a lipid phase composed of fully hydrogenated microalgae oil and soybean oil in simple and interesterified blends. The FHMO concentration contributed to a high content of saturated fatty acids in the blends, and the majority presence of TAG S3 (mainly StStSt) before and after the randomization, despite the increase in the S2U concentration. These characteristics can affect the thermal parameters of NLCs composed of interesterified blends when compared to simple blends. The higher thermal parameters and higher SFC were observed for the NLC 70:30S, due to the higher FHMO concentration. On the other hand, this thermal characteristic affected the physical behavior of the NLCs. The droplet size of the interesterified blends and the lower FHMO ratio (60:40I) resulted in a higher droplet size and heterogeneous distribution of NLCs, with no effect on the zeta potential, which was adequate for all NLCs evaluated. The turbidimetric analysis showed instability of the NCLs composed of 60:40I (creaming and flocculation/coalescence) and the worst TSI values. Concerning the encapsulation efficiency, the encapsulation of fish oil was effective, with a little oil release until 30 days of storage, with no negative impact on the oxidative stability of NLCs, which presented low values. Over time, a reduction of the physical stability, encapsulation efficiency, and oxidative stability of all NLCs was observed. Although the low FHMO concentration and the interesterification reaction affected negatively the stability of nanoparticles, the encapsulation of fish oil was effective for all the NLCs. The fish oil, due to its low melting point and low crystallinity, can be properly encapsulated into the NLCs composed of FHMO: SO in simple or interesterified blends. The NLCs made with interesterified blends is more effective for the encapsulation of bioactive compounds with low melting point and high crystallinity, resulting in a more disorganized colloidal system that

favors the self-assembly crystals. Therefore, as expected, the nanostructured lipid carrier was an adequate system to protect fish oil and provide benefits for application in food with no unpleasant flavor and odor characteristics.

CRediT authorship contribution statement

Kamila Ramponi Rodrigues de Godoi Fernandes: Conceptualization, Methodology, Investigation, Formal analysis, Writing – original draft. Mayanny Gomes da Silva: Methodology, Formal analysis, Review. Mirna Lucia Gigante: Supervision, Resources. Ana Paula Badan Ribeiro: Conceptualization, Writing – review & editing, Supervision, Funding acquisition, Resources, Project administration.

Declaration of Competing Interest

The authors declare that they have no known competing financial interests or personal relationships that could have appeared to influence the work reported in this paper.

Acknowledgments

Ana Paula Badan Ribeiro thank CNPq (303429/2018-6) for productivity grant and São Paulo Research Foundation-FAPESP (16/11261-8). Kamila Ramponi Rodrigues de Godoi Fernandes thank CNPq (140789/2017-0) for PhD scholarship grant. This study was financed in part by the “Coordenação de Aperfeiçoamento de Pessoal de Nível Superior - Brazil (CAPES)”–Finance Code 001.

5. References

Agrawal, Y., Petkar, K. C., & Sawant, K. K. (2010). Development, evaluation and clinical studies of Acitretin loaded nanostructured lipid carriers for topical treatment of psoriasis. International Journal of Pharmaceutics, 401(1), 93–102. https://doi.org/https://doi.org/10.1016/j.ijpharm.2010.09.007

Akhoond Zardini, A., Mohebbi, M., Farhoosh, R., & Bolurian, S. (2018). Production and characterization of nanostructured lipid carriers and solid lipid

nanoparticles containing lycopene for food fortification. Journal of Food Science and Technology, 55(1), 287–298. https://doi.org/10.1007/s13197-017-2937-5.

AOCS. (2009). Official methods and recommended practices of the American Oil Chemists' Society (6th Editio). https://doi.org/http://dx.doi.org/10.1002/0471740039.vec0152

Artiga-Artigas, M., Lanjari-Pérez, Y., & Martín-Belloso, O. (2018). Curcumin-loaded nanoemulsions stability as affected by the nature and concentration of surfactant. Food Chemistry, 266(June), 466–474. https://doi.org/10.1016/j.foodchem.2018.06.043

Assadpour, E., & Mahdi Jafari, S. (2019). A systematic review on nanoencapsulation of food bioactive ingredients and nutraceuticals by various nanocarriers. Critical Reviews in Food Science and Nutrition, 59(19), 3129–3151. https://doi.org/10.1080/10408398.2018.1484687

Awad, T. S., Helgason, T., Weiss, J., Decker, E. A., & McClements, D. J. (2009). Effect of omega-3 fatty acids on crystallization, polymorphic transformation and stability of tripalmitin solid lipid nanoparticle suspensions. Crystal Growth and Design, 9(8), 3405–3411. https://doi.org/10.1021/cg8011684

Babazadeh, A., Ghanbarzadeh, B., & Hamishehkar, H. (2016). Novel nanostructured lipid carriers as a promising food grade delivery system for rutin. Journal of Functional Foods, 26, 167–175. https://doi.org/10.1016/j.jff.2016.07.017

Bertoni, S., Passerini, N., & Albertini, B. (2021). Liquid lipids act as polymorphic modifiers of tristearin-based formulations produced by melting technologies. Pharmaceutics, 13(7). https://doi.org/10.3390/pharmaceutics13071089

Bruxel, F., Laux, L., Fraga, M., Koester, L., & Teixeira, H. (2012). Nanoemulsions as prospective drug delivery systems. Química Nova, 35(9), 1827–1840. https://doi.org/10.24959/nphj.14.1926

Campos, R. (2005). Fat Crystal Networks. In Fat Crystal Networks (pp. 267–349). Marcell Dekker Inc.

Chiu, M. C., & Gioielli, L. A. (2002). Conteúdo De Gordura Sólida Da Gordura Abdominal De Frango , De. Ciênc. Tecnol. Aliment., 22(2), 151–157.

Das, S., Ng, W. K., & Tan, R. B. H. (2012). Are nanostructured lipid carriers (NLCs) better than solid lipid nanoparticles (SLNs): Development, characterizations and comparative evaluations of clotrimazole-loaded SLNs and NLCs? European Journal of Pharmaceutical Sciences, 47(1), 139–151. https://doi.org/10.1016/j.ejps.2012.05.010

de Souza Queirós, M., Viriato, R. L. S., Vega, D. A., Ribeiro, A. P. B., & Gigante, M. L. (2020). Milk fat nanoemulsions stabilized by dairy proteins. Journal of Food Science and Technology, 57(9), 3295–3304. https://doi.org/10.1007/s13197-020-04362-0

Demetzos, C. (2008). Differential Scanning Calorimetry (DSC): A tool to study the thermal behavior of lipid bilayers and liposomal stability. Journal of Liposome Research, 18(3), 159–173. https://doi.org/10.1080/08982100802310261

Deng, L. (2021). Current Progress in the Utilization of Soy-Based Emulsifiers in. Foods, 10(6), 1354.

Elmowafy, M., Ibrahim, H. M., Ahmed, M. A., Shalaby, K., Salama, A., & Hefesha, H. (2017). Atorvastatin-loaded nanostructured lipid carriers (Nlcs): Strategy to overcome oral delivery drawbacks. Drug Delivery, 24(1), 932–941. https://doi.org/10.1080/10717544.2017.1337823

Esfahani, R., Jafari, S. M., Jafarpour, A., & Dehnad, D. (2019). Loading of fish oil into nanocarriers prepared through gelatin-gum Arabic complexation. Food Hydrocolloids, 90(December 2018), 291–298. https://doi.org/10.1016/j.foodhyd.2018.12.044

Faridi Esfanjani, A., Assadpour, E., & Jafari, S. M. (2018). Improving the bioavailability of phenolic compounds by loading them within lipid-based nanocarriers. Trends in Food Science and Technology, 76(March 2017), 56–66. https://doi.org/10.1016/j.tifs.2018.04.002

Filho, N. R. A., Mendes, O. L., & Lanças, F. M. (1995). Computer prediction of triacylglycerol composition of vegetable oils by HRGC. Chromatographia, 40(9–10), 557–562. https://doi.org/10.1007/BF02290268

Foster, D. W. (2004). The role of the carnitine system in human metabolism. Annals of the New York Academy of Sciences, 1033, 1–16. https://doi.org/10.1196/annals.1320.001

Ghorbanzade, T., Jafari, S. M., Akhavan, S., & Hadavi, R. (2017). Nano-encapsulation of fish oil in nano-liposomes and its application in fortification of yogurt. Food Chemistry, 216, 146–152. https://doi.org/10.1016/j.foodchem.2016.08.022

Giorgio, L. Di, Salgado, P. R., & Mauri, A. N. (2019). Food Hydrocolloids Encapsulation of fi sh oil in soybean protein particles by emulsi fi cation and spray drying. Food Hydrocolloids, 87(July 2018), 891–901. https://doi.org/10.1016/j.foodhyd.2018.09.024

Godoi, K. R. R. de, Basso, R. C., Ming, C. C., Silva, V. M. da, Cunha, R. L. da, Barrera-Arellano, D., & Ribeiro, A. P. B. (2019). Physicochemical and rheological properties of soybean organogels: Interactions between different structuring agents. Food Research International, 124. https://doi.org/10.1016/j.foodres.2019.05.023

Godoi-Fernandes, K. R. R. de, Silva, M. G., Cardoso, L.P., & Ribeiro, A. P. B. (2023a). Effect of chemical interesterification on physico-chemical properties of soybean oil and fully hydrogenated microalgae oil blends. *Food Research International*,*submitted but not published yet.

Godoi-Fernandes, K. R. R. de, Silva, M. G., Gigante, M. L., & Ribeiro, A. P. B. (2023b). Effect of static crystallization protocol on polymorphism and microstructure of interesterified lipid matrices rich in stearic acid. *Food Research International*,*submitted but not published yet.

Godoi-Fernandes, K. R. R. de, Silva, M. G., Cardoso, L.P., & Ribeiro, A. P. B. (2023c). Simple and interesterified lipid blends for formulating food-grade nanostructured lipid carriers. *Colloids and surfaces A: Physicochemical and engineering aspects*,*submitted but not published yet.

Grimaldi, R., Gonçalves, L. A. G., & Ando, M. Y. (2005). Otimização da reação de interesterificaç ão química do óleo de palma. Quimica Nova, 28(4), 633–636. https://doi.org/10.1590/s0100-40422005000400015

Hartman, L., & Lago, R. C. A. (1973). Rapid preparation of fatty acid methyl esters from lipids. Lab. Pract., 22(January), 475-476,494.

Hashemi, F. S., Farzadnia, F., Aghajani, A., Ahmadzadeh NobariAzar, F., & Pezeshki, A. (2020). Conjugated linoleic acid loaded nanostructured lipid carrier as a potential antioxidant nanocarrier for food applications. Food Science and Nutrition, February, 1–11. https://doi.org/10.1002/fsn3.1712

Huang, J., Wang, Q., Li, T., Xia, N., & Xia, Q. (2017). Nanostructured lipid carrier (NLC) as a strategy for encapsulation of quercetin and linseed oil: Preparation and in vitro characterization studies. Journal of Food Engineering, 215, 1–12. https://doi.org/10.1016/j.jfoodeng.2017.07.002

Huck-Iriart, C., Pizones Ruiz-Henestrosa, V. M., Candal, R. J., & Herrera, M. L. (2013). Effect of Aqueous Phase Composition on Stability of Sodium Caseinate/Sunflower oil Emulsions. Food and Bioprocess Technology, 6(9), 2406–2418. https://doi.org/10.1007/s11947-012-0901-y

Jun-xia, X., Hai-yan, Y., & Jian, Y. (2011). Microencapsulation of sweet orange oil by complex coacervation with soybean protein isolate/gum Arabic. Food Chemistry, 125(4), 1267–1272. https://doi.org/10.1016/j.foodchem.2010.10.063

Kang, W., Guo, L., Fan, H., Meng, L., & Li, Y. (2012). Flocculation, coalescence and migration of dispersed phase droplets and oil-water separation in heavy oil emulsion. Journal of Petroleum Science and Engineering, 81, 177–181. https://doi.org/10.1016/j.petrol.2011.12.011

Katouzian, I., Faridi Esfanjani, A., Jafari, S. M., & Akhavan, S. (2017). Formulation and application of a new generation of lipid nano-carriers for the food bioactive ingredients. Trends in Food Science and Technology, 68, 14–25. https://doi.org/10.1016/j.tifs.2017.07.017

Kumbhar, D. D., & Pokharkar, V. B. (2013). Engineering of a nanostructured lipid carrier for the poorly water-soluble drug, bicalutamide: Physicochemical investigations. Colloids and Surfaces A: Physicochemical and Engineering Aspects, 416(1), 32–42. https://doi.org/10.1016/j.colsurfa.2012.10.031

Lacatusu, I., Mitrea, E., Badea, N., Stan, R., Oprea, O., & Meghea, A. (2013). Lipid nanoparticles based on omega-3 fatty acids as effective carriers for lutein delivery. Preparation and in vitro characterization studies. Journal of Functional Foods, 5(3), 1260–1269. https://doi.org/10.1016/j.jff.2013.04.010

Lalia, A. Z., & Lanza, I. R. (2016). Insulin-sensitizing effects of omega-3 fatty acids: Lost in translation? Nutrients, 8(6). https://doi.org/10.3390/nu8060329

Li, Y., Li, M., Qi, Y., Zheng, L., Wu, C., Wang, Z., & Teng, F. (2020). Preparation and digestibility of fish oil nanoemulsions stabilized by soybean protein isolate-phosphatidylcholine. Food Hydrocolloids, 100(July 2019), 105310. https://doi.org/10.1016/j.foodhyd.2019.105310

Liu, C. H., & Wu, C. T. (2010). Optimization of nanostructured lipid carriers for lutein delivery. Colloids and Surfaces A: Physicochemical and Engineering Aspects, 353(2–3), 149–156. https://doi.org/10.1016/j.colsurfa.2009.11.006

Liu, F., Zhu, Z., Ma, C., Luo, X., Bai, L., Decker, E. A., Gao, Y., & McClements, D. J. (2016). Fabrication of Concentrated Fish Oil Emulsions Using Dual-Channel Microfluidization: Impact of Droplet Concentration on Physical Properties and Lipid Oxidation. Journal of Agricultural and Food Chemistry, 64(50), 9532–9541. https://doi.org/10.1021/acs.jafc.6b04413

Llinares, R., Ramírez, P., Carmona, J., Carrillo, F., & Munñoz, J. (2018). Formulation and optimization of emulsions based on bitter fennel essential oil and EO/BO block copolymer surfactant. Colloids and Surfaces A: Physicochemical and Engineering Aspects, 536(July 2017), 142–147. https://doi.org/10.1016/j.colsurfa.2017.07.027

Ludtke, F. L., Stahl, M. A., Zaia, B. G., & Ribeiro, A. P. B. (2017). Characterization of Lipid Matrices for Obtaining Nanostructured Lipid Carriers. In 17th AOCS Latin American Congress and Exhibition on Fats, Oils, and Lipids.

Marangoni, A. G., & Rosseau, D. (2002). The effects of interesterification on the physical properties of fats. In A. G. Marangoni & S. S. Narine (Eds.), Physical Properties of Lipids. Marcell Dekker Inc.

Marhamati, M., Ranjbar, G., & Rezaie, M. (2021). Effects of emulsifiers on the physicochemical stability of Oil-in-water Nanoemulsions: A critical review. Journal of Molecular Liquids, 340, 117218. https://doi.org/10.1016/j.molliq.2021.117218

McClements, D. J. (2004). Protein-stabilized emulsions. Current Opinion in Colloid and Interface Science, 9(5), 305–313. https://doi.org/10.1016/j.cocis.2004.09.003

Mohammadi, M., Assadpour, E., & Jafari, S. M. (2019). Encapsulation of food ingredients by nanostructured lipid carriers (NLCs). In Lipid-Based Nanostructures for Food Encapsulation Purposes. Elsevier Inc. https://doi.org/10.1016/b978-0-12-815673-5.00007-6

Mohammadi, M., Pezeshki, A., Abbasi, M. M., Ghanbarzadeh, B., & Hamishehkar, H. (2017). Vitamin D3-loaded nanostructured lipid carriers as a potential approach for fortifying food beverages; in vitro and in vivo evaluation.

Advanced Pharmaceutical Bulletin, 7(1), 61–71. https://doi.org/10.15171/apb.2017.008

Munin, A., & Edwards-Lévy, F. (2011). Encapsulation of natural polyphenolic compounds; a review. In Pharmaceutics (Vol. 3, Issue 4). https://doi.org/10.3390/pharmaceutics3040793

Nazarzadeh, E., Anthonypillai, T., & Sajjadi, S. (2013). On the growth mechanisms of nanoemulsions. Journal of Colloid and Interface Science, 397, 154–162. https://doi.org/10.1016/j.jcis.2012.12.018

Nguyen, H. M., Hwang, I. C., Park, J. W., & Park, H. J. (2012). Enhanced payload and photo-protection for pesticides using nanostructured lipid carriers with corn oil as liquid lipid. Journal of Microencapsulation, 29(6), 596–604. https://doi.org/10.3109/02652048.2012.668960

O'Brien, R. D. (2009). Chapter 1 - Raw Materials. In Fats and Oils: Formulating and Processing for Applications (Third Edit, pp. 1–66). CRC Press.

Ojagh, S. M., & Hasani, S. (2018). Characteristics and oxidative stability of fish oil nano-liposomes and its application in functional bread. Journal of Food Measurement and Characterization, 12(2), 1084–1092. https://doi.org/10.1007/s11694-018-9724-5

Park, S. J., Garcia, C. V., Shin, G. H., & Kim, J. T. (2017). Development of nanostructured lipid carriers for the encapsulation and controlled release of vitamin D3. Food Chemistry, 225, 213–219. https://doi.org/10.1016/j.foodchem.2017.01.015

Pathakoti, K., Manubolu, M., & Hwang, H. M. (2017). Nanostructures: Current uses and future applications in food science. Journal of Food and Drug Analysis, 25(2), 245–253. https://doi.org/10.1016/j.jfda.2017.02.004

Patra, J. K., & Baek, K. H. (2014). Green Nanobiotechnology: Factors Affecting Synthesis and Characterization Techniques. Journal of Nanomaterials, 2014. https://doi.org/10.1155/2014/417305

Perica, M. M., & Delaš, I. (2011). Essential fatty acids and psychiatric disorders. Nutrition in Clinical Practice, 26(4), 409–425. https://doi.org/10.1177/0884533611411306

Pezeshki, A., Hamishehkar, H., Ghanbarzadeh, B., Fathollahy, I., Keivani Nahr, F., Khakbaz Heshmati, M., & Mohammadi, M. (2019). Nanostructured

lipid carriers as a favorable delivery system for β-carotene. Food Bioscience, 27(January 2018), 11–17. https://doi.org/10.1016/j.fbio.2018.11.004

Pinto, F., de Barros, D. P. C., & Fonseca, L. P. (2018). Design of multifunctional nanostructured lipid carriers enriched with α-tocopherol using vegetable oils. Industrial Crops and Products, 118(April), 149–159. https://doi.org/10.1016/j.indcrop.2018.03.042

Poonia, N., Kaur Narang, J., Lather, V., Beg, S., Sharma, T., Singh, B., & Pandita, D. (2019). Resveratrol loaded functionalized nanostructured lipid carriers for breast cancer targeting: Systematic development, characterization and pharmacokinetic evaluation. Colloids and Surfaces B: Biointerfaces, 181(February), 756–766. https://doi.org/10.1016/j.colsurfb.2019.06.004

Qian, C., Decker, E. A., Xiao, H., & McClements, D. J. (2013). Impact of lipid nanoparticle physical state on particle aggregation and β-carotene degradation: Potential limitations of solid lipid nanoparticles. Food Research International, 52(1), 342–349. https://doi.org/10.1016/j.foodres.2013.03.035

Ribeiro, A. P. B., Basso, R. C., Grimaldi, R., Gioielli, L. A., & Gonçalves, L. A. G. (2009). Instrumental Methods for the Evaluation of Interesterified Fats. Food Analytical Methods, 2(4), 281–302.

Ribeiro, A. P. B., Masuchi, M. H., Miyasaki, E. K., Domingues, M. A. F., Stroppa, V. L. Z., de Oliveira, G. M., & Kieckbusch, T. G. (2015). Crystallization modifiers in lipid systems. Journal of Food Science and Technology, 52(7), 3925–3946. https://doi.org/10.1007/s13197-014-1587-0

Rocha, J. C. B., Lopes, J. D., Mascarenhas, M. C. N., Arellano, D. B., Guerreiro, L. M. R., & da Cunha, R. L. (2013). Thermal and rheological properties of organogels formed by sugarcane or candelilla wax in soybean oil. Food Research International, 50(1), 318–323. https://doi.org/10.1016/j.foodres.2012.10.043

Sadati Behbahani, E., Ghaedi, M., Abbaspour, M., Rostamizadeh, K., & Dashtian, K. (2019). Curcumin loaded nanostructured lipid carriers: In vitro digestion and release studies. Polyhedron, 164, 113–122. https://doi.org/10.1016/j.poly.2019.02.002

Salminen, H., Gömmel, C., Leuenberger, B. H., & Weiss, J. (2016). Influence of encapsulated functional lipids on crystal structure and chemical stability in solid lipid nanoparticles: Towards bioactive-based design of delivery

systems. Food Chemistry, 190, 928–937. https://doi.org/10.1016/j.foodchem.2015.06.054

Salvia-Trujillo, L., McClements, D. J., & Martín-Belloso, O. (2021). Nanoemulsion design for the delivery of omega-3 fatty acids. In Omega-3 Delivery Systems: Production, Physical Characterization and Oxidative Stability. Elsevier Inc. https://doi.org/10.1016/B978-0-12-821391-9.00016-8

Santos, V. da S., Braz, B. B., Silva, A. Á., Cardoso, L. P., Ribeiro, A. P. B., & Santana, M. H. A. (2019). Nanostructured lipid carriers loaded with free phytosterols for food applications. Food Chemistry, 298(May), 125053. https://doi.org/10.1016/j.foodchem.2019.125053

Shah, R., Eldridge, D., Palombo, E., & Harding, I. (2015). Production Techniques. https://doi.org/10.1007/978-3-319-10711-0_3

Shahparast, Y., Eskandani, M., Rajaei, A., & Khosroushahi, A. Y. (2019). Preparation, physicochemical characterization and oxidative stability of omega-3 fish oil/α-tocopherol-co-loaded nanostructured lipidic carriers. In Advanced Pharmaceutical Bulletin (Vol. 9, Issue 3, pp. 393–400). https://doi.org/10.15171/apb.2019.046

Silva, M. G., de Godoi, K. R. R., Gigante, M. L., Cardoso, L. P., & Ribeiro, A. P. B. (2022). Nanostructured lipid carriers for delivery of free phytosterols: Effect of lipid composition and chemical interesterification on physical stability. Colloids and Surfaces A: Physicochemical and Engineering Aspects, 640(January), 128425. https://doi.org/10.1016/j.colsurfa.2022.128425

Silva, R. C., De Martini Soares, F. A. S., Maruyama, J. M., Dagostinho, N. R., Silva, Y. A., Ract, J. N. R., & Gioielli, L. A. (2016). Microscopic approach of the crystallization of tripalmitin and tristearin by microscopy. Chemistry and Physics of Lipids, 198, 1–9. https://doi.org/10.1016/j.chemphyslip.2016.04.004

Souto, E., Severino, P., Santana, M. H., & Pinho, S. (2011). NANOPARTÍCULAS DE LIPÍDIOS SÓLIDOS: MÉTODOS CLÁSSICOS DE PRODUÇÃO LABORATORIAL. Quimica Nova, 34(8), 1323–1327.

Stan, C. (2001). Codex standard for named vegetable oils. 8, 11–25.

Sulciner, M. L., Serhan, C. N., Gilligan, M. M., Mudge, D. K., Chang, J., Gartung, A., Lehner, K. A., Bielenberg, D. R., Schmidt, B., Dalli, J., Greene, E. R., Gus-Brautbar, Y., Piwowarski, J., Mammoto, T., Zurakowski, D., Perretti, M., Sukhatme, V. P., Kaipainen, A., Kieran, M. W., … Panigrahy, D. (2018).

Resolvins suppress tumor growth and enhance cancer therapy. Journal of Experimental Medicine, 215(1), 115–140. https://doi.org/10.1084/jem.20170681

Tadros, T., Izquierdo, P., Esquena, J., & Solans, C. (2004). Formation and stability of nano-emulsions. Advances in Colloid and Interface Science, 108–109, 303–318. https://doi.org/10.1016/j.cis.2003.10.023

Tamjidi, F., Shahedi, M., Varshosaz, J., & Nasirpour, A. (2013). Nanostructured lipid carriers (NLC): A potential delivery system for bioactive food molecules. Innovative Food Science and Emerging Technologies, 19, 29–43. https://doi.org/10.1016/j.ifset.2013.03.002

Tamjidi, F., Shahedi, M., Varshosaz, J., & Nasirpour, A. (2014). Design and characterization of astaxanthin-loaded nanostructured lipid carriers. Innovative Food Science and Emerging Technologies, 26, 366–374. https://doi.org/10.1016/j.ifset.2014.06.012

Teng, W., Zhao, L., Yang, S., Zhang, C., Liu, M., Luo, J., Jin, J., Zhang, M., Bao, C., Li, D., Xiong, W., Li, Y., & Ren, F. (2019). The hepatic-targeted, resveratrol loaded nanoparticles for relief of high fat diet-induced nonalcoholic fatty liver disease. Journal of Controlled Release, 307(April), 139–149. https://doi.org/10.1016/j.jconrel.2019.06.023

Thrandur, H., Awad, T. S., Kristberg, K., Eric, A. D., David, J. M. A., & Jochen, W. (2009). Impact of surfactant properties on oxidative stability of ??-carotene encapsulated within solid lipid nanoparticles. Journal of Agricultural and Food Chemistry, 57(17), 8033–8040. https://doi.org/10.1021/jf901682m

Timms, R. E. (1984). Phase behaviour of fats and their mixtures. Progress in Lipid Research, 23(1), 1–38. https://doi.org/10.1016/0163-7827(84)90004-3

Trujillo-Cayado, L. A., Alfaro, M. C., & Muñoz, J. (2018). Effects of ethoxylated fatty acid alkanolamide concentration and processing on D-limonene emulsions. Colloids and Surfaces A: Physicochemical and Engineering Aspects, 536(June 2017), 198–203. https://doi.org/10.1016/j.colsurfa.2017.06.010

Vellido-Perez, J. A., Ochando-Pulido, J. M., Brito-de la Fuente, E., & Martinez-Ferez, A. (2021). Novel emulsions–based technological approaches for the protection of omega–3 polyunsaturated fatty acids against oxidation processes – A comprehensive review. Food Structure, 27(December 2020), 100175. https://doi.org/10.1016/j.foostr.2021.100175

Venugopalan, V. K., Gopakumar, L. R., Kumaran, A. K., Chatterjee, N. S., Soman, V., Peeralil, S., Mathew, S., McClements, D. J., & Nagarajarao, R. C. (2021). Encapsulation and protection of omega-3-rich fish oils using food-grade delivery systems. Foods, 10(7), 1–20. https://doi.org/10.3390/foods10071566

Vieira, R., Severino, P., Nalone, L. A., Souto, S. B., Silva, M., Lucarini, M., Durazzo, A., & Santini, A. (2020). Sucupira Oil-Loaded Nanostructured Lipid Carriers (NLC): Lipid Screening, Factorial Design, Release Profile, and Cytotoxicity. 029(6), 1–22.

Wang, J. L., Dong, X. Y., Wei, F., Zhong, J., Liu, B., Yao, M. H., Yang, M., Zheng, C., Quek, S. Y., & Chen, H. (2014). Preparation and characterization of novel lipid carriers containing microalgae oil for food applications. Journal of Food Science, 79(2). https://doi.org/10.1111/1750-3841.12334

Xu, B., Kang, W., Meng, L., Yang, R., Liu, S., & Zhang, L. (2013). Synthesis, aggregation behavior and emulsification characteristic of a multi-sticker amphiphilic polymer. Journal of Macromolecular Science, Part A: Pure and Applied Chemistry, 50(3), 302–309. https://doi.org/10.1080/10601325.2013.755855

Yang, Ying, & McClements, D. J. (2013). Vitamin E bioaccessibility: Influence of carrier oil type on digestion and release of emulsified α-tocopherol acetate. Food Chemistry, 141(1), 473–481. https://doi.org/10.1016/j.foodchem.2013.03.033

Ye, Q., Georges, N., & Selomulya, C. (2018). Microencapsulation of active ingredients in functional foods: From research stage to commercial food products. Trends in Food Science and Technology, 78(January), 167–179. https://doi.org/10.1016/j.tifs.2018.05.025

Yuan, Y., Gao, Y., Zhao, J., & Mao, L. (2008). Characterization and stability evaluation of β-carotene nanoemulsions.pdf. In Food Research International (Vol. 41, pp. 61–68).

Zheng, M., Falkeborg, M., Zheng, Y., Yang, T., & Xu, X. (2013). Formulation and characterization of nanostructured lipid carriers containing a mixed lipids core. Colloids and Surfaces A: Physicochemical and Engineering Aspects, 430, 76–84. https://doi.org/10.1016/j.colsurfa.2013.03.070

5. Discussão Geral

Conforme previamente mencionado, o presente estudo teve como objetivo principal avaliar o impacto da reação de interesterificação em bases compostas de FHMO:SO em diferentes proporções e processamento (blends simples ou quimicamente interesterificados) e verificar qual o impacto do uso destas frações como fase lipídica em NLCs para encapsulação de óleo de peixe.

Neste sentido, avaliando-se as matérias-primas utilizadas no estudo, o SO analisado mostrou composição em ácidos graxos coerente com informações da literatura, enquanto o FHMO, devido à sua composição original rica em ácido oleico, resultou em um óleo totalmente hidrogenado com alto teor de ácido esteárico (92.85%), concentração não encontrada em nenhuma fonte vegetal. É importante salientar que o ácido esteárico (C18:0) possui efeito aterogênico neutro, ou seja, não causa aumento dos níveis das lipoproteínas de alta densidade, também chamadas de LDL colesterol.

Nos blends avaliados (90:10, 80:20, 70:30, 60:40, 50:50 FHMO: SO) houve teor de ácidos graxos saturados proporcionais à adição de FHMO. Do ponto de vista tecnológico, a adição de óleos totalmente hidrogenados contendo majoritariamente ácidos graxos saturados de cadeia longa, como C18, são requeridos em bases lipídicas que necessitam de maior ponto de fusão, resistência térmica e mecânica, além de serem utilizados como aceleradores de cristalização. Neste sentido, a gama de blends produzidos pode fornecer tais características de forma diversa, já que as variações nos teores de SO e FHMO garantem perfis distintos aos blends lipídicos.

Para os blends avaliados, antes ou após a randomização, houve predominância de triestearina (SSS) devido ao expressivo teor de ácido esteárico do FHMO. Para os blends interesterificados observou-se aumento de TAG S_2U, com redução nos demais TAG de forma concomitante quando comparado às frações simples. Em geral, comparando-se a fração simples à sua correspondente interesterificada, houve aumento dos teores de PSS e SOO, com manutenção ou diminuição nos teores de SSS após a reação.

Para avaliar o real impacto desta mudança, a análise de regioespecificidade mostrou ligeira predominância de ácidos graxos saturados nas posições sn 1,3, sempre superior a quantidade de ácidos graxos saturados na posição sn 2,

característico da distribuição natural em matrizes vegetais nos blends simples. Após a reação de interesterificação química houve diminuição da quantidade de ácidos graxos saturados em todas as posições nas concentrações em que o FHMO foi adicionado de forma majoritária.

Estes resultados impactaram diretamente nos perfis de fusão e cristalização das bases lipídicas. Com isso, a diminuição de FHMO dos blends simples reduziu os teores de TAG S3 com aumento proporcional principalmente nos teores de SU2 e SU3. Com isso, as temperaturas iniciais e finais de cristalização e fusão, assim como a entalpia diminuíram proporcionalmente ao teor de S3. Após a randomização, no entanto, estes parâmetros se modificaram juntamente com a distribuição das classes triacilglicerólicas.

Ao impactar nos parâmetros de cristalização em geral, o teor de sólidos e a velocidade de cristalização também são influenciados. Os blends obtidos tiveram perfis de SFC proporcionais à quantidade de FHMO adicionado, devido ao teor de ácidos graxos saturados na composição do *hardfat*. Já em função da randomização houve ligeira diferenciação nos perfis de gordura sólida com curvas menos acentuadas para os blends interesterificados e maiores valores de SFC para os blends simples. Esta diferença antes e após a randomização deve-se à composição triacilglicerólica de cada blend obtido, aspecto que também direcionará a aplicação, sendo que todos os blends simples poderiam ser direcionados para aplicação em caldos em cubos, sopas, granulados, matrizes para micro e nanopartículas, que necessitam de resistência e estabilidade física à temperatura ambiente (25°C), enquanto os blends interesterificados apresentam maior característica de plasticidade e possibilidade de aplicações.

Não menos importante, o SFC permite ainda avaliar a compatibilidade entre as matérias-primas utilizadas nos blends através do diagrama de iso-sólidos/compatibilidade em que os blends simples apresentaram ocorrência de efeito eutético nas proporções de 70% e 90% de FHMO, o que indica incompatibilidade entre os materiais de partida, enquanto nos blends interesterificados houve maior compatibilidade entre o SO e FHMO.

Quanto à velocidade de cristalização, as isotermas realizadas a 25°C nos blends simples se estabilizaram mais rapidamente do que os blends interesterificados e, conforme esperado, a adição do SO ao FHMO promoveu redução no teor de sólidos máximo (SFC_{max}) e os blends interesterificados

tiveram menor SFC_{max}. Em relação ao tempo de indução da cristalização (τ_{SFC}), os blends simples apresentaram tempos de indução iguais (2 minutos), enquanto os blends interesterificados apresentaram maior tempo, proporcionalmente à concentração de SO (de 2 a 4.25 minutos). Para os valores de K, a velocidade de cristalização foi menor nos blends interesterificados quando comparados às mesmas proporções em sua forma simples, o que condiz com os valores para SFC_{max} e τ_{SFC}. O valor de n apresentou números fracionários na grande maioria dos blends, com diferenciação entre as frações antes e após a randomização com valores de n = 1 ou n= 2, respectivamente. Este resultado indica que a nucleação dos blends simples seria preferencialmente instantânea e com cristais do tipo agulha, já a nucleação após a randomização poderia se modificar ou não, podendo ser de cristal do tipo agulha ou disco com nucleação instantânea ou esporádica em todos os blends interesterificados.

Estas observações foram confirmadas por imagens de microscopia sob luz polarizada, em que se visualizou a formação de cristais em formato de discos. Após a randomização, no entanto, foram obtidos cristais menores, com formatos do tipo discos ou agulhas e maior área cristalizada. Neste sentido, devido ao aumento do número absoluto de cristais e redução do diâmetro cristalino de forma simultânea nos blends interesterificados, a possibilidade de maior formação de aglomerados se confirmou através da avaliação de porcentagem de área cristalizada e formação de clusters, que foi superior para os blends simples. Esta avaliação, ao ser realizada ao longo de 60 dias de armazenamento, indicou que análise quantitativa através das imagens de microestrutura fica dificultada devido à grande cristalinidade do sistema, mas, nos blends com menores concentrações de FHMO (60:40 e 50:50) é possível visualizar ligeiras mudanças nas imagens.

Adicionalmente a estes parâmetros, avaliou-se o tempo de meia vida de cristalização, ou seja, o tempo necessário para cristalizar 50% da totalidade do sistema lipídico. Este tempo foi sempre menor para os blends simples quando comparadas às suas frações interesterificadas correspondentes, resultado já esperado em função da maior velocidade de cristalização observada e menor tempo de indução dos blends antes da randomização. A dimensão reduzida dos cristais observada nos blends interesterificados é considerada um fator positivo para a aplicação de gorduras em alimentos.

Com isso, para os blends simples, observou-se predominância da forma polimórfica β, enquanto após a reação de interesterificação houve predominância da forma polimórfica β' indicando que são blends com menor cristalinidade na temperatura de análise.

Portanto, para todos os blends avaliados, o processo de interesterificação foi eficaz na redução do tamanho dos cristais, fornecendo estabilidade física e ampliando as possibilidades de aplicação da base lipídica. Este conjunto de informações corroboram os resultados de polimorfismo, uma vez que o processo de interesterificação modificou o hábito cristalino das gorduras, observando-se predominância significativa do polimorfo β′ após a reação, caracterizados por cristais menores e plasticidade desejáveis em produtos como margarinas e gorduras para produtos de panificação e confeitaria.

Com respeito ao primeiro protocolo de cristalização (lenta – 25°C por todo o tempo de avaliação) observou-se forma polimórfica β em todos os blends simples com presença concomitante de β' no blend 50:50S após 60 dias e os blends 90:10I, 60:40I e 50:50I apresentaram o hábito polimórfico β' indefinidamente e de forma isolada, assim como o blend 80:20I apresentou as formas β e β' simultaneamente em todo o tempo de avaliação.

Durante o período avaliado, observou-se diminuição no diâmetro máximo e médio dos cristais e na porcentagem de área cristalizada em todos os blends. Contudo, o diâmetro médio e máximo dos cristais foi sempre maior antes do que após a randomização e proporcionais aos teores de FHMO, possivelmente associado à presença mais frequente de cristais do tipo β nos blends simples e ao aumento de TAG S_3 proporcionalmente ao teor de FHMO

Em relação à avaliação em método de cristalização rápida (24h a 5°C e 24h a 25°C – Método 2) houve predominância da forma polimórfica β' nos blends interesterificados e β nos blends simples após 48 horas de armazenamento, o que se modificou após 7 dias, quando houve aparecimento da forma β nos blends interesterificados. A concomitância de polimorfos pode ocorrer devido à formação de cristais favorecidos pela composição triacilglicerólica e pelo protocolo de cristalização usado, sendo que este fato decorre, principalmente, em situações de super-resfriamento, conforme avaliado no Método 2. O diâmetro médio seguiu a mesma tendência, com diminuição do parâmetro ao longo do

tempo para todos os blends. Este resultado refletiu diretamente no parâmetro de área cristalizada em que houve diminuição da área total cristalizada.

Portanto, além da randomização, a estabilização da gordura através do Método 2, apesar de direcionar a formação de hábito polimórfico β, também favorece o aparecimento de β' ao longo do tempo, sendo capaz de modificar o polimorfismo dos cristais. Isso se deve à fusão de cristais do tipo β que podem ter sido formados através da indução por baixas temperaturas de forma rápida, e que não garantiu devida estabilidade cristalina. Neste sentido, com o aumento da temperatura para 25°C, houve fusão destes cristais e possibilidade de formação de novos cristais do tipo β'. Outro motivo pelo qual os cristais β' podem surgir ao longo do tempo é devido à cristalização tardia, pois, com a presença majoritária de SO, podem haver frações lipídicas que se cristalizarão ao longo do tempo. E, por fim, ainda pode-se ter ocorrido o fenômeno do Oswald Ripening, em que há dissolução de cristais pequenos e agregação dos cristais mais estáveis e maiores presentes na fase lipídica.

Com tudo isso, é possível indicar que os blends interesterificados e a cristalização rápida (5°C/24h) seriam as condições mais indicadas para aplicações em NLCs, já que não há transição monotrópica. Os cristais formados no início da cristalização se mantêm ou são gerados novos cristais, porém do tipo β', adequado para aplicação.

Assim, as combinações de FHMO:SO 90:10, 80:20, 70:30 e 60:40 (FHMO:SO m:m) foram utilizadas como fase lipídica de forma simples e interesterificadas em NLCs com avaliação durante 60 dias.

Nesta aplicação, foi possível distinguir a maioria das formas polimórficas presentes, porém esta identificação foi bastante dificultada devido ao teor de água nas formulações. Em alguns NLCs (90:10S, 90:10I, 70:30I e 60:40I) foi possível observar o aparecimento tardio da forma polimórfica β', menos estável, possivelmente devido à cristalização tardia da tripalmitina ou até mesmo ao efeito da interesterificação. Portanto, o comportamento do material lipídico em macro e nanoescala foram bastante similares, o que pode ser atribuído à metodologia de estabilização e à composição triacilglicerólica após a reação de interesterificação.

Em relação aos parâmetros térmicos, os NLCs formulados a partir de blends interesterificados apresentaram valores de temperaturas iniciais e finais de cristalização e fusão, além da entalpia, inferiores aos dos blends simples, assim como ocorreu na fase bulk. Em função do teor de ácidos graxos saturados, conforme a diminuição da proporção de FHMO nas frações, houve redução em todos os parâmetros de fusão (T_p, T_i, T_f e ΔH) nos NLCs avaliados, também de forma similar à fase lipídica bulk.

Após a adição do composto bioativo, os NLCs 70:30 e 60:40 foram avaliados ao longo de 30 dias, e o tempo de armazenamento não afetou nenhum dos parâmetros térmicos avaliados, pois não houve diferença estatisticamente significativa considerando-se a mesma amostra após 48 horas, 7, 15 ou 30 dias. A proporção de FHMO:SO nos NLCs influenciou os parâmetros de fusão sendo que os NLCs com maior proporção de FHMO (70:30) apresentaram maiores valores para todos os parâmetros quando comparados à proporção 60:40. Já a comparação entre matrizes lipídicas interesterificadas e simples, observou-se que as matrizes interesterificadas apresentaram menores valores quando comparados às matrizes simples com o mesmo tempo de armazenamento e proporção de FHMO:SO. Assim, a reação de interesterificação tende a reduzir a resistência térmica do sistema pela diminuição da proporção de TAGs S_3. Entretanto, ao comparar-se os NLCs sem adição do composto bioativo e com óleo de peixe adicionado, não se observou diferença no comportamento térmico.

Através dos parâmetros de fusão foi possível avaliar o Índice de Recristalização (RI) da fase lipídica nas nanoemulsões. O IR observado para os NLCs foi baixo (entre 0.78% e 1.46%), e sem diferença significativa entre os blends utilizados.

Em relação ao SFC, observou-se que, para os blends simples com maiores teores de FHMO (90:10 e 80:20) houve aumento do SFC logo após a cristalização estática (48h), com manutenção até os 60 dias de armazenamento a 25°C. Já para os NLCs contendo blends nas proporções 70:30S e 60:40S, observou-se maior SFC inicial (após as primeiras 48h de armazenamento) com posterior redução do parâmetro. De modo geral, o SFC diminuiu em função do tempo em todos os NLCs avaliados, enquanto não se observou diferença significativa entre os NLCs compostos de fração lipídica simples e interesterificada. Porém, o SFC teve influência, principalmente, da quantidade

de FHMO. Este efeito já era esperado visto que a inclusão e o aumento de óleo totalmente hidrogenado nos blends simples ou interesterificados tendem a aumentar o ponto de fusão

Para os NLCs carregados com óleo de peixe, houve redução do SFC devido à desorganização mais intensa do sistema, promovida pela própria adição do composto, altamente poli-insaturado, com reduzido ponto de fusão, assim como detectado no comportamento de fusão. Já a diminuição gradativa do SFC ao longo do tempo de armazenamento, que não foi observada nos NLCs sem a adição do composto após 7 dias, pode indicar certa incompatibilidade entre as matrizes lipídicas adicionadas, já que há significativas diferenças de estrutura química e espacial.

Em função da estabilidade das nanopartículas, a distribuição de tamanho representada por média da superfície (D 3,2) não variou em função do tempo, assim como não foram observadas diferenças expressivas nos NLCs obtidos com blends simples ou randomizados. Assim, quando o óleo de peixe foi adicionado, verificou-se que, logo após a obtenção (48h), apenas o NLC obtido com fase lipídica 60:40S mostrou-se significativamente menor do que as demais. Aos 15 dias, observou-se comportamento diferente para todos os NLCs, sendo que a fração 60:40S resultou em menor D3,2 e a fração 70:30I a maior, com subsequente redução do parâmetro em todos os blends ao longo do tempo. Estes resultados indicam que há maior influência do teor de ácidos graxos saturados e predominância de TAGs S3 no parâmetro D3,2, do que da reação de interesterificação.

É possível correlacionar diretamente o valor do SPAN com o parâmetro de D3,2, visto que, com o decorrer do tempo de armazenamento, houve diminuição do tamanho das partículas e também do SPAN, o que indica que a redução no D3,2 promoveu maior homogeneização do sistema favorecendo a estabilidade física. Quando os teores de adição de óleo de peixe estão abaixo de 1% não se observa aumento no tamanho das partículas, que pode ser um indicativo de encapsulação adequada. Neste sentido, o SPAN dos NLCs com óleo de peixe obtidos de frações lipídicas interesterificadas foram maiores do que àqueles com frações simples durante todo o tempo de análise (30 dias). Quanto ao teor de FHMO, observou-se menor valor de SPAN para NLCs obtidos com fração lipídica simples.

O índice de polidispersidade (PDI) mostrou que as nanoemulsões constituídas de blends interesterificados originaram sistemas mais homogêneos, com valores maiores de PDI para os NLCs compostos de blends simples e com maior proporção de FHMO. Este perfil pode estar associado ao polimorfismo preferencial da fração lipídica, já que os cristais do tipo β' foram visualizados apenas nas matrizes interesterificadas e na matriz com maior concentração de FHMO. Em função do tempo, os parâmetros mostraram-se similares para os NLCs antes e depois da adição do composto bioativo.

Acerca do potencial zeta, observou-se diminuição deste parâmetro em todas as nanoemulsões ao longo do tempo, independente da matéria-prima lipídica utilizada. De forma comparativa, os NLCs formulados com blends interesterificados e com menor teor de FHMO apresentaram maiores valores de potencial zeta, portanto, podem ser considerados mais estáveis. Com o tempo, a redução pode estar relacionada ao polimorfismo predominante nos NLCs e à possível cristalização tardia ou recristalização das matrizes lipídicas, em que houve formação de cristais do tipo β' na fase lipídica bulk. Com a adição do óleo de peixe, os NLCs 60:40S e 70:30I foram considerados mais estáveis ao longo do tempo. Em geral, o parâmetro de potencial zeta foi maior nos NLCs com a adição do composto bioativo, o que indica que, apesar de apresentar tamanho de partícula aumentado, há maior estabilidade ao longo do tempo e dispersão das partículas independentemente da fase lipídica utilizada no NLC em que o óleo de peixe foi adicionado.

Na análise de turbidimetria, alguns fenômenos de desestabilização comuns em emulsões podem ser observados nos NLCs sem composto bioativo. Assim, os NLCs contendo as proporções 90:10S e 90:10I apresentaram sedimentação, que se acentuou ao longo do tempo, sendo que a fração randomizada apresentou também cremeação aos 60 dias de análise. Com a fração lipídica 80:20 ocorreu sedimentação e cremeação após 60 dias na mistura simples e após 15 dias na mistura randomizada. Já na fração 70:30 ocorreu o fenômeno de cremeação, sendo que a fração simples ainda mostrou características de floculação/coalescência de forma concomitante após 60 dias de análise. Por fim, os NLCs com blends 60:40 antes e após a randomização apresentaram características do fenômeno de cremeação, floculação/coalescência, sem variação expressiva ao longo do tempo de análise. Com isso, observou-se que

todos os NLCs mostraram desestabilização ao longo tempo, principalmente após 60 dias de armazenamento, independente da randomização ou proporção das blends lipídicas utilizadas.

Após a adição do óleo de peixe nos NLCs, a variação do backscttering mostrou desestabilização (em forma de sedimentação, cremeação, coalescência ou floculação) a partir de 7 dias de armazenamento sendo que houve intensificação ao longo do tempo de avaliação. Nos NLCs contendo fase lipídica constituída de blends interesterificados (60:40I e 70:30I) observou-se o fenômeno de cremeação a partir de 7 dias de armazenamento, sendo que na fração 60:40I houve floculação e coalescência das partículas de forma concomitante. Já nos NLCs produzidos com blends simples (60:40S e 70:30S) como fase lipídica observou-se, além do fenômeno de cremeação, também sedimentação ao longo do tempo de armazenamento. Em relação à interesterificação, principalmente o NLC contendo fase lipídica 60:40I, apresentou cremeação, floculação e coalescência. Estes resultados foram similares aos NLCs sem composto bioativo, portanto, não há influência da presença do óleo de peixe na desestabilização das nanoemulsões.

Em relação ao índice de estabilidade TSI (Turbiscan Stability Index), verifica-se que os NLCs contendo fases lipídicas com menores teores de FHMO apresentaram maior TSI, indicando maior desestabilização da amostra, que foi intensificada ao longo do tempo de análise, assim como observado pelo perfil de backscattering e potencial zeta para as mesmas proporções. Após a adição do composto bioativo, os NLCs mostraram resultado divergente quanto ao TSI, pois, quando o óleo de peixe foi adicionado, houve maior propensão aos fenômenos de desestabilização quando a fase lipídica era composta por bases interesterificadas, mas não houve diferença entre as proporções de FHMO. Este efeito pode ter ocorrido devido ao direcionamento para a forma polimórfica menos estável, β’, causada pela reação de interesterificação, e que pode ter se intensificado com a adição do composto bioativo. Este efeito colabora para a maior desorganização estrutural do sistema, em função do baixo ponto de fusão e polimorfismo preferencial β’.

O óleo de peixe possui baixo ponto de fusão e também não direciona a formação de cristais para a forma mais estável, do tipo β, podendo favorecer a desorganização estrutural dos NLCs. Em ambos os casos, com ou sem a adição

de óleo de peixe, os fenômenos de desestabilização observados podem estar relacionados às condições de obtenção dos NLCs, como o número de ciclos, uso de alta pressão e temperatura elevada, assim como pelo tamanho da partícula e viscosidade do sistema.

Além disso, no presente trabalho, observou-se alta e satisfatória EE dos NLCs em todos os tempos de análise, independentemente da fase lipídica utilizada. Esta elevada capacidade de incorporação dos NLCs pode dever-se à alta compatibilidade entre os materiais de parede, o composto bioativo encapsulado (de natureza lipofílica) e também ao baixo ponto de fusão do mesmo, que não influencia ou favorece uma cristalização mais intensa do sistema. Além disso, apesar de notar-se mínima diminuição da EE ao longo do tempo de armazenamento, este parâmetro esteve sempre acima de 80%, caracterizando ótima capacidade de encapsulação.

Como esperado, o índice de peróxido apresentou aumento ao longo do tempo de armazenamento. Acredita-se que a exposição da fase lipídica (considerando-se os materiais de parede e o composto bioativo lipofílico) a alta temperatura durante o processo de fusão completa, incorporação e obtenção da pré e nanoemulsão por homogeneização a alta pressão a quente pode ter favorecido o aumento do IP já nas primeiras 48 horas de avaliação. Este efeito possivelmente seria maior para as matrizes interesterificadas visto que a exposição à temperatura elevada destas matrizes ocorre já durante a reação de interesterificação química, que acontece a 90°C. No entanto, o aumento gradual do parâmetro ao longo do tempo pode ser explicado pela continuidade do mecanismo de reação em cadeia típico da oxidação lipídica.

Considerando que as nanoemulsões poderão ser aplicadas em matrizes alimentares complexas, as características físicas deverão ser avaliadas e consideradas, principalmente, no produto final. Portanto, os resultados avaliados a nível nanométrico serão considerados para direcionar as conclusões sobre as nanoemulsões. Neste sentido, a interesterificação e o uso de menores teores de ácidos graxos saturados podem ser mais indicadas para aplicações em matrizes alimentares.

6. Conclusão geral

Ao avaliar combinações de óleo de soja e óleo de microalgas totalmente hidrogenado, em diferentes proporções, em misturas simples ou quimicamente interesterificadas, foi possível observar que os blends interesterificados apresentaram menor ponto de fusão, redução no teor de sólidos máximo no equilíbrio isotérmico, maior linearidade do perfil de sólidos, maior compatibilidade entre as matérias-primas, maior tempo de indução de cristalização devido à diferenciação do comportamento térmico e, consequentemente, modificação morfológica e polimórfica. Observou-se, ainda, maiores quantidades e menores diâmetros das estruturas cristalinas, e maior ocorrência da configuração β', que é desejável para aplicação em NLCs.

Todas estas características de cristalização foram atribuídas à reordenação dos ácidos graxos na molécula de glicerol causada pela reação de interesterificação, em que houve redução de TAG S3 com simultâneo aumento de S_2U. Com isso, as características finais das gorduras estruturadas possibilitaram a ampliação da aplicabilidade em produtos de base lipídica que necessitem de aeração como margarinas e produtos de panificação e confeitaria.

Já ao avaliar-se as diferentes metodologias de cristalização (lenta ou rápida) e o armazenamento ao longo de 60 dias, nos blends simples identificou-se cristais do tipo discos grandes, enquanto após a randomização, os mesmos blends apresentaram cristais do tipo agulhas diminutas, com direcionamento para a configuração cristalina β'. De acordo com a metodologia de cristalização rápida (24h/5°C e depois a 25°C) houve maior densidade cristalina após 48 horas, com cristais de menor diâmetro médio e máximo, e maior quantidade de área cristalizada quando comparado ao método de cristalização lenta (24h/25°C). Além disso, esta metodologia de cristalização rápida resultou em alteração do hábito polimórfico β para o β' possivelmente relacionado à um efeito de fusão dos cristais formados rapidamente, mais frágeis, com posterior recristalização em nova polimórfica (β') ou ao amadurecimento de Ostwald, que favorece a dissolução de cristais menores reduzindo a área cristalizada ao longo do tempo de armazenamento. Já a metodologia de cristalização lenta (24h/25°C) resultou em rede cristalina mais estável, com aparecimento tardio de forma

polimórfica β’ e estabilização majoritariamente em forma polimórfica β mesmo nos blends interesterificados.

Desta forma, escolheu-se a metodologia de cristalização rápida para aplicação das frações lipídicas nos NLCs já que houve direcionamento para a forma polimórfica β’ com esta metodologia e menor velocidade das transições monotrópicas.

Avaliando-se os NLCs com as frações lipídicas representadas por 90:10, 80:20, 70:30 e 60:40 FHMO:SO (m:m), as características das nanoemulsões foram dependentes do teor de FHMO, visto que o aumento da concentração do óleo totalmente hidrogenado levou ao aumento da resistência térmica, SFC e tamanho de partícula, além de menores valores de potencial zeta, com maior susceptibilidade à agregação das partículas e desestabilização do sistema. Já nos NLCs de frações interesterificadas houve menor resistência térmica e menor SFC, assim como maior homogeneidade de distribuição nos diâmetros das partículas e menor tendência à agregação e desestabilização do sistema. O hábito polimórfico predominante de todas as nanoemulsões foi β, mas a visualização dos picos lipídicos foi dificultada pela água cristalizada presente, o que pode ter ocultado picos de cristais do tipo β’. Ao longo do tempo de armazenamento, todos os NLCs sofreram desestabilização física observada através da avaliação por Turbiscan. Com isso, NLCs constituídos por blends interesterificados e com menores quantidades de FHMO mostraram-se mais estáveis, com ocorrência tardia de instabilidade durante o armazenamento a 25°C.

Ao incluir o óleo de peixe nos NLCs de proporção 60:40 e 70:30 (FHMO:SO m:m) em misturas simples e interesterificadas, observou-se que o óleo de peixe, devido às suas características de baixa cristalinidade e ponto de fusão, foi possível obter-se boa eficiência de encapsulação. Quanto ao impacto da adição do óleo de peixe nas características da nanoemulsão, observou-se que o uso da estrutura foi eficiente para encapsulação, independentemente da fração lipídica utilizada demonstrando grande valia na técnica para reduzir os impactos organolépticos do óleo de peixe e aumentar o seu consumo pela população.

7. Referências

AGRAWAL, Y.; PETKAR, K. C.; SAWANT, K. K. Development, evaluation and clinical studies of Acitretin loaded nanostructured lipid carriers for topical treatment of psoriasis. **International Journal of Pharmaceutics**, v. 401, n. 1, p. 93–102, 2010.

AHMADI, L.; WRIGHT, A. J.; MARANGONI, A. G. Chemical and enzymatic interesterification of tristearin / triolein-rich blends : **Microstructure and polymorphism**. p. 1025–1034, 2008.

AKHOOND ZARDINI, A. et al. Production and characterization of nanostructured lipid carriers and solid lipid nanoparticles containing lycopene for food fortification. **Journal of Food Science and Technology**, v. 55, n. 1, p. 287–298, 2018.

ANTONIOSI FILHO, N. R. A.; MENDES, O. L.; LANÇAS, F. M. Computer prediction of triacylglycerol composition of vegetable oils by HRGC. **Chromatographia**, v. 40, n. 9–10, p. 557–562, 1995.

AOCS. Official methods and recommended practices of the American Oil Chemists' Society. 6th Editio ed. Champaign, 2009.

ARAÚJO, J. et al. Nanostructured lipid carriers for triamcinolone acetonide delivery to the posterior segment of the eye. **Colloids and Surfaces B: Biointerfaces,** v. 88, n. 1, p. 150–157, 2011.

ARTICLE, R. et al. Current Status of Solid Lipid Nanoparticles : A Review. v. 3, n. 4, p. 1–10, 2018.

ARTIGA-ARTIGAS, M.; LANJARI-PÉREZ, Y.; MARTÍN-BELLOSO, O. Curcumin-loaded nanoemulsions stability as affected by the nature and concentration of surfactant. **Food Chemistry**, v. 266, n. June, p. 466–474, 2018.

ASBRIDGE, D. D. Soybeans vs.Other vegetable oils as a source of edible oil products. In: ERICKSON, D. R. (Ed.). . Pratical Handbook and soybean processing and utilization. Illinois: AOCS Press, 2015. p. 1–9.

ASSADPOUR, E.; MAHDI JAFARI, S. A systematic review on nanoencapsulation of food bioactive ingredients and nutraceuticals by various nanocarriers. **Critical Reviews in Food Science and Nutrition**, v. 59, n. 19, p. 3129–3151, 2019.

AWAD, T. S. et al. Effect of omega-3 fatty acids on crystallization, polymorphic transformation and stability of tripalmitin solid lipid nanoparticle suspensions. **Crystal Growth and Design**, v. 9, n. 8, p. 3405–3411, 2009.

AZIZI, M. et al. Improvement of physicochemical properties of encapsulated echium oil using nanostructured lipid carriers. **Food Chemistry**, v. 246, n. September 2017, p. 448–456, 2018.

BABAZADEH, A.; GHANBARZADEH, B.; HAMISHEHKAR, H. Novel nanostructured lipid carriers as a promising food grade delivery system for rutin. **Journal of Functional Foods**, v. 26, p. 167–175, 2016.

BADEA, G. et al. Use of various vegetable oils in designing photoprotective nanostructured formulations for UV protection and antioxidant activity. **Industrial Crops and Products**, v. 67, p. 18–24, 2015.

BALLESTRA, D. Produce trans-free fats - Interchem® Technology, [s.d.]. Disponível em: <https://www.desmetballestra.com/oils-fats/fat-modification/interesterification/chemical-interesterification>

BASOVA, M. M. Fatty acid composition of lipids in microalgae. **International Journal on Algae**, v. 7, n. 1, p. 33–57, 2005.

BELOQUI, A. et al. Nanostructured lipid carriers : Promising drug delivery systems for future clinics. Nanomedicine: **Nanotechnology, Biology, and Medicine,** v. 12, n. 1, p. 143–161, 2016.

BERČÍKOVÁ, M. et al. Physical Properties of Structured Fats and Fat Blends Based on the Long Chain Fatty Acids. **Food Biophysics**, v. 15, n. 1, p. 143–152, 2020.

BERNAL, D. J.; FOWLER, R. H. A Theory of Water and Ionic Solution, with Particular Reference to Hydrogen and Hydroxyl Ions. **The Journal of Chemical Physics**, v. 1, n. 8, 1933.

BERTON-CARABIN, C. C.; COUPLAND, J. N.; ELIAS, R. J. Effect of the lipophilicity of model ingredients on their location and reactivity in emulsions and solid lipid nanoparticles. **Colloids and Surfaces A: Physicochemical and Engineering Aspects**, v. 431, p. 9–17, 2013.

BERTONI, S.; PASSERINI, N.; ALBERTINI, B. Liquid lipids act as polymorphic modifiers of tristearin-based formulations produced by melting technologies. **Pharmaceutics**, v. 13, n. 7, 2021.

BOGEVIK, A. S. et al. Enzymatic Interesterification of Heterotrophic Microalgal Oil with Rapeseed Oil to Decrease the Levels of Tripalmitin. **European Journal of Lipid Science and Technology**, v. 120, n. 7, p. 1–10, 2018.

BÖSCH, S. et al. Trans Fat Free by 2023—A Building Block of the COVID-19 Response. **Frontiers in Nutrition**, v. 8, n. March, p. 1–7, 2021.

BOT, A.; FLÖTER, E. Application in Fat-Continuous Emulsions (Spreads). Edible Oil Processing (2nd Edition), p. 223–249, 2013.

BOUZIDI, L.; NARINE, S. S. Relationships between molecular structure and kinetic and thermodynamic controls in lipid systems. Part II: Phase behavior and transformation paths of SSS, PSS and PPS saturated triacylglycerols - Effect of chain length mismatch. **Chemistry and Physics of Lipids**, v. 165, n. 1, p. 77–88, 2012.

BRAIPSON-DANTHINE, S.; DEROANNE, C. Influence of SFC, microstructure and polymorphism on texture (hardness) of binary blends of fats involved in the preparation of industrial shortenings. **Food Research International**, v. 37, n. 10, p. 941–948, 2004.

BRASIL. Informe Técnico n. 63, de 3 de outubro de 2014. ANVISA – Agência Nacional de Vigilância Sanitária, 2014.

BROUWER, I. A. The public health rationale for reducing saturated fat intakes: Is a maximum of 10% energy intake a good recommendation? **Nutrition Bulletin**, v. 45, n. 3, p. 271–280, 2020.

BRUNSTEINER, M. et al. Toward a Molecular Understanding of Crystal Agglomeration. **Crystal Growth & Design**, v. 5, n. 1, p. 3–16, 1 jan. 2005.

BRUXEL, F. et al. Nanoemulsions as prospective drug delivery systems. **Química Nova**, v. 35, n. 9, p. 1827–1840, 2012.

BUNJES, H.; UNRUH, T. Characterization of lipid nanoparticles by differential scanning calorimetry, X-ray and neutron scattering. **Advanced Drug Delivery Reviews**, v. 59, n. 6, p. 379–402, 2007.

CAMPOS, R. Fat Crystal Networks. In: Fat Crystal Networks. New York: Marcell Dekker Inc., 2005. p. 267–349.

CHIPLUNKAR, P. P.; PRATAP, A. P. Ultrasound Assisted Synthesis of Hydroxylated Soybean Lecithin from Crude Soybean Lecithin as an Emulsifier. **J Oleo Sci.** v. 1108, n. 10, p. 1101–1108, 2017.

CHIU, M. C.; GIOIELLI, L. A. Conteúdo De Gordura Sólida Da Gordura Abdominal De Frango , De. **Ciênc. Tecnol. Aliment**., v. 22, n. 2, p. 151–157, 2002.

CHONG, C. L. et al. Thermal and structural behaviour of crude palm oil: Crystallisation at very slow cooling rate. **European Journal of Lipid Science and Technology**, v. 109, n. 4, p. 410–421, 2007.

CHOPIN-DOROTEO, M. et al. The Effect of Shearing in the Thermo-mechanical Properties of Candelilla Wax and Candelilla Wax-Tripalmitin Organogels. **Food Biophysics**, v. 6, n. 3, p. 359–376, 2011.

COHEN, Z.; NORMAN, H. A.; HEIMER, Y. M. Microalgae as a source of omega3 fatty acids. **World Review of Nutrition and Dietetics**, v. 77, p. 1–31, 1995.

CRUPKIN, M.; ZAMBELLI, A. Detrimental impact of trans fats on human health: Stearic acid-rich fats as possible substitutes. **Comprehensive Reviews in Food Science and Food Safety**, v. 7, n. 3, p. 271–279, 2008.

CURI, R. et al. Entendendo a gordura: os ácidos graxos. 1a ed. Editora Manole, 2002.

D'AGOSTINI, D. Obtenção de lipídios estruturados por interesterificação de triacilgliceróis de cadeia média e longa.Universidade de São Paulo, 2014.

DA MATA, A. M. B. et al. Dietary Lipid Intake Influences the Alpha-tocopherol Levels in Human Milk. **Journal of pediatric gastroenterology and nutrition**, v. 70, n. 6, p. 858–863, 2020.

DAS, S.; NG, W. K.; TAN, R. B. H. Are nanostructured lipid carriers (NLCs) better than solid lipid nanoparticles (SLNs): Development, characterizations and comparative evaluations of clotrimazole-loaded SLNs and NLCs? **European Journal of Pharmaceutical Sciences**, v. 47, n. 1, p. 139–151, 2012.

DASSANAYAKE, L. S. K.; KODALI, D. R.; UENO, S. Formation of oleogels based on edible lipid materials. **Current Opinion in Colloid and Interface Science**, v. 16, n. 5, p. 432–439, 2011.

DE GRAEF, V. et al. Effect of TAG composition on the solid fat content profile, microstructure, and hardness of model fat blends with identical saturated fatty acid content. **European Journal of Lipid Science and Technology**, v. 114, n. 5, p. 592–601, 2012.

DEHNAD, D. et al. Thermal and antimicrobial properties of chitosan-nanocellulose films for extending shelf life of ground meat. **Carbohydrate Polymers**, v. 109, p. 148–154, 2014.

DEMETZOS, C. Differential Scanning Calorimetry (DSC): A tool to study the thermal behavior of lipid bilayers and liposomal stability. **Journal of Liposome Research**, v. 18, n. 3, p. 159–173, 2008.

DEMODARAN, S.; PARKIN, K. L.; FENNEMA, O. L. Química de Alimentos de Fennema. Forth edit ed. Porto Alegre: Editora Artmed, 2010.

DENG, L. Current Progress in the Utilization of Soy-Based Emulsifiers in. **Foods,** v. 10, n. 6, p. 1354, 2021.

DRUSCH, S. et al. Physicochemical characterization and oxidative stability of fish oil encapsulated in an amorphous matrix containing trehalose. **Food Research International**, v. 39, n. 7, p. 807–815, 2006.

ELMOWAFY, M. et al. Atorvastatin-loaded nanostructured lipid carriers (Nlcs): Strategy to overcome oral delivery drawbacks. **Drug Delivery**, v. 24, n. 1, p. 932–941, 2017.

ELNAGGAR, Y. S. R.; EL-MASSIK, M. A.; ABDALLAH, O. Y. Fabrication, appraisal, and transdermal permeation of sildenafil citrate-loaded nanostructured lipid carriers versus solid lipid nanoparticles. **International journal of nanomedicine**, v. 6, p. 3195–3205, 2011.

ESFAHANI, R. et al. Loading of fish oil into nanocarriers prepared through gelatin-gum Arabic complexation. **Food Hydrocolloids**, v. 90, n. December 2018, p. 291–298, 2019.

FAGERIA, N. K.; BALIGAR, V. C.; JONES, C. A. Growth and Mineral Nutrition of Field Crops. In: Third Edit ed. Boca Raton: CRC Press, 2010. p. 551.

FANG, J. Y. et al. Lipid nanoparticles as vehicles for topical psoralen delivery: Solid lipid nanoparticles (SLN) versus nanostructured lipid carriers (NLC). **European Journal of Pharmaceutics and Biopharmaceutics**, v. 70, n. 2, p. 633–640, 2008.

FARIDI ESFANJANI, A.; ASSADPOUR, E.; JAFARI, S. M. Improving the bioavailability of phenolic compounds by loading them within lipid-based nanocarriers. **Trends in Food Science and Technology**, v. 76, n. March 2017, p. 56–66, 2018.

FOSTER, D. W. The role of the carnitine system in human metabolism. Annals of the New York Academy of Sciences. Anais...2004

FOUBERT, I. et al. Modelling two-step isothermal fat crystallization. Journal of Food Engineering, v. 75, n. 4, p. 551–559, 2006.

GHANBARZADEH, B.; KEIVANI, F.; MOHAMMADI, M. Encapsulation of food ingredients by solid lipid nanoparticles (SLNs). Elsevier Inc., 2019.

GHASEMI FARD, S. et al. How does high DHA fish oil affect health? A systematic review of evidence. **Critical Reviews in Food Science and Nutrition**, v. 59, n. 11, p. 1684–1727, 2019.

GHORBANZADE, T. et al. Nano-encapsulation of fish oil in nano-liposomes and its application in fortification of yogurt. **Food Chemistry**, v. 216, p. 146–152, 2017.

GHOTRA, B. S.; DYAL, S. D.; NARINE, S. S. Lipid shortenings: A review. **Food Research International**, v. 35, n. 10, p. 1015–1048, 2002.

GIORGIO, L. DI; SALGADO, P. R.; MAURI, A. N. Food Hydrocolloids Encapsulation of fi sh oil in soybean protein particles by emulsi fi cation and spray drying. **Food Hydrocolloids**, v. 87, n. July 2018, p. 891–901, 2019.

GODOI, K. R. R. DE et al. Physicochemical and rheological properties of soybean organogels: Interactions between different structuring agents. **Food Research International**, v. 124, 2019.

GOMES, M. et al. Nanostructured lipid carriers for delivery of free phytosterols : Effect of lipid composition and chemical interesterification on physical stability. **Colloids and Surfaces A: Physicochemical and Engineering Aspects**, v. 640, n. January, p. 128425, 2022.

GRIMALDI, R.; GONÇALVES, L. A. G.; ANDO, M. Y. Otimização da reação de interesterificaç ão química do óleo de palma. **Quimica Nova**, v. 28, n. 4, p. 633–636, 2005.

GUEDES, A. M. M. et al. Physicochemical Properties of Interesterified Blends of Fully Hydrogenated Crambe abyssinica Oil and Soybean Oil. **Journal of American Oil Chemistry Society**, v. 91, n. 1, p. 111–123, 2014.

GUNSTONE, F. D.; HARWOOD, J. L.; DIJKSTRA, A. T. The Lipid Handbook. In: The lipid handbook. 3a Edição ed. Boca Raton: CRC Press, 2007. p. 37–141.

GUPTA, S. et al. Systematic Approach for the Formulation and Optimization of Solid Lipid Nanoparticles of Efavirenz by High Pressure Homogenization Using Design of Experiments for Brain Targeting and Enhanced Bioavailability. v. 2017, 2017.

HAMMOND, E. G. et al. Soybean Oil. **Bailey's Industrial Oil and Fat Products**, n. 1, p. 577–653, 2005.

HARTMAN, L.; LAGO, R. C. A. Rapid preparation of fatty acid methyl esters from lipids. **Lab. Pract**., v. 22, n. January, p. 475- 476,494, 1973.

HASHEMI, F. S. et al. Conjugated linoleic acid loaded nanostructured lipid carrier as a potential antioxidant nanocarrier for food applications. **Food Science and Nutrition**, n. February, p. 1–11, 2020.

HERRERA, M. L. et al. Isothermal crystallization of hydrogenated sunflower oil: II. Growth and solid fat content. JAOCS, **Journal of the American Oil Chemists'** Society, v. 76, n. 1, p. 1–6, 1999.

HERRERA, M. L.; DE LEÓN GATTI, M.; HARTEL, R. W. A kinetic analysis of crystallization of a milk fat model system. **Food Research International**, v. 32, n. 4, p. 289–298, 1999.

HERRERA, M. L.; MARQUEZ ROCHA, F. J. Effects of sucrose ester on the kinetics of polymorphic transition in hydrogenated sunflower oil. **Journal of the American Oil Chemists' Society**, v. 73, n. 3, p. 321–326, 1996.

HIMAWAN, C.; STAROV, V. M.; STAPLEY, A. G. F. Thermodynamic and kinetic aspects of fat crystallization. **Advances in Colloid and Interface Science**, v. 122, n. 1–3, p. 3–33, 2006.

HOLSER, R. Encapsulation of polyunsaturated fatty acid esters with solid lipid particles. **Lipid Insights**, v. 5, p. 1–5, 2012.

HUANG, J. et al. Nanostructured lipid carrier (NLC) as a strategy for encapsulation of quercetin and linseed oil: Preparation and in vitro characterization studies. **Journal of Food Engineering**, v. 215, p. 1–12, 2017.

HUCK-IRIART, C. et al. Effect of Aqueous Phase Composition on Stability of Sodium Caseinate/Sunflower oil Emulsions. **Food and Bioprocess Technology**, v. 6, n. 9, p. 2406–2418, 2013.

HULLA, J. E.; SAHU, S. C.; HAYES, A. W. Nanotechnology: History and future. **Human and Experimental Toxicology**, v. 34, n. 12, p. 1318–1321, 2015.

IFEDUBA, E. A.; MARTINI, S.; AKOH, C. C. Enzymatic Interesterification of High Oleic Sunflower Oil and Tripalmitin or Tristearin. JAOCS, **Journal of the American Oil Chemists' Society**, v. 93, n. 1, p. 61–67, 2016.

INOUE, T. et al. Solid-liquid phase behavior of binary fatty acid mixtures: 2. Mixtures of oleic acid with lauric acid, myristic acid, and palmitic acid. **Chemistry and Physics of Lipids**, v. 127, n. 2, p. 161–173, 2004.

INSTITUTO BRASILEIRO DE GEOGRAFIA E ESTATISTICA, I. Pesquisa de Orçamentos Familiares 2017 - 2018 - Primeiros Resultados, 2018.

JAFARI, S. M. et al. Hydrophobicity, thermal and micro-structural properties of whey protein concentrate-pullulan-beeswax films. **International Journal of Biological Macromolecules**, v. 80, p. 506–511, 2015.

JAFARI, S. M. et al. Encapsulation by nanoemulsions. Elsevier Inc., 2017.

JAFARI, S. M.; ESFANJANI, A. F. Instrumental analysis and characterization of nanocapsules. In: Nanoencapsulation Technologies for the Food and Nutraceutical Industries. Elsevier Inc., 2017. p. 524–544.

JAFARI, S. M.; HE, Y.; BHANDARI, B. Effectiveness of encapsulating biopolymers to produce sub-micron emulsions by high energy emulsification techniques. **Food Research International**, v. 40, n. 7, p. 862–873, 2007.

JI, S. et al. Synthesis, Purification, and Characterization of a Structured Lipid Based on Soybean Oil and Coconut Oil and Its Applications in Curcumin-Loaded Nanoemulsions. **European Journal of Lipid Science and Technology**, v. 122, n. 10, p. 1–10, 2020.

JUN-XIA, X.; HAI-YAN, Y.; JIAN, Y. Microencapsulation of sweet orange oil by complex coacervation with soybean protein isolate/gum Arabic. **Food Chemistry**, v. 125, n. 4, p. 1267–1272, 2011.

KAMBOJ, S.; BALA, S.; NAIR, A. B. Review Article **Solid lipid nanoparticles** : v. 5, n. 2, 2010.

KANG, W. et al. Flocculation, coalescence and migration of dispersed phase droplets and oil-water separation in heavy oil emulsion. **Journal of Petroleum Science and Engineering**, v. 81, p. 177–181, 2012.

KARABULUT, I.; TURAN, S.; ERGIN, G. Effects of chemical interesterification on solid fat content and slip melting point of fat/oil blends. **European Food Research and Technology**, v. 218, n. 3, p. 224–229, 2004.

KATOUZIAN, I. et al. Formulation and application of a new generation of lipid nano-carriers for the food bioactive ingredients. **Trends in Food Science and Technology**, v. 68, p. 14–25, 2017.

KHARAT, M.; MCCLEMENTS, D. J. Fabrication and characterization of nanostructured lipid carriers (NLC) using a plant-based emulsifier: Quillaja saponin. **Food Research International**, v. 126, n. July, p. 108601, 2019.

KHOSHNOUDI-NIA, S.; FORGHANI, Z.; JAFARI, S. M. A systematic review and meta-analysis of fish oil encapsulation within different micro/nanocarriers. **Critical Reviews in Food Science and Nutrition**, v. 0, n. 0, p. 1–22, 2020.

KOK, L. L. et al. Trans-free margarine from highly saturated soybean oil. JAOCS, **Journal of the American Oil Chemists' Society**, v. 76, n. 10, p. 1175–1181, 1999.

KOVAČEVIĆ, A. B. et al. Solid lipid nanoparticles (SLN) stabilized with polyhydroxy surfactants: Preparation, characterization and physical stability investigation. **Colloids and Surfaces A: Physicochemical and Engineering Aspects**, v. 444, p. 15–25, 2014a.

KOVAČEVIĆ, A. B. et al. Solid lipid nanoparticles (SLN) stabilized with polyhydroxy surfactants: Preparation, characterization and physical stability investigation. **Colloids and Surfaces A: Physicochemical and Engineering Aspects**, v. 444, p. 15–25, 2014b.

KRIS-ETHERTON, P. M.; GRIEGER, J. A.; ETHERTON, T. D. Dietary reference intakes for DHA and EPA. **Prostaglandins Leukotrienes and Essential Fatty Acids**, v. 81, n. 2–3, p. 99–104, 2009.

KUMBHAR, D. D.; POKHARKAR, V. B. Engineering of a nanostructured lipid carrier for the poorly water-soluble drug, bicalutamide: Physicochemical investigations. **Colloids and Surfaces A: Physicochemical and Engineering Aspects**, v. 416, n. 1, p. 32–42, 2013.

KURATKO, C. N.; SALEM, N. Docosahexaenoic acid from algal oil. European **Journal of Lipid Science and Technology**, v. 115, n. 9, p. 965–976, 2013.

LACATUSU, I. et al. Lipid nanoparticles based on omega-3 fatty acids as effective carriers for lutein delivery. Preparation and in vitro characterization studies. **Journal of Functional Foods**, v. 5, n. 3, p. 1260–1269, 2013.

LALIA, A. Z.; LANZA, I. R. Insulin-sensitizing effects of omega-3 fatty acids: Lost in translation? Nutrients, v. 8, n. 6, 2016.

LAWLER, P. J.; DIMICK, P. S. Crystallization and Polymorphism of Fats. In: Food Lipids: Chemistry, Nutrition, and Biotechnology. .

LEÃO, K. M. M. et al. Physicochemical characterization and antimicrobial activity in novel systems containing buriti oil and structured lipids nanoemulsions. **Biotechnology Reports**, v. 24, 2019.

LEE, J. H. . et al. Preparation of Interesterified Plastic Fats from Fats and Oils Free of Trans Fatty Acid. **Journal of Agricultural and Food Chemistry**, v. 56, p. 4039–4046, 2008.

LI, Y. et al. Preparation and digestibility of fish oil nanoemulsions stabilized by soybean protein isolate-phosphatidylcholine. **Food Hydrocolloids**, v. 100, n. July 2019, p. 105310, 2020.

LIANG, L. et al. In vitro release of α-tocopherol from emulsion-loaded β-lactoglobulin gels. **International Dairy Journal**, v. 20, n. 3, p. 176–181, 2010.

LIU, C. H.; WU, C. T. Optimization of nanostructured lipid carriers for lutein delivery. **Colloids and Surfaces A: Physicochemical and Engineering Aspects**, v. 353, n. 2–3, p. 149–156, 2010.

LIU, F. et al. Fabrication of Concentrated Fish Oil Emulsions Using Dual-Channel Microfluidization: Impact of Droplet Concentration on Physical Properties and Lipid Oxidation. **Journal of Agricultural and Food Chemistry**, v. 64, n. 50, p. 9532–9541, 2016.

LIVNEY, Y. D. Nanostructured delivery systems in food: Latest developments and potential future directions. **Current Opinion in Food Science**, v. 3, p. 125–135, 2015.

LLINARES, R. et al. Formulation and optimization of emulsions based on bitter fennel essential oil and EO/BO block copolymer surfactant. **Colloids and Surfaces A: Physicochemical and Engineering Aspects**, v. 536, n. July 2017, p. 142–147, 2018.

LUDTKE, F. L. et al. Characterization of Lipid Matrices for Obtaining Nanostructured Lipid Carriers. In: 17th AOCS Latin American Congress and Exhibition on Fats, Oils, and Lipids. Cancún, 2017.

LUO, Y.; TENG, Z.; WANG, Q. Development of zein nanoparticles coated with carboxymethyl chitosan for encapsulation and controlled release of vitamin D3. **Journal of Agricultural and Food Chemistry**, v. 60, n. 3, p. 836–843, 2012.

LUYKX, D. M. et al. A review of analytical methods for the identification and characterization of nano delivery systems in food. **J Agric Food Chem**, v. 56, n. 18, p. 8231–8247, 2008.

MA, P. et al. LWT - Food Science and Technology Preparation of curcumin-loaded emulsion using high pressure homogenization : Impact of oil phase and

concentration on physicochemical stability. **LWT - Food Science and Technology**, v. 84, p. 34–46, 2017.

MADUREIRA, A. R. et al. Characterization of solid lipid nanoparticles produced with carnauba wax for rosmarinic acid oral delivery. **RSC Advances**, v. 5, n. 29, p. 22665–22673, 2015.

MATOS-JR, F. E. et al. Effect of feed preparation on the properties and stability of ascorbic acid microparticles produced by spray chilling. **LWT - Food Science and Technology**, v. 75, p. 251–260, 2017.

MARANGONI, A. G. On the use and misuse of the avrami equation in characterization of the kinetics of fat crystallization. **Journal of the American Oil Chemists' Society**, v. 75, n. 10, p. 1465–1467, 1998.

MARANGONI, A. G.; CAMPOS, R. Fat Crystal Networks, 2005.

MARANGONI, A. G.; ROSSEAU, D. The effects of interesterification on the physical properties of fats. In: MARANGONI, A. G.; NARINE, S. S. (Eds.) Physical Properties of Lipids. New York: Marcell Dekker Inc., 2002.

MARHAMATI, M.; RANJBAR, G.; REZAIE, M. Effects of emulsifiers on the physicochemical stability of Oil-in-water Nanoemulsions: A critical review. **Journal of Molecular Liquids**, v. 340, p. 117218, 2021.

MARTINI, S.; HERRERA, M. L.; HARTEL, R. W. Effect of cooling rate on crystallization behavior of milk fat fraction/sunflower oil blends. JAOCS, **Journal of the American Oil Chemists' Society**, v. 79, n. 11, p. 1055–1062, 2002.

MARTINI, S.; HERRERA, M. L.; MARANGONI, A. New technologies to determine solid fat content on-line. JAOCS, **Journal of the American Oil Chemists' Society**, v. 82, n. 5, p. 313–317, 2005.

MCCLEMENTS, D. J. Protein-stabilized emulsions. **Current Opinion in Colloid and Interface Science**, v. 9, n. 5, p. 305–313, 2004.

MCCLEMENTS, D. J. Crystals and crystallization in oil-in-water emulsions: Implications for emulsion-based delivery systems. **Advances in Colloid and Interface Science**, v. 174, p. 1–30, 2012.

MCCLEMENTS, D. J. Advances in nanoparticle and microparticle delivery systems for increasing the dispersibility, stability, and bioactivity of phytochemicals. **Biotechnology Advances**, v. 38, n. August 2018, p. 107287, 2020.

MCCLEMENTS, D. J.; JAFARI, S. M. Chapter 1 - General Aspects of Nanoemulsions and Their Formulation. In: JAFARI, S. M.; MCCLEMENTS, D. J. (Eds.). Nanoemulsions. Academic Press, p. 3–20, 2018.

MCCLEMENTS, D. J. Standardization of Nanoparticle Characterization : Methods for Testing Properties , Stability , and Functionality of Edible Nanoparticles Standardization of Nanoparticle Characterization. **Crit Rev Food Sci Nutr**. v. 8398, 2016.

MEHNERT, W.; MÄDER, K. Solid lipid nanoparticles: Production, characterization and applications. **Advanced Drug Delivery Reviews**, v. 64, n. SUPPL., p. 83–101, 2012.

MENG, Z. et al. Comparative analysis of lipid composition and thermal, polymorphic, and crystallization behaviors of granular crystals formed in beef tallow and palm oil. **Journal of Agricultural and Food Chemistry**, v. 59, n. 4, p. 1432–1441, 2011.

MENSINK, R. P. Effects of stearic acid on plasma lipid and lipoproteins in humans. **Lipids,** 2005.

METIN, S.; HARTEL, R. W. Fats and Oils. Bailey's Industrial Oil and Fat Products, p. 45–76, 2005.

MICHAEL ESKIN, N. A.; LIST, G. R. Food applications of lipids. Food Lipids: Chemistry, Nutrition, and Biotechnology, Fourth Edition, p. 421–451, 2017.

MISKANDAR, M. S. et al. Quality of margarine: Fats selection and processing parameters. **Asia Pacific Journal of Clinical Nutrition**, v. 14, n. 4, p. 387–395, 2005.

MOHAMMADI, M. et al. Vitamin D3-loaded nanostructured lipid carriers as a potential approach for fortifying food beverages; in vitro and in vivo evaluation. **Advanced Pharmaceutical Bulletin**, v. 7, n. 1, p. 61–71, 2017.

MOHAMMADI, M.; ASSADPOUR, E.; JAFARI, S. M. Encapsulation of food ingredients by nanostructured lipid carriers (NLCs). Elsevier Inc., 2019.

MONTENEGRO, R.; LANDFESTER, K. Metastable and stable morphologies during crystallization of alkanes in miniemulsion droplets. **Langmuir**, v. 19, n. 15, p. 5996–6003, 2003.

MORSELLI RIBEIRO, M. D. M. et al. Comparison between enzymatic and chemical interesterification of high oleic sunflower oil and fully hydrogenated

soybean oil**. European Journal of Lipid Science and Technology**, v. 119, n. 2, p. 1–9, 2017.

MÜLLER, R. H. et al. Nanostructured Lipid Carriers (NLC): The Second Generation of Solid Lipid Nanoparticles. In: DRAGICEVIC, N.; MAIBACH, H. I. (Eds.) Percutaneous Penetration Enhancers Chemical Methods in Penetration Enhancement: Nanocarriers. Berlin, Heidelberg: Springer Berlin Heidelberg, 2016. p. 161–185.

NARINE, S. S.; HUMPHREY, K. L. A comparison of lipid shortening functionality as a function of molecular ensemble and shear: Microstructure, polymorphism, solid fat content and texture. **Food Research International**, v. 37, n. 1, p. 28–38, 2004.

NARINE, S. S.; MARANGONI, A. G. Microscopic and rheological studies of fat crystal networks. **Journal of Crystal Growth**, v. 198–199, n. pt 2, p. 1315–1319, 1999.

NASCIMENTO, I. A. et al. Screening Microalgae Strains for Biodiesel Production: Lipid Productivity and Estimation of Fuel Quality Based on Fatty Acids Profiles as Selective Criteria. **Bioenergy Research**, v. 6, n. 1, p. 1–13, 2013.

NGUYEN, H. M. et al. Enhanced payload and photo-protection for pesticides using nanostructured lipid carriers with corn oil as liquid lipid. **Journal of Microencapsulation**, v. 29, n. 6, p. 596–604, 2012.

O'BRIEN, R. D. Interesterification. In: Fats and Oils: Formulating and Processing for Applications. CRC Press, 2009a. p. 122–132.

O'BRIEN, R. D. Chapter 1 - Raw Materials. In: Fats and Oils: Formulating and Processing for Applications. Third Edit ed. Boca Raton: CRC Press, 2009b. p. 1–66.

O'KEEFE, S. F.; SARNOSKI, P. J. Nomenclature and Classification of Lipids. In: AKOH, C. C. (Ed.) Food Lipids: Chemistry, Nutrition, and Biotechnology. Fourth Edi ed. Boca Raton: p. 1029.

OH, J. H. et al. Stabilizing polymorphic transitions of tristearin using diacylglycerols and sucrose polyesters. JAOCS, **Journal of the American Oil Chemists' Society**, v. 82, n. 1, p. 13–19, 2005.

OJAGH, S. M.; HASANI, S. Characteristics and oxidative stability of fish oil nano-liposomes and its application in functional bread. **Journal of Food Measurement and Characterization**, v. 12, n. 2, p. 1084–1092, 2018.

OLIVEIRA, P. D. et al. Chemical interesterification of blends with palm stearin and patawa oil. **Food Chemistry**, v. 215, p. 369–376, 2017.

OLIVEIRA, G. M. et al. Effect of the addition of hardfats on technological properties of palm oil : solid fat content , consistency and crystallization kinetic. **International Congress on Engineering and Food**., 2011.

OLIVEIRA, G. M. et al. Hard fats as additives in palm oil and its relationships to crystallization process and polymorphism. **LWT - Food Science and Technology**, v. 63, n. 2, p. 1163–1170, 2015.

PACHECO, C. et al. Optimization of Reaction Conditions in the Enzymatic Interesterification of Soybean Oil and Fully Hydrogenated Soybean Oil to Produce Plastic Fats. **Journal of American Oil Chemistry Society**, v. 90, p. 391–400, 2013.

PANDE, G.; AKOH, C. C. Enzymatic modification of lipids for trans-free margarine. **Lipid Technology**, v. 25, n. 2, p. 31–33, 2013.

PARK, S. J. et al. Fabrication and optimization of EGCG-loaded nanoparticles by high pressure homogenization. **Journal of Applied Polymer Science**. v. 43269, p. 1–7, 2016.

PARK, S. J. et al. Development of nanostructured lipid carriers for the encapsulation and controlled release of vitamin D3. **Food Chemistry**, v. 225, p. 213–219, 2017.

PATHAKOTI, K.; MANUBOLU, M.; HWANG, H. M. Nanostructures: Current uses and future applications in food science. **Journal of Food and Drug Analysis**, v. 25, n. 2, p. 245–253, 2017.

PATRA, J. K.; BAEK, K. H. Green Nanobiotechnology: Factors Affecting Synthesis and Characterization Techniques. **Journal of Nanomaterials**, v. 2014, 2014.

PÉREZ, B.; LI, J.; GUO, Z. Chemistry and properties of lipids and phospholipids. In: AKOH, C. C. (Ed.). . Food Lipids: Chemistry, Nutrition, and Biotechnology. Fouth Edit ed. Boca Raton: CRC Press, 2017. p. 1029.

PERICA, M. M.; DELAŠ, I. Essential fatty acids and psychiatric disorders. **Nutrition in Clinical Practice**, v. 26, n. 4, p. 409–425, 2011.

PEZESHKI, A. et al. Nanostructured lipid carriers as a favorable delivery system for β-carotene. **Food Bioscience**, v. 27, n. January 2018, p. 11–17, 2019.

PIMENTEL-MORAL, S. et al. Lipid nanocarriers for the loading of polyphenols – A comprehensive review. **Advances in Colloid and Interface Science**, v. 260, p. 85–94, 2018.

PINTO, F.; DE BARROS, D. P. C.; FONSECA, L. P. Design of multifunctional nanostructured lipid carriers enriched with α-tocopherol using vegetable oilsIndustrial **Crops and Products**, v. 118, n. April, p. 149–159, 2018.

POONIA, N. et al. Nanostructured lipid carriers : versatile oral delivery vehicle. **Future Sci AO**. v. 2, 2016.

POONIA, N. et al. Resveratrol loaded functionalized nanostructured lipid carriers for breast cancer targeting: Systematic development, characterization and pharmacokinetic evaluation. **Colloids and Surfaces B: Biointerfaces**, v. 181, n. February, p. 756–766, 2019.

PURI, A. et al. Lipid-Based Nanoparticles as Pharmaceutical Drug Carriers : From Concepts to Clinic. **Crit Rev Ther Drug Carrier Syst. v**. 26, n. 6, p. 523–580, 2009.

QUEIRÓS, M. S. et al. Milk fat nanoemulsions stabilized by dairy proteins. **Journal of Food Science and Technology**, v. 57, n. 9, p. 3295–3304, 2020.

QIAN, C. et al. Impact of lipid nanoparticle physical state on particle aggregation and β-carotene degradation: Potential limitations of solid lipid nanoparticles. **Food Research International,** v. 52, n. 1, p. 342–349, 2013.

QUEIRÓS, M. DE S. et al. Development of solid lipid nanoparticle and nanostructured lipid carrier with dairy ingredients. **International Dairy Journal**, v. 130, 2022.

RASHID, N. A. et al. Effects of chemical interesterification on the physicochemical properties of palm stearin and rice bran oil blends. **Jurnal Teknologi**, v. 5, p. 21–27, 2016.

RASHID, N. A.; KAMARULZAMANA, N. A.; OMARB, Z. Effect of chemical and enzymatic interesterification on the physicochemical properties of palm oil and. Palm kernel oil blends. **Jurnal Teknologi**, v. 2, p. 19–25, 2016.

REIS, L. V. DE C. et al. Evaluation of nanostructured lipid carriers produced with interesterified buriti oil. **Food Technology and Biotechnology**, v. 58, n. 3, p. 284–294, 2020.

RIBEIRO, A. P. B. et al. Interesterificação química: Alternativa para obtenção de gorduras zero trans. **Quimica Nova**, v. 30, n. 5, p. 1295–1300, 2007.

RIBEIRO, A. P. B. et al. Instrumental Methods for the Evaluation of Interesterified Fats. **Food Analytical Methods**, v. 2, n. 4, p. 281–302, 2009a.

RIBEIRO, A. P. B. et al. Thermal behavior, microstructure, polymorphism, and crystallization properties of zero trans fats from soybean oil and fully hydrogenated soybean oil. **Food Biophysics**, v. 4, n. 2, p. 106–118, 2009b.

RIBEIRO, A. P. B. et al. Influence of chemical interesterification on thermal behavior, microstructure, polymorphism and crystallization properties of canola oil and fully hydrogenated cottonseed oil blends. **Food Research International**, v. 42, n. 8, p. 1153–1162, 2009c.

RIBEIRO, A. P. B. et al. Thermal behavior, microstructure, polymorphism, and crystallization properties of zero trans fats from soybean oil and fully hydrogenated soybean oil. **Food Biophysics**, v. 4, n. 2, p. 106–118, 2009d.

RIBEIRO, A. P. B. et al. Interesterificação química de óleo de soja e óleo de soja totalmente hidrogenado: influência do tempo de reação. **Química Nova**, v. 32, n. 4, p. 939–945, 2009e.

RIBEIRO, A. P. B. et al. Interesterification: Alternative for obtaining zero trans fat bases for food applications. **Food research International**, 2009.

RIBEIRO, A. P. B. et al. Hardfats as crystallization modifiers of cocoa butter. **European Journal of Lipid Science and Technology**, v. 115, p. 1462–1473, 2013a.

RIBEIRO, A. P. B. et al. Crystallization modifiers in lipid systems. **Journal of Food Science and Technology**, v. 52, n. 7, p. 3925–3946, 2015.

RIBEIRO, A. P. B. et al. Effects of chemical interesterification on the triacylglycerols, solid fat contents and crystallization kinetics of palm oil-based fats. Proceedings of the 20th USENIX Security Symposium, v. 2, n. 1, p. 369–376, 2017a.

RIBEIRO, M. D. M. M. et al. Synthesis of structured lipids containing behenic acid from fully hydrogenated Crambe abyssinica oil by enzymatic interesterification. **Journal of Food Science and Technology**, v. 54, n. 5, p. 1146–1157, 2017b.

RIBEIRO, M. D. M. M. et al. Enzymatic synthesis of structured lipids from liquid and fully hydrogenated high oleic sunflower oil. **International Journal of Food Properties**, v. 21, n. 1, p. 702–716, 2018.

ROCHA, J. C. B. et al. Thermal and rheological properties of organogels formed by sugarcane or candelilla wax in soybean oil. **Food Research International**, v. 50, n. 1, p. 318–323, 2013.

ROGERS, M. A. et al. Fat crystal networks. Food Materials Science: Principles and Practice, p. 369–414, 2008.

ROSSEAU, D.; MARANGONI, A. G. Chemical Interesterification of Food Lipids: Theory and Practice. In: AKOH, C. C.; MIN, D. B. (Eds.). . Food Lipids : Chemistry, Nutrition, and Biotechnology. Second Edi ed. New York: Marcel Dekker, Inc, 2002. p. 1014.

ROUSSEAU, D.; MARANGONI, A. G. The effects of interesterification on physical and sensory attributes of butterfat and butterfat-canola oil spreads. **Food Research International**, v. 31, n. 5, p. 381–388, 1998.

ROUSSEAU, D.; MARANGONI, A. G.; JEFFREY, K. R. The influence of chemical interesterification on the physicochemical properties of complex fat systems. 2. morphology and polymorphism. JAOCS, **Journal of the American Oil Chemists' Society**, v. 75, n. 12, p. 1833–1839, 1998.

SADATI BEHBAHANI, E. et al. Curcumin loaded nanostructured lipid carriers: In vitro digestion and release studies. **Polyhedron**, v. 164, p. 113–122, 2019.

SALMINEN, H. et al. Formation of solid shell nanoparticles with liquid ω-3 fatty acid core. **Food Chemistry**, v. 141, n. 3, p. 2934–2943, 2013.

SALMINEN, H. et al. Influence of encapsulated functional lipids on crystal structure and chemical stability in solid lipid nanoparticles: Towards bioactive-based design of delivery systems. **Food Chemistry**, v. 190, p. 928–937, 2016.

SALVIA-TRUJILLO, L. et al. Edible Nanoemulsions as Carriers of Active Ingredients: A Review. **Annual Review of Food Science and Technology**, v. 8, n. 1, p. 439–466, 2017.

SALVIA-TRUJILLO, L.; MCCLEMENTS, D. J.; MARTÍN-BELLOSO, O. Nanoemulsion design for the delivery of omega-3 fatty acids. Elsevier Inc., 2021.

SAMPATH, H.; NTAMBI, J. M. The fate and intermediary metabolism of stearic acid. **Lipids,** v. 40, n. 12, p. 1187–1191, 2005.

SANTOS, R. et al. I Diretriz sobre o consumo de Gorduras e Saúde Cardiovascular. **Arquivo Brasileiro de Cardiologia**, v. 100, p. 1–40, 2013.

SANTOS, V. DA S. et al. Nanostructured lipid carriers loaded with free phytosterols for food applications. **Food Chemistry**, v. 298, n. May, p. 125053, 2019a.

SANTOS, V. DA S. et al. Crystallization, Polymorphism and Stability of Nanostructured Lipid Carriers Developed with Soybean Oil, Fully Hydrogenated Soybean Oil and Free Phytosterols for Food Applications. **Journal of Nanotechnology Research**, v. 01, n. 01, p. 1–22, 2019b.

SATO, K.; UENO, S. Polymorphism in fats and oils. Bailey's Industrial Oil and Fat Products, v. 1, p. 77–120, 2005.

SCRIMGEOUR, C. Chemistry of Fatty Acids. Bailey's Industrial Oil and Fat Products, p. 1–43, 2005.

SHAHPARAST, Y. et al. Preparation, physicochemical characterization and oxidative stability of omega-3 fish oil/α-tocopherol-co-loaded nanostructured lipidic carriers**. Advanced Pharmaceutical Bulletin**, 2019.

SHI, Y.; LIANG, B.; HARTEL, R. W. Crystal morphology, microstructure, and textural properties of model lipid systems. JAOCS, **Journal of the American Oil Chemists' Society**, v. 82, n. 6, p. 399–408, 2005.

SHTAY, R.; PING, C.; SCHWARZ, K. Development and characterization of solid lipid nanoparticles (SLNs) made of cocoa butter : A factorial design study. **Journal of Food Engineering**, v. 231, p. 30–41, 2018.

SIEKMANN, B.; WESTESEN, K. Thermoanalysis of the recrystallization process of melt-homogenized glyceride nanoparticles. **Colloids and Surfaces B: Biointerfaces**, v. 3, n. 3, p. 159–175, 1994.

SILVA, M. G. et al. Developed and characterization of nanostructured lipid carriers containing food-grade interesterified lipid phase for food application. **Food Research International**, v. 155, n. October 2021, p. 111119, 2022a.

SILVA, M. G. et al. Nanostructured lipid carriers for delivery of free phytosterols: Effect of lipid composition and chemical interesterification on physical stability. **Colloids and Surfaces A: Physicochemical and Engineering Aspects**, v. 640, n. January, p. 128425, 2022b.

SILVA, R. C. et al. Microscopic approach of the crystallization of tripalmitin and tristearin by microscopy. **Chemistry and Physics of Lipids**, v. 198, p. 1–9, 2016.

SILVA SANTOS, V.; BADAN RIBEIRO, A. P.; ANDRADE SANTANA, M. H. Solid lipid nanoparticles as carriers for lipophilic compounds for applications in foods. **Food Research International**, v. 122, n. September 2017, p. 610–626, 2019.

DAN, N. Compound release from nanostructured lipid carriers (NLCs). Journal of Food Engineering, v. 171, p. 37–43, 2016.

SILVA, A. C. et al. Preparation, characterization and biocompatibility studies on risperidone-loaded solid lipid nanoparticles (SLN): High pressure homogenization versus ultrasound. Colloids and Surfaces B: **Biointerfaces**, v. 86, n. 1, p. 158–165, 2011.

SIVAKANTHAN, S.; MADHUJITH, T. Current trends in applications of enzymatic interesterification of fats and oils: A review**. LWT**, v. 132, n. July, p. 109880, 2020.

SOLEIMANIAN, Y. et al. Propolis wax nanostructured lipid carrier for delivery of β sitosterol: Effect of formulation variables on physicochemical properties. Food Chemistry, v. 260, n. March, p. 97–105, 2018.

SOUTO, E. et al. Nanopartículas de lipídios sólidos: métodos clássicos de produção laboratorial**. Quimica Nova**, v. 34, n. 8, p. 1323–1327, 2011.

SPERANZA, P.; MACEDO, G.; RIBEIRO, A. P. B. Lipase catalyzed interesterification of Amazonian patauá oil and palm stearin for preparation of specific-structured oils. **Journal of Food Science and Technology**, v. 52, p. 8268–8275, 2015.

STAN, C. Codex standard for named vegetable oils. v. 8, p. 11–25, 2001.

SULCINER, M. L. et al. Resolvins suppress tumor growth and enhance cancer therapy. **Journal of Experimental Medicine**, v. 215, n. 1, p. 115–140, 2018.

SWANSON, D.; BLOCK, R.; MOUSA, S. A. Omega-3 Fatty Acids EPA and DHA: Health Benefits Throughout Life. **Advances in Nutrition**, v. 3, n. 1, p. 1–7, 2012.

TADROS, T. et al. Formation and stability of nano-emulsions. **Advances in Colloid and Interface Science**, v. 108–109, p. 303–318, 2004.

TAKEUCHI, M.; UENO, S.; SATO, K. Crystallization kinetics of polymorphic forms of a molecular compound constructed by SOS (1,3-distearoyl-2-oleoyl-sn-glycerol) and SSO (1,2-distearoyl-3-oleoyl-rac-glycerol). **Food Research International**, v. 35, n. 10, p. 919–926, 2002.

TAMJIDI, F. et al. Nanostructured lipid carriers (NLC): A potential delivery system for bioactive food molecules. Innovative **Food Science and Emerging Technologies**, v. 19, p. 29–43, 2013.

TAMJIDI, F. et al. Design and characterization of astaxanthin-loaded nanostructured lipid carriers. Innovative **Food Science and Emerging Technologies**, v. 26, p. 366–374, 2014.

TANG, D.; MARANGONI, A. G. Microstructure and fractal analysis of fat crystal networks. JAOCS, **Journal of the American Oil Chemists' Society**, v. 83, n. 5, p. 377–388, 2006.

TENG, W. et al. The hepatic-targeted, resveratrol loaded nanoparticles for relief of high fat diet-induced nonalcoholic fatty liver disease. **Journal of Controlled Release**, v. 307, n. April, p. 139–149, 2019.

THRANDUR, H. et al. Impact of surfactant properties on oxidative stability of ??-carotene encapsulated within solid lipid nanoparticles. **Journal of Agricultural and Food Chemistry**, v. 57, n. 17, p. 8033–8040, 2009.

TIKEKAR, R. V; NITIN, N. Effect of physical state (solid vs. liquid) of lipid core on the rate of transport of oxygen and free radicals in solid lipid nanoparticles and emulsion. **Soft Matter**, v. 7, n. 18, p. 8149–8157, 2011.

TRUJILLO-CAYADO, L. A.; ALFARO, M. C.; MUÑOZ, J. Effects of ethoxylated fatty acid alkanolamide concentration and processing on D-limonene emulsions. **Colloids and Surfaces A: Physicochemical and Engineering Aspects**, v. 536, n. June 2017, p. 198–203, 2018.

VALENZUELA, A.; DELPLANQUE, B.; TAVELLA, M. Stearic acid: a possible substitute for trans fatty acids from industrial origin. **Grasas y Aceites**, v. 62, n. 2, p. 131–138, 2011.

VELLIDO-PEREZ, J. A. et al. Novel emulsions–based technological approaches for the protection of omega–3 polyunsaturated fatty acids against oxidation processes – A comprehensive review. **Food Structure**, v. 27, n. December 2020, p. 100175, 2021.

VENUGOPALAN, V. K. et al. Encapsulation and protection of omega-3-rich fish oils using food-grade delivery systems. **Foods**, v. 10, n. 7, p. 1–20, 2021.

VIEIRA, R. et al. Sucupira Oil-Loaded Nanostructured Lipid Carriers (NLC): Lipid Screening, Factorial Design, Release Profile, and Cytotoxicity. **Molecules**. v. 029, n. 6, p. 1–22, 2020.

WANG, J. et al. From microalgae oil to produce novel structured triacylglycerols enriched with unsaturated fatty acids. **Bioresource Technology**, v. 184, p. 405–414, 2015.

WANG, J. L. et al. Preparation and characterization of novel lipid carriers containing microalgae oil for food applications. **Journal of Food Science**, v. 79, n. 2, 2014a.

WANG, J. L. et al. Preparation and characterization of novel lipid carriers containing microalgae oil for food applications. **Journal of Food Science**, v. 79, n. 2, 2014b.

WASSELL, P.; YOUNG, N. W. G. Food applications of trans fatty acid substitutes. International **Journal Of Food Science And Technology**, v. 42, n. 5, p. 503–517, 2007.

WEISS, J. et al. Solid lipid nanoparticles as delivery systems for bioactive food components. **Food Biophysics**, v. 3, n. 2, p. 146–154, 2008.

WENDEL, A.; STAFF, U. Lecithin. In: Kirk-Othmer Encyclopedia of Chemical Technology. p. 1–19, 2000.

WITAYAUDOM, P.; KLINKESORN, U. Effect of surfactant concentration and solidification temperature on the characteristics and stability of nanostructured lipid carrier (NLC) prepared from rambutan (Nephelium lappaceum L.) kernel fat. **Journal of Colloid and Interface Science**, v. 505, p. 1082–1092, 2017.

WORLD HEALTH ORGANIZATION. Countdown To 2023: WHO report on global trans-fat elimination 2020. Geneva, 2020.

WRIGHT, A. J. et al. Rheological Properties of Milkfat and Butter Concise Reviews in Food Science. **Journal of Food Science**, v. 66, n. 8, p. 1056–1071, 2001.

WRIGHT, A. J.; NARINE, S. S.; MARANGONI, A. G. Comparison of experimental techniques used in lipid crystallization studies. **Journal of the American Oil Chemists' Society**, v. 77, n. 12, p. 1239–1242, 2000.

XU, B. et al. Synthesis, aggregation behavior and emulsification characteristic of a multi-sticker amphiphilic polymer. **Journal of Macromolecular Science**, Part A: Pure and Applied Chemistry, v. 50, n. 3, p. 302–309, 2013.

YANG, Y. et al. The effect of oil type on the aggregation stability of nanostructured lipid carriers. **Journal of Colloid and Interface Science**, v. 418, p. 261–272, 2014.

YANG, Y.; MCCLEMENTS, D. J. Vitamin E bioaccessibility: Influence of carrier oil type on digestion and release of emulsified α-tocopherol acetate. **Food Chemistry**, v. 141, n. 1, p. 473–481, 2013.

YAP, P.; MAN, J. DE; MAN, L. DE. Polymorphism of palm oil and palm oil products. **Journal of the American Oil Chemist's Society**, v. 66, n. 5, p. 693–697, 1989.

YE, Q.; GEORGES, N.; SELOMULYA, C. Microencapsulation of active ingredients in functional foods: From research stage to commercial food products. **Trends in Food Science and Technology**, v. 78, n. January, p. 167–179, 2018.

YOON, G.; PARK, J. W.; YOON, I.-S. Solid lipid nanoparticles (SLNs) and nanostructured lipid carriers (NLCs): recent advances in drug delivery. **Journal of Pharmaceutical Investigation**, v. 43, n. 5, p. 353–362, 2013.

YUAN, Y. et al. Characterization and stability evaluation of β-carotene nanoemulsions. **Food Research International**, 2008.

ZEITOUN, M. A. M. et al. Physical properties of interesterified fat blends. **Journal of the American Oil Chemists' Society**, v. 70, n. 5, p. 467–471, 1993.

ZHANG, Z. et al. Effects of chemical interesterification on the triacylglycerols, solid fat contents and crystallization kinetics of palm oil-based fats. **Food and Function**, v. 10, n. 11, p. 7553–7564, 2019.

ZHENG, M. et al. Formulation and characterization of nanostructured lipid carriers containing a mixed lipids core. **Colloids and Surfaces A: Physicochemical and Engineering Aspects**, v. 430, p. 76–84, 2013.

ZHU, T. et al. Comparative study on crystallization behaviors of physical blend- and interesterified blend-based special fats. **Journal of Food Engineering**, v. 241, n. May 2018, p. 33–40, 2019.

ZHU, T. WEI et al. Mechanistic insight into the relationship between triacylglycerol and crystallization of lipase-catalyzed interesterified blend of palm stearin and vegetable oil. **Food Chemistry**, v. 260, n. March, p. 306–316, 2018.